B cell and antibody differentiation

The contribution of glycans to repertoire diversification and classification

Koers, J.

Publication date
2023

Document Version
Final published version

B cell and antibody differentiation

JANA KOERS • 2023

B cell and antibody differentiation

the contribution of glycans to repertoire diversification and classification

JANA KOERS

B cell and antibody differentiation

the contribution of glycans to repertoire diversification and classification

By

JANA KOERS

The research described in this thesis was performed at the department of Immunopathology of Sanquin Research (Amsterdam, the Netherlands) from 2017 until 2022. The research was financially supported by the Landsteiner Foundation for Blood Transfusion under Grant1626 (LSBR; www.lsbr.nl). The printing of this thesis is financially supported by Sanquin Research.

ISBN: 978-94-6458-929-0

Cover design by Mieke van den Heuvel & Alex Butenko
Lay-out by Alex Butenko & Wouter Aalberts, persoonlijkproefschrift.nl
Printed by Ridderprint

B cell and antibody differentiation

the contribution of glycans to repertoire diversification and classification

ACADEMISCH PROEFSCHRIFT

ter verkrijging van de graad van doctor
aan de Universiteit van Amsterdam
op gezag van Rector Magnificus
Prof. dr. ir. P.P.C.C. Verbeek
ten overstaan van een door het College voor Promoties ingestelde commissie,
in het openbaar te verdedigen in de Agnietenkapel
op vrijdag 24 maart 2023, te 13:00 uur

door

Jana Koers

geboren te Nijmegen

PROMOTIECOMMISSIE

Promotor:	Prof. dr. S.M. van Ham	Universiteit van Amsterdam
Co-promotor:	dr. T. Rispens	Sanquin Research
Overige leden:	Prof. dr. S. Brul	Universiteit van Amsterdam
	Prof. dr. N.A. Bos	Rijksuniversiteit Groningen
	Prof. dr. M. van Egmond	Vrije Universiteit Amsterdam
	Prof. dr. C.E. van der Schoot	Universiteit van Amsterdam
	dr. M. van der Burg	Leids Universitair Medisch Centrum
	dr. J.M.I. Vos	Amsterdam UMC
	dr. J.E.J. Guikema	Universiteit van Amsterdam

Faculteit der Natuurwetenschappen, Wiskunde en Informatica

TABLE OF CONTENTS

CHAPTER 1

General introduction and scope of this thesis

INNATE AND ADAPTIVE IMMUNE RESPONSES

The human immune system is a highly sophisticated network of cells and proteins that evolved to protect the body against harmful pathogens. The human immune system has two lines of defense, innate and adaptive immunity, that co-operate to facilitate rapid and specific clearance of pathogens. Innate immune responses serve as a first line of defense against pathogens as these act rapidly upon infection. They depend on the complement system, phagocytic and secretory cells that recognize broadly conserved features of pathogens, with each innate component acting in a pathogen-class specific (viruses, bacteria, fungi, parasites) fashion[1–3]. Adaptive immune responses are generated more slowly, but have high specificity for the pathogen and depend on the activation of B and T cells[4]. In addition, these responses provide long-lasting protection as immunological memory is generated and allows for rapid and specific response to re-call infection of the same pathogen, or their related variants[5]. A fundamental feature of the immune system is the ability to distinguish self from non-self. Occasionally, the systems fails to make this distinction which can lead to self-damaging immune responses and can drive pathology and the generation of autoimmune diseases[6]. Although the innate and adaptive immune systems are different, their collaboration is essential to facilitate rapid and specific clearance of pathogens: the innate immune system enables the generation of an adaptive immune response, while the latter acts by enhancement of the functions of the innate immune system.

B cell development and maturation

B cells recognize antigens by using their antigen receptors, or B cell receptors (BCRs). The immense variety of antigen receptor specificities in the human B cell pool enables the generation of immune response to virtually any pathogen. This diverse repertoire of BCRs is generated during B cell development. Most B cells develop in the bone marrow from common lymphoid progenitor cells. Here they receive specific signals from the specialized microenvironment to commit to B cell lineage development. Throughout life new B cell are continuously generated and leave the bone marrow to populate peripheral secondary lymphoid organs (SLOs), e.g. lymph nodes, spleen and mucosal lymphoid tissues. SLOs are highly organized structures connected to the blood and lymphatics system and constantly sample and collect circulating antigens which can activate the SLO populating immune cells to initiate adaptive immune responses[7,8].

B cell development begins by rearrangement of the heavy (H) chain locus by assembly of one of many V, D and J gene segments in the pro-B cell. Around two thirds of the VDJ_H rearrangements is nonproductive. If failure occurs on both alleles transition towards the pre-B cell stage is ceased and surface expression of both BCRs is prevented. If VDJ_H rearrangements result in a functional heavy chain this pre-B cell receptor is expressed in the cytoplasm and on the cell surface. In the next stage rearrangement of the light chain

gene is rearranged in a similar fashion, but does not include a D segment. By a successful rearrangement of the light chain a complete BCR molecule can be expressed on the cell surface accompanied by several other co-receptor molecules, such as CD79, Igα and Igβ, CD19, CD45 at the cell surface, for efficient signal transduction upon antigen binding.

Within the bone marrow, immature B cells that express properly rearranged BCRs are tested for reactivity to self-antigens. In early stages of B cell development, only IgM is expressed. Immature B cells that express IgM BCRs that crosslink self-antigens development is arrested. This mechanism is known as clonal deletion[9]. Other mechanisms, within or outside of the bone marrow, that deal with self-reactive immature B cells are receptor editing, the induction of a permanent state of unresponsiveness to antigen, or anergy, and immunological ignorance. These mechanisms all contribute that the B cell populations in the SLOs will be relatively limited in recognition of self-antigens and are mainly pathogen-specific. Occasionally, self-reactive B cells are able to escape elimination. This does not necessarily lead to pathology, but if sustained reaction to self occurs, with generation of effector cells and molecules, such as destructive autoantibodies, autoimmune diseases can develop.

To complete development, immature B cells that pass central tolerance within the bone marrow migrate to the spleen, currently at the maturation stage of transitional B cell, to populate the medullary vascular sinuses. Here, B cells compete for access to the follicles in lymphoid tissues to receive essential survival factors, such as BAFF, provided by follicular dendritic cells (FDCs). In the spleen these B cells differentiate into follicular (FO) B cells or marginal zone (MZ) B cells[10] depending on received signals[11–14], and fulfill different functions[11]. These FO B cells are now considered matured, and are commonly referred to as naive B cells. Naive B cells co-express IgM and IgD BCRs on their surface. IgM and IgD perform many of the same roles and can largely substitute for one another[15]. However, naive B cells that recognize ‘self’ decrease their levels of IgM but retain high levels of IgD on their surface which subsequently drives these B cells into anergy[16,17]. The distribution of naive B cells throughout peripheral lymphoid tissues is controlled by chemoattractant cytokines (chemokines) secreted by stromal cells and bone marrow derived cells and the expression of chemokine receptors on the B cell surface. Naive B cells constitutively express CXCR5 and are attracted to the follicles, where its ligand CXCL13 is expressed by FDCs predominantly[18].

B cell fate decision: memory B cells, plasmablasts and plasma cells

B cell responses to infection or immunization can broadly be divided into T cell-dependent B cell responses that feature a germinal center (GC) reaction and T cell-independent B cell responses that lack GCs and feature B cell proliferation and differentiation at extrafollicular sites. Both responses will be discussed in more detail in this section.

T cell-independent B cell responses

Activation of B cells occurs trough different mechanisms depending on several factors, such as the molecular nature of the antigen. Antibody responses to most protein antigens require T cell help for B cell activation, however humans with T cell deficiencies still generate antibodies against many bacterial antigens[19]. These T cell-independent (TI) responses lack GCs and feature B cell proliferation and differentiation into plasmablasts (PBs) at extrafollicular sites and are often induced by repeated, non-protein bacterial antigens such as polysaccharides and lipopolysaccharides[20]. TI antigens display structural repetitive epitopes that allow for cross-linking of multiple BCRs. Activation of the B cell trough the BCRs results in the upregulation of toll-like receptors (TLRs) that interact with pathogen-associated molecular patterns (PAMPs), including glycans like LPS and nucleic acids like CpG[21]. The combination of BCR and TLR activation generally leads to the generation of short-lived PBs that secrete low-affinity IgM antibodies[22]. Although these responses do not mount high-affinity antibodies or B cell memory, they are an essential part of the first line defense against invading extracellular pathogens since they arise earlier that TD responses that require priming and clonal expansion of T helper cells and are thus able to provide a speedily support to the actions of the innate immune system.

T cell-dependent B cell responses

T cell-dependent (TD) antibody responses require help of CD4 T cells and are elicited by TD protein antigens. These antigens have been designated T-dependent, as individuals that lack or have deficient T cells do not elicit an antibody response to these antigens[23]. TD B cell responses feature a GC reaction that occurs within follicles of SLOs (**Figure 1**). However, also TD B cell responses often are preceded by a short phase of extrafollicular proliferation and differentiation. During the initial extrafollicular response, an early wave of naive B cells differentiate with help of activated CD4 T cells (pre-T follicular helper cells) into plasmablasts (PBs) and early memory B cells (MBCs). These cells display limited levels of somatic hypermutation and affinity maturation[22,24–26].

Naive CD4 T cells that recirculate through SLOs can recognize antigen on major histocompatibility complex class II (MHCII) molecules presented by dendritic cells (DCs), populating the T cell zone, using their T cell receptors (TCR)[27]. After recognition, the activated T cell receives DC-derived co-stimulatory signals such as CD80/86, and cytokines that promote expansion and differentiation into effector T helper cells and T follicular helper cells (Tfh)[28,29]. These Tfh cells migrate from the T cell zone to the border of the B cell zone in search for a cognate B cell. In the B cell zone resting naive B cells can recognize antigen presented by FDCs via their BCRs[30,31]. This interaction leads to activation and migration of the naive B cells, like the Tfh cell, to the T/B cell zone border. This migration is driven by up and down regulation of several chemokine receptors, such as CCR7 and CXCR5, on the B and T cell surface[32–34] and production of chemokine receptor

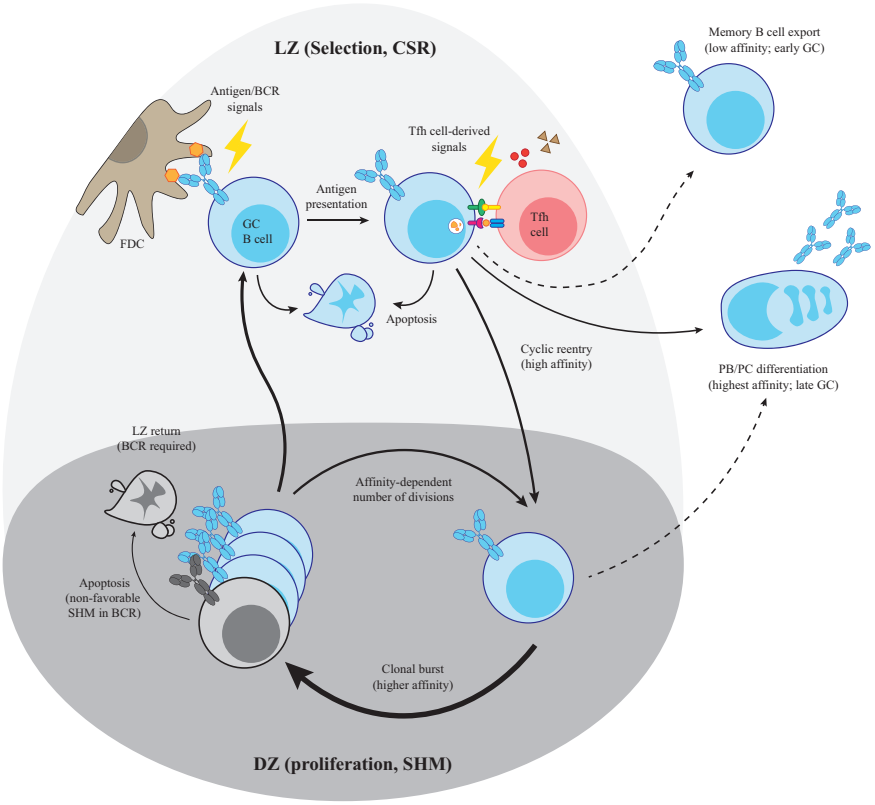

Figure 1. Cellular mechanisms of germinal center selection. *Model depicting events and decision points as GC B cells progress through the steps of affinity-based selection and differentiation. GC, germinal center; BCR, B cell receptor; DZ, dark zone; LZ, light zone; Tfh, T follicular helper cell; FDC, follicular dendritic cell; MBC, memory B cell; PB, plasmablast; PC, plasma cell; SHM, somatic hypermutation; CSR, class switch recombination.*

ligands, including CXCL19, CXCL21 and CXCL13, by T/B zone restricted stromal cells, DCs and FDCs[18,32,35]. After BCR-antigen recognition activated naive B cells the antigen is internalized, processed into antigenic peptides and presented onto MHCII molecules on the B cell surface. Cognate Tfh cells recognize and bind the presented peptide:MHCII complex via their T cell receptor (TCR) and provide both cell-bound and secreted effector molecules that synergize in activating the GC B cell. The interaction between CD40 ligand (CD40L) on the Tfh cell and CD40 on the B cell surface activating the NF-κB pathway and triggering B cell proliferation[36]. B cells that recognized antigen but did not receive subsequent CD40L co-stimulation will go into apoptosis. The second component of Tfh cells help is the secretion of cytokines, such as IL-21 and/ or IL-4 that promote GC B cell proliferation, maintenance and differentiation in PBs and long-lived PCs[37–39]. After receiving these signals the activated B cells start to proliferate and a first fate decision is

made. Activated B cells either differentiate into extrafollicular ASCs or GC-independent early MBCs, or move into the follicle to initiate GC generation[22,24–26,40,41]. Affinity for the antigen is a major driver of the fate decision choice. Activated B cells with relatively high affinity will differentiate in short-lived extrafollicular ASCs[42,43] to ensure a first wave of protection by pathogen-opsonization and immune complex formation to initiate pathogen clearance and subsequent antigen presentation by FDCs, important for driving the GC reaction. The GC-independent MBCs display lower affinity BCRs than do contemporary GC B cells[26,44,45]. These cells ensure plasticity for the memory pool as these can be recruited later in the same response or reactivated during recall responses upon secondary antigen encounter. Activated B cells that enter the follicles, accompanied by their cognate Tfh cells, start to upregulate Bcl-6[46,47]. During an ongoing GC reaction the follicles can be subdivided into two distinct regions, the dark zone (DZ) and the light zone (LZ), where distinct B cell intrinsic processes take place. Within the DZ, GC B cells will go through multiple rounds of division during which mutation may accumulate within the BCR V region by the process of somatic hypermutation (SHM). In the LZ, B cells that acquired affinity improving mutations are selected and at this site also class switch recombination takes place which may occur as early as the pre-GC stages[48–50]. The segregation of proliferation/hypermutation and antigen-driven selection/CSR between DZ and LZ requires that GC B cells migrate dynamically between these two compartments, a framework known as cyclic reentry[51] and is driven by temporal expression of the chemokine receptor CXCR4[52,53].

Besides VDJ recombination, B cells can undergo two additional genetic modifications, somatic hypermutation and class switch recombination, that aim to increase the affinity for the antigen and alter the biological properties of the immunoglobulin following secretion, respectively (**Figure 2**). The process of somatic hypermutation introduces single point mutations that typically accumulate predominantly in the three hypervariable regions (CDR1-3) of the variable domains of the BCR. This results in part of the BCR repertoire changing from germline to somatically mutated BCRs, that generally display a structural decrease in conformational flexibility, slower antigen dissociation rates, and increased binding selectivity. These mutations generate the sequence diversity upon which affinity-based selection will act. Class switch recombination alters the isotype of the BCR via irreversible nonhomologous DNA recombination at switch regions on the heavy chain locus by excision and ligation of C genes. BCRs of different isotypes have different modes of intracellular signaling and upon secretion all have distinct effector functions. Isotype selection is dictated by cytokines secreted by Tfh cells and is discussed in more detail below. Both processes share similar molecular mechanisms and rely on the expression of the enzyme activation-induced cytidine deaminase (AID)[54–56]. AID is highly expressed in GC B cells and expression is induced by CD40 engagement, IL-4, BCR crosslinking and TLR activating agents including LPS and CpG[57–61]. AID preferably targets hotspots within ssDNA and converts cytosine bases to uracils. The introduction of uracil triggers

several types of DNA repair pathways including mismatch repair (MMR) and base excision repair (BER)[62–66]. These will initiate the excision of uracils and generally results in DNA repair with high fidelity. Hence, non-canonical MMR and BER, that recruit low-fidelity polymerases like Polη and REV, are essential for transition or transversion mutations in SHM and double-strand brake formation required for CSR[67–69].

In the LZ, FDCs continue to present antigen. Higher affinity GC B cells, that obtained favorable SHM, have prolonged interaction with FDCs and internalize more antigen conferring an advantage in obtaining Tfh cell help[70,71]. This promotes survival and regulates dwell time and number of selection cycles. Often, SHM lead to BCRs with decreased rather than enhanced affinity, and these B cells, failing to bind and internalize antigen, do not receive survival signals and go into apoptosis. Within a GC, the GC B cell repertoire changes and becomes less diverse with predominantly high affinity clones, a process known as affinity maturation[72]. After initial fate decision choice for GC reactive B cells, GC B cells can be positively selected to exit the GC reaction as PCs, plasmablasts (PBs) -the precursors of PCs that also secrete antibodies[73]- or as MBCs[44,74], which, upon re-exposure to antigen, will rapidly differentiate into PCs[75] or re-enter the GC reaction for further diversification[76,77]. The cues and factors that determine whether a GC B cells differentiates into a MBCs, PBs or PCs are an active area of investigation and are still incompletely understood and is further discussed below.

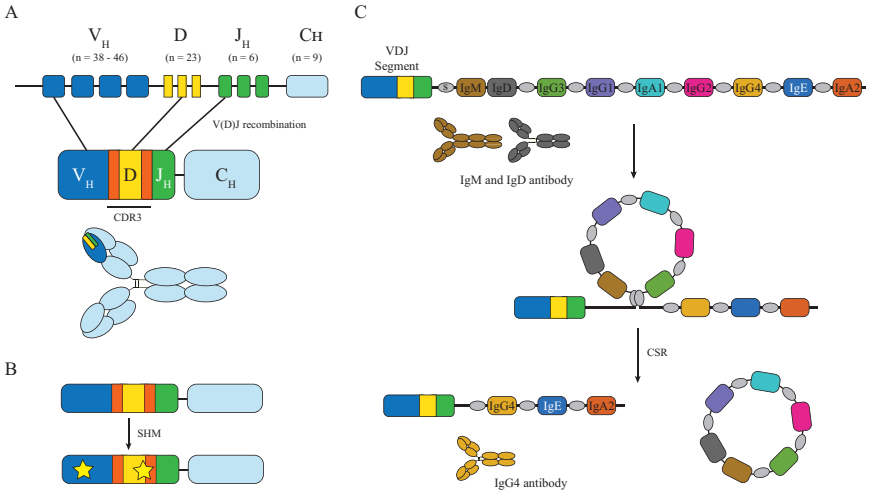

Figure 2. Schematic overview of V(D)J recombination, somatic hypermutation and class switch recombination at the immunoglobulins heavy chain. *(**A**) V(D)J recombination: heavy chain V regions are constructed from three separate gene segments, one of many V, D and J gene segments. Light chain V region construction works similarly except for the absence of a D segment (not shown). (**B**) Somatic hypermutation (SHM) results in mutations (yellow stars) being introduced into the V_H, altering the affinity of the antibody for its antigen. (**C**) Class switch recombination (CSR): the initial μ C_H are replaced by C_H of another isotype by joining and excision of two switch regions (s), modifying the effector activity but not its antigen specificity.*

Memory B cells

The establishment of immunological memory enables the immune system to respond more rapidly and specifically to pathogens and their variants, that have been encountered previously[78]. Those pathogens enter the body trough infections but also trough vaccination, in case of the latter aiming to prevent disease. MBCs are long-lived and quiescent cells poised to response quickly upon antigen recall[76,77]. Little is known about the cues that drive B cells to differentiate into MBCs[79,80]. Classically, the generation of both MBCs and PBs/PCs has been attributed exclusively to the GC reaction. However, recent studies suggest that early MBCs are also formed after contact with activated T cells at the border of the B-T zones and prior to the onset of GCs during protein immunizations[24,81–84]. In mice it was recently observed that the contribution of MBCs within recall responses is more limited than previously thought. Upon secondary antigen exposure limited MBCs reenter secondary GCs, which mainly contain B cells without prior GC experience or detectable clonal expansion, suggestive to be naive B cells[85]. Also their contribution to the PB/PC compartments was minor and derived from a small subset of MBCs differentiated from precursor clones with higher germline affinity during the primary response. Whether TI B cell responses are able to generate MBCs is less clear, but has also been described in some amount[86,87]. Several studies have pointed towards "master transcription factors" promoting MBC differentiation, but transcription factors unique to MBCs have not been found. As MBCs are formed prior to or early in the GC response they feature fewer somatic hypermutations and are of lower affinity as compared to PCs[88,89]. GC B cells that express high levels of Bach2 are suggested to be precursors of MBCs[44]. The timing of memory formation is supported by the observation that Bach2 is only expressed in early GC B cells. ZBTB32, KLF2[90], ABF-1[91,92], HHEX, TLE3[93] and STAT5[94,95] have been associated with MBC generation, as well as timing[80] and absence of IL-21/ Tfh cell help[39,96,97]. Identification of MBCs using surface markers also proves difficult as markers are not shared between mice and humans, such as CD80 and PD-L2[92,98], or not shared between different memory subsets[99], including CD27[100–103] and CCR6[26,104]. Further studies into molecular mechanisms indispensable for MBC generation and markers for identification are needed.

Plasmablasts and plasma cells

Shortly after antigen recognition, B and T cells interact at the T cell border. Some B cells migrate to extrafollicular regions and initiate PB differentiation where they proliferation and secrete antibodies which can be isotype switched and contain few V region mutations[50,105–107]. PBs expand rapidly and since their half-life is only a few days there is high recruitment of new PB precursors during ongoing responses.

Concurrently, other B cells migrate into B cell follicles and commit to the GC B cell fate. High affinity for antigen favors differentiation of GC B cells into proliferative PBs, some of which subsequently enter the quiescent PC compartment. As with positive selection, Tfh

cell help, specifically CD40L stimulation, is thought to play a prominent role in driving cells toward the PB fate[108]. PCs differ from GC B cells and MBCs in terms of affinity and SHM, as affinity of PCs is almost uniformly high[88] and lower affinity cells are absent. The differentiation of GC B cells into PBs and subsequently into PCs is characterized by distinct transcriptional and morphological changes. PB/PC differentiation requires the repression of several GC-associated TFs, such as PAX-5 and BCL6, and upregulation of BLIMP1, IRF4 and XBP-1s[109–115].

Given the fact that 20% of the proteins produced by PCs are antibodies it is no wonder that they contain an enlarged protein machinery. PCs that remain in the lymphoid organs are usually short-lived. PCs that exit the SLOs by downregulation of CXCR5 and upregulation of S1PR1 enter circulation and either move to sites of infection via CXCR3-mediated migration or enter the bone marrow by upregulation of CXCR4[114]. Long-lived PCs are able to migrate into survival niches in the bone marrow and continue their antibody production there, often for decades. It is unclear what drives a PCs to become short- or long-lived, but potentially selection advantages or a different phenotype might enable long-lived PCs to migrate into these survival niches.

Characterization of B cell differentiation by glycan remodeling

Glycans can be found attached to proteins and are abundantly found on cellular surfaces and common glycan structures include O- and *N*-linked glycans. Glycans are important for proper protein folding, cell-cell interaction, lymphocyte migration and antibody effector functions[116]. Distinct global O-glycosylation profiles allow for segregation of different B cell subsets during B cell differentiation (**Figure 3**). Naive B cells exhibit sialylated, elongated O-glycans, which become transiently non-sialylated and subsequently progressively shortened during GC and post-GC stages[117]. These alterations in O-glycan profiles arises from differential expression of glycan-modifying enzymes, including ST3Gal1 and GCNT1. Lectins, glycan-binding proteins, are useful for characterizing B cell subsets based on their glycan-binding profiles. PNA (peanut agglutinin) in combination with other surface markers, is used to detect GC B cells[118,119], whereas lectins Jacalin and HPA bind to MBCs and PBs[117]. It was noted that alterations in glycosylation occur to a significant extend on CD45, a central regulator of BCR signaling, since binding of two anti-CD45 antibodies (B220 and MEM55), which recognize distinct glycan-dependent epitopes, switched during B cell differentiation[117,120–123]. Different glycan profiles may not only generate phenotypic differences but potentially also provide functional differences by their ability to interact in *cis* or *trans* with endogenous lectins such as galectins and SIGLECs[124,125].

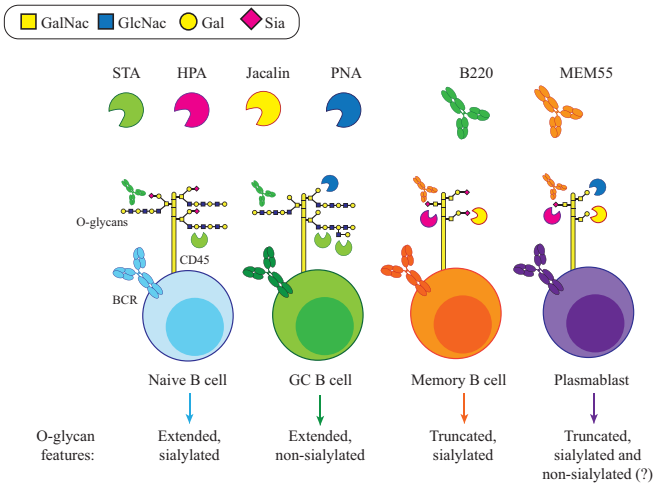

Figure 3. O-glycosylation phenotype of human B cell subsets and expression of associated CD45 glycoforms and their lectin and anti-CD45 antibody binding profiles. *Glycan features that are inconclusive are marked with a "?". GalNAc, N-acetylgalactosamine; GlcNAc, N-acetylglucosamine; Gal, galactose; Sia, sialic acid; BCR, B cell receptor; GC, germinal center; STA, solanum tuberosum agglutinin; HPA, Helix pomatia agglutinin; PNA, peanut agglutinin.*

Antibodies

Antibodies, or immunoglobulins, rapidly recognize and neutralize invading pathogens and leave a signature of clearance recognized by other host immune mechanisms. Antibodies exist as monomers and oligomers. The monomers are Y-shaped and consist of two linked heavy chains each paired with a light chain and constitute two distinct regions, a Fab region that determines the antibody specificity and is responsible for antigen binding and a crystallizable fragment (Fc) that exerts the effector functions of the antibody.

The variable region

The variable region (V region) is the N-terminal part of the Fab, of which each antibody has two identical (**Figure 2**). It comprises multiple loops, that constitute three complementarity determining regions (CDR1, CDR2 and CDR3) that are imperative for antigen binding and harbor the highest diversity in the variable domain. CDR1 and CDR2 are encoded in the germline sequences whereas the CDR3 is generated during initial BCR formation in the bone marrow, by a mechanism known as V(D)J-recombination introduced above[126]. The CDRs from both heavy and light chains form the antigen binding site which can be shaped differently depending on the shape of the antigen. Typically however, only a few amino acid residues contribute to the paratope, particularly those within the CDR3 of the heavy chain[127]. A single antibody harbors two or more identical antigen-binding sites which allow for binding to multivalent antigens (such as polysaccharides on bacteria) and immune complex formation.

The constant region

The constant region, or Fc region, is composed of constant domains from both heavy chains and attributes the effector capacities of the antibody. After antibody opsonization of the pathogen several clearance pathways are in place, including complement-dependent cytotoxicity (CDC), antibody-dependent cellular phagocytosis (ADCP), and antibody-dependent cell-mediated cytotoxicity (ADCC). During CDC, the classical complement pathway is triggered by C1q binding to opsonizing antibodies, resulting in the formation of a membrane attack complex and lysis of the pathogen. During ADCP and ADCC, effector cells with FcRs, such as macrophages and NK cells, are recruited via opsonizing antibodies and get activated by receptor cross-linking resulting in release of cytotoxic molecules or phagocytosis all leading to clearance of the pathogen. During an immune response different C region isotypes can be expressed in the B cell progeny. The route of antigen entry into the body, its chemical composition and the released cytokines steer isotype class switching decisions and only occurs after antigen stimulation. B cells can switch isotype via irreversible nonhomologous DNA recombination at switch regions on the heavy chain locus by excision and ligation of C genes. Antibody isotype switching increases the functional diversity of the antibody response as it allows for the generation of antibodies with the same antigen specificity but distinct effector functions (**Figure 2**).

The antibody classes and subclasses

Humans have five classes or isotypes of antibodies IgM, IgD, IgG, IgA, IgE (**Figure 4**) and for IgG and IgA several subclasses are defined. Isotype switching is regulated, amongst others, by cytokines such as IL-4, IL-10, IL-13, IL-21 and TGFβ[128–130], and isotype-switched antibodies are associated with different types of pathogenic infections. Viral infections are associated with IgG1 and IgG3, bacteria induce IgG1 and IgG2, parasitic infections elicit IgG4 and IgE, and mucosal pathogens induce IgA antibodies. Different antibody isotypes differ in biological properties, functional target sites and induced routes of antigen-clearance[131–133].

IgM

The secreted form of IgM is a pentameric multimer, composed of five monomers and a J-chain polypeptide that promotes polymerization. Most IgM molecules are present in the bloodstream where it has a half-life of 10 days. IgM is the first antibody to be expressed in the early stages of an immune response in anticipation of affinity matured antibodies. The affinity of a single IgM monomeric subunit is often low, due to the lack of SHM and affinity maturation, however due to the multiple binding sites of the pentameric structure its overall binding strength, or avidity, can be much greater towards multivalent antigens such as viral particles. Not surprisingly, IgM antibodies often recognize repetitive epitopes such as polysaccharides on bacteria. IgM is a potent activator of the classical complement pathway by binding of C1q leading to antigen opsonization and complement-mediated cytolysis.

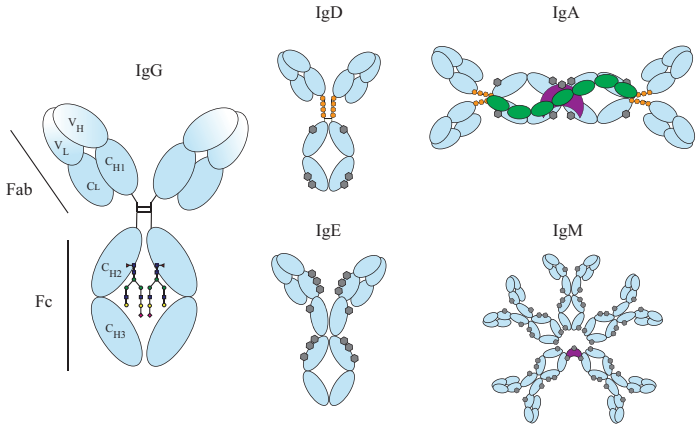

Figure 4. Immunoglobulin isotypes and their sites of glycosylation. *Each immunoglobulin is comprised of two heavy chains (V_H + $C_{H1-3/4}$) and two light chains (V_L + C_L). IgG, IgD, and IgA have a flexible hinge region that link the antigen-binding Fab region to the Fc effector region. For IgG the N-glycan structure is represented for other isotypes O-glycosylation sites are depicted as orange hexagons and N-glycosylation sites are depicted as grey hexagons. The depicted glycans are important for the structural integrity of the antibodies and their effector function. J-chain in purple and secretory component in green.*

IgD

Membrane-bound IgD differs from IgM in that it has a hinge region making this molecule structurally more flexible than IgM, which may explain why the dual expression of IgD and IgM on one B cells improves antigen recognition[16]. IgD antibodies are present in low quantities in serum, and have a high susceptibility for proteolytic enzymes resulting in a serum half-life of only 3 days. Although IgD is often described as having an insignificant role in immune responses, recent evidence suggest that secreted IgD is involved in mucosal immunity[134,135]. IgD expressing B cells are also enriched in autoreactivity. Elevated levels of IgD and reduced IgM expression hallmark anergic B cells that recognize self-antigens and comprise ~30% of naive B cells in human peripheral blood[134,136–139].

IgA

IgA has two subclasses (IgA1 and IgA2) and can be secreted as monomers as well as dimers, and small quantities of larger oligomers. Monomeric IgA is found in serum whereas dimeric secretory IgA (sIgA) is produced locally by PCs in the lamina propria of the gut. IgA dimers contain a J-chain and after poly-Ig receptor-mediated secretion over epithelial borders a polypeptide called the secretory component. At mucosal surfaces, IgA functions as a barrier for pathogens by covering the epithelial cells, interfering with pathogen-epithelial receptor binding and cross-linking of pathogens resulting in clearance. In the blood, although weak in activating complement, complexed IgA can provoke strong pro-inflammatory responses like ADCC and phagocytosis via Fcα-receptor I (FcαRI) binding expressed on immune effector cells. However, also opposing anti-inflammatory properties have been described proposing a protective role for IgA in autoimmunity[140].

IgG

IgG is the most abundant antibody class in serum and extracellular fluids. IgG antibodies have the lowest molecular weight attributed by the low number of Fc glycans, a single highly conserved *N*-glycosylation site at the asparagine 297 residue on each heavy chain. The half-life of circulating IgG is between 7-21 days depending on the IgG subclass and characteristics of the V region[141]. The increased half-life of IgG compared to other antibody classes is attributed to its association with the neonatal Fc receptor (FcRn) that leads to recycling and minimal endosomal degradation[142]. There are four IgG subclasses in humans, IgG1, IgG2, IgG3 and IgG4, named in decreasing order of abundance in serum. IgG subclass antibodies share over 90% homology in amino acid sequence, but all have a unique profile with respect to antigen binding, immune complex formation, complement activation, and triggering of effector cells[131].

IgG1

IgG1 antibody responses are induced by variety of pathogens, including viruses and bacteria, via binding to soluble protein antigens and membrane proteins, and are often accompanied by lower levels of IgG3 in the initial stage of the response. IgG1 antibodies can effectively bind C1q initiating CDC and FcγRs initiating ADCC[131]. As IgG1 is the most abundant subclass in healthy human serum, deficiencies in IgG1 often lead to lowered total IgG levels and are associated with recurrent infections.

IgG2

Responses restricted to IgG2 include responses to bacterial capsular polysaccharide antigens and represents the bulk of the reactivity to many glycans[143]. Unlike IgG1, IgG2 is limited to engage effector functions due lowered binding to effector molecules, e.g. FcRs, and due to restricted conformational flexibility because of its relatively short hinge region[144]. Nevertheless, IgG2 antibodies can activate complement mainly at high antigen densities[145,146]. Interestingly, IgG2 antibodies have greater resistance to microbial proteases such as Staphylococcus aureus gluV8 and Streptococcus pyogenes IdeS[147], mostly due to the unique sequence of their lower hinge region. This feature may provide an evolutionary advantage for IgG2 antibodies in dealing with encapsulated, protease-producing pathogens.

IgG3

IgG3 antibodies are pro-inflammatory antibodies with efficient effector functions and high Fab arm flexibility due to their extended hinge region[148,149]. IgG3 responses are elicited against viruses, specific bacteria and parasites expressing protein antigens[143,150,151]. IgG3 antibodies often arise early against protein antigens upon infection and are followed-up by IgG1. Antibody responses exclusively inducing IgG3 are rare, but have been observed for anti-hinge antibodies[152], which bind to the exposed hinge region of cleaved IgG molecules.

IgG4

IgG4 antibodies are generally considered anti-inflammatory, as they are poor activator of immune cell-mediated cytotoxicity and unable to crosslink antigens due to Fab-arm exchange-induced functional monovalency[153–156]. IgG4 responses are associated with prolonged or repeated antigen exposure[157–160] and are predominantly induced by Tfh cell derived cytokines IL-4 and IL-21[161,162]. IgG4 antibody responses are observed during allergy where the relief of allergic symptoms correlates with increasing IgG4 levels, linking this subclass to tolerance induction[163]. Moreover, IgG4 antibody responses are found in helminth or filarial parasite infections[164] and are associated with several autoimmune diseases, amongst which IgG4-related disease (IRD), MuSK myasthenia gravis and pemphigus vulgaris[165]. While in MuSK myasthenia gravis and pemphigus vulgaris IgG4 autoantibodies are pathogenic, in IRD their contribution to disease needs to be determined.

IgE

Similar to IgM, IgE monomers have no hinge region and the Fc region consists of four constant domains. IgE is the least abundant and has the shortest half-life of all antibody isotypes in serum, approximately 2 days[133]. Generation of IgE antibodies presumably occurs in incomplete GCs leading to low-affinity IgE antibodies[166] and switch requires either IL-4 from Tfh cells or IL-13 from T_H2 cells[133,161,167]. IgE antibodies are well known for their role in mediating allergic reactions, but are also important in the defense against parasites[168]. Although they are poor activators of complement, IgE antibodies have powerful effector functions through binding to Fc receptors FcεRI and FcεRII/CD23 on mast cells and basophils[169]. Bound IgE mediates mast cell degranulation of biologically active mediators in an antigen-specific manner which is central to the initiation and propagation of immediate hypersensitivity reactions which can lead to various allergic diseases, but also anaphylactic shock.

Autoantibodies

Various autoimmune diseases are characterized by the presence of antibodies that recognize self-antigens, so-called autoantibodies. These autoantibodies have escaped elimination and for some diseases, including MuSK myasthenia gravis and pemphigus vulgaris, their contribution to pathology has been established[170–172]. Autoantibody-mediated clearance of red blood cells and platelets is observed in autoimmune hemolytic anemia and thrombocytopenic purpura (TTP). Here, autoantibodies directed against platelets and red blood cells induce phagocytosis or complement-mediated lysis[173,174]. Autoantibodies can also interfere with cell-cell interactions or cell functions resulting in systemic inflammation and tissue damage, as is seen in pemphigus vulgaris[175] and MuSK myasthenia gravis[176]. The presence of autoantibodies is a common feature of many autoimmune diseases and for some diseases these can be useful for diagnosis and classification and for others may announce the disease status or predict further clinical evolution of the disease[177–180].

Antibody repertoire diversification

The human antibody repertoire is immensely variable and able to generate an antibody response to virtually any pathogen/substance, often with multiple antibodies capable of recognizing a particular pathogen via different epitopes. Although still controversial, the naive or germline antibody repertoire is currently estimated to consist of ~10^{15} independent members[181,182]. However, the number of B cells in the body at a given moment in time is limited by the individual's total number of B cells and history of antigen encounter. The theoretical diversity of the human antibody repertoire is the result of a number of diversification strategies. The 'core' combinatorial diversity is generated by the process of V(D)J recombination and the joining of V, (D), and J genes by random nucleotide junctions. In addition, antibody diversification is mediated by the process of somatic hypermutation and class switch recombination, described in more detail earlier. Furthermore, antibodies can undergo a magnitude of post-translational modifications, such as *N*- and O-linked glycosylation, cysteinylation, deamination, oxidation and carbamylation[183]. Although post-translational modifications of antibodies has been studied for decades the full impact of the microheterogeneity on antibody function is less well understood. These multiple layers of different diversification strategies combined gives rise to a myriad of distinct antibody molecules with large activity and potency differences.

Antibody Fab glycosylation

Antibodies are glycoproteins and all antibodies classes have one or more conserved *N*-linked glycans within the constant region (**Figure 4**). For IgG *N*-linked glycans attached to the heavy chain position N297[184] are well studied and major immunoregulatory functions have been attributed to these glycans[185,186]. In addition to Fc glycans, the variable domains of antibodies may also contain *N*-linked glycans. In healthy individuals, it is estimated that 11-14% of IgG antibodies display V region glycans, so-called Fab glycans[187–191]. The presence of Fab glycans in other antibody isotypes, apart from IgG, is less clear since their quantification is challenging due to the presence of additional conserved *N*-linked glycans, i.e. in the C_{H1} domains of IgM and IgE and O-linked glycans in the hinge regions of IgD, IgA and IgG3. Fab glycans are linked to *N*-glycosylation sites (Asn-X-Ser/Thr [where X is any amino acid but proline]) and are mainly the result of somatic hypermutation, as *N*-glycosylation sites are largely absent in the germline antibody repertoire[192]. Although the existence of Fab glycans is well established, the mechanisms and functions of Fab glycosylation remain poorly understood. Nevertheless, it is not unlikely that Fab glycosylation can have an impact on immune function since they are found more frequently in autoimmune diseases and certain B cell lymphomas[193]. The characterization of and occurrence in physiological and pathological conditions of this specific type of antibody diversification is one of the main topics of this thesis.

Structural features of Fab glycans

There are three main types of *N*-linked glycans; high-mannose-, complex- and hybrid-type glycans. Glycans found on IgG, both Fab and Fc, are generally complex-type *N*-linked glycans that exhibit a high degree of conformational flexibility. Compared with IgG Fc glycans, IgG Fab glycans contain high levels of sialic acid, galactose, and bisecting *N*-acetylglucosamine and low levels of core fucose[191,194–196], with slight alterations observed during aging and pregnancy[197]. High-mannose-type glycans are rare and estimated to be found on ~ 4% of IgG in healthy individuals[198,199]. The presence of a glycosylation site within the antibody V region does not guarantee the presence of a glycan. The glycosylation of V region sites follows along the classical *N*-glycosylation pathway. Why certain sites are occupied and others are not, is not fully understood. For one, sites can stay unoccupied due to inaccessibility for glycosidases to attach the initial sugar moiety simply because the site is unexposed within the three-dimensional antibody structure[199]. However, several studies have shown that sites, even though exposed, can still lack a glycan[187,200] which suggest that inaccessibly is not the only mechanism driving unoccupied glycan sites. Other mechanisms that influence glycosylation site occupancy may be the type of motif: Asn-X-Ser motifs were three times more common as Asn-X-Thr motifs, but tend to be less often glycosylated[187]. In addition, the type of amino acids surrounding the glycosylation motifs but also expression levels of enzymes required for glycosylation may also play a role.

Functional attributes of antibody Fab glycosylation

Several functional attributes have been observed or proposed for the role of Fab glycans in immunity (**Figure 5**). Fab glycans on antibodies can influence antigen binding, either by increasing[199,201–204] or decreasing[199,201,205] binding affinity. However, in many cases antibody affinity will remain essentially unaffected when Fab glycans are present or removed. In addition, it is thought that via steric hinderance Fab glycans can prevent protein-protein interactions, as exemplified by interfering with binding of FVII to von Willebrand Factor[206]. Furthermore, Fab glycans showed to affect *in vivo* antibody half-live by altering stability and aggregation[201,207–210]. This was recapitulated *in vitro*, and the introduction of Fab glycans could improve antibody stability whereas removing naturally acquired Fab glycans deteriorated stability. Not only the presence or absence of the glycan, but also the glycan structure seems to be important for their function. It was observed that removal of terminal sialic acid on Fab glycans could decrease antigen binding affinity[187,211] but did not affect the stability of the antibody[207,210]. Finally, Fab glycans may participate in glycan-lectin interactions thereby modulating inhibitory receptor signaling (i.e. SIGLEC CD22 on the B cell surface[212]) or act as surrogate antigen to mediate BCR-crosslinking[205,213].

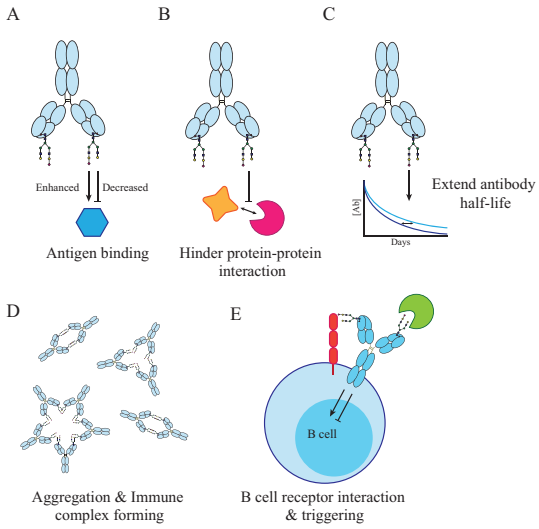

Figure 5. Influence of Fab glycosylation on antibody function. *Fab glycans can (**A**) enhance or decrease antigen binding, (**B**) hinder interaction between proteins by steric hindrance, (**C**) extend antibody half-life as a result of sialylation, (**D**) affect antibody aggregation and immune complex formation, and may (**E**) alter B cell receptor signaling via cis and trans interactions with lectins.*

Selection of Fab glycosylated antibodies

Fab glycans may accumulate as a natural byproduct of somatic hypermutation. However, in recent years a growing body of evidence indicates that the acquisition of Fab glycans is subject to multiple selection mechanisms. Although *N*-glycosylation sites can be acquired across the entire V region of both heavy and light chains, there is preferential introduction of sites within and flanking CDRs due to an inherent bias in the germline variable domain repertoire[187]. The majority of sites is located at 'progenitor glycosylation sites', positions for which a single mutation would suffice to introduce an *N*-glycosylation site, that specifically cluster around CDRs. The biased distribution of sites may be subject to several selection mechanism, such as the higher mutation frequency in CDRs compared to the framework regions (FWRs) or introduction of glycosylation sites within the FWR is more likely to disrupt antibody folding. Moreover, another bias was observed when Fab glycosylation levels were compared amongst IgG subclasses. IgG4 antibodies had a 2-fold higher level of Fab glycosylation compared to the other IgG subclasses[187]. In addition, Fab glycosylation levels have been analyzed for several IgG antibody responses with different specificities. It was observed that several responses had increased levels of IgG Fab glycosylation (anti-PLA2, -ADL, -CCP), others showed a decrease (anti-RhD) and some showed similar levels (anti-TT, anti-NTZ) compared to total IgG[187]. The variation of Fab glycosylation levels for antibodies with different isotypes and specificities suggests that Fab glycosylation is subject to selection during antigen-specific antibody responses. It is not fully understood how B cells with Fab glycosylated BCRs convey a survival advantage. Fab glycans acquired during

antigen-specific immune responses may provide the antibody with improved stability compared to non Fab glycosylation variants, potentially offering an *in vivo* selection advantage. In addition, Fab glycans on BCRs may interact with cellular lectins. A likely scenario involves the highly sialylated Fab glycans on BCRs to interact with sialic acid-binding immunoglobulin-type lectins (SIGLECs), such as CD22 an inhibitory co-receptor of the BCR on the B cell surface. By interacting with CD22, or other cellular lectins, the threshold for activation may be modified, leading to a selective advantage for B cells that have Fab glycosylated BCRs.

Fab glycans in physiological and pathological conditions

The amount of glycans or the composition of the glycan may vary for a given antibody response, but can also change during certain physiological and pathological conditions. This suggest that glycans may play a role in or are informative for the (patho)physiological status of an antibody.

During pregnancy Fab glycans contain more sialic acid and less bisecting GlcNAc than after delivery[194]. Although not confirmed, this specific modulation of Fab glycan composition is suggested to minimize unwanted reactivity towards the fetus. In line, in nonimmunized rats 80% of Fab glycosylated IgG conferred autoreactivity, whereas this was only 40% for non-Fab glycosylated rat IgG[214], suggesting that Fab glycans may be introduced to eliminate autoreactivity. Furthermore, IVIg treatment has been proven successful for the treatment of symptoms in a number of autoimmune diseases, like rheumatoid arthritis, SLE, iTTP. The precise mechanism of the therapeutic effect is not established, however a growing body of evidence suggest that the Fab glycosylated fraction of IVIg mediates, at least in part, the observed anti-inflammatory activity[215].

ACPA autoantibodies in rheumatoid arthritis are characterized by a high prevalence of Fab glycans[216]. Furthermore, patients with IgG4-related disease did not only exhibited increased IgG4 titers but also levels of Fab glycans[217]. The role of Fab glycosylation for any of these conditions has not been established and it is unclear what determines the levels of Fab glycosylation for a specific response, but might relate to the type of antigen recognized or the chronicity/abundance of antigen exposure.

Elevated levels of Fab glycans have not only been observed in autoimmune diseases, but also for certain lymphomas, including follicular lymphoma and primary cutaneous follicle center cell lymphoma[218–221]. Tumor-associated Fab glycans are rich in high-mannose glycans, that are rarely found in non-pathological conditions. The corresponding Fc glycans are complex-type glycans confirming that the normal *N*-glycan pathway is functional[222,223], and suggest a specific role for these oligomannoses in lymphomas. Similar to Fab glycans in autoimmunity, it has been postulated that Fab glycans on lymphoma BCRs interact

with microenvironmental lectins and thereby gain additional growth and survival signals[205,213,224,225]. Intriguingly, as both autoimmune disease and B cell malignancies arise from poor immune regulation they might feature an unappreciated shared pathogenic mechanism, involving elevated levels of Fab glycans, that is worth exploring. In addition, the sialic acid enriched fraction of IVIg may be a potential therapeutic option to explore for patients with autoimmune diseases or B cell malignancies.

SCOPE OF THIS THESIS

Repertoire diversification and classification for both B cells and antibodies arises, among others, from post-translational attachment of glycan moieties to cellular proteins or onto antibodies. Several B cell differentiation stages are characterized by the presence of distinctly composed glycans on proteins on the B cell surface and antibodies can harbor Fab glycans in addition to conserved Fc glycans. The importance of glycosylation is emerging in immunity, and critical roles for glycans involve lymphocyte migration, effector functions and pathogen recognition. Moreover, a growing body of evidence points towards the immunomodulatory effects of glycans via their interactions with endogenous and exogenous lectins. At the same time, many unanswered questions remain with regards to the role of glycans in immunity. The focus of this thesis therefore lies on the contribution of surface glycans to B cell subset classification and clarifying the role of antibody repertoire diversification by Fab glycans during health and autoimmune diseases.

Antibody Fab glycosylation per se and the location of glycan sites within V regions may be driven by antigen specific properties. Therefore, the acquisition of *N*-glycosylation sites by naive B cells in presence and absence of antigen *in vitro* may be informative. For this purpose it is essential that studies are performed using true naive B cells that have non-mutated BCRs to acknowledge *in vitro* induced somatic hypermutation and potentially acquired *N*-glycosylation site patterns. Current strategies for isolation of naive B cells make use of CD27 expression to discriminate antigen-experienced and inexperienced B cells as CD27 expression correlates with having mutated BCRs. However, a substantial fraction of isotype-switched and non-isotype switched B cells that do not express CD27 carry mutated BCRs. In **Chapter 2** we investigated if we could improve current naive B cell identification strategies by including a glycan-dependent B cell subset marker.

Distinct glycosylation profiles of CD45 are used to segregate B cell subsets. Anti-CD45RB antibody MEM55 recognizes a glycan-dependent epitope associated with memory B cells and plasmablasts. There is however a small fraction of non-memory B cells and plasmablasts that also bind this antibody. In **Chapter 3** we studied these and other B cell subsets segregated by CD45RB glycosylation, CD27 and Ig isotype expression and analyzed their IGHV repertoire and *in vitro* functionality.

In **Chapter 4** we improved previously established human naive B cell cultures to better recapitulate the human germinal center response *in vitro*. Here, we established TD and TI B cell cultures performed with low B cell numbers, relevant when working with sparse patient material.

A major factor often overlooked in *in vitro* cultures is the partial pressure of oxygen (pO_2) in healthy human tissues (pO_2 ~3-6%) and the presence of distinctive hypoxic regions (pO_2 ~0.5-1%) within the germinal center microenvironment. The role of variations in pO_2 on human B cell differentiation, and fate decision into MBCs and ASCs has not been studied. In fact, the vast majority of studies is carried out at atmospheric oxygen levels, which is much higher than proliferating B cells will encounter. Variations in pO_2 are likely to affect the amplitude of B cell differentiation, due to profound effects of cellular metabolism as well as direct effects on transcriptional regulation. In **Chapter 5** we investigated the effect of physiological relevant pO_2 on B cell fate decision and class switch recombination.

BCRs and antibodies can acquire glycans on *N*-glycosylation sites present in their V regions of which most emerge during antigen-specific B cell responses by the process of somatic hypermutation. Basic knowledge about patterns of V region *N*-glycosylation at different stages of B cell development is scarce. In **Chapter 6** we therefore established patterns of *N*-glycosylation sites in V regions of naive and memory B cell repertoires by analyzing the V region distribution and acquisition of *N*-glycosylation sites.

Although several autoantibody responses have been characterized with increased levels of Fab glycans, it is not known whether this is a general characteristic acquired by antibodies that develop in the context of autoimmunity. In **Chapter 7** we performed a disease-overarching study and determined the level of Fab glycosylation on ten different autoantibody responses in a broad range of autoimmune diseases.

In **Chapter 8** we investigated if elevated levels of Fab glycans are specific for antibodies that develop in the context of autoimmunity or also develop in other inflammatory-contexts, such as anti-hinge antibodies found in inflammatory proteolytic microenvironments. The association of anti-hinge antibody responses and their level of Fab glycosylation are compared between rheumatoid arthritis patients and healthy individuals.

Finally, a general summary about the most relevant findings of this thesis and how they relate to current literature is presented in **Chapter 9.** Understanding the role of glycans in B cell and antibody biology is important as it may provide insights in the phenotypic and functional progression from differentiating B cell subsets and if Fab glycans on autoantibodies, may aid in diagnostics, be indicative of disease progression or contribute to pathogenesis.

REFERENCES

1. Fujita T. Evolution of the lectin-complement pathway and its role in innate immunity. *Nat Rev Immunol*. 2002;2(5):346-353. doi:10.1038/nri800
2. Holers VM. Complement and its receptors: new insights into human disease. *Annu Rev Immunol*. 2014;32:433-459. doi:10.1146/annurev-immunol-032713-120154
3. Janeway CAJ, Medzhitov R. Innate immune recognition. *Annu Rev Immunol*. 2002;20:197-216. doi:10.1146/annurev.immunol.20.083001.084359
4. Iwasaki A, Medzhitov R. Control of adaptive immunity by the innate immune system. *Nat Immunol*. 2015;16(4):343-353. doi:10.1038/ni.3123
5. Bonilla FA, Oettgen HC. Adaptive immunity. *J Allergy Clin Immunol*. 2010;125(2 Suppl 2):S33-40. doi:10.1016/j.jaci.2009.09.017
6. Wang L, Wang F-S, Gershwin ME. Human autoimmune diseases: a comprehensive update. *J Intern Med*. 2015;278(4):369-395. doi:10.1111/joim.12395
7. Heesters BA, van der Poel CE, Das A, Carroll MC. Antigen Presentation to B Cells. *Trends Immunol*. 2016;37(12):844-854. doi:10.1016/j.it.2016.10.003
8. Batista FD, Harwood NE. The who, how and where of antigen presentation to B cells. *Nat Rev Immunol*. 2009;9(1):15-27. doi:10.1038/nri2454
9. Nemazee D. Mechanisms of central tolerance for B cells. *Nat Rev Immunol*. 2017;17(5):281-294. doi:10.1038/nri.2017.19
10. King JK, Ung NM, Paing MH, et al. Regulation of Marginal Zone B-Cell Differentiation by MicroRNA-146a. *Front Immunol*. 2016;7:670. doi:10.3389/fimmu.2016.00670
11. Allman D, Pillai S. Peripheral B cell subsets. *Curr Opin Immunol*. 2008;20(2):149-157. doi:10.1016/j.coi.2008.03.014
12. Pillai S, Cariappa A. The follicular versus marginal zone B lymphocyte cell fate decision. *Nat Rev Immunol*. 2009;9(11):767-777. doi:10.1038/nri2656
13. Stadanlick JE, Kaileh M, Karnell FG, et al. Tonic B cell antigen receptor signals supply an NF-kappaB substrate for prosurvival BLyS signaling. *Nat Immunol*. 2008;9(12):1379-1387. doi:10.1038/ni.1666
14. Tan JB, Xu K, Cretegny K, et al. Lunatic and manic fringe cooperatively enhance marginal zone B cell precursor competition for delta-like 1 in splenic endothelial niches. *Immunity*. 2009;30(2):254-263. doi:10.1016/j.immuni.2008.12.016
15. Geisberger R, Lamers M, Achatz G. The riddle of the dual expression of IgM and IgD. *Immunology*. 2006;118(4):429-437. doi:10.1111/j.1365-2567.2006.02386.x
16. Noviski M, Mueller JL, Satterthwaite A, Garrett-Sinha LA, Brombacher F, Zikherman J. IgM and IgD B cell receptors differentially respond to endogenous antigens and control B cell fate. *Elife*. 2018;7. doi:10.7554/eLife.35074
17. Noviski M, Zikherman J. Control of autoreactive B cells by IgM and IgD B cell receptors: maintaining a fine balance. *Curr Opin Immunol*. 2018;55:67-74. doi:10.1016/j.coi.2018.09.015
18. Ansel KM, Ngo VN, Hyman PL, et al. A chemokine-driven positive feedback loop organizes lymphoid follicles. *Nature*. 2000;406(6793):309-314. doi:10.1038/35018581

19. Weller S, Faili A, Garcia C, et al. CD40-CD40L independent Ig gene hypermutation suggests a second B cell diversification pathway in humans. *Proc Natl Acad Sci U S A*. 2001;98(3):1166-1170. doi:10.1073/pnas.98.3.1166

20. Mond JJ, Vos Q, Lees A, Snapper CM. T cell independent antigens. *Curr Opin Immunol*. 1995;7(3):349-354. doi:10.1016/0952-7915(95)80109-x

21. Bekeredjian-Ding I, Jego G. Toll-like receptors--sentries in the B-cell response. *Immunology*. 2009;128(3):311-323. doi:10.1111/j.1365-2567.2009.03173.x

22. Elsner RA, Shlomchik MJ. Germinal Center and Extrafollicular B Cell Responses in vaccination, immunity and autoimmunity. *Immunity*. 2020;53(6):1136-1150. doi:10.1016/j.immuni.2020.11.006. Germinal

23. Allen RC, Armitage RJ, Conley ME, et al. CD40 ligand gene defects responsible for X-linked hyper-IgM syndrome. *Science*. 1993;259(5097):990-993. doi:10.1126/science.7679801

24. Weisel FJ, Zuccarino-Catania G V., Chikina M, Shlomchik MJ. A Temporal Switch in the Germinal Center Determines Differential Output of Memory B and Plasma Cells. *Immunity*. 2016;44(1):116-130. doi:10.1016/j.immuni.2015.12.004

25. Laidlaw BJ, Cyster JG. Transcriptional regulation of memory B cell differentiation. *Nat Rev Immunol*. 2021;21(4):209-220. doi:10.1038/s41577-020-00446-2

26. Suan D, Kräutler NJ, Maag JL V, et al. CCR6 Defines Memory B Cell Precursors in Mouse and Human Germinal Centers, Revealing Light-Zone Location and Predominant Low Antigen Affinity. *Immunity*. 2017;47(6):1142-1153.e4. doi:10.1016/j.immuni.2017.11.022

27. Panda S, Ding JL. Natural antibodies bridge innate and adaptive immunity. *J Immunol*. 2015;194(1):13-20. doi:10.4049/jimmunol.1400844

28. Chen L, Flies DB. Molecular mechanisms of T cell co-stimulation and co-inhibition. *Nat Rev Immunol*. 2013;13(4):227-242. doi:10.1038/nri3405

29. Crotty S. Follicular helper CD4 T cells (TFH). *Annu Rev Immunol*. 2011;29:621-663. doi:10.1146/annurev-immunol-031210-101400

30. Allen CDC, Cyster JG. Follicular dendritic cell networks of primary follicles and germinal centers: phenotype and function. *Semin Immunol*. 2008;20(1):14-25. doi:10.1016/j.smim.2007.12.001

31. Heesters BA, Myers RC, Carroll MC. Follicular dendritic cells: dynamic antigen libraries. *Nat Rev Immunol*. 2014;14(7):495-504. doi:10.1038/nri3689

32. Förster R, Schubel A, Breitfeld D, et al. CCR7 coordinates the primary immune response by establishing functional microenvironments in secondary lymphoid organs. *Cell*. 1999;99(1):23-33. doi:10.1016/s0092-8674(00)80059-8

33. Hardtke S, Ohl L, Förster R. Balanced expression of CXCR5 and CCR7 on follicular T helper cells determines their transient positioning to lymph node follicles and is essential for efficient B-cell help. *Blood*. 2005;106(6):1924-1931. doi:10.1182/blood-2004-11-4494

34. Arnold CN, Campbell DJ, Lipp M, Butcher EC. The germinal center response is impaired in the absence of T cell-expressed CXCR5. *Eur J Immunol*. 2007;37(1):100-109. doi:10.1002/eji.200636486

35. Ngo VN, Tang HL, Cyster JG. Epstein-Barr virus-induced molecule 1 ligand chemokine is expressed by dendritic cells in lymphoid tissues and strongly attracts naive T cells and activated B cells. *J Exp Med*. 1998;188(1):181-191. doi:10.1084/jem.188.1.181

36. Mackus WJM, Lens SMA, Medema RH, et al. Prevention of B cell antigen receptor-induced apoptosis by ligation of CD40 occurs downstream of cell cycle regulation. *Int Immunol*. 2002;14(9):973-982. doi:10.1093/intimm/dxf065

37. Weinstein JS, Herman EI, Lainez B, et al. T FH cells progressively differentiate to regulate the germinal center response. *Nat Immunol*. 2016;17(10):1197-1205. doi:10.1038/ni.3554

38. Chou C, Verbaro DJ, Tonc E, et al. The Transcription Factor AP4 Mediates Resolution of Chronic Viral Infection through Amplification of Germinal Center B Cell Responses. *Immunity*. 2016;45(3):570-582. doi:10.1016/j.immuni.2016.07.023

39. Linterman MA, Beaton L, Yu D, et al. IL-21 acts directly on B cells to regulate Bcl-6 expression and germinal center responses. *J Exp Med*. 2010;207(2):353-363. doi:10.1084/jem.20091738

40. Mak TW, Shahinian A, Yoshinaga SK, et al. Costimulation through the inducible costimulator ligand is essential for both T helper and B cell functions in T cell-dependent B cell responses. *Nat Immunol*. 2003;4(8):765-772. doi:10.1038/ni947

41. De Silva NS, Klein U. Dynamics of B cells in germinal centres. *Nat Rev Immunol*. 2015;15(3):137-148. doi:10.1038/nri3804

42. Shih T-AY, Meffre E, Roederer M, Nussenzweig MC. Role of BCR affinity in T cell dependent antibody responses in vivo. *Nat Immunol*. 2002;3(6):570-575. doi:10.1038/ni803

43. Paus D, Phan TG, Chan TD, Gardam S, Basten A, Brink R. Antigen recognition strength regulates the choice between extrafollicular plasma cell and germinal center B cell differentiation. *J Exp Med*. 2006;203(4):1081-1091. doi:10.1084/jem.20060087

44. Shinnakasu R, Inoue T, Kometani K, et al. Regulated selection of germinal-center cells into the memory B cell compartment. *Nat Immunol*. 2016;17(7):861-869. doi:10.1038/ni.3460

45. Wong R, Belk JA, Govero J, et al. Affinity-Restricted Memory B Cells Dominate Recall Responses to Heterologous Flaviviruses. *Immunity*. 2020;53(5):1078-1094.e7. doi:10.1016/j.immuni.2020.09.001

46. Kitano M, Moriyama S, Ando Y, et al. Bcl6 Protein Expression Shapes Pre-Germinal Center B Cell Dynamics and Follicular Helper T Cell Heterogeneity. *Immunity*. 2011;34(6):961-972. doi:10.1016/j.immuni.2011.03.025

47. Finkin S, Hartweger H, Oliveira TY, Kara EE, Nussenzweig MC. Protein Amounts of the MYC Transcription Factor Determine Germinal Center B Cell Division Capacity. *Immunity*. 2019;51(2):324-336.e5. doi:10.1016/j.immuni.2019.06.013

48. Roco JA, Mesin L, Binder SC, et al. Class-Switch Recombination Occurs Infrequently in Germinal Centers. *Immunity*. 2019;51(2):337-350.e7. doi:10.1016/j.immuni.2019.07.001

49. Marshall JL, Zhang Y, Pallan L, et al. Early B blasts acquire a capacity for Ig class switch recombination that is lost as they become plasmablasts. *Eur J Immunol*. 2011;41(12):3506-3512. doi:10.1002/eji.201141762

50. Cunningham AF, Gaspal F, Serre K, et al. Salmonella induces a switched antibody response without germinal centers that impedes the extracellular spread of infection. *J Immunol*. 2007;178(10):6200-6207. doi:10.4049/jimmunol.178.10.6200

51. Kepler TB, Perelson AS. Cyclic re-entry of germinal center B cells and the efficiency of affinity maturation. *Immunol Today*. 1993;14(8):412-415. doi:10.1016/0167-5699(93)90145-B

52. Victora GD, Schwickert TA, Fooksman DR, et al. Germinal center dynamics revealed by multiphoton microscopy with a photoactivatable fluorescent reporter. *Cell*. 2010;143(4):592-605. doi:10.1016/j.cell.2010.10.032

53. Allen CDC, Ansel KM, Low C, et al. Germinal center dark and light zone organization is mediated by CXCR4 and CXCR5. *Nat Immunol*. 2004;5(9):943-952. doi:10.1038/ni1100

54. Xu Z, Pone EJ, Al-Qahtani A, Park S-R, Zan H, Casali P. Regulation of aicda expression and AID activity: relevance to somatic hypermutation and class switch DNA recombination. *Crit Rev Immunol*. 2007;27(4):367-397. Accessed September 7, 2017. http://www.ncbi.nlm.nih.gov/pubmed/18197815

55. Muramatsu M, Kinoshita K, Fagarasan S, Yamada S, Shinkai Y, Honjo T. *Class Switch Recombination and Hypermutation Require Activation-Induced Cytidine Deaminase (AID), a Potential RNA Editing Enzyme*. Vol 102.; 2000.

56. Revy P, Muto T, Levy Y, et al. *Activation-Induced Cytidine Deaminase (AID) Deficiency Causes the Autosomal Recessive Form of the Hyper-IgM Syndrome (HIGM2) HIGM2 Patients (and in AID / Mice) Demonstrates the Absolute Requirement for AID in Several Crucial Steps of B Cell Terminal Differentiation Necessary for Efficient Antibody Responses. Production of Highly Efficient Neutralizing Antibodies Re-Kazuo Kinoshita, 2 Tasuku Honjo, 2 Quires Affinity Maturation of Antibody Responses. This*. Vol 102.; 2000.

57. Muramatsu M, Sankaranand VS, Anant S, et al. Specific expression of activation-induced cytidine deaminase (AID), a novel member of the RNA-editing deaminase family in germinal center B cells. *J Biol Chem*. 1999;274(26):18470-18476. doi:10.1074/jbc.274.26.18470

58. Jabara H, Laouini D, Tsitsikov E, et al. The binding site for TRAF2 and TRAF3 but not for TRAF6 is essential for CD40-mediated immunoglobulin class switching. *Immunity*. 2002;17(3):265-276. doi:10.1016/s1074-7613(02)00394-1

59. Zan H, Wu X, Komori A, Holloman WK, Casali P. AID-dependent generation of resected double-strand DNA breaks and recruitment of Rad52/Rad51 in somatic hypermutation. *Immunity*. 2003;18(6):727-738. doi:10.1016/s1074-7613(03)00151-1

60. Jain A, Ma CA, Lopez-Granados E, et al. Specific NEMO mutations impair CD40-mediated c-Rel activation and B cell terminal differentiation. *J Clin Invest*. 2004;114(11):1593-1602. doi:10.1172/JCI21345

61. Schrader CE, Linehan EK, Mochegova SN, Woodland RT, Stavnezer J. Inducible DNA breaks in Ig S regions are dependent on AID and UNG. *J Exp Med*. 2005;202(4):561-568. doi:10.1084/jem.20050872

62. Xu Z, Fulop Z, Zhong Y, Evinger AJ 3rd, Zan H, Casali P. DNA lesions and repair in immunoglobulin class switch recombination and somatic hypermutation. *Ann N Y Acad Sci*. 2005;1050:146-162. doi:10.1196/annals.1313.119

63. Kenter AL. Class switch recombination: an emerging mechanism. *Curr Top Microbiol Immunol*. 2005;290:171-199. doi:10.1007/3-540-26363-2_8

64. Martomo SA, Gearhart PJ. Somatic hypermutation: subverted DNA repair. *Curr Opin Immunol*. 2006;18(3):243-248. doi:10.1016/j.coi.2006.03.007

65. Stavnezer J, Schrader CE. Mismatch repair converts AID-instigated nicks to double-strand breaks for antibody class-switch recombination. *Trends Genet*. 2006;22(1):23-28. doi:10.1016/j.tig.2005.11.002

66. Casali P, Pal Z, Xu Z, Zan H. DNA repair in antibody somatic hypermutation. *Trends Immunol*. 2006;27(7):313-321. doi:10.1016/j.it.2006.05.001

67. Xu Z, Zan H, Pal Z, Casali P. DNA replication to aid somatic hypermutation. *Adv Exp Med Biol*. 2007;596:111-127. doi:10.1007/0-387-46530-8_10

68. Jansen JG, Langerak P, Tsaalbi-Shtylik A, van den Berk P, Jacobs H, de Wind N. Strand-biased defect in C/G transversions in hypermutating immunoglobulin genes in Rev1-deficient mice. *J Exp Med*. 2006;203(2):319-323. doi:10.1084/jem.20052227

69. Faili A, Aoufouchi S, Weller S, et al. DNA polymerase eta is involved in hypermutation occurring during immunoglobulin class switch recombination. *J Exp Med*. 2004;199(2):265-270. doi:10.1084/jem.20031831

70. Natkanski E, Lee W-Y, Mistry B, Casal A, Molloy JE, Tolar P. B cells use mechanical energy to discriminate antigen affinities. *Science*. 2013;340(6140):1587-1590. doi:10.1126/science.1237572

71. Allen CDC, Okada T, Tang HL, Cyster JG. Imaging of germinal center selection events during affinity maturation. *Science*. 2007;315(5811):528-531. doi:10.1126/science.1136736

72. Victora GD, Nussenzweig MC. Germinal centers. *Annu Rev Immunol*. 2012;30:429-457. doi:10.1146/annurev-immunol-020711-075032

73. Shapiro-Shelef M, Calame K. Regulation of plasma-cell development. *Nat Rev Immunol*. 2005;5(3):230-242. doi:10.1038/nri1572

74. Laidlaw BJ, Schmidt TH, Green JA, Allen CDC, Okada T, Cyster JG. The Eph-related tyrosine kinase ligand Ephrin-B1 marks germinal center and memory precursor B cells. *J Exp Med*. 2017;214(3):639-649. doi:10.1084/jem.20161461

75. Gray D. Immunological memory. *Annu Rev Immunol*. 1993;11:49-77. doi:10.1146/annurev.iy.11.040193.000405

76. Dogan I, Bertocci B, Vilmont V, et al. Multiple layers of B cell memory with different effector functions. *Nat Immunol*. 2009;10(12):1292-1299. doi:10.1038/ni.1814

77. Pape KA, Taylor JJ, Maul RW, Gearhart PJ, Jenkins MK. Different B cell populations mediate early and late memory during an endogenous immune response. *Science*. 2011;331(6021):1203-1207. doi:10.1126/science.1201730

78. Amanna IJ, Carlson NE, Slifka MK. Duration of humoral immunity to common viral and vaccine antigens. *N Engl J Med*. 2007;357(19):1903-1915. doi:10.1056/NEJMoa066092

79. Tangye SG, Tarlinton DM. Memory B cells: effectors of long-lived immune responses. *Eur J Immunol*. 2009;39(8):2065-2075. doi:10.1002/eji.200939531

80. Good-Jacobson KL, Shlomchik MJ. Plasticity and heterogeneity in the generation of memory B cells and long-lived plasma cells: the influence of germinal center interactions and dynamics. *J Immunol*. 2010;185(6):3117-3125. doi:10.4049/jimmunol.1001155

81. Inamine A, Takahashi Y, Baba N, et al. Two waves of memory B-cell generation in the primary immune response. *Int Immunol*. 2005;17(5):581-589. doi:10.1093/intimm/dxh241

82. Takemori T, Kaji T, Takahashi Y, Shimoda M, Rajewsky K. Generation of memory B cells inside and outside germinal centers. *Eur J Immunol*. 2014;44(5):1258-1264. doi:10.1002/eji.201343716

83. Weisel F, Shlomchik M. Memory B Cells of Mice and Humans. *Annu Rev Immunol*. 2017;35:255-284. doi:10.1146/annurev-immunol-041015-055531

84. Toyama H, Okada S, Hatano M, et al. Memory B cells without somatic hypermutation are generated from Bcl6-deficient B cells. *Immunity*. 2002;17(3):329-339. doi:10.1016/s1074-7613(02)00387-4

85. Mesin L, Schiepers A, Ersching J, et al. Restricted Clonality and Limited Germinal Center Reentry Characterize Memory B Cell Reactivation by Boosting. *Cell*. 2020;180(1):92-106.e11. doi:10.1016/j.cell.2019.11.032

86. Obukhanych T V., Nussenzweig MC. T-independent type II immune responses generate memory B cells. *J Exp Med*. 2006;203(2):305-310. doi:10.1084/jem.20052036

87. Berkowska MA, Driessen GJA, Bikos V, et al. Human memory B cells originate from three distinct germinal center-dependent and -independent maturation pathways. *Blood*. 2011;118(8):2150-2158. doi:10.1182/blood-2011-04-345579

88. Smith KG, Light A, Nossal GJ, Tarlinton DM. The extent of affinity maturation differs between the memory and antibody-forming cell compartments in the primary immune response. *EMBO J*. 1997;16(11):2996-3006. doi:10.1093/emboj/16.11.2996

89. Smith KG, Light A, O'Reilly LA, Ang SM, Strasser A, Tarlinton D. bcl-2 transgene expression inhibits apoptosis in the germinal center and reveals differences in the selection of memory B cells and bone marrow antibody-forming cells. *J Exp Med*. 2000;191(3):475-484. doi:10.1084/jem.191.3.475

90. Wang Y, Shi J, Yan J, et al. Germinal-center development of memory B cells driven by IL-9 from follicular helper T cells. *Nat Immunol*. 2017;18(8):921-930. doi:10.1038/ni.3788

91. Chiu Y-K, Lin I-Y, Su S-T, et al. Transcription factor ABF-1 suppresses plasma cell differentiation but facilitates memory B cell formation. *J Immunol*. 2014;193(5):2207-2217. doi:10.4049/jimmunol.1400411

92. Zuccarino-Catania G V., Sadanand S, Weisel FJ, et al. CD80 and PD-L2 define functionally distinct memory B cell subsets that are independent of antibody isotype. *Nat Immunol*. 2014;15(7):631-637. doi:10.1038/ni.2914

93. Laidlaw BJ, Duan L, Xu Y, Vazquez SE, Cyster JG. The transcription factor Hhex cooperates with the corepressor Tle3 to promote memory B cell development. *Nat Immunol*. 2020;21(9):1082-1093. doi:10.1038/s41590-020-0713-6

94. Tunyaplin C, Shaffer AL, Angelin-Duclos CD, Yu X, Staudt LM, Calame KL. Direct repression of prdm1 by Bcl-6 inhibits plasmacytic differentiation. *J Immunol*. 2004;173(2):1158-1165. doi:10.4049/jimmunol.173.2.1158

95. Scheeren FA, Naspetti M, Diehl S, et al. STAT5 regulates the self-renewal capacity and differentiation of human memory B cells and controls Bcl-6 expression. *Nat Immunol*. 2005;6(3):303-313. doi:10.1038/ni1172

96. Zotos D, Coquet JM, Zhang Y, et al. IL-21 regulates germinal center B cell differentiation and proliferation through a B cell-intrinsic mechanism. *J Exp Med*. 2010;207(2):365-378. doi:10.1084/jem.20091777

97. Inoue T, Shinnakasu R, Kawai C, et al. Exit from germinal center to become quiescent memory B cells depends on metabolic reprograming and provision of a survival signal. *J Exp Med*. 2021;218(1). doi:10.1084/jem.20200866

98. Weisel NM, Joachim SM, Smita S, et al. Surface phenotypes of naive and memory B cells in mouse and human tissues. *Nat Immunol*. 2022;23(1):135-145. doi:10.1038/s41590-021-01078-x

99. Sanz I, Wei C, Jenks SA, et al. Challenges and opportunities for consistent classification of human b cell and plasma cell populations. *Front Immunol*. 2019;10(OCT):1-17. doi:10.3389/fimmu.2019.02458

100. Wei C, Anolik J, Cappione A, et al. A New Population of Cells Lacking Expression of CD27 Represents a Notable Component of the B Cell Memory Compartment in Systemic Lupus Erythematosus. *J Immunol*. 2007;178(10):6624-6633. doi:10.4049/jimmunol.178.10.6624

101. Moir S, Ho J, Malaspina A, et al. Evidence for HIV-associated B cell exhaustion in a dysfunctional memory B cell compartment in HIV-infected viremic individuals. *J Exp Med*. 2008;205(8):1797-1805. doi:10.1084/jem.20072683

102. Sanz I, Wei C, Lee FEH, Anolik J. Phenotypic and functional heterogeneity of human memory B cells. *Semin Immunol*. 2008;20(1):67-82. doi:10.1016/j.smim.2007.12.006

103. Della Valle L, Dohmen SE, Verhagen OJHM, Berkowska MA, Vidarsson G, Ellen van der Schoot C. The Majority of Human Memory B Cells Recognizing RhD and Tetanus Resides in IgM + B Cells . *J Immunol*. 2014;193(3):1071-1079. doi:10.4049/jimmunol.1400706

104. Elgueta R, Marks E, Nowak E, et al. CCR6-dependent positioning of memory B cells is essential for their ability to mount a recall response to antigen. *J Immunol*. 2015;194(2):505-513. doi:10.4049/jimmunol.1401553

105. Di Niro R, Lee S-J, Vander Heiden JA, et al. Salmonella Infection Drives Promiscuous B Cell Activation Followed by Extrafollicular Affinity Maturation. *Immunity*. 2015;43(1):120-131. doi:10.1016/j.immuni.2015.06.013

106. Schröder AE, Greiner A, Seyfert C, Berek C. Differentiation of B cells in the nonlymphoid tissue of the synovial membrane of patients with rheumatoid arthritis. *Proc Natl Acad Sci U S A*. 1996;93(1):221-225. doi:10.1073/pnas.93.1.221

107. Nzula S, Going JJ, Stott DI. Antigen-driven clonal proliferation, somatic hypermutation, and selection of B lymphocytes infiltrating human ductal breast carcinomas. *Cancer Res*. 2003;63(12):3275-3280.

108. Heise N, De Silva NS, Silva K, et al. Germinal center B cell maintenance and differentiation are controlled by distinct NF-κB transcription factor subunits. *J Exp Med*. 2014;211(10):2103-2118. doi:10.1084/jem.20132613

109. Carotta S, Willis SN, Hasbold J, et al. The transcription factors IRF8 and PU.1 negatively regulate plasma cell differentiation. *J Exp Med*. 2014;211(11):2169-2181. doi:10.1084/jem.20140425

110. Saito M, Gao J, Basso K, et al. A signaling pathway mediating downregulation of BCL6 in germinal center B cells is blocked by BCL6 gene alterations in B cell lymphoma. *Cancer Cell*. 2007;12(3):280-292. doi:10.1016/j.ccr.2007.08.011

111. Klein U, Casola S, Cattoretti G, et al. Transcription factor IRF4 controls plasma cell differentiation and class-switch recombination. *Nat Immunol*. 2006;7(7):773-782. doi:10.1038/ni1357

112. Sciammas R, Shaffer AL, Schatz JH, Zhao H, Staudt LM, Singh H. Graded expression of interferon regulatory factor-4 coordinates isotype switching with plasma cell differentiation. *Immunity*. 2006;25(2):225-236. doi:10.1016/j.immuni.2006.07.009

113. Tellier J, Nutt SL. Plasma cells: The programming of an antibody-secreting machine. *Eur J Immunol*. 2019;49(1):30-37. doi:10.1002/eji.201847517

114. Nutt SL, Hodgkin PD, Tarlinton DM, Corcoran LM. The generation of antibody-secreting plasma cells. *Nat Rev Immunol*. 2015;15(3):160-171. doi:10.1038/nri3795

115. Ding BB, Bi E, Chen H, Yu JJ, Ye BH. IL-21 and CD40L Synergistically Promote Plasma Cell Differentiation through Upregulation of Blimp-1 in Human B Cells. *J Immunol*. 2013;190(4):1827-1836. doi:10.4049/jimmunol.1201678

116. Maverakis E, Kim K, Shimoda M, et al. Glycans in the immune system and The Altered Glycan Theory of Autoimmunity: a critical review. *J Autoimmun*. 2015;57:1-13. doi:10.1016/j.jaut.2014.12.002

117. Giovannone N, Antonopoulos A, Liang J, et al. Human B Cell Differentiation Is Characterized by Progressive Remodeling of O-Linked Glycans. *Front Immunol*. 2018;9:2857. doi:10.3389/fimmu.2018.02857

118. Rose ML, Malchiodi F. Binding of peanut lectin to thymic cortex and germinal centres of lymphoid tissue. *Immunology*. 1981;42(4):583-591.

119. Mesin L, Ersching J, Victora GD. Germinal Center B Cell Dynamics. *Immunity*. 2016;45(3):471-482. doi:10.1016/j.immuni.2016.09.001

120. Koethe S, Zander L, Koster S, et al. Pivotal Advance: CD45RB glycosylation is specifically regulated during human peripheral B cell differentiation. *J Leukoc Biol*. 2011;90(1):5-19. doi:10.1189/jlb.0710404

121. Jackson SM, Harp N, Patel D, et al. Key developmental transitions in human germinal center B cells are revealed by differential CD45RB expression. *Blood*. 2009;113(17):3999-4007. doi:10.1182/blood-2008-03-145979

122. Bleesing JJH, Fleisher TA. Human B cells express a CD45 isoform that is similar to murine B220 and is downregulated with acquisition of the memory B-cell marker CD27. *Cytometry B Clin Cytom*. 2003;51(1):1-8. doi:10.1002/cyto.b.10007

123. Rodig SJ, Shahsafaei A, Li B, Dorfman DM. The CD45 isoform B220 identifies select subsets of human B cells and B-cell lymphoproliferative disorders. *Hum Pathol*. 2005;36(1):51-57. doi:10.1016/j.humpath.2004.10.016

124. Giovannone N, Liang J, Antonopoulos A, et al. Galectin-9 suppresses B cell receptor signaling and is regulated by I-branching of N-glycans. *Nat Commun*. 2018;9(1):3287. doi:10.1038/s41467-018-05770-9

125. Coughlin S, Noviski M, Mueller JL, et al. An extracatalytic function of CD45 in B cells is mediated by CD22. *Proc Natl Acad Sci U S A*. 2015;112(47):E6515-24. doi:10.1073/pnas.1519925112

126. Schroeder HWJ, Cavacini L. Structure and function of immunoglobulins. *J Allergy Clin Immunol*. 2010;125(2 Suppl 2):S41-52. doi:10.1016/j.jaci.2009.09.046

127. Xu JL, Davis MM. Diversity in the CDR3 Region of V H Is Sufficient for Most Antibody Specificities. *Immunity*. 2000;13(1):37-45.

128. Pène J, Gauchat J-F, Lécart S, et al. Cutting edge: IL-21 is a switch factor for the production of IgG1 and IgG3 by human B cells. *J Immunol*. 2004;172(9):5154-5157. doi:10.4049/jimmunol.172.9.5154

129. Punnonen J, Aversa G, Cocks BG, et al. Interleukin 13 induces interleukin 4-independent IgG4 and IgE synthesis and CD23 expression by human B cells. *Proc Natl Acad Sci U S A*. 1993;90(8):3730-3734. doi:10.1073/pnas.90.8.3730

130. Zan H, Cerutti A, Dramitinos P, Schaffer A, Casali P. CD40 engagement triggers switching to IgA1 and IgA2 in human B cells through induction of endogenous TGF-beta: evidence for TGF-beta but not IL-10-dependent direct S mu-->S alpha and sequential S mu-->S gamma, S gamma-->S alpha DNA recombination. *J Immunol*. 1998;161(10):5217-5225.

131. Vidarsson G, Dekkers G, Rispens T. IgG subclasses and allotypes: from structure to effector functions. *Front Immunol*. 2014;5:520. doi:10.3389/fimmu.2014.00520

132. Woof JM, Kerr MA. The function of immunoglobulin A in immunity. *J Pathol*. 2006;208(2):270-282. doi:10.1002/path.1877

133. Wade-Vallance AK, Allen CDC. Intrinsic and extrinsic regulation of IgE B cell responses. *Curr Opin Immunol*. 2021;72:221-229. doi:10.1016/j.coi.2021.06.005

134. Gutzeit C, Chen K, Cerutti A. The enigmatic function of IgD: some answers at last. *Eur J Immunol*. 2018;48(7):1101-1113. doi:10.1002/eji.201646547

135. Shan M, Carrillo J, Yeste A, et al. Secreted IgD Amplifies Humoral T Helper 2 Cell Responses by Binding Basophils via Galectin-9 and CD44. *Immunity*. 2018;49(4):709-724.e8. doi:10.1016/j.immuni.2018.08.013

136. Merrell KT, Benschop RJ, Gauld SB, et al. Identification of Anergic B Cells within a Wild-Type Repertoire. *Immunity*. 2006;25(6):953-962. doi:10.1016/j.immuni.2006.10.017

137. Wardemann H, Yurasov S, Schaefer A, Young JW, Meffre E, Nussenzweig MC. Predominant autoantibody production by early human B cell precursors. *Science (80-)*. 2003;301(5638):1374-1377. doi:10.1126/science.1086907

138. Duty JA, Szodoray P, Zheng NY, et al. Functional anergy in a subpopulation of naive B cells from healthy humans that express autoreactive immunoglobulin receptors. *J Exp Med*. 2009;206(1):139-151. doi:10.1084/jem.20080611

139. Quách TD, Manjarrez-Orduño N, Adlowitz DG, et al. Anergic responses characterize a large fraction of human autoreactive naive B cells expressing low levels of surface IgM. *J Immunol*. 2011;186(8):4640-4648. doi:10.4049/jimmunol.1001946

140. Ben Mkaddem S, Rossato E, Heming N, Monteiro RC. Anti-inflammatory role of the IgA Fc receptor (CD89): from autoimmunity to therapeutic perspectives. *Autoimmun Rev*. 2013;12(6):666-669. doi:10.1016/j.autrev.2012.10.011

141. Mankarious S, Lee M, Fischer S, et al. The half-lives of IgG subclasses and specific antibodies in patients with primary immunodeficiency who are receiving intravenously administered immunoglobulin. *J Lab Clin Med*. 1988;112(5):634-640.

142. Roopenian DC, Akilesh S. FcRn: the neonatal Fc receptor comes of age. *Nat Rev Immunol*. 2007;7(9):715-725. doi:10.1038/nri2155

143. Ferrante A, Beard LJ, Feldman RG. IgG subclass distribution of antibodies to bacterial and viral antigens. *Pediatr Infect Dis J*. 1990;9(8 Suppl):S16-24.

144. Ryazantsev S, Tischenko V, Nguyen C, Abramov V, Zav'yalov V. Three-dimensional structure of the human myeloma IgG2. *PLoS One*. 2013;8(6):e64076. doi:10.1371/journal.pone.0064076

145. Michaelsen TE, Garred P, Aase A. Human IgG subclass pattern of inducing complement-mediated cytolysis depends on antigen concentration and to a lesser extent on epitope patchiness, antibody affinity and complement concentration. *Eur J Immunol*. 1991;21(1):11-16. doi:10.1002/eji.1830210103

146. Garred P, Michaelsen TE, Aase A. The IgG subclass pattern of complement activation depends on epitope density and antibody and complement concentration. *Scand J Immunol*. 1989;30(3):379-382. doi:10.1111/j.1365-3083.1989.tb01225.x

147. Brezski RJ, Jordan RE. Cleavage of IgGs by proteases associated with invasive diseases: an evasion tactic against host immunity? *MAbs*. 2010;2(3):212-220. doi:10.4161/mabs.2.3.11780

148. Damelang T, Rogerson SJ, Kent SJ, Chung AW. Role of IgG3 in Infectious Diseases. *Trends Immunol*. 2019;40(3):197-211. doi:10.1016/j.it.2019.01.005

149. Giuntini S, Granoff DM, Beernink PT, Ihle O, Bratlie D, Michaelsen TE. Human IgG1, IgG3, and IgG3 Hinge-Truncated Mutants Show Different Protection Capabilities against Meningococci Depending on the Target Antigen and Epitope Specificity. *Clin Vaccine Immunol*. 2016;23(8):698-706. doi:10.1128/CVI.00193-16

150. Richards JS, Stanisic DI, Fowkes FJI, et al. Association between naturally acquired antibodies to erythrocyte-binding antigens of Plasmodium falciparum and protection from malaria and high-density parasitemia. *Clin Infect Dis an Off Publ Infect Dis Soc Am*. 2010;51(8):e50-60. doi:10.1086/656413

151. Roussilhon C, Oeuvray C, Müller-Graf C, et al. Long-term clinical protection from falciparum malaria is strongly associated with IgG3 antibodies to merozoite surface protein 3. *PLoS Med*. 2007;4(11):e320. doi:10.1371/journal.pmed.0040320

152. Brezski RJ, Knight DM, Jordan RE. The Origins, Specificity, and Potential Biological Relevance of Human Anti-IgG Hinge Autoantibodies. *Sci World J*. 2011;11:1153-1167. doi:10.1100/tsw.2011.107

153. Bruhns P, Iannascoli B, England P, et al. Specificity and affinity of human Fcgamma receptors and their polymorphic variants for human IgG subclasses. *Blood*. 2009;113(16):3716-3725. doi:10.1182/blood-2008-09-179754

154. van der Zee JS, van Swieten P, Aalberse RC. Inhibition of complement activation by IgG4 antibodies. *Clin Exp Immunol*. 1986;64(2):415-422.

155. van der Neut Kolfschoten, Marijn Schuurman J, Losen M, Bleeker WK, et al. Anti-Inflammatory Activity of Human IgG4 Antibodies by Dynamic Fab Arm Exchange. *Sciene*. 2007;317(September):1554-1558.

156. Lighaam LC, Rispens T. The Immunobiology of Immunoglobulin G4. *Semin Liver Dis*. 2016;36(3):200-215. doi:10.1055/s-0036-1584322

157. Aalberse ROBC, Schuurman J. 2002_Immunology_IgG4 breaking the rules.pdf. Published online 2002.

158. Hussain R, Poindexter RW, Ottesen EA. Control of allergic reactivity in human filariasis. Predominant localization of blocking antibody to the IgG4 subclass. *J Immunol*. 1992;148(9):2731-2737.

159. Jutel M, Jaeger L, Suck R, Meyer H, Fiebig H, Cromwell O. Allergen-specific immunotherapy with recombinant grass pollen allergens. *J Allergy Clin Immunol*. 2005;116(3):608-613. doi:10.1016/j.jaci.2005.06.004

160. Aalberse RC, Dieges PH, Knul-Bretlova V, Vooren P, Aalbers M, van Leeuwen J. IgG4 as a blocking antibody. *Clin Rev Allergy*. 1983;1(2):289-302. doi:10.1007/BF02991163

161. Liang H-E, Reinhardt RL, Bando JK, Sullivan BM, Ho I-C, Locksley RM. Divergent expression patterns of IL-4 and IL-13 define unique functions in allergic immunity. *Nat Immunol*. 2011;13(1):58-66. doi:10.1038/ni.2182

162. Kubo M. The role of IL-4 derived from follicular helper T (TFH) cells and type 2 helper T (TH2) cells. *Int Immunol*. 2021;33(12):717-722. doi:10.1093/intimm/dxab080

163. Jutel M, Akdis CA. Immunological mechanisms of allergen-specific immunotherapy. *Allergy*. 2011;66(6):725-732. doi:10.1111/j.1398-9995.2011.02589.x

164. McSorley HJ, Maizels RM. Helminth infections and host immune regulation. *Clin Microbiol Rev*. 2012;25(4):585-608. doi:10.1128/CMR.05040-11

165. Huijbers MG, Plomp JJ, van der Maarel SM, Verschuuren JJ. IgG4-mediated autoimmune diseases: a niche of antibody-mediated disorders. *Ann N Y Acad Sci*. 2018;1413(1):92-103. doi:10.1111/nyas.13561

166. Davies JM, Platts-Mills TA, Aalberse RC. The enigma of IgE+ B-cell memory in human subjects. *J Allergy Clin Immunol*. 2013;131(4):972-976. doi:10.1016/j.jaci.2012.12.1569

167. Harada Y, Tanaka S, Motomura Y, et al. The 3' enhancer CNS2 is a critical regulator of interleukin-4-mediated humoral immunity in follicular helper T cells. *Immunity*. 2012;36(2):188-200. doi:10.1016/j.immuni.2012.02.002

168. Mukai K, Tsai M, Starkl P, Marichal T, Galli SJ. IgE and mast cells in host defense against parasites and venoms. *Semin Immunopathol*. 2016;38(5):581-603. doi:10.1007/s00281-016-0565-1

169. Sutton BJ, Davies AM, Bax HJ, Karagiannis SN. IgE Antibodies: From Structure to Function and Clinical Translation. *Antibodies (Basel, Switzerland)*. 2019;8(1). doi:10.3390/antib8010019

170. Fichtner ML, Vieni C, Redler RL, et al. Affinity maturation is required for pathogenic monovalent IgG4 autoantibody development in myasthenia gravis. *J Exp Med*. 2020;217(12). doi:10.1084/JEM.20200513

171. Catrina A, Krishnamurthy A, Rethi B. Current view on the pathogenic role of anti-citrullinated protein antibodies in rheumatoid arthritis. *RMD open*. 2021;7(1). doi:10.1136/rmdopen-2020-001228

172. Hacker MK, Janson M, Fairley JA, Lin M-S. Isotypes and antigenic profiles of pemphigus foliaceus and pemphigus vulgaris autoantibodies. *Clin Immunol*. 2002;105(1):64-74. doi:10.1006/clim.2002.5259

173. Pos W, Luken BM, Sorvillo N, Kremer Hovinga JA, Voorberg J. Humoral immune response to ADAMTS13 in acquired thrombotic thrombocytopenic purpura. *J Thromb Haemost*. 2011;9(7):1285-1291. doi:10.1111/j.1538-7836.2011.04307.x

174. Berentsen S, Sundic T. Red blood cell destruction in autoimmune hemolytic anemia: role of complement and potential new targets for therapy. *Biomed Res Int*. 2015;2015:363278. doi:10.1155/2015/363278

175. Ruocco V, Ruocco E, Lo Schiavo A, Brunetti G, Guerrera LP, Wolf R. Pemphigus: Etiology, pathogenesis, and inducing or triggering factors: Facts and controversies. *Clin Dermatol*. 2013;31(4):374-381. doi:10.1016/j.clindermatol.2013.01.004

176. Huijbers MG, Vink A-FD, Niks EH, et al. Longitudinal epitope mapping in MuSK myasthenia gravis: implications for disease severity. *J Neuroimmunol*. 2016;291:82-88. doi:10.1016/j.jneuroim.2015.12.016

177. Steiner G, Smolen J. Autoantibodies in rheumatoid arthritis and their clinical significance. *Arthritis Res*. 2002;4 Suppl 2(Suppl 2):S1-5. doi:10.1186/ar551

178. Prüßmann W, Prüßmann J, Koga H, et al. Prevalence of pemphigus and pemphigoid autoantibodies in the general population. *Orphanet J Rare Dis*. 2015;10(1):1-8. doi:10.1186/s13023-015-0278-x

179. Damoiseaux J, Andrade LE, Fritzler MJ, Shoenfeld Y. Autoantibodies 2015: From diagnostic biomarkers toward prediction, prognosis and prevention. *Autoimmun Rev*. 2015;14(6):555-563. doi:10.1016/j.autrev.2015.01.017

180. Hafkenscheid L, Bondt A, Scherer HU, et al. Structural analysis of variable domain glycosylation of anti-citrullinated protein antibodies in rheumatoid arthritis reveals the presence of highly sialylated glycans. *Mol Cell Proteomics*. 2017;16(2):278-287. doi:10.1074/mcp.M116.062919

181. Briney B, Inderbitzin A, Joyce C, Burton DR. Commonality despite exceptional diversity in the baseline human antibody repertoire. *Nature*. 2019;566(7744):393-397. doi:10.1038/s41586-019-0879-y

182. Schroeder HWJ. Similarity and divergence in the development and expression of the mouse and human antibody repertoires. *Dev Comp Immunol*. 2006;30(1-2):119-135. doi:10.1016/j.dci.2005.06.006

183. Maverakis E, Kim K, Shimoda M, et al. Glycans In The Immune system and The Altered Glycan Theory of Autoimmunity: A Critical Review. *J Autoimmun*. 2015;(0):1-13. doi:10.1007/978-3-642-16712-6_100386

184. Huber R, Deisenhofer J, Colman PM, Matsushima M, Palm W. Crystallographic structure studies of an IgG molecule and an Fc fragment. *Nature*. 1976;264(5585):415-420. doi:10.1038/264415a0

185. Dekkers G, Rispens T, Vidarsson G. Novel Concepts of Altered Immunoglobulin G Galactosylation in Autoimmune Diseases. *Front Immunol*. 2018;9(March). doi:10.3389/fimmu.2018.00553

186. Wang TT. IgG Fc Glycosylation in Human Immunity. *Curr Top Microbiol Immunol*. 2019;423:63-75. doi:10.1007/82_2019_152

187. van de Bovenkamp FS, Derksen NIL, Ooievaar-de Heer P, et al. Adaptive antibody diversification through N -linked glycosylation of the immunoglobulin variable region. *Proc Natl Acad Sci U S A*. 2018;115(8):1901-1906. doi:10.1073/pnas.1711720115

188. Guhr T, Bloem J, Derksen NIL, et al. Enrichment of sialylated IgG by lectin fractionation does not enhance the efficacy of immunoglobulin G in a murine model of immune thrombocytopenia. *PLoS One*. 2011;6(6):1-8. doi:10.1371/journal.pone.0021246

189. Käsermann F, Boerema DJ, Rüegsegger M, et al. Analysis and functional consequences of increased Fab-sialylation of intravenous immunoglobulin (IVIG) after lectin fractionation. *PLoS One*. 2012;7(6):e37243. doi:10.1371/journal.pone.0037243

190. Stadlmann J, Weber A, Pabst M, et al. A close look at human IgG sialylation and subclass distribution after lectin fractionation. *Proteomics*. 2009;9(17):4143-4153. doi:10.1002/pmic.200800931

191. Anumula KR. Quantitative glycan profiling of normal human plasma derived immunoglobulin and its fragments Fab and Fc. *J Immunol Methods*. 2012;382(1-2):167-176. doi:10.1016/j.jim.2012.05.022

192. Lefranc M. IMGT, the International ImMunoGeneTics Information System. *Cold Spring Harb Protoc*. 2011(6):595-603.

193. Vletter EM, Koning MT, Scherer HU, Veelken H, Toes REM. A Comparison of Immunoglobulin Variable Region N-Linked Glycosylation in Healthy Donors, Autoimmune Disease and Lymphoma. *Front Immunol*. 2020;11(February):1-12. doi:10.3389/fimmu.2020.00241

194. Bondt A, Rombouts Y, Selman MHJ, et al. Immunoglobulin G (IgG) Fab Glycosylation Analysis Using a New Mass Spectrometric High-throughput Profiling Method Reveals Pregnancy-associated Changes. *Mol Cell Proteomics*. 2014;13(11):3029-3039. doi:10.1074/mcp.M114.039537

195. Holland M, Yagi H, Takahashi N, et al. Differential glycosylation of polyclonal IgG, IgG-Fc and IgG-Fab isolated from the sera of patients with ANCA-associated systemic vasculitis. *Biochim Biophys Acta - Gen Subj*. 2006;1760(4):669-677. doi:10.1016/j.bbagen.2005.11.021

196. van de Bovenkamp FS, Derksen NIL, Ooijevaar-de Heer P, Rispens T. The enzymatic removal of immunoglobulin variable domain glycans by different glycosidases. *J Immunol Methods*. 2019;467:58-62. doi:10.1016/j.jim.2019.02.005

197. Bondt A, Wuhrer M, Kuijper TM, Hazes JMW, Dolhain RJEM. Fab glycosylation of immunoglobulin G does not associate with improvement of rheumatoid arthritis during pregnancy. *Arthritis Res Ther*. 2016;18(1):1-6. doi:10.1186/s13075-016-1172-1

198. van de Bovenkamp FS, Hafkenscheid L, Rispens T, Rombouts Y. The Emerging Importance of IgG Fab Glycosylation in Immunity. *J Immunol*. 2016;196(4):1435-1441. doi:10.4049/jimmunol.1502136

199. Wright A, Tao M, Kabat EA, Morrison SL. Antibody variable region glycosylation : position effects on antigen binding and carbohydrate structure. *EMBO*. 1991;10(10):2717-2723.

200. Petrescu AJ, Milac AL, Petrescu SM, Dwek RA, Wormald MR. Statistical analysis of the protein environment of N-glycosylation sites: Implications for occupancy, structure, and folding. *Glycobiology*. 2004;14(2):103-114. doi:10.1093/glycob/cwh008

201. Coloma MJ, Trinh RK, Martinez AR, Morrison SL. Position Effects of Variable Region Carbohydrate on the Affinity and In Vivo Behavior of an Anti-(1 → 6) Dextran Antibody. Published online 2018.

202. Wallick BYSC, Kabat EA, Morrison SL. Glycosylation of a VH residue of a monoclonal antibody against alpha (1----6) dextran increases its affinity for antigen. *JEM*. 1988;168(September):1099-1109.

203. Tachibana H, Kim J, Shirahata S. Building high affinity human antibodies by altering the glycosylation on the light chain variable region in N -acetylglucosamine-supplemented hybridoma cultures. *Cytotechnology*. 1997;23(1-3):151-159.

204. Leibiger H, Wu D, Stigler R, Marx U. Variable domain-linked oligosaccharides of human monoclonal IgG: structure and influence on antigen binding. *Biochem J*. 1999;538:529-538.

205. Schneider D, Dühren-von Minden M, Alkhatib A, et al. Lectins from opportunistic bacteria interact with acquired variable-region glycans of surface immunoglobulin in follicular lymphoma. *Blood*. 2015;125(21):3287-3296. doi:10.1182/blood-2014-11-609404

206. Jacquemin M. Variable region heavy chain glycosylation determines the anticoagulant activity of a factor VIII antibody. *Haemophilia*. 2010;16(102):16-19. doi:10.1111/j.1365-2516.2010.02233.x

207. Goletz, SA, Czyk, D, Stoeckl L. Fab-glycosylated antibodies. Patent WO 2012/020065. Published online 2012.

208. Courtois F, Agrawal NJ, Lauer TM, Trout BL. Rational design of therapeutic mAbs against aggregation through protein engineering and incorporation of glycosylation motifs applied to bevacizumab. *MAbs*. 2016;8(1):99-112. doi:10.1080/19420862.2015.1112477

209. Middaugh CR, Litman GW. Atypical glycosylation of an IgG monoclonal cryoimmunoglobulin. *J Biol Chem*. 1987;262(8):3671-3673.

210. van de Bovenkamp F, Derksen N, van Breemen M, et al. Variable Domain N -linked glycans acquired During antigen-specific immune responses can contribute to immunoglobulin g antibody stability. *Front Immunol*. 2018;9(April):1-9. doi:10.3389/fimmu.2018.00740

211. Khurana S, Raghunathan V, Salunke DM. The variable domain glycosylation in a monoclonal antibody specific to GnRH modulates antigen binding. *Biochem Biophys Res Commun*. 1997;234(2):465-469. doi:10.1006/bbrc.1997.5929

212. Wong KL, Li Z, Ma F, et al. SM03, an Anti-CD22 Antibody, Converts Cis-to-Trans Ligand Binding of CD22 against α2,6-Linked Sialic Acid Glycans and Immunomodulates Systemic Autoimmune Diseases. *J Immunol*. Published online June 2022. doi:10.4049/jimmunol.2100820

213. Coelho V, Krysov S, Ghaemmaghami AM, et al. Glycosylation of surface Ig creates a functional bridge between human follicular lymphoma and microenvironmental lectins. *Proc Natl Acad Sci U S A*. 2010;107(43):18587-18592. doi:10.1073/pnas.1009388107

214. Canellada A, Gentile T, Dokmetjian J, Margni RA, Margni RA. Occurrence, properties, and function of asymmetric IgG molecules isolated from non-immune sera. *Immunol Invest*. 2002;31(2):107-120. doi:10.1081/IMM-120004802

215. Schwab I, Mihai S, Seeling M, Kasperkiewicz M, Ludwig RJ, Nimmerjahn F. Broad requirement for terminal sialic acid residues and FcγRIIB for the preventive and therapeutic activity of intravenous immunoglobulins in vivo. *Eur J Immunol*. 2014;44(5):1444-1453. doi:10.1002/eji.201344230

216. Rombouts Y, Willemze A, Van Beers JJBC, et al. Extensive glycosylation of ACPA-IgG variable domains modulates binding to citrullinated antigens in rheumatoid arthritis. *Ann Rheum Dis*. 2016;75(3):578-585. doi:10.1136/annrheumdis-2014-206598

217. Culver EL, van de Bovenkamp FS, Derksen NIL, et al. Unique patterns of glycosylation in IgG4-related disease and primary sclerosing cholangitis. *J gastroentol Hepatol*. Published online 2018. doi:10.1111/jgh.14512

218. Zhu D, Mccarthy H, Ottensmeier CH, Johnson P, Hamblin TJ, Stevenson FK. Acquisition of potential N-glycosylation sites in the immunoglobulin variable region by somatic mutation is a distinctive feature of follicular lymphoma. 2018;99(7):2562-2569.

219. Koning MT, Quinten E, Zoutman WH, et al. Acquired N-Linked Glycosylation Motifs in B-Cell Receptors of Primary Cutaneous B-Cell Lymphoma and the Normal B-Cell Repertoire. *J Invest Dermatol*. 2019;139(10):2195-2203. doi:10.1016/j.jid.2019.04.005

220. Zhu D, Ottensmeier CH, Du M, Mccarthy H. Incidence of potential glycosylation sites in immunoglobulin variable regions distinguishes between subsets of Burkitt ' s lymphoma and mucosa-associated lymphoid tissue lymphoma. 2003;22:217-222.

221. Sachen KL, Strohman MJ, Singletary J, et al. Self-antigen recognition by follicular lymphoma B-cell receptors. *Blood*. 2012;120(20):4182-4190. doi:10.1182/blood-2012-05-427534

222. McCann KJ, Ottensmeier CH, Callard A, et al. Remarkable selective glycosylation of the immunoglobulin variable region in follicular lymphoma. *Mol Immunol*. 2008;45(6):1567-1572. doi:10.1016/j.molimm.2007.10.009

223. Radcliffe CM, Arnold JN, Suter DM, et al. Human follicular lymphoma cells contain oligomannose glycans in the antigen-binding site of the B-cell receptor. *J Biol Chem*. 2007;282(10):7405-7415. doi:10.1074/jbc.M602690200

224. Amin R, Mourcin F, Uhel F, et al. DC-SIGN-expressing macrophages trigger activation of mannosylated IgM B-cell receptor in follicular lymphoma. *Blood*. 2015;126(16):1911-1920. doi:10.1182/blood-2015-04-640912

225. Linley A, Krysov S, Ponzoni M, Johnson PW, Packham G, Stevenson FK. Lectin binding to surface Ig variable regions provides a universal persistent activating signal for follicular lymphoma cells. doi:10.1182/blood-2015-04-640805

CHAPTER 2

Improving naive B cell isolation by absence of CD45RB glycosylation and CD27 expression in combination with BCR isotype

Jana Koers*, Sabrina Pollastro*, Simon Tol, Ilse T.G. Niewold, Pauline A. van Schouwenburg, Niek de Vries and Theo Rispens
*These authors contributed equally

Published in the European Journal of Immunology (2022)

ABSTRACT

In past years *ex vivo* and *in vivo* experimental approaches involving human naive B cells have proven fundamental for elucidation of mechanisms promoting B cell differentiation in both health and disease. For such studies, it is paramount that isolation strategies yield a population of bona fide naive B cells, i.e., B cells that are phenotypically and functionally naive, clonally non-expanded and have non-mutated B cell receptor (BCR) variable regions. In this study different combinations of common as well as recently identified B cell markers were compared to isolate naive B cells from human peripheral blood. High-throughput BCR sequencing was performed to analyze levels of somatic hypermutation and clonal expansion. Additionally, contamination from mature mutated B cells intrinsic to each cell-sorting strategy was evaluated and how this impacts the purity of obtained populations. Our results show that current naive B cell isolation strategies harbor contamination from non-naive B cells, and use of $CD27^{-}IgD^{+}$ is adequate but can be improved by including markers for CD45RB glycosylation and IgM. The finetuning of naive B cell classification provided herein will harmonize research lines using naive B cells, and will improve B cell profiling during health and disease, e.g. during diagnosis, treatment and vaccination strategies.

INTRODUCTION

Naive B cells are the basis of humoral immunity. After differentiation in the bone marrow, resting naive B cells start to circulate in peripheral blood where they can become activated upon antigen encounter and directly differentiate into low-affinity antibody secreting cells (ASCs), or mature within germinal centers (GC) into memory B cells and high-affinity ASCs expressing B cell receptors (BCRs) of different isotypes[1–3].

Commonly, the isolation of naive B cell from peripheral blood for further *in vitro* functional characterization relies on few phenotypic surface markers, among which absence of CD27 and presence of IgD is most frequently used[4–6]. Co-stimulatory molecule CD27, a member of the TNF-receptor superfamily, is constitutively expressed on 20-40% of peripheral blood B cells[7] and is associated with greater cell size[8,9], increased proliferation capacity[10,11], increased antigen presentation[12] and detectible levels of somatic hypermutation[13,14] in the BCRs, all hallmarks of antigen experience. However, approximately 5% of the isotype switched and non-switched B cells in peripheral blood display mutated BCRs in the absence of CD27 expression[9,15–17]. These mutated $CD27^-$ B cells have a different BCR-repertoire, are in a different maturation stage, and respond, like memory B cells, more rapidly to *in vitro* stimulation[8,10,17,18]. Including IgD expression improves isolation of naive B cells, as this excludes most of the mutated $CD27^-$ B cells. IgD is co-expressed with IgM on the B cell surface in defined windows during development, i.e. only after maturation within the spleen. However, a large proportion of $CD27^-IgD^+$ B cells (~30%) have reduced IgM expression, representing a population of anergic B cells that recognize self-antigens. These cells have been observed in autoimmune diseases, e.g. in active SLE[19–23]. Hence, the use of CD27 and IgD alone might not represent the most optimal strategy to isolate bona fide naive B cells, i.e. B cells that are naive from a phenotypical and functional point of view.

In this respect, we and others have recently identified glycosylation of CD45RB, an isoform of CD45, as a novel marker to identify antigen-primed B cells, independent of CD27 and BCR isotype expression[5,17,24–27]. The glycan-dependent CD45RB (RB) epitope can be detected using the mAb MEM-55[24]. This marker in combination with CD27 and BCR isotype, may be useful to better define bona fide naive B cells in humans.

In this study we aimed to define an optimal sorting strategy to isolate bona fide naive B cells. We interrogated eleven cell-sorted naive B cell populations from healthy adult peripheral blood using different combinations of known and new phenotypic markers of naive B cells. We used high-throughput BCR repertoire sequencing to analyze the level of somatic hypermutation and clonal expansion for each sorted population. Here we observed that in many of the commonly used naive B cell sorting strategies contamination occurs of highly mutated B cells, which was inherent to the marker selection for cell-sorting.

Including markers for RB and IgM in combination with CD27 and IgD improved currently used cell-sorting strategies and yielded a population of phenotypical naive B cells with minimal contamination by clonally expanded and/or somatically hypermutated B cells.

MATERIALS AND METHODS

Human B cell isolation

Buffy coats were obtained from anonymized healthy adult donors with written informed consent in accordance to the guidelines established by the Sanquin Medical Ethical Committee and in line with the Declaration of Helsinki. Human peripheral blood mononucleated cells (PBMCs) were isolated from fresh buffy coats (n = 3) using Ficoll gradient centrifugation (lymphoprep; Axis-Shield PoC AS) and CD19+ cells were isolated by positive selection using magnetic Dynabeads (Invitrogen). CD19+ cells were resuspended in B cell culture medium (RPMI medium supplemented with FCS (5%, Bodinco), penicillin (100 U/mL, Invitrogen), streptomycin (100 µg/mL, Invitrogen), β-mercaptoethanol (50 µM, Sigma-Aldrich), L-glutamine (2mM, Invitrogen), human apo-transferrin (20 µg/mL, Sigma-Aldrich) depleted for IgG using protein A sepharose (GE Healthcare) supplemented with 20% DMSO) and stored in liquid nitrogen.

Cell sorting

Cryopreserved CD19+ cells were thawed into B cell culture medium and pelleted for 5min at 300g. Cells were resuspended in PBA (PBS supplemented with 0.1% bovine serum albumin) and surface stained for 30 minutes at 4°C. Singlet viable CD19+ cells were acquired using a lymphocyte gate (FSC-A and SSC-A), single cell gate (SSC-A/SSC-H) and subsequent gating on cells that express CD19 but remain negative in the LIVE/DEAD Fixable Near-IR channel. Singlet viable CD19+ B cells were further separated into eleven subsets based on the expression of a single or multiple markers, including CD27, CD38, CD45RB glycosylation, IgD, IgM, IgG, and IgA. For each subset 105 B cells were cell-sorted (FACS Aria III, BD Biosciences) into RNA LoBind tubes (eppendorf). The gating strategy is provided in **Figure 1A**. Additional technical replicate samples (n = 12) were sorted from the same donors for several S, C and memory subsets (**Figure S2**).

Antibodies

CD19+ cells were surface stained using the following antibodies: anti-CD19 (clone SJ25C1, 562947), anti-CD38 (clone HB7, 646851), anti-IgD (clone IA6, 2561315), anti-IgM (clone G20-127, 562977) from BD Biosciences. Anti-IgG (MH16-1, M1268) from Sanquin Reagents. Anti-IgA (polyclonal, 2050-09) from SouthernBiotech. Anti-CD27 (clone O323, 25-0279-42) from ThermoFisher. Anti-CD45RB (clone MEM-55, 310205) from Biolegend. Each antibody was titrated to optimal staining concentration using PBMCs.

B cell receptor repertoire sequencing

Repertoire amplification was performed as previously described[28]. Briefly, specific complementary DNA (cDNA) of BCR molecules was synthesized using a BCR heavy chain joining gene primer tagged with a 9-nucleotide Unique Molecular Identifier (UMI). After cDNA synthesis an Exonuclease I (Thermo Fisher Scientific) treatment was carried out followed by a multiplexed PCR with 6 primers covering all BCR heavy chain variable genes (primer details are available upon request). Amplified libraries were purified, quantified and sequenced via Illumina Miseq 2 x 300 technology according to the sequencing platform manufacturer's manual (Illumina, San Diego, California, USA).

B cell receptor repertoire dataset construction and mutation analysis

Reads retrieved from the sequencing platform were processed using pRESTO[29]. Low quality reads (phred score < 25) were filtered out using the FilterSeq.py quality function. The MaskPrimers.py function was used to identify and mask the IGHV primers and to cut the sequence after and including the IGHJ primer. UMI-based consensus sequences were created with the max.error parameter of the BuildConsensus.py function set to 0.1 and paired-end reads were assembled using the AssemblePairs.py function. Additional filtering was applied to obtain datasets of unique consensus sequences represented by a minimum of 3 aligned UMIs using IMGT/HighV-QUEST[30]. Aligned sequences were further processed using Change-O[31]. Output of the IMGT/HighV-QUEST was parsed using the MakeDb.py function and only functional rearrangements were selected. Germline sequences were reconstructed using the CreateGermlines.py function. Each unique nucleotide sequence spacing from the IGHV gene to the IGHJ gene was regarded as a BCR. Clonal frequency for each BCR was calculated as the number of different UMIs associated to the BCR divided by the total number of unique UMIs in the sample. The clonal expansion index was calculated as the Gini index on the distribution of the number of unique UMIs per BCR in each sample[32] using the renyi function in the "vegan" R package[33] (version 2.5-6). IGHV and IGHJ gene usage was calculate using the geneUsage function in the "immunarch" R package[34] (version 0.6.5). Analysis of somatic hypermutation (SHM) was performed using the "SHazaM" R package[31] (version 0.2.1) which compared each BCR sequence to its reconstructed germline. Mean SHM counts and median SHM counts were then calculated for each sample as respectively the mean and the median of the mutations distribution carried by each BCR sequence in the sample. For the three analyzed buffy's the observed SHM was calculated as the mean of the three observations. To correct for the percentage of cellular contamination from a contaminating subset C %CX, the corrected mean µ_SX was calculated from the observed mean SHM for each naive subset µ_SX and observed mean SHM for the contaminating population µCX using the following formula:

$$corrected\ \mu_{SX} = \frac{100 * \ observed\ \mu_{SX} - \sum_i (\%_{C_iX} \ * \ \mu_{C_iX})}{100 - \sum_i \%_{C_iX}}$$

Raw sequencing data have been deposited at NCBI Sequence Read Archive (BioProject: PRJNA856112) and processed repertoires are available upon request to the corresponding author.

Statistical analysis

Differences between groups were analyzed using a one-way ANOVA and Tukey's multiple comparison test (each group against every other group). In the comparisons against all S-subsets, all single data points from S-subsets were pooled together and a Kruskal-Wallis test followed by a Dunn's multiple comparison test (each group against pooled S-subsets only) was performed. Correlations were determined using a Spearman rank correlation test. A p value <0.05 was considered significant. The statistical analysis was carried out using GraphPad Prism 9.1.1.

RESULTS

Examination of different cell-sorting strategies to obtain naive B cells from human peripheral blood

We interrogated eleven different strategies to determine an optimal strategy for cell-sorting bona fide naive B cells using a single or multiple B cell identity surface markers, including CD19, CD27, CD38, CD45RB glycosylation (RB), IgM, IgD, IgG and IgA (**Figure 1A**, gating strategy in blue, pre-gating of singlet, viable $CD19^+$ cells in **Figure S1A**). These sorted populations are hereafter regarded as sample (S) subsets (**Figure 1B**). Subsets S1 to S6 are all $CD27^-$ populations, with additional gating for BCR isotype expression. Subsets S7 to S9 are RB^- populations and subsets S10 to S11 are both $CD27^-$ and RB^- with additional BCR isotype gating. Additionally, we sorted five $CD27^-$ or RB^- populations expected to harbor non-naive B cells that could potentially contaminate the S-subsets and were therefore designated contaminating (C) subsets (**Figure 1A**, gating strategy in light pink). Subsets C1 and C2 represent isotype-switched or IgM^+IgD^- $CD27^-$ B cells that have previously been described to carry mutated BCRs and are functionally distinct from naive B cells[13,35,36]. Subset C3 represents $IgMD^+RB^+$ B cells for which we have recently shown that these cells still have low mutations levels but are functionally distinct from $IgMD^+RB^-$ cells[17], while subset C4 represents $CD38^+$ activated naive B cells. Finally, subset C5 represents B cells that are $CD27^+$ but RB^- with previously reported high mutation levels[5]. $CD27^+IgM^+$ (IgMmem) and $CD27^+IgG/IgA^+$ (Smem) B cells were sorted as control populations, representing antigen-experienced memory B cell populations characterized by mutated BCRs (**Figure 1A**, gating strategy in dark pink). Classification strategy and frequency within $CD19^+$ cells are reported for each population (**Figure 1B**). For each subset 10^5 cells were sorted from peripheral blood of healthy adult donors (n = 3) and next-generation sequencing of the immunoglobulin heavy chain variable (IGHV) genes

and VDJ-junction, followed by BCR repertoire analysis was performed (**Figure 1C**). For each cell-sorted subset the efficiency of sequencing and the number of obtained sequences are provided (**Figure S1B and C**). Additional technical replicate samples were sorted for several S, C, and memory subsets and their comparison is reported in **Figure S2**.

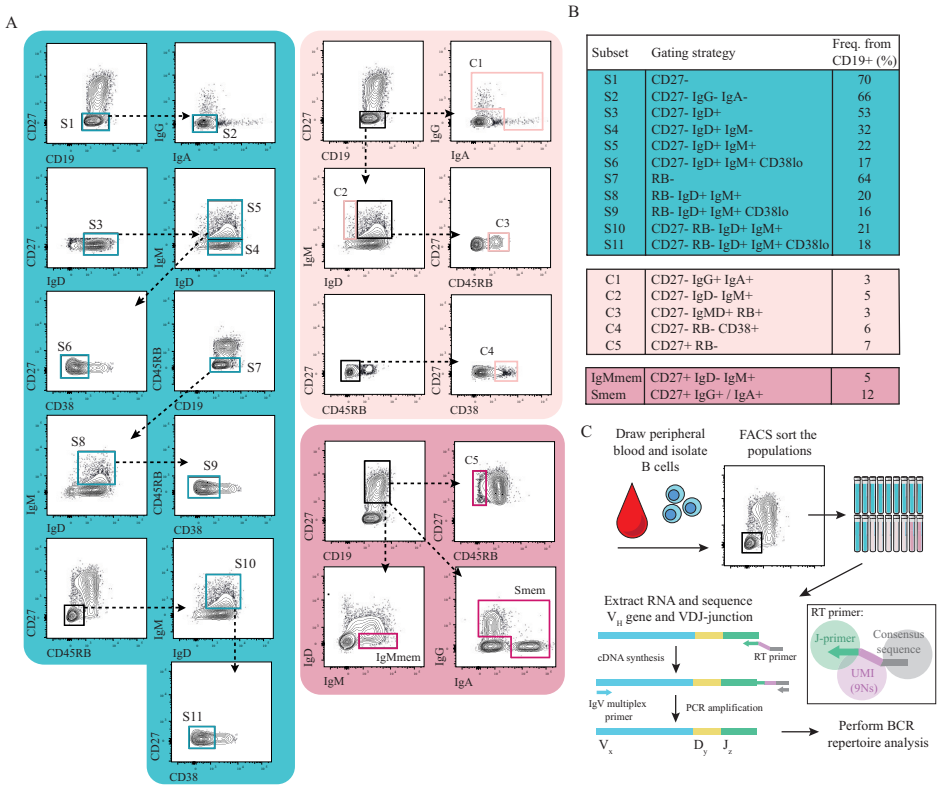

Subset	Gating strategy	Freq. from CD19+ (%)
S1	CD27-	70
S2	CD27- IgG- IgA-	66
S3	CD27- IgD+	53
S4	CD27- IgD+ IgM-	32
S5	CD27- IgD+ IgM+	22
S6	CD27- IgD+ IgM+ CD38lo	17
S7	RB-	64
S8	RB- IgD+ IgM+	20
S9	RB- IgD+ IgM+ CD38lo	16
S10	CD27- RB- IgD+ IgM+	21
S11	CD27- RB- IgD+ IgM+ CD38lo	18
C1	CD27- IgG+ IgA+	3
C2	CD27- IgD- IgM+	5
C3	CD27- IgMD+ RB+	3
C4	CD27- RB- CD38+	6
C5	CD27+ RB-	7
IgMmem	CD27+ IgD- IgM+	5
Smem	CD27+ IgG+ / IgA+	12

Figure 1. Overview of FACS cell-sorting and BCR repertoire strategies for obtaining naive B cells from human peripheral blood. *(A) Representative gating strategy for sorting sample (S), contaminating (C), and memory B cell subsets from healthy adult donor peripheral blood by flow cytometry. Pre-gating of singlet, viable CD19⁺ cells in **Figure S1A**. (B) Table shows the classification and frequency of studied subsets within CD19⁺ cells for three biological replicates in one independent experiment. (C) Experimental overview (n = 3). The reproducibility was shown by using several technical replicate samples for each donors presented in **Figure S2**.*

Repertoire analysis in cell-sorted B cell subsets

The BCR repertoire of the different cell-sorted subsets was analyzed to compare the level of somatic hypermutation and clonal expansion. First, we performed in-depth analysis of the somatic hypermutation levels (**Figure 2A-D**). No significant differences were observed in the mean mutation counts among S-subsets, where values ranged from 0.66 ± 0.06 (mean ± s.d.) for S10 to 1.40 ± 0.48 for S7 (**Figure 2A** for mean and **Figure S3A** for median mutation

counts). Among C-subsets, only C1 and C5 showed significantly higher mean mutation counts compared to S-subsets (C1: 8.80 ± 2.14, C5: 13.4 ± 4.07, mean ± s.d., p-value ≤0.05 for C1 and p-value ≤0.01 for C5 versus pooled S-subsets). As expected, IgMmem and Smem both displayed significantly higher mutation counts compared to all S-subsets (IgMem: 9.66 ± 0.89, Smem: 15.1 ± 2.93, mean ± s.d., p-value ≤0.05 for IgMem and p-value ≤0.01 for Smem versus pooled S-subsets). Next, we analyzed the percentage of non-mutated BCRs present in each subset (**Figure 2B**). No significant differences were observed among S-subsets and C3 and C4 (average S-subsets: 75.2% ± 3.9%, C3: 59.3% ± 4.7%, C4: 74.0%

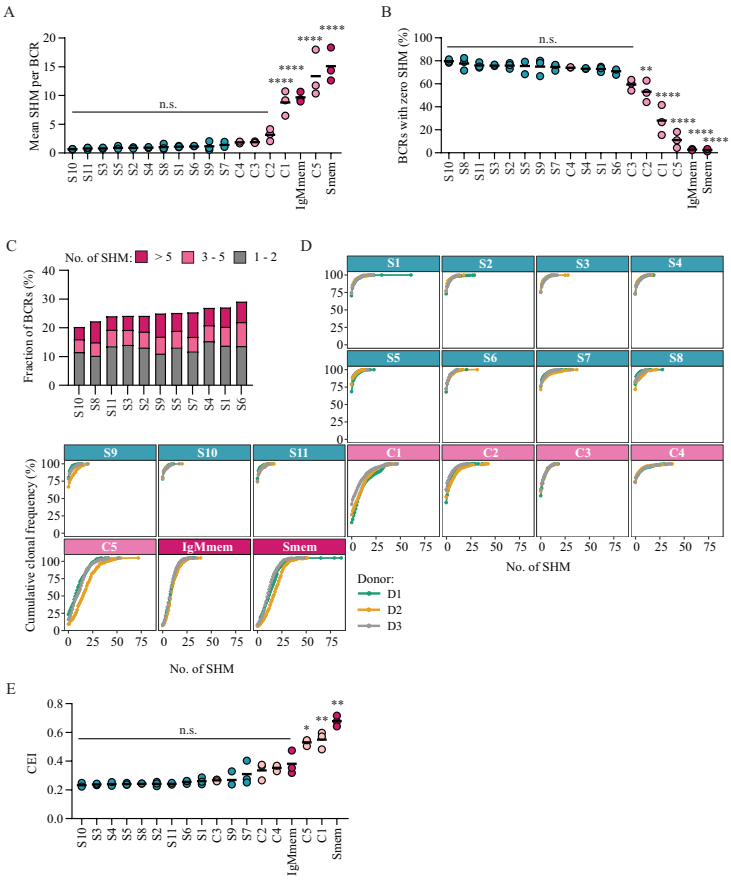

Figure 2. Analysis of somatic hypermutation (SHM) and clonal expansion in cell-sorted subsets. *(**A**) Mean SHM per BCR and (**B**) percentage of BCRs with zero SHM in the BCR repertoire of cell-sorted B cell subsets from healthy donor peripheral blood. (**C**) Fraction of repertoire consisting of BCRs with 1 or 2, 3 to 5 or more than 5 mutations (expressed as percentage of total BCRs). Statistical differences were determined using a Kruskal-Wallis with a Dunn's multiple comparison test. *p < 0.05, **p < 0.01, ****p < 0.0001, n.s. = not significant. (**D**) Cumulative frequency distribution of mutations in the BCR repertoire for S, C and memory subsets. Different colors represent different donors. (**E**) Clonal expansion index (CEI). Data displays three biological replicates in one independent experiment. The reproducibility was shown by using several technical replicate samples for each donors presented in **Figure S2**. Single dots represent single donors, black lines depict means and subsets are ordered by increasing (A and C) or decreasing (B) mean.*

± 0.5%, mean ± s.d.). However, C1, C2, and C5 showed a significantly lower percentage of non-mutated BCRs compared to S-subsets (C1: 28.0% ± 13.1%, C2: 53.1% ± 9.4%, C5: 11.2% ± 7.0, mean ± s.d., p-value ≤0.05versus pooled S-subsets). Of note, C5 showed very similar values compared IgMmem and Smem (IgMmem: 2.8% ± 0.5%, Smem: 2.4% ± 1.1%, mean ± s.d., p-value = n.s. versus C5). When focusing on mutated BCRs found in S-subsets, we observed that on average 12.9% of the repertoire was composed of BCRs with 1 or 2 mutations (**Figure 2C**, grey bars). Surprisingly, also highly mutated BCRs with more than 5 mutations could be detected (average BCRs with >5 SHM in S-subsets: 6.3%, dark pink bars). The overall impact on the repertoire of non-mutated and mutated BCRs for each sorted subset is reported in **Figure 2D**. Next, we evaluated the level of clonal expansion by the use of the clonal expansion index (CEI) and again observed no significant differences among the S-subsets, and a significant increase in clonal expansion only in the C-subsets C1 and C5 compared to the S-subsets (C1: 0.55 ± 0.06, C5: 0.53 ± 0.02, mean ± s.d., p-value ≤0.001 for C1 and p ≤0.05 for C5 versus pooled S-subsets; **Figure 2E**). However, a significant correlation was observed between the level of somatic hypermutation and clonal expansion in the analyzed S-subset (**Figure S3B**) and S7, S9, S6 and S1 showed both the highest mean mutations count and the highest clonal expansion index among all S-subsets. Correlation between mutation counts and clonal expansion at single BCR level for all sorted subsets is reported in **Figure S3C**. Additional BCR repertoire parameters such as average CDR3 length (**Figure S3D**) and IGHV and IGHJ gene usage (**Figure S3E and F**) did not show large differences among S-subsets. In conclusion, subtle differences were observed between mean mutation counts, the frequency of non-mutated BCRs and the clonal expansion index among S-subsets. Among the contaminating subsets, C1 and C5 showed the most substantial and significant differences from S-subsets indicating that these populations do in fact contain relevant hypermutated and clonal expanded BCRs that can potentially contaminate S-subsets.

Analysis of the contamination level by C-subsets in S-subsets

The analysis of the BCR repertoire in the different S-subsets revealed subtle differences among tested cell-sorting strategies, based on which it would be difficult to decide on an outcompeting strategy. However, we did observe that some of the C-subsets do in fact carry more mutated and expanded BCRs compared to S-subset and that BCRs with more than 5 mutations were detected with variable levels in all S-subsets. Hence, the level of C-subset contamination, inherent to each specific cell-sorting strategy, could likely affect the purity of the obtained naive B cell population, thus playing an additionally role in the decision for the best isolation strategy for bona fide naive B cells. To test this, we first determined the percentage of cells coming from C-subsets present in each S-subset by flow cytometry (**Figure 3A**). Among the highly mutated contaminating subsets, C1 was found back in all but one S-subset, S2, while C5 was found in only three S-subsets, S7, S8 and S9. To evaluate the impact of contamination by C-cells on S-subset mutation levels, we corrected the mean

mutation count of each S-subsets by subtracting the weighted mean mutation count of each C-subset that is present (**Figure 3B**). S7, S8 and S9 showed major correction of their mean mutation counts most likely due to the high percentage of highly mutated C5 cells present in these subsets. Accordingly, these three subsets also showed the highest percentage highly mutated BCRs (SHM >5) within their repertoire among S-subsets (**Figure 3C**). On the contrary, subsets S4, S10 and S11 showed only minor corrections of their mean mutation count. In these subsets the contaminating populations were only the virtually non-mutated C4 and a low frequency of highly mutated C1 (~1%). S10 and S11 also showed the lowest percentage of highly mutated BCRs. For S-subsets S1, S2, S3, S5 and S6 which showed various level of contamination by C-subsets intermediate correction of their mean mutation count was observed. Overall, there was a correlation between the percentage contamination from mutated C1 and C5 cells and the percentage of highly mutated BCRs found in S-subset (**Figure 3D**, r = 0.77**). There was, however, no correlation observed between C-cell contamination and CEI, indicating that the highly mutated C-cells are not clonally expanded (**Figure 3E**). Taken together these results confirm that based on the selected cell-sorting strategy little or a substantial amount of highly mutated B cells can contaminate the naive B cell target population impacting the overall mutation level but not the clonal expansion level.

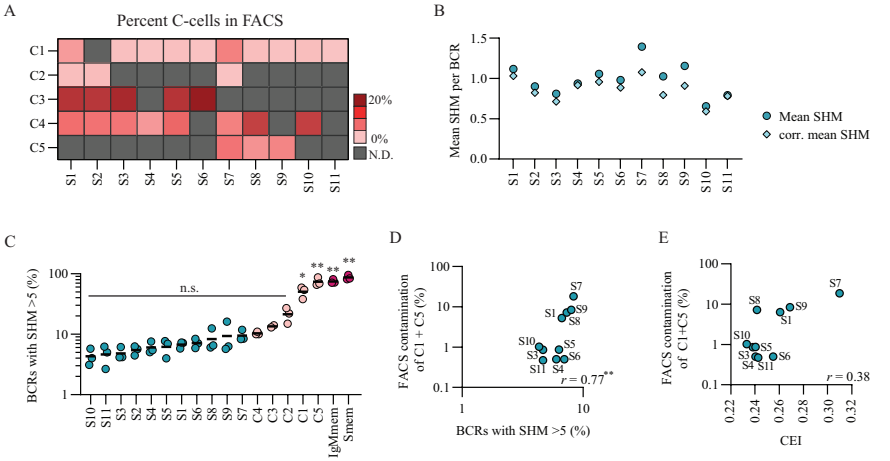

Figure 3. Contamination by C-cells impacts overall BCR mutation levels. *(**A**) Heat map of the mean percentage of C-cell contamination for each S-subset. (**B**) Dot plot depicts the observed mean SHM and the corrected mean SHM for each S-subset. (**C**) The percentage of BCRs with more than 5 mutations (SHM) in the BCR repertoire of S, C and memory subsets. Black lines depict means and each dot is an individual donor and subsets are ordered by increasing mean. Statistical differences were determined using a Kruskal-Wallis with a Dunn's multiple comparison test. *p < 0.05, **p < 0.01, n.s. = not significant. (**D**) Correlation between FACS C1 and C5 subset contamination and the percentage of BCRs with >5 SHM for S-subsets. (**E**) Correlation between FACS C1 and C5 subset contamination and CEI. For correlation plots the Spearman rank correlation coefficient (r) is represented at the right side of each graph and dots represent average value of n = 3. Data displays three biological replicates in one independent experiment.*

Ranking of sorting strategies to obtain naive B cells

After having analyzed the level of mutations and clonal expansion in the BCR repertoire and the level of sorting-derived contamination for each S-subset, we combined relevant parameters such as, mean SHM, % BCRs with zero SHM, % BCRs with >5 SHMs, and % of contaminating C-cells and composed a ranking of the best sorting strategy to obtain bona fide naive B cells (**Table I**). The number of markers used for isolation is also reported but was not included in the ranking calculation. S10, S11 and S3 ranked as the top 3 sorting strategies, scoring best in all considered parameters. On the contrary, subsets S7, S9, S6 and S1 were among the worst performing sorting strategies. The remaining subsets S2, S4, S5 and S8 scored intermediate.

DISCUSSION

The aim of this study was to evaluate and optimize naive B cell cell-sorting strategies from human peripheral blood to acquire a population of non-mutated, non-expanded and phenotypical non-antigen experienced B cell population. Here we show that current naive B cell isolation strategies using $CD27^-IgD^+$ are adequate but can be improved considerably by including markers for IgM and CD45RB glycosylation.

CD27 expression is used in general to separate naive from antigen-experienced B cells as its expression correlates with detectible levels of somatic hypermutation in the V region, regardless of cells being IgD^- or IgM/IgD^+[7,13,14]. Here we show that the isolation of naive B cells using only CD27 negativity (S1 subset) was not optimal and ranked 8th out of the 11 tested strategies, due to high mean mutation level and low percentage of non-mutated BCRs. This is most likely due to the presence of contaminating $CD27^-$ cells that carry highly mutated BCRs, such as $CD27^-IgG^+/IgA^+$ cells (C1 subset) or $CD27^-IgD^-IgM^+$ cells (C2 subset). The removal of these switched and non-switched CD27- cells, respectively in subsets S2 and S4, reduced the mean SHM from 1.2 to 0.90 for S2 and 0.94 for S4 while also reducing the percentage of contaminating highly mutated cells (S1: 29.4%; S2: 18.7%; S4: 1.0%; **Figure 3**). Another commonly used strategy to isolate naive B cells, i.e., $CD27^-IgD^+$ (S3 subset), showed low levels of mutated BCRs (mean SHM = 0.81) and ended up in the top 3 of best sorting strategies (**Table I**). However, it must be noted that there is a large fraction (~30%) of anergic B cells ($CD27^-IgD^+IgM^{low}$ B cells) present when using this isolation strategy[19,20]. Although functional evaluation of the different subsets was beyond the scope of this paper others have shown the reduced responsiveness of these IgD^+IgM^{low} B cells *in vitro*[22,23]. Therefore, depending on the experimental aim for which the naive B cell are isolated, it might be more appropriate to also include a marker for IgM by which CD27- B cells with dual expression of IgM and IgD can be isolated (S5 subset, mean SHM = 0.89). Moreover, within cells with dual expression of IgM and IgD, a small percentage

Table I. Ranking of sorting strategies to isolate non-clonally expanded non-mutated naive B cells

Subset	Classification	No. of markers*	Mean SHM	BCRs 0 SHM	BCRs >5 SHM	FACS C-cells	CEI	Total Score	Rank
S10	CD27- RB- IgD+ IgM+	4	1	1	1	4	1	8	1
S11	CD27- RB- IgD+ IgM+ $CD38^{lo}$	5	2	3	2	1	7	15	2
S3	CD27- IgD+	2	3	4	3	3	2	15	3
S2	CD27- IgG- IgA-	3	5	5	4	5	6	25	4
S4	CD27-IgD+ IgM-	3	6	9	5	2	3	25	5
S5	CD27- IgD+ IgM+	3	4	6	6	9	4	29	6
S8	RB- IgD+ IgM+	3	7	2	9	8	5	31	7
S1	CD27-	1	8	10	7	6	9	40	8
S6	CD27- IgD+ IgM+ $CD38^{lo}$	4	9	11	8	7	8	43	9
S9	RB- IgD+ IgM+ $CD38^{lo}$	4	10	7	10	10	10	47	10
S7	RB-	1	11	8	11	11	11	52	11

**For all sorting strategies markers for CD19 and viability were also included. This parameter is not included in the ranking calculation.*

of cells also expressed IgG or IgA (~1%) that likely represent a population of cells that recently underwent class-switching. The exclusion of these cells by also including markers for IgG and IgA in cell-sorting strategies may further improve naive B cell isolation and is particularly important when studying the process of IgG and IgA class-switching.

Recently, we and others have identified glycosylation of CD45RB (RB) as a novel marker to identify antigen-primed B cells, independent of CD27 and BCR isotype expression[5,17,24,25]. However, the use of RB negativity alone (S7 subset), proved to be the least optimal strategy to cell-sort naive B cells, yielding the subset with the highest mean SHM (1.40), highest percentage of BCRs with >5 SHM and highest percentage of contaminating cells. Although a large fraction of cells in this population still harbors non-mutated BCRs (75%), the presence of contaminating $CD27^{+}RB^{-}$ cells with high mutation levels (C5, mean SHM = 13.36) is likely responsible for the poor performance of this strategy. By including IgM and IgD surface expression (S8 subset) the BCR mutation levels reduced somewhat but remained relatively high (mean SHM = 1.03). This could be explained the fact that ~15% of $CD27^{+}RB^{-}$ cells also have dual expression of IgM and IgD[17]. Thus, using RB alone or in combination with BCR isotype markers does not seem to outperform current isolation strategies using CD27 expression, and is even suboptimal. However, when cell-sorting using RB^{-} is combined with $CD27^{-}$ or $CD27^{-}IgD^{+}$ a lower mutation level was observed, likely due to the loss of mutated $CD27^{-}IgMD^{+}RB^{+}$ (C3 subset) which account for 20% of the contamination in CD27-/ $CD27^{-}IgD^{+}$ sorted subsets (**Figure 3A and C**). The addition of IgM expression, $CD27^{-}RB^{-}IgD^{+}IgM^{+}$ (S10 subset), yielded the B cell population with the lowest mean SHM (0.65), highest percentage of BCRs with zero SHM and lowest percentage of BCRs >5 SHM, ranking in fact number one among the tested strategies.

Whether this is also the preferred strategy during pathological conditions, for example autoimmune diseases, needs to be investigated in PBMCs from patients.

Naive B cells that become positive for CD38, are described to be activated and to participate in the GC reaction, where multiple rounds of affinity selection will lead to the accumulation of SHM in their BCRs. It is unclear whether $CD27^{-}RB^{-}CD38^{+}$ B cells found in peripheral blood (C4 subsets) are naive B cells that have recently been activated or did already participate in the GC reaction and therefore display mutated BCRs[27]. Here we observed that these cells have minimal BCR mutations (mean SHM = 1.84), but do show higher levels of clonal expansion compared to S-subsets (Clonal expansion index 0.35 in C4 versus 0.25 on average for S-subsets) (**Figure 2E, S3C**). This suggest that $CD27^{-}RB^{-}CD38^{+}$ B cells in peripheral blood have been activated by antigen and started to proliferate but have not yet been subjected to the process of somatic hypermutation.

Contrary to what is expected from antigen-naive B cells that have not yet undergone clonal expansion and somatic hypermutation in a GC reaction, the mean mutation count in the BCR repertoire of naive B cell subsets in this study and in other studies[32,37] is higher than 0. Furthermore, we observed that only around 80% of repertoires found in S-subsets contained BCRs with zero SHM while around 13% contained BCR with 1 or 2 SHM (**Figure S4A**). The latter was shown to be independent from the level of FACS contamination from mutated cells (**Figure S4B**), opposite to what was observed for the percentage of BCRs >5 SHM (**Figure 3D**). Therefore, the mutations found in BCRs with 1 or 2 SHM are likely to be errors introduced by the technical procedure of PCR amplification and sequencing. This was confirmed when analyzing the distribution and type of mutations across the antibody V region in BCRs with 1 or 2 SHM compared to BCRs with >5 SHM in S-subsets versus memory subsets (**Figure S4B and C**). In fact, it became apparent that reads with 1 or 2 mutations within S-subsets did not follow natural occurring mutational patterns, which was observed in both BCRs with 1 or 2 SHM and BCRs with >5 SHM from IgMmem and Smem. Therefore, one must consider that upon performing repertoire analysis using current methodologies one can expect a baseline error level of approximately 1 to 2 SHM for naive B cells.

In summary, we showed that although some of the most widely adopted sorting strategies for naive B cell isolation (such as $CD27^{-}IgD^{+}$) are adequate to obtain a B cell population with virtually non-mutated BCR, others (such as $CD27^{-}$ or RB^{-}) deliver a naive B cell population with increased contamination of B cells with mutated BCRs. We therefore propose that exclusion of CD27 expression and CD45RB glycosylation with dual expression of IgM and IgD (thus $CD27^{-}RB^{-}IgD^{+}IgM^{+}$) provides a more stringent but improved strategy to obtain a purified naive B cell population. Finetuning naive B cell classification will improve interrogation and monitoring of B cell profiles during health and disease, diagnosis

and treatment, and vaccination strategies. Phenotypic B cell analysis, BCR analysis, and functional *in vitro* assays are vital to further elucidate the mechanisms driving B cell maturation and their contribution in mediating autoimmune diseases and cancer.

Acknowledgements

The authors would like to thank Mirjam van der Burg, PhD, for guidance in designing the research and critically reviewing the manuscript. This study was supported by Landsteiner Foundation for Blood Transfusion research (Grant1626).

Author contributions

JK, SP, PS, MB and TR designed research. JK, ST, and IN performed research. SP and JK analyzed data. JK, SP, MB, NV and TR wrote the paper. All authors critically reviewed the manuscript, gave final approval of the version to be published, and agreed to be accountable for all aspects of the work ensuring that questions related to the accuracy or integrity of any part of the work are appropriately investigated and resolved.

Financial support

This study was supported by Landsteiner Foundation for Blood Transfusion Research (Grant1626).

Disclosure statement

The authors declare no commercial or financial conflicts of interest.

Data availability statement

The data that support the findings of this study are openly available in NCBI Sequence Read Archive at https://www.ncbi.nlm.nih.gov/sra, reference number PRJNA856112.

Ethics approval

Buffy coats were obtained from anonymized healthy adult donors with written informed consent in accordance to the guidelines established by the Sanquin Medical Ethical Committee and in line with the Declaration of Helsinki.

REFERENCES

1. Obukhanych TV, Nussenzweig MC. T-independent type II immune responses generate memory B cells. *J Exp Med*. 2006;203(2):305-310. doi:10.1084/jem.20052036
2. Weisel FJ, Zuccarino-Catania GV, Chikina M, Shlomchik MJ. A Temporal Switch in the Germinal Center Determines Differential Output of Memory B and Plasma Cells. *Immunity*. 2016;44(1):116-130. doi:10.1016/j.immuni.2015.12.004
3. Elsner RA, Shlomchik MJ. Germinal Center and Extrafollicular B Cell Responses in vaccination, immunity and autoimmunity. *Immunity*. 2020;53(6):1136-1150. doi:10.1016/j.immuni.2020.11.006. Germinal
4. Sanz I, Wei C, Jenks SA, et al. Challenges and opportunities for consistent classification of human b cell and plasma cell populations. *Front Immunol*. 2019;10(OCT):1-17. doi:10.3389/fimmu.2019.02458
5. Glass DR, Tsai AG, Oliveria JP, et al. An Integrated Multi-omic Single-Cell Atlas of Human B Cell Identity. *Immunity*. 2020;53(1):217-232.e5. doi:10.1016/j.immuni.2020.06.013
6. Weisel NM, Joachim SM, Smita S, et al. Surface phenotypes of naive and memory B cells in mouse and human tissues. *Nat Immunol*. 2022;23(1):135-145. doi:10.1038/s41590-021-01078
7. Klein U, Rajewsky K, Küppers R. Human immunoglobulin (Ig)M+IgD+ peripheral blood B cells expressing the CD27 cell surface antigen carry somatically mutated variable region genes: CD27 as a general marker for somatically mutated (memory) B cells. *J Exp Med*. 1998;188(9):1679-1689. doi:10.1084/jem.188.9.1679
8. Agematsu K, Nagumo H, Yang FC, et al. B cell subpopulations separated by CD27 and crucial collaboration of CD27 + B cells and helper T cells in immunoglobulin production. *Eur J Immunol*. 1997;27(8):2073-2079. doi:10.1002/eji.1830270835
9. Wirths S, Lanzavecchia A. ABCB1 transporter discriminates human resting naive B cells from cycling transitional and memory B cells. *Eur J Immunol*. 2005;35(12):3433-3441. doi:10.1002/eji.200535364
10. Tangye SG, Avery DT, Deenick EK, Hodgkin PD. Intrinsic Differences in the Proliferation of Naive and Memory Human B Cells as a Mechanism for Enhanced Secondary Immune Responses. *J Immunol*. 2003;170(2):686-694. doi:10.4049/jimmunol.170.2.686
11. Macallan DC, Wallace DL, Zhang V, et al. B-cell kinetics in humans: Rapid turnover of peripheral blood memory cells. *Blood*. 2005;105(9):3633-3640. doi:10.1182/blood-2004-09-3740
12. Good KL, Avery DT, Tangye SG. Resting Human Memory B Cells Are Intrinsically Programmed for Enhanced Survival and Responsiveness to Diverse Stimuli Compared to Naive B Cells. *J Immunol*. 2009;182(2):890-901. doi:10.4049/jimmunol.182.2.890
13. Dunn-Walters DK, Isaacson PG, Spencer J. MGZ of Human Spleen Is a Reservoir of Memory. *J Exp Med*. 1995;182(August):559-566.
14. Pascual BV, Liu Y, Magalski A, Bouteiller O De, Banchereau J, Capra JD. Analysis of Somatic mutation in Five B cell Subsets of Human Tonsil. *J Exp Med*. 1994;180.
15. Wei C, Anolik J, Cappione A, et al. A New Population of Cells Lacking Expression of CD27 Represents a Notable Component of the B Cell Memory Compartment in Systemic Lupus Erythematosus. *J Immunol*. 2007;178(10):6624-6633. doi:10.4049/jimmunol.178.10.6624
16. Fecteau JF, Côté G, Néron S. A New Memory CD27 − IgG + B Cell Population in Peripheral Blood Expressing V H Genes with Low Frequency of Somatic Mutation . *J Immunol*. 2006;177(6):3728-3736. doi:10.4049/jimmunol.177.6.3728
17. Koers J, Pollastro S, Tol S, et al. CD45RB Glycosylation and Ig Isotype Define Maturation of Functionally Distinct B Cell Subsets in Human Peripheral Blood. *Front Immunol*. 2022;13:1-8. doi:10.3389/fimmu.2022.891316
18. Wu YC, Kipling D, Leong HS, Martin V, Ademokun AA, Dunn-Walters DK. High-throughput immunoglobulin repertoire analysis distinguishes between human IgM memory and switched memory B-cell populations. *Blood*. 2010;116(7):1070-1078. doi:10.1182/blood-2010-03-275859

19. Gutzeit C, Chen K, Cerutti A. The enigmatic function of IgD: some answers at last. *Eur J Immunol*. 2018;48(7):1101-1113. doi:10.1002/eji.201646547
20. Merrell KT, Benschop RJ, Gauld SB, et al. Identification of Anergic B Cells within a Wild-Type Repertoire. *Immunity*. 2006;25(6):953-962. doi:10.1016/j.immuni.2006.10.017
21. Wardemann H, Yurasov S, Schaefer A, Young JW, Meffre E, Nussenzweig MC. Predominant autoantibody production by early human B cell precursors. *Science (80-)*. 2003;301(5638):1374-1377. doi:10.1126/science.1086907
22. Duty JA, Szodoray P, Zheng NY, et al. Functional anergy in a subpopulation of naive B cells from healthy humans that express autoreactive immunoglobulin receptors. *J Exp Med*. 2009;206(1):139-151. doi:10.1084/jem.20080611
23. Quách TD, Manjarrez-Orduño N, Adlowitz DG, et al. Anergic responses characterize a large fraction of human autoreactive naive B cells expressing low levels of surface IgM. *J Immunol*. 2011;186(8):4640-4648. doi:10.4049/jimmunol.1001946
24. Koethe S, Zander L, Koster S, et al. Pivotal Advance: CD45RB glycosylation is specifically regulated during human peripheral B cell differentiation. *J Leukoc Biol*. 2011;90(1):5-19. doi:10.1189/jlb.0710404
25. Bemark M, Friskopp L, Saghafian-Hedengren S, et al. A glycosylation-dependent CD45RB epitope defines previously unacknowledged CD27-IgMhigh B cell subpopulations enriched in young children and after hematopoietic stem cell transplantation. *Clin Immunol*. 2013;149(3 PB):421-431. doi:10.1016/j.clim.2013.08.011
26. Zhao Y, Uduman M, Siu JHY, et al. Spatiotemporal segregation of human marginal zone and memory B cell populations in lymphoid tissue. *Nat Commun*. 2018;9(1). doi:10.1038/s41467-018-06089-1
27. Jackson SM, Harp N, Patel D, et al. Key developmental transitions in human germinal center B cells are revealed by differential CD45RB expression. *Blood*. 2009;113(17):3999-4007. doi:10.1182/blood-2008-03-145979
28. Pollastro S, de Bourayne M, Balzaretti G, et al. Characterization and Monitoring of Antigen-Responsive T Cell Clones Using T Cell Receptor Gene Expression Analysis. *Front Immunol*. 2021;11(February):1-11. doi:10.3389/fimmu.2020.609624
29. Vander Heiden JA, Yaari G, Uduman M, et al. PRESTO: A toolkit for processing high-throughput sequencing raw reads of lymphocyte receptor repertoires. *Bioinformatics*. 2014;30(13):1930-1932. doi:10.1093/bioinformatics/btu138
30. Giudicelli V, Chaume D, Lefranc MP. IMGT/GENE-DB: A comprehensive database for human and mouse immunoglobulin and T cell receptor genes. *Nucleic Acids Res*. 2005;33:256-261. doi:10.1093/nar/gki010
31. Gupta NT, Vander Heiden JA, Uduman M, Gadala-Maria D, Yaari G, Kleinstein SH. Change-O: A toolkit for analyzing large-scale B cell immunoglobulin repertoire sequencing data. *Bioinformatics*. 2015;31(20):3356-3358. doi:10.1093/bioinformatics/btv359
32. Bashford-Rogers RJM, Bergamaschi L, McKinney EF, et al. Analysis of the B cell receptor repertoire in six immune-mediated diseases. *Nature*. 2019;574(7776):122-126. doi:10.1038/s41586-019-1595-3
33. Oksanen J, Legendre P, O'Hara B, Stevens MHH, Oksanen MJ, Suggests M. The vegan package. *Community Ecol Packag*. 2007;10:631-637.
34. ImmunoMind Team. immunarch: An R Package for Painless Bioinformatics Analysis of T-Cell and B-Cell Immune Repertoires. 2019. doi:10.1186/s12859-015-0613-1>.License
35. Sanz I, Wei C, Lee FEH, Anolik J. Phenotypic and functional heterogeneity of human memory B cells. *Semin Immunol*. 2008;20(1):67-82. doi:10.1016/j.smim.2007.12.006
36. Berkowska MA, Driessen GJA, Bikos V, et al. Human memory B cells originate from three distinct germinal center-dependent and -independent maturation pathways. *Blood*. 2011;118(8):2150-2158. doi:10.1182/blood-2011-04-345579
37. Heiden JA Vander, Stathopoulos P, Julian Q, et al. Dysregulation of B Cell Repertoire Formation in Myasthenia Gravis Patients Revealed through Deep Sequencing. *J Immunol*. 2017;198(4):1460-1473. doi:10.4049/jimmunol.1601415

SUPPLEMENTARY MATERIAL

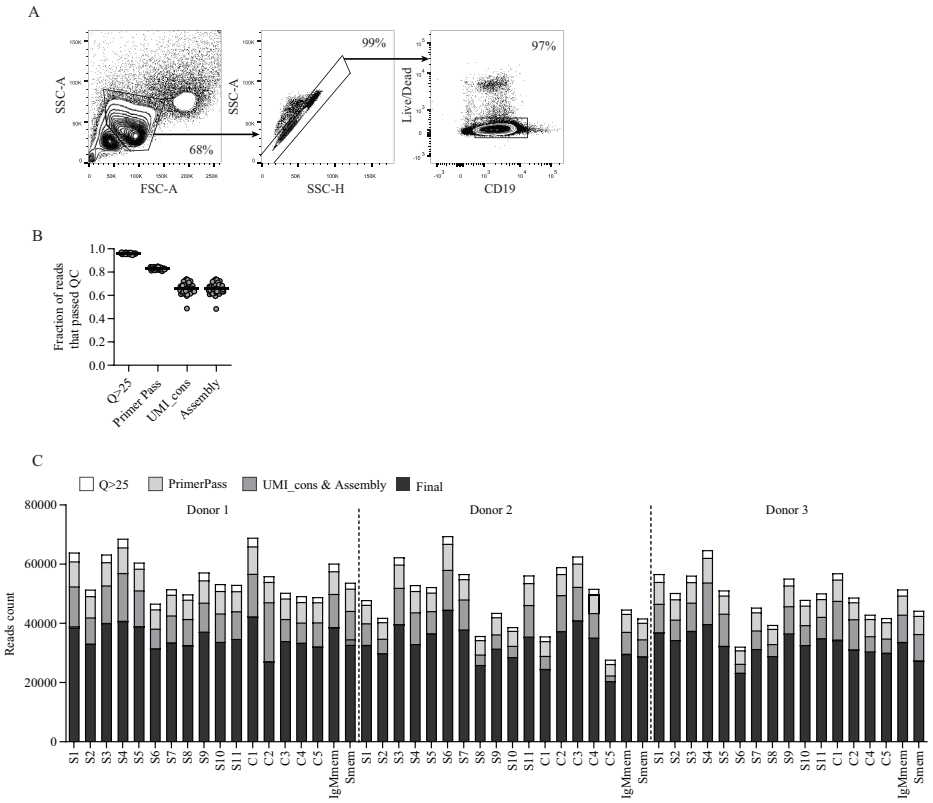

Figure S1. FACS pre-gating and BCR repertoire sequencing performance. ***(A)*** *Cryopreserved CD19⁺ magnetic bead isolated B cells were pre-gated to obtain singlet, viable CD19⁺ cells for cell-sorting (Representative example in Figure 1A).* ***(B)*** *Dotplot depicting the fraction of sequenced reads that successfully passed each step of the bioinformatic pipeline.* ***(C)*** *Barplot depicting the loss in absolute reads counts during each step of the bioinformatic pipeline. Q>25: quality filtering with phred-score >25; Primer Pass: masking or removal of sequencing IGHV and IGHJ primers; UMI_cons: creation of UMI-consensus reads; Assembly: assembly of paired read 1 and read 2; Final: final reads used for the analysis.*

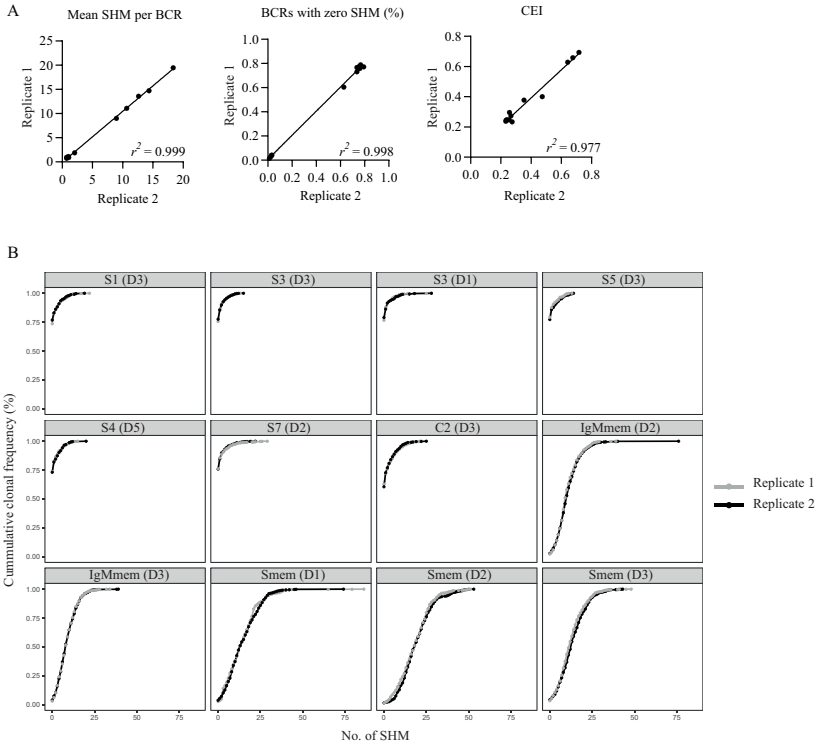

Figure S2. Reproducibility of BCR sequencing for technical replicates. *(**A**) X, y plots depicting mutation levels, percentage of BCRs with zero mutations and clonal expansion (CEI) between technical replicate samples. Linear regression (r2) is presented on the right side of each graph. (**B**) Cumulative frequency distribution of mutations in the BCR repertoire for several S, C and memory subsets for technical replicate 1 (grey) and technical replicate 2 (black). Donor = D.*

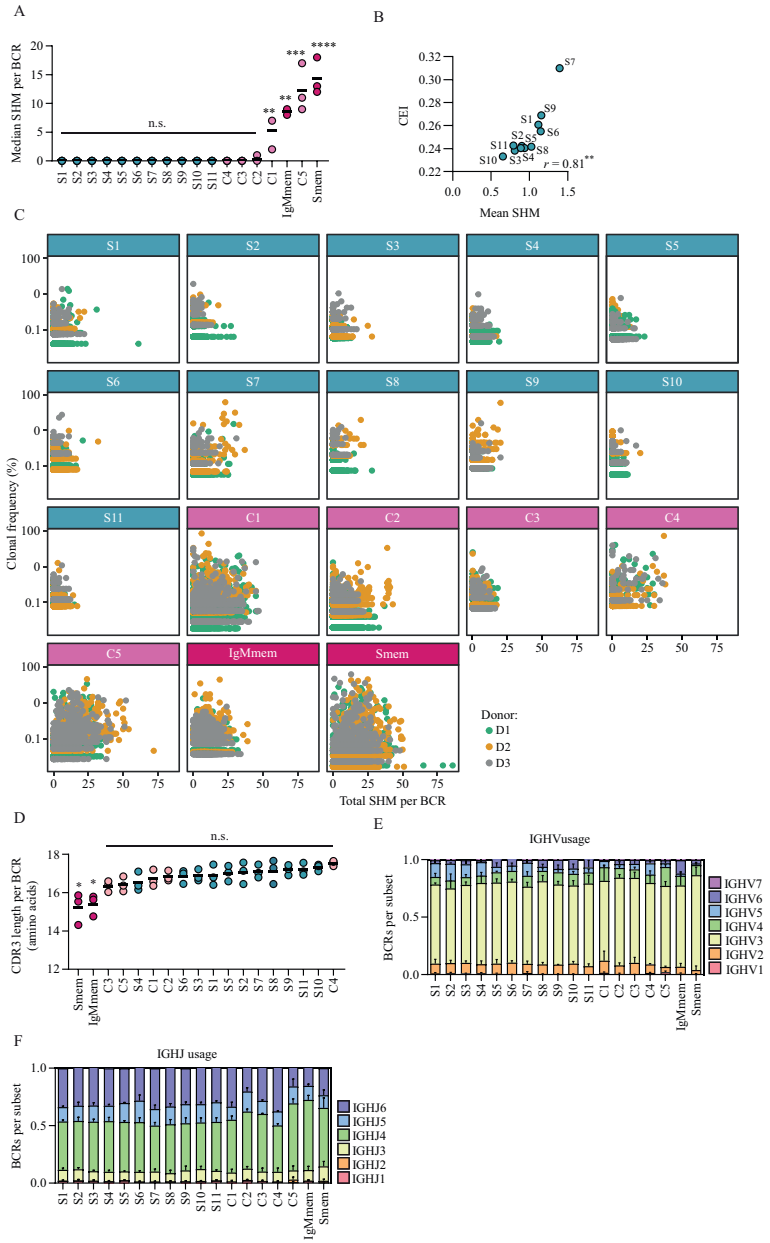

Figures S3. BCR repertoire analysis. ***(A)*** *Median SHM per BCR and* ***(B)*** *Correlation between the clonal expansion index (CEI) and the mean SHM for each S-subset. Spearman rank correlation coefficient (r) is represented at the right side of the graph.* ***(C)*** *Scatterplot depicting the clonal frequency and the total SHM count in single BCRs for each sorted subset. Different colors represent different donors.* ***(D)*** *Mean CDR3 length in the BCR repertoire of cell-sorted B cell subsets from healthy adult donor peripheral blood (n = 3).* ***(E)*** *IGHV and* ***(F)*** *IGHJ gene usage in BCR repertoires. Dots represent mean individual donors and black lines depict means. Statistical differences were determined using a Kruskal-Wallis with Dunn's post-test. *p < 0.05, **p < 0.01, ***p < 0.001, ****p < 0.0001, n.s. = not significant. Data displays three biological replicates in one independent experiment.*

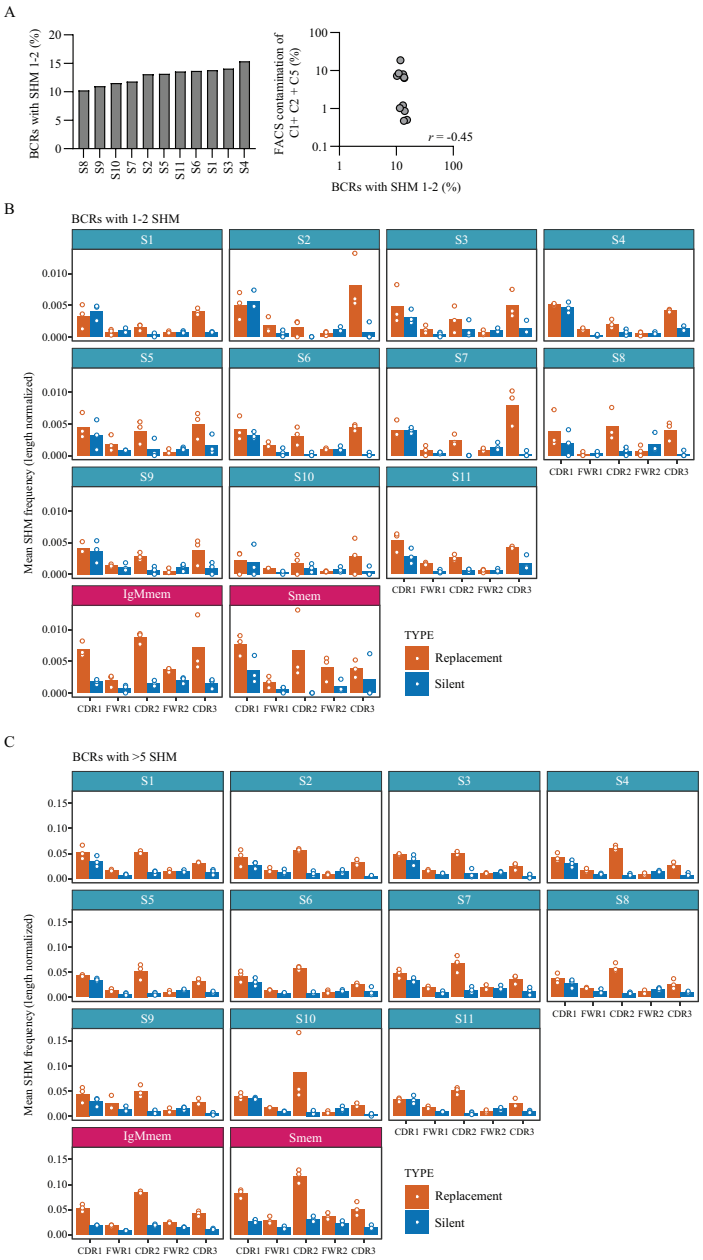

Figure S4. Distribution and type of SHM. *(**A**) The percentage of BCRs with 1 or 2 SHM for each naive subset and their correlation with the FACS cellular contamination from subset C1, C2 and C5 (n = 3). Spearman rank correlation coefficient (r) is represented at the right side of the graph. (**B**) Bar graphs show mean frequency distribution of mutations per IGHV gene region and per type of mutation in BCRs with 1 or 2 SHM for naive and memory subsets. Bars depict means and each dot represent a single donor. (**C**) As in (B) but for BCRs with more than 5 mutations. Data displays three biological replicates in one independent experiment. CDR: Complementary Determining Region; FWR: Frame Working Region.*

CHAPTER 3

CD45RB glycosylation and Ig isotype define maturation of functionally distinct B cell subsets in human peripheral blood

Jana Koers, Sabrina Pollastro, Simon Tol, Ingrid Pico-Knijnenburg,
Ninotska I.L. Derksen, Pauline A. van Schouwenburg,
Mirjam van der Burg, S. Marieke van Ham and Theo Rispens

Published in Frontiers in Immunology (2022)

ABSTRACT

Glycosylation of CD45RB (RB$^+$) has recently been identified to mark antigen-experienced B cells, independent of their CD27 expression. By using a novel combination of markers including CD45RB glycosylation, CD27 and IgM/IgD isotype expression we segregated human peripheral blood B cell subsets and investigated their IGHV repertoire and *in vitro* functionality. We observed distinct maturation stages for CD27$^-$RB$^+$ cells, defined by differential expression of non-switched Ig isotypes. CD27$^-$RB$^+$ cells, which only express IgM, were more matured in terms of Ig gene mutation levels and function as compared to CD27$^-$RB$^+$ cells that express both IgM and IgD or cells that were CD27$^-$RB$^-$. Moreover, CD27$^-$RB$^+$IgM$^+$ cells already showed remarkable rigidity in IgM isotype commitment, different from CD27$^-$RB$^+$IgMD$^+$ and CD27$^-$RB$^-$ cells that still demonstrated great plasticity in B cell fate decision. Thus, glycosylation of CD45RB is indicative for antigen-primed B cells, which are, dependent on the Ig isotype, functionally distinct.

INTRODUCTION

B cell development and the formation of a highly diverse pool of long-lived antibody-secreting cells and memory B cells is crucial for the humoral immune response and lasting immunological memory. During the course of an immune response, the immunoglobulin (Ig) gene is changed by the process of somatic hypermutation (SHM), class switch recombination (CSR), and selection in response to antigen stimulation. Hypermutated and class-switched Ig genes are a characteristic of memory B cells along with the loss of IgD expression. Gain of CD27 expression, often combined with absent IgD expression, is commonly used to discriminate human memory B cells from naive B cells. However, a substantial proportion of $CD27^-$ B cells in healthy adults displays mutated and isotype-switched Ig genes like memory B cells[1–3], which disputes the feasibility of using CD27 as a truly discriminative memory marker. Mutated $CD27^-$ cells are present at birth[4] and account for 5% of the peripheral blood B cell population in healthy adults[1]. The function of these putative $CD27^-$ memory cells and their relationship to $CD27^+$ cells is not well understood but increased frequencies have been observed during aging[5], in autoimmunity[6] and several viral infections[7,8]. The lack of markers to distinguish naive B cells from memory B cells resulted in novel strategies for B cell classification using phenotypical differences in addition to CD27 and Ig isotype[9]. Several studies identified changes in site-specific O-linked glycosylation of CD45RB during human B cell differentiation in various secondary lymphoid organs and blood[10–14]. This glycan-dependent CD45RB epitope can be detected using the mAb MEM-55 and within human peripheral blood, glycosylation of CD45RB (RB^+) was absent on naive B cells, but highly expressed on $CD27^+$ cells and on a small fraction of switched and non-switched $CD27^-$ B cells[10]. Next-generation sequencing of the Ig heavy chain variable (IGHV) genes revealed that these $CD27^-RB^+$ cells displayed intermediate levels of somatic mutations, higher than $CD27^-RB^-$ but lower than $CD27^+RB^+$ cells[1,14], suggesting that these B cells are antigen-primed and no longer naive. On the other hand, these $CD27^-RB^+$ cells, with high IgM levels, were found with increased frequencies in young children and early after hematopoietic stem cell transplantation (HSCT)[11], suggesting an immature rather than memory stage. Thus, CD45RB glycosylation, in combination with CD27 expression and Ig isotype, may serve as an additional marker to improve classification of human naive and memory B cells. Here, we investigated human peripheral blood B cell subsets segregated by CD45RB glycosylation, CD27 and IgM/IgD isotype expression and studied their IGHV repertoire and *in vitro* functionality.

MATERIALS AND METHODS

Human B cell isolation

Buffy coats were obtained from anonymized adult healthy donors with written informed consent in accordance to the guidelines established by the Sanquin Medical Ethical Committee and in line with the Declaration of Helsinki. Human peripheral blood mononucleated cells (PBMCs) were isolated from buffy coats using Ficoll gradient centrifugation (lymphoprep; Axis-Shield PoC AS) and CD19$^+$ cells were isolated by positive selection using magnetic Dynabeads (Invitrogen).

FACS sorting

Cryopreserved CD19$^+$ cells were surface stained in PBA (PBS supplemented with 0.1% bovine serum albumin) for 30 min at 4°C and washed in PBA. A LIVE/DEAD cell staining (ThermoFisher scientific) was used to label and exclude non-viable cells. B cells were gated as singlet, viable, CD19$^+$ cells and were segregated further into six subsets using surface marker expression of: CD27, CD38, CD45RB-glycosylation, IgD, IgM, IgG, and IgA. Subsets were FACS-sorted (FACS Aria III, BD Biosciences) into RTL buffer (Sigma-Aldrich) for next-generation sequencing or in PBA for *in vitro* stimulation assays.

Antibodies

CD19$^+$ cells were surface stained using the following antibodies: anti-CD19 (clone SJ25C1, 562947), anti-CD38 (clone HB7, 646851), anti-IgD (clone IA6, 2561315), anti-IgM (clone G20-127, 562977) from BD Biosciences. Anti-IgG (MH16-1, M1268) from Sanquin Reagents. Anti-IgA (polyclonal, 2050-09) from SouthernBiotech. Anti-CD27 (clone O323, 25-0279-42) from ThermoFisher. Anti-CD45RB (clone MEM-55, 310205) from Biolegend.

Immune repertoire sequencing

5000 B cells were sorted per subset per donor (n = 3), lysed and gDNA was extracted according to the manufacturer's instructions (Qiagen). IgH rearrangements were amplified in a multiplex PCR using forward primers V_H1-6 FR1 (BIOMED-2) and J_H consensus reverse primers with a Molecular Identifier (MID)-tag. A total of 40 PCR cycles were performed and a heat stable polymerase with proof-reading activity was used (AmpliTaq Gold DNA polymerase, Thermo Fisher). Equal quantities of PCR products were pooled and purified by gel extraction (MinElute gel extraction kit, Qiagen) and Agencourt AMPure XP beads (Backman Coulter) and quantified by fluorescence using the Qubit 2.0 Fluorometer (Invitrogen). Sequencing was performed using a Illumina Miseq run in standard mode using a v3 kit.

Repertoire and Mutation analysis

Reads retrieved from the sequencing platform were processed using pRESTO[15]. Briefly, paired-ends reads were assembled using the AssemblePairs.py function and assembled reads with a phred score < 25 were removed. V_H, J_H primers and MID-tags were annotated and masked using the MaskPrimers.py function. Obtained datasets were then submitted to IMGT/HighV-QUEST [16,17] for alignment. Aligned sequences were further processed using Change-O[18]. Output of the IMGT/HighV-QUEST was parsed using the MakeDb.py function[18] and only functional rearrangements were selected. Analysis of somatic hypermutation was performed using the SHazaM R package (version 0.2.1) after germline sequence reconstruction using the CreateGermlines.py function from Change-O. All data here presented are performed on a final dataset of unique nucleotidic sequences (spacing from the IGHV to the IGHJ gene, primers excluded). Due to the lack of unique molecular identifiers (UMIs) in the amplification protocol, it was not possible to properly correct for technical artifacts such as PCR and sequencing errors. Therefore, we removed reads that occurred only once (singletons) with the assumption that technical artifacts occur randomly and independently of each sample's origin and are therefore equally distributed in all analyzed samples. Information on the total and unique rearrangements per sample, before and after singletons exclusion, and IGHV and IGHJ gene representation is reported in **Table SI**. Raw sequencing data have been deposited at NCBI Sequence Read Archive (BioProject: PRJNA816414) and processed repertoires are available upon request to the corresponding author.

In vitro stimulation assays

T cell-dependent (TD) stimulation assays. 96- well flat-bottom plates were seeded with $0.01x10^6$ irradiated 3T3 fibroblast cells expressing human CD40L per well in B cell medium (RPMI medium supplemented with FCS (5%, Bodinco), penicillin (100 U/mL, Invitrogen), streptomycin (100 µg/mL, Invitrogen), β-mercaptoethanol (50 µM, Sigma-Aldrich), L-glutamine (2mM, Invitrogen), and human apo-transferrin (20 µg/mL, Sigma-Aldrich) depleted for IgG using protein A sepharose (GE Healthcare)) and adhered overnight. The generation of CD40L expressing fibroblasts is described elsewhere[19]. The next day, B cell medium supplemented with recombinant human IL-21 (50ng/ml, Preprotech) or IL-21 and IL-4 (50ng/ml and 25ng/ml, Preprotech) was added to the seeded 3T3-CD40L cells. B cell subsets (**Figure 2A**) were directly sorted into the plates in a density of 250 cells/well. After ten days of culture, survival, isotype switching, differentiation and Ig secretion was assessed using flow cytometry and ELISA.

T cell-independent (TI) stimulation assays. 96- well flat-bottom plates were seeded with 10.000 B cells from each subset per well supplemented with either 0.1µM CpG ODN (Invivogen) or 1µM R848 (Invivogen), in the presence of 1µg/ml anti-IgM $F(ab')_2$ (JacksonImmunoResearch). After seven days of culture B cell survival, isotype switching, differentiation and Ig secretion were assessed using flow cytometry and ELISA.

IgM, IgG, and IgA ELISA of culture supernatants

IgM, IgG, and IgA expression levels were measured as described previously[19]. In brief, 96-well maxisorb plates were coated with monoclonal anti-IgM, anti-IgG, or anti-IgA (2µg/ml MH15-1, 2µg/ml MH16-1, or 1µg/ml MH14-01-M08, Sanquin reagents) and culture supernatants were incubated for 1h. Secreted IgM, IgG, or IgA was detected using HRP-conjugated mouse anti-human IgM, IgG, or IgA (1µg/ml MH15-1, 1µg/ml MH16-1, or 1µg/ml MH14-1, Sanquin reagents) in HPE (Sanquin reagents). The ELISA was developed using TMB substrate, stopped by addition of 0.2M H_2SO_4 and absorbance was measured at 450 and 540 nm. OD values were normalized to values of a reference serum pool that was included in each plate. To properly determine IgM production, *in vitro* stimulation assays described above, were also performed in the absence of anti-IgM $F(ab')_2$ as this compound interferes with the IgM ELISA resulting in an incomplete picture of the IgM production. Of note, the presence of anti-IgM $F(ab')_2$ may alter IgM production during culture.

Statistical analysis

Differences between groups were analyzed using a Friedman analysis of variance for non-parametric repeated measures followed by a Dunn's multiple comparison test. A p value <0.05 was considered significant. The statistical analysis was carried out using GraphPad Prism 9.1.1.

RESULTS

B cell subsets separated based on CD45RB glycosylation and CD27 expression feature differential Ig isotype usage

Human peripheral blood $CD19^+CD38^{lo}$ B cells (**Figure S1A**, pre-gating strategy) can be segregated into four populations based on their CD45RB glycosylation (RB) and CD27 expression levels (**Figure 1A**). The $CD27^-RB^-$ (55%) and $CD27^+RB^+$ (28%) populations are more prevalent compared to $CD27^-RB^+$ (9.5%) and $CD27^+RB^-$ (7%) (**Figure 1B**). Within these populations differential Ig isotype usage was observed, with $CD27^+$ cells enriched for IgG and IgA and $CD27^-$ cells mostly being IgM^+ and/or IgD^+ (**Figure 1C**). Within $CD27^+$ populations, the Ig isotype usage was quite similar, despite cells being RB^+ or RB^-. By contrast, within $CD27^-$ populations, there was an increased prevalence of all IgD^- subsets within the RB^+ population. By isotype-specific gating around 13% of the $CD19^+$ cells were left unannotated, in line with a recent study[14]. These cells are not mislabeled IgE^+ B cells as these are extremely rare in healthy peripheral blood[20]. The Ig^{lo} cells were found across all four populations and likely represent a mixture of isotypes found on cells that recently underwent class-switching. Thus, the $CD27^-RB^+$ population features more isotype-switched cells than the $CD27^-RB^-$ population, a difference not observed within $CD27^+$ populations.

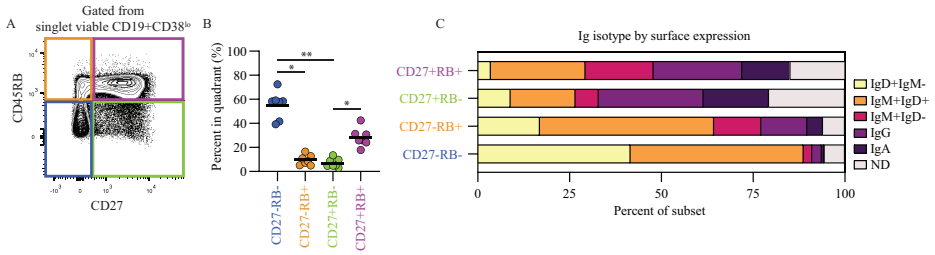

Figure 1. B cells within subsets separated based on CD45RB glycosylation and CD27 expression feature differential Ig isotype usage. *(A) Representative biaxial CD45RB/CD27 plot gated from singlet viable CD19^{+}CD38^{lo} cells (**Figure S1A**). (**B**) Percent of B cells in each quadrant, as in (A), for seven biological replicates (healthy adults) each composed of two technical replicates over three independent experiments. (**C**) VH-isotype usage per quadrant. ND, not determined. Black lines depict mean values. Statistical differences were determined using a Friedman analysis of variance and Dunn's multiple comparison test. * $p < 0.05$, ** $p < 0.01$.*

CD45RB glycosylation marks antigen-primed B cells independent of CD27 expression

To refine discrimination of CD27/RB populations we included Ig isotype expression for enhanced characterization. In the current study we focused on characterizing the non-isotype switched (IgM and IgD) B cells but excluded CD27^{-}IgD^{+}IgM^{-} B cells that represent a population of anergic B cells that recognize self-antigens[21–23]. Based on the expression of CD27, CD45RB glycosylation and IgM and IgD we discriminated four CD27^{-} populations (**Figure 2A**, **Figure S1B**): CD27^{-}RB^{-}IgM^{+}IgD^{+} [IgMD^{+}RB^{-}], CD27^{-}RB^{-}IgM^{+}IgD^{-} [IgM^{+}RB^{-}], CD27^{-}RB^{+}IgM^{+}IgD^{+} [IgMD^{+}RB^{+}], and CD27^{-}RB^{+}IgM^{+}IgD^{-} [IgM^{+}RB^{+}]. In addition, two CD27^{+}RB^{+} populations were included: IgM^{+}IgD^{-} memory B cells [IgMmem] and isotype-switched memory B cells [IgG/Amem]. Subset classifications are depicted (table, **Figure 2A**). All subsets were gated on being CD38^{lo} to exclude CD38^{+} transitional B cells and CD38^{+} ASCs. Combined the CD27^{-} subsets make up ~30% of the adult human peripheral blood B cell population with the largest fraction being IgMD^{+}RB^{-} cells (n = 7, **Figure 2B**). To investigate the levels of somatic hypermutation in the six different subsets we performed next-generation sequencing of IGHV genes (n = 3). We observed increased somatic mutations in V_H-regions of both memory B cell subsets (IgMmem and IgG/Amem), in line with previous studies[24,25]. V_H-mutations were virtually absent for IgMD^{+}RB^{-} cells and not significantly increased for both IgM^{+}RB^{-} and IgMD^{+}RB^{+} subsets compared to IgMD^{+}RB^{-} cells (**Figure 2C**). Remarkably, IgM^{+}RB^{+} cells had comparable mutation counts as IgMmem, but less than IgG/Amem. Similar results were observed when analyzing the entire cumulative distribution of mutations in the Ig repertoire (**Figure 2D**). In addition, IgM^{+}RB^{+} cells displayed a reduction in V_H-CDR3 length[25,26], also similar to IgMmem (**Figure 2E**). Taken together, IgM^{+}RB^{+} cells show characteristic that associate with being antigen-primed despite being CD27^{-}.

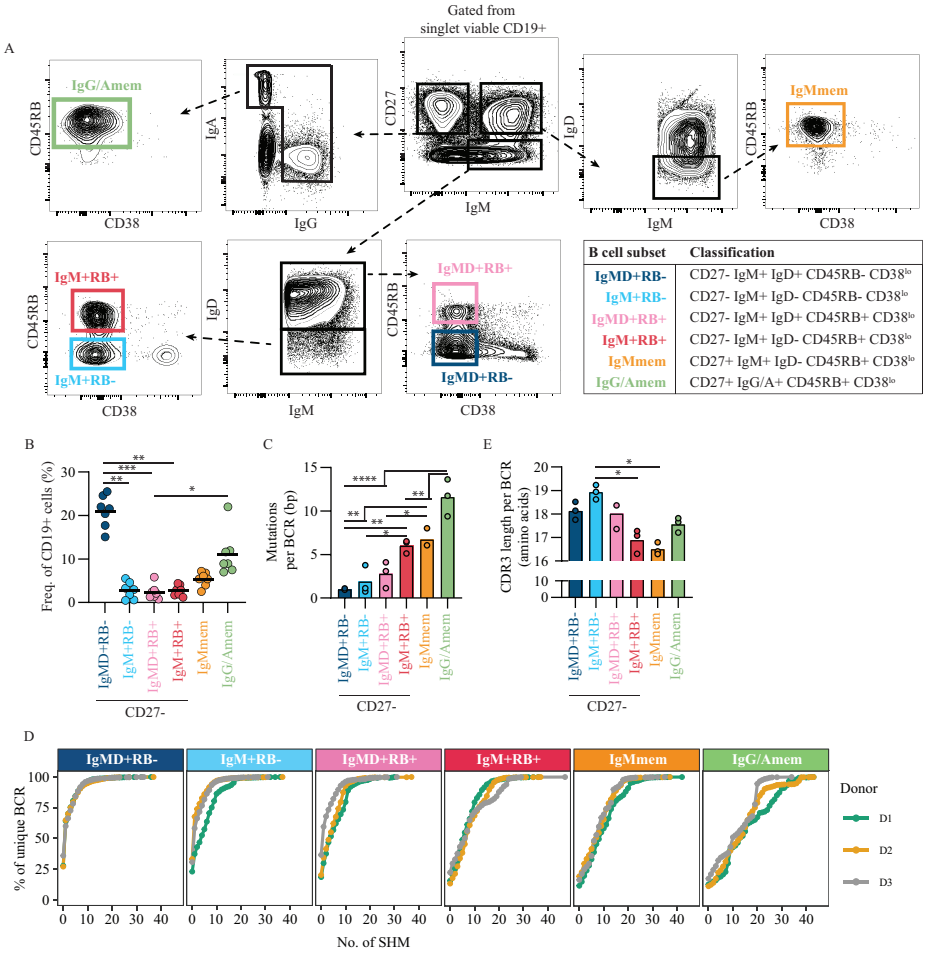

Figure 2. CD45RB glycosylation marks antigen-primed B cells independent of CD27 expression. ***(A)*** *Representative gating strategy for cell-sorting B cell subsets from healthy donor peripheral blood CD19⁺ pre-isolated B cells by flow cytometry. Gated from singlet viable CD19⁺ cells (**Figure S1B**). Table shows the classification of subsets.* ***(B)*** *Frequency of subsets within CD19⁺ cells, for seven biological replicates each composed of two technical replicates over three independent experiments.* ***(C)*** *Mean number of mutations per Ig gene (healthy adults, n = 3) and* ***(D)*** *Cumulative frequency distribution of mutations in the Ig repertoire in the different B cell subsets. Different colored lines represent different donors.* ***(E)*** *mean V_H-CDR3 length from cell-sorted B cell subsets (healthy adults, n = 3). Bars and black lines depict mean values. Statistical differences were determined using a Friedman analysis of variance and Dunn's multiple comparison test. * p < 0.05, ** p < 0.01, *** p < 0.001, **** p < 0.0001.*

CD45RB glycosylation, combined with Ig isotype, identifies functionally distinct B cell subsets

Apart from expression of mutated V_H genes, memory B cells can be distinguished from naive B cells by more efficient proliferation and differentiation into antibody-secreting cells (ASCs) upon stimulation[26,27]. Given that the IgM^+RB^+ subset carried somatic mutations they may also functionally resemble memory B cells. Therefore, we studied their *in vitro* functionality, and of the other $CD27^-$ subsets, using T cell-dependent (TD) and -independent (TI) stimulation and analyzed survival, differentiation and isotype-switching potential.

The six B cell subsets were cell-sorted and cultured on CD40L-expressing cells in the presence of IL-21 for 10 days. Survival and/or proliferation was similar for most subsets (**Figure S2A**). Compared to $IgMD^+RB^-$ cells, IgM^+RB^+ cells showed increased differentiation towards activated and/or memory-like B cells (MBCs, $CD27^+CD38^-$, **Figure 3A and B**). Within IgMmem and IgG/Amem populations, that were sorted as being $CD27^+$, we observed downregulation of CD27 expression, a phenomenon previously observed by others upon *in vitro* culture of memory B cells[28,29]. Interestingly, IgM^+RB^+ cells, but not $IgMD^+RB^+$ cells, had poor IgG switching potential, a feature shared with IgMmem (**Figure 3C**). The addition of IL-4, a TD cytokine known to enhance isotype switch to IgG, had limited additional effects and did not alleviate the reduced IgG switch observed for IgM^+RB^+ cells (**Figure S2B-F**). Furthermore, the IgM^+RB^+ subset showed increased differentiation into functional ASCs ($CD27^+CD38^+$, **Figure 3A, D and E, Figure S2G**), however, this was less in comparison to IgG/Amem. $IgMD^+RB^+$ cells, although not significant, did show a trend in increased MBC and ASC formation compared to $IgMD^+RB^-$ and IgM^+RB^- cells, but less in comparison to IgM^+RB^+ cells (**Figure 3B, D and E**). Differentiation of B cells also occurs during T cell-independent (TI) immune responses that generally results in the formation of ASCs that secrete low-affinity IgM antibodies[30]. Since IgM^+RB^+ cells showed reduced isotype switch to IgG upon *in vitro* TD stimulation we studied their functionality, and of the other CD27- subsets, upon *in vitro* TI stimulation. After 7 days of TI stimulation with CpG ODN (TLR9 activator) and anti-IgM, IgM^+RB^+ and $IgMD^+RB^+$ subsets, but not IgM^+RB^- and $IgMD^+RB^-$ subsets, were able to differentiate into memory-like B cells (**Figure 3F**), albeit, much less when compared to TD stimulation. Furthermore, IgM^+RB^+ and $IgMD^+RB^+$ subsets showed a trend towards increased differentiation into functional ASCs as was observed for IgMmem and IgG/Amem, albeit to various degrees (**Figure 3G**, **Figure S3A**), and with limited isotype switching (**Figure S3B**). Subsets responded in a similar fashion when stimulated with R848 (TLR7/TLR8 agonist) and anti-IgM for 7 days (**Figure S4**). Thus, different from $IgMD^+RB^+$, IgM^+RB^- and $IgMD^+RB^-$ subsets, IgM^+RB^+ cells showed a higher propensity for MBC differentiation with an IgM isotype commitment.

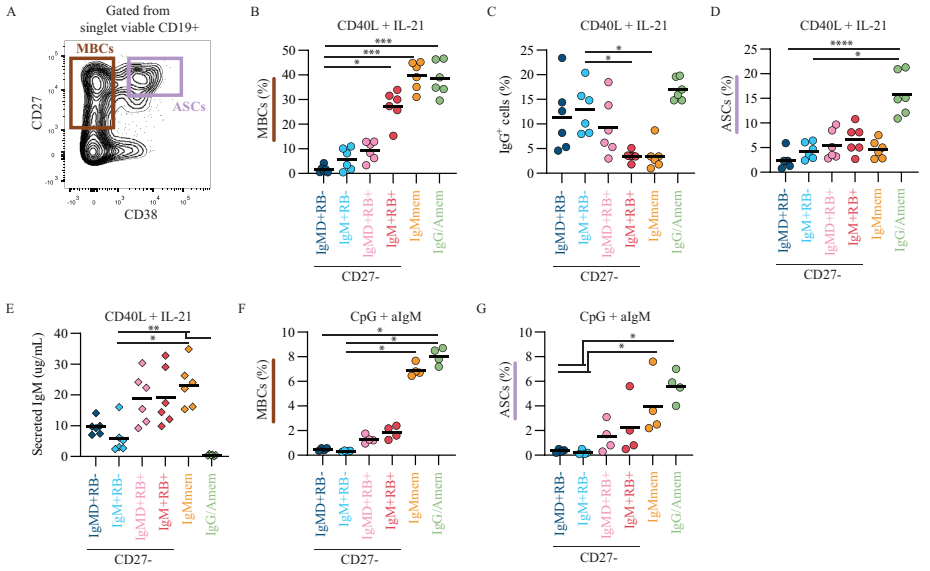

Figure 3. CD45RB glycosylation, combined with Ig isotype, marks functionally distinct B cell subsets. *B cell subsets were cultured with TD-stimulation of CD40L-expressing 3T3s in the presence of IL-21 (50ng/ml) for 10 days (six biological replicates each consisting of two technical replicates over two independent experiments). (**A**) Representative biaxial CD27/CD38 FACS plot after 10 days of TD culture. The formation of (**B**) MBCs (CD27+CD38-) (**C**) IgG+ B cells, and (**D**) ASCs (CD27+CD38+) was measured using flow cytometry. (**E**) Cumulative IgM secretion measured in culture supernatants using ELISA at day 10 (n = 6). B cell subsets were cultured with TI-stimulation of CpG ODN (0.1μM) and anti-IgM-F(ab')$_2$ (1μg/ml) for 7 days (four biological replicates each consisting of two technical replicates). The formation of (**F**) MBCs and (**G**) ASCs was measured using flow cytometry. Black lines depict mean values. Statistical differences were determined using a Friedman analysis of variance and Dunn's multiple comparison test. * $p < 0.05$, ** $p < 0.01$, *** $p < 0.001$, **** $p < 0.0001$.*

DISCUSSION

Here, by using a novel combination of markers including CD45RB glycosylation, CD27 and IgM/IgD isotype expression we segregated human peripheral blood B cell subsets and investigated their IGHV repertoire and *in vitro* functionality. **Table I** summarizes for each of the studied B cell subset their V_H mutation status and *in vitro* functionality.

IgMD$^+$ RB$^-$ cells displayed virtually absent levels of somatic hypermutation, indicating that this population corresponds to "classical" naive B cells. IgM$^+$RB$^-$ and IgMD$^+$RB$^+$ cells were both in repertoire and *in vitro* functionality similar to IgMD$^+$RB$^-$ cells. Because IgM$^+$RB$^-$ cells were gated on being CD38^{lo} we do not assume that they represent human T1 B cells that are often characterized by a CD24^{hi}CD38^{hi} phenotype[31]. Circulating IgM$^+$RB$^+$ cells carried mutated V_H genes and reduced CDR3 length which implies previous antigen-priming. This suggests that these cells are at a later stage of development with regards

Table I. Summary of B cell subset discriminating factors

B cell subset	V_H mutations	MBC TD-stim.	IgG+ TD-stim.	IgM secr. TD-stim.	MBC TI-stim.
IgMD+RB-	low	-	+	+/-	-
IgM+RB-	low	-	+	+/-	-
IgMD+RB+	low	-	+	+	-
IgM+RB+	int	+	-	+	-
IgMmem	int	+	-	+	+
IgG/Amem	high	+	+	-	+

MBC = memory B cell differentiation, TD = T cell-dependent, TI = T cell-independent

to affinity maturation as compared to the other $CD27^-$ subsets. In line, IgM^+RB^+ cells also showed improved ability to develop into functional ASCs using TI and TD *in vitro* stimulations. $IgMD^+RB^+$ cells, although not significant and less in comparison to IgM^+RB^+, did show a trend in increased MBC and ASC formation compared to $IgMD^+RB^-$ and IgM^+RB^- cells. These data indicate that $CD27^-RB^+$ populations fall within the continuum of naive B cells that progress towards memory B cells and ASCs and do not represent a population of exhausted memory B cells with downregulated CD27, as was proposed previously[5]. In addition, the absence of CD45RB glycosylation to define 'true' human naive B cells may advance current strategies using CD27 and IgD. Even though using the glycosylation epitope on CD45RB helps to identify antigen-primed B cells among $CD27^-$ cell, there is, however, a population of $CD27^+$ cells, presumed memory B cells, that are RB^-, meaning that glycosylation of CD45RB does not mark all antigen primed B cells.

We show that IgM^+RB^+ cells have properties in common with $CD27^+IgM^+IgD^-RB^+$ cells (IgMmem). IgM^+RB^+ cells seem to have an early lineage commitment to the IgM isotype as they showed reduced ability to isotype-switch to IgG, similar to IgMmem but in steep contrast to the other CD27- subsets. Moreover, CD27 expression was higher on IgM^+RB^+ cells after 10 days of TD culture compared to the other $CD27^-$ subsets which shows that with the same level of stimulation these cells had enhanced capacity to differentiate towards a memory phenotype. IgM memory B cells are important for the generation of a broadly cross-reactive memory repertoire with lower affinity BCRs to protect against a plethora of pathogens and their variants[32–34]. The early lineage commitment of IgM^+RB^+ cells to the IgM isotype might represent a mechanism to ensure replenishment of the IgM memory pool for lasting B cell immunity. In contrast, the efficient IgG isotype-switching seen for $IgMD^+RB^+$ cells suggests this subset has more plasticity in B cell fate decision. Thus, within RB+ cells, differential expression of IgM and IgD, discriminates two functionally distinct B cell subsets. In line, for $CD27^+RB^+$ subsets, only IgG/Amem, but not IgMmem, outperformed both $CD27^-RB^+$ subsets in ASC differentiation. This suggest that expression of just CD27 or CD45RB glycosylation upon B cell activation is not indicative for enhanced ASC differentiation, but also relies on the Ig isotype. The notion that the Ig isotype imprints

the subsequent fate of the B cell upon recall responses is consistent with data obtained from mouse and human *in vitro* models indicating that in general the IgM memory B cells re-entered germinal centers to undergo multiple rounds of expansion, somatic hypermutation and selection, whereas IgG memory B cells preferentially differentiated into ASCs[35–37].

In this study we did not analyze memory subsets with differential expression of IgM and IgD and only included the CD27$^+$IgM$^+$IgD$^-$RB$^+$ subset (IgMmem). For CD27$^+$IgM$^+$IgD$^+$ cells it has been described that they have fewer V_H-gene mutation than CD27$^+$IgM$^+$IgD$^-$ and class-switched CD27+ cells but more mutations than naive (CD27$^-$IgM$^+$IgD$^+$) and CD27$^+$IgM$^-$IgD$^+$ cells[38]. CD27$^+$IgM$^-$IgD$^+$ cells only make up a small fraction of CD27$^+$ cells (7.5%, **Figure 1C**). Within CD27+RB+ cells, CD27$^+$IgM$^+$IgD$^+$ cells make up around 25% cells and are present to a lesser degree within the CD27$^+$RB$^-$ population (16%, **Figure 1C**). Whether, the presence or absence of glycosylated CD45RB on CD27$^+$ cells with differential IgM and IgD expression impacts the level of detectible V_H-gene mutations and *in vitro* functionality remains unclear.

Previous studies reported increased frequencies of CD27$^-$RB$^+$ cells that expressed high levels of IgM in young children and early after hematopoietic stem cell transplantation[11]. Unfortunately, the dual IgM/IgD expression on these cells was not determined. Therefore, we cannot assign with certainty whether these are CD27$^-$IgM$^+$RB$^+$ or the CD27$^-$IgMD$^+$RB$^+$ cells. As these cells have increased frequency in children it may be more likely that these are the CD27$^-$IgMD$^+$RB$^+$ cells described here that have fewer mutations and showed a naive-like behavior. However, cord blood and fetal tissues also accommodate a small population of mutated CD27$^+$IgM$^+$IgD$^+$ B cells[39,40]. These subsets may represent a first-line defense mechanism that respond rapidly upon both TD and TI activation.

The findings presented here provide novel insights in the phenotypic and functional progression from naive B cells via CD27$^-$RB$^+$ cells to memory B cells in human peripheral blood. In conclusion, glycosylation of CD45RB is indicative for antigen-primed B cells, which are, dependent on the Ig isotype, functionally distinct.

Author contributions

JK, SP, ST, PS, MB and TR designed research. JK, ST, IP and ND performed research. JK, SP and ND analyzed data. JK, SP and TR wrote the paper. All authors critically reviewed the manuscript, gave final approval of the version to be published, and agreed to be accountable for all aspects of the work ensuring that questions related to the accuracy or integrity of any part of the work are appropriately investigated and resolved.

Financial support

This study was supported by Landsteiner Foundation for Blood Transfusion Research (Grant1626).

Disclosure statement

There are no commercial or financial conflicts of interest.

Data availability statement

The datasets presented in this study can be found in online repositories. The names of the repository/repositories and accession number(s) can be found below: NCBI, accession code: PRJNA816414

Ethics approval

Ethical review and approval was not required for the study on human participants in accordance with the local legislation and institutional requirements. The patients/participants provided their written informed consent to participate in this study.

REFERENCES

1. Sanz I, Wei C, Lee FEH, Anolik J. Phenotypic and functional heterogeneity of human memory B cells. *Semin Immunol*. 2008;20(1):67-82. doi:10.1016/j.smim.2007.12.006
2. Berkowska MA, Driessen GJA, Bikos V, et al. Human memory B cells originate from three distinct germinal center-dependent and -independent maturation pathways. *Blood*. 2011;118(8):2150-2158. doi:10.1182/blood-2011-04-345579
3. Dunn-Walters DK, Isaacson PG, Spencer J. MGZ of Human Spleen Is a Reservoir of Memory. *J Exp Med*. 1995;182(August):559-566.
4. van Gent R, van Tilburg CM, Nibbelke EE, et al. Refined characterization and reference values of the pediatric T- and B-cell compartments. *Clin Immunol*. 2009;133(1):95-107. doi:10.1016/j.clim.2009.05.020
5. Colonna-Romano G, Bulati M, Aquino A, et al. A double-negative (IgD-CD27-) B cell population is increased in the peripheral blood of elderly people. *Mech Ageing Dev*. 2009;130(10):681-690. doi:10.1016/j.mad.2009.08.003
6. Wei C, Anolik J, Cappione A, et al. A New Population of Cells Lacking Expression of CD27 Represents a Notable Component of the B Cell Memory Compartment in Systemic Lupus Erythematosus. *J Immunol*. 2007;178(10):6624-6633. doi:10.4049/jimmunol.178.10.6624
7. Moir S, Ho J, Malaspina A, et al. Evidence for HIV-associated B cell exhaustion in a dysfunctional memory B cell compartment in HIV-infected viremic individuals. *J Exp Med*. 2008;205(8):1797-1805. doi:10.1084/jem.20072683
8. Rojas OL, Narváez CF, Greenberg HB, Angel J, Franco MA. Characterization of rotavirus specific B cells and their relation with serological memory. *Virology*. 2008;380(2):234-242. doi:10.1016/j.virol.2008.08.004
9. Zuccarino-Catania G V., Sadanand S, Weisel FJ, et al. CD80 and PD-L2 define functionally distinct memory B cell subsets that are independent of antibody isotype. *Nat Immunol*. 2014;15(7):631-637. doi:10.1038/ni.2914
10. Koethe S, Zander L, Koster S, et al. Pivotal Advance: CD45RB glycosylation is specifically regulated during human peripheral B cell differentiation. *J Leukoc Biol*. 2011;90(1):5-19. doi:10.1189/jlb.0710404
11. Bemark M, Friskopp L, Saghafian-Hedengren S, et al. A glycosylation-dependent CD45RB epitope defines previously unacknowledged CD27-IgMhigh B cell subpopulations enriched in young children and after hematopoietic stem cell transplantation. *Clin Immunol*. 2013;149(3 PB):421-431. doi:10.1016/j.clim.2013.08.011
12. Jackson SM, Harp N, Patel D, et al. Key developmental transitions in human germinal center B cells are revealed by differential CD45RB expression. *Blood*. 2009;113(17):3999-4007. doi:10.1182/blood-2008-03-145979
13. Zhao Y, Uduman M, Siu JHY, et al. Spatiotemporal segregation of human marginal zone and memory B cell populations in lymphoid tissue. *Nat Commun*. 2018;9(1). doi:10.1038/s41467-018-06089-1
14. Glass DR, Tsai AG, Oliveria JP, et al. An Integrated Multi-omic Single-Cell Atlas of Human B Cell Identity. *Immunity*. 2020;53(1):217-232.e5. doi:10.1016/j.immuni.2020.06.013
15. Vander Heiden JA, Yaari G, Uduman M, et al. PRESTO: A toolkit for processing high-throughput sequencing raw reads of lymphocyte receptor repertoires. *Bioinformatics*. 2014;30(13):1930-1932. doi:10.1093/bioinformatics/btu138

16. Lefranc M. IMGT, the International ImMunoGeneTics Information System. *Cold Spring Harb Protoc*. 2011(6):595-603.

17. Brochet X, Lefranc M, Giuidicelli V. IMGT / V-QUEST : the highly customized and integrated system for IG and TR standardized V-J and V-D-J sequence analysis. *Nucleic Acids Res*. 2008;36:503-508. doi:10.1093/nar/gkn316

18. Gupta NT, Vander Heiden JA, Uduman M, Gadala-Maria D, Yaari G, Kleinstein SH. Change-O: A toolkit for analyzing large-scale B cell immunoglobulin repertoire sequencing data. *Bioinformatics*. 2015;31(20):3356-3358. doi:10.1093/bioinformatics/btv359

19. Unger PPA, Verstegen NJM, Marsman C, et al. Minimalistic in vitro culture to drive human naive b cell differentiation into antibody-secreting cells. *Cells*. 2021;10(5). doi:10.3390/cells10051183

20. Jiménez-Saiz R, Ellenbogen Y, Bruton K, et al. Human BCR analysis of single-sorted, putative IgE+ memory B cells in food allergy. *J Allergy Clin Immunol*. 2019;144(1):336-339.e6. doi:10.1016/j.jaci.2019.04.001

21. Gutzeit C, Chen K, Cerutti A. The enigmatic function of IgD: some answers at last. *Eur J Immunol*. 2018;48(7):1101-1113. doi:10.1002/eji.201646547

22. Quách TD, Manjarrez-Orduño N, Adlowitz DG, et al. Anergic responses characterize a large fraction of human autoreactive naive B cells expressing low levels of surface IgM. *J Immunol*. 2011;186(8):4640-4648. doi:10.4049/jimmunol.1001946

23. Merrell KT, Benschop RJ, Gauld SB, et al. Identification of Anergic B Cells within a Wild-Type Repertoire. *Immunity*. 2006;25(6):953-962. doi:10.1016/j.immuni.2006.10.017

24. Wu YC, Kipling D, Leong HS, Martin V, Ademokun AA, Dunn-Walters DK. High-throughput immunoglobulin repertoire analysis distinguishes between human IgM memory and switched memory B-cell populations. *Blood*. 2010;116(7):1070-1078. doi:10.1182/blood-2010-03-275859

25. DeKosky BJ, Lungu OI, Park D, et al. Large-scale sequence and structural comparisons of human naive and antigen-experienced antibody repertoires. *Proc Natl Acad Sci U S A*. 2016;113(19):E2636-E2645. doi:10.1073/pnas.1525510113

26. Wu YCB, Kipling D, Dunn-Walters DK. The relationship between CD27 negative and positive B cell populations in human peripheral blood. *Front Immunol*. 2011;2:1-12. doi:10.3389/fimmu.2011.00081

27. Deenick EK, Avery DT, Chan A, et al. Naive and memory human B cells have distinct requirements for STAT3 activation to differentiate into antibody-secreting plasma cells. *J Exp Med*. 2013;210(12):2739-2753. doi:10.1084/jem.20130323

28. Racanelli V, Frassanito MA, Leone P, et al. Antibody Production and In Vitro Behavior of CD27-Defined B-Cell Subsets: Persistent Hepatitis C Virus Infection Changes the Rules. *J Virol*. 2006;80(8):3923-3934. doi:10.1128/jvi.80.8.3923-3934.2006

29. van Asten SD, Unger P-P, Marsman C, et al. Soluble FAS Ligand Enhances Suboptimal CD40L/IL-21–Mediated Human Memory B Cell Differentiation into Antibody-Secreting Cells. *J Immunol*. 2021;207(2):449-458. doi:10.4049/jimmunol.2001390

30. Obukhanych T V., Nussenzweig MC. T-independent type II immune responses generate memory B cells. *J Exp Med*. 2006;203(2):305-310. doi:10.1084/jem.20052036

31. Sims GP, Ettinger R, Shirota Y, Yarboro CH, Illei GG, Lipsky PE. Identification and characterization of circulating human transitional B cells. *Blood*. 2005;105(11):4390-4398. doi:10.1182/blood-2004-11-4284

32. Burton BR, Tennant RK, Love J, Titball RW, Wraith DC, White HN. Variant proteins stimulate more IgM+ GC B-cells revealing a mechanism of cross-reactive recognition by antibody memory. *Elife*. 2018;7:1-14. doi:10.7554/eLife.26832

33. Keating R, Hertz T, Wehenkel M, et al. Protective Immunity To Lethal Influenza Infections. *Nat Immunol*. 2013;14(12):1266-1276. doi:10.1038/ni.2741.mTOR

34. Weill JC, Reynaud CA. IgM memory B cells: specific effectors of innate-like and adaptive responses. *Curr Opin Immunol*. 2020;63:1-6. doi:10.1016/j.coi.2019.09.003

35. Dogan I, Bertocci B, Vilmont V, et al. Multiple layers of B cell memory with different effector functions. *Nat Immunol*. 2009;10(12):1292-1299. doi:10.1038/ni.1814

36. Pape KA, Taylor JJ, Maul RW, Gearhart PJ, K. MJ. Different B cell populations mediate early and late memory during an endogenous immune response. *Science (80-).* 2011;331(6021):1203-1207. doi:10.1016/j.earlhumdev.2006.05.022

37. Seifert M, Przekopowitz M, Taudien S, et al. Functional capacities of human igm memory b cells in early inflammatory responses and secondary germinal center reactions. *Proc Natl Acad Sci U S A*. 2015;112(6):E546-E555. doi:10.1073/pnas.1416276112

38. Bautista D, Vásquez C, Ayala-Ramírez P, et al. Differential Expression of IgM and IgD Discriminates Two Subpopulations of Human Circulating IgM+IgD+CD27+ B Cells That Differ Phenotypically, Functionally, and Genetically. *Front Immunol*. 2020;11(May):1-19. doi:10.3389/fimmu.2020.00736

39. Weller S, Faili A, Garcia C, et al. CD40-CD40L independent Ig gene hypermutation suggests a second B cell diversification pathway in humans. *Proc Natl Acad Sci U S A*. 2001;98(3):1166-1170. doi:10.1073/pnas.98.3.1166

40. Scheeren FA, Nagasawa M, Weijer K, et al. T cell-independent development and induction of somatic hypermutation in human IgM+IgD+CD27+ B cells. *J Exp Med*. 2008;205(9):2033-2042. doi:10.1084/jem.20070447

SUPPLEMENTARY MATERIAL

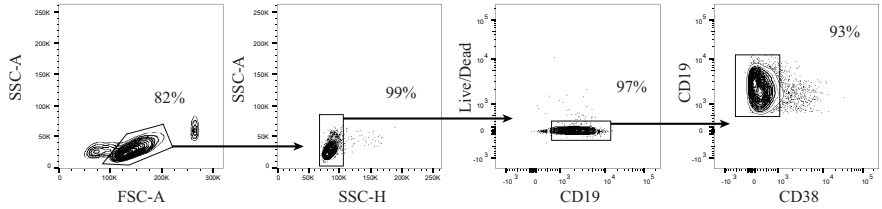

Figure S1A. Gating strategy. *Cryopreserved CD19⁺ magnetic bead isolated B cells were pre-gated to obtain singlet viable CD19⁺CD38^{lo} cells for flow cytometry (Figure 1A).*

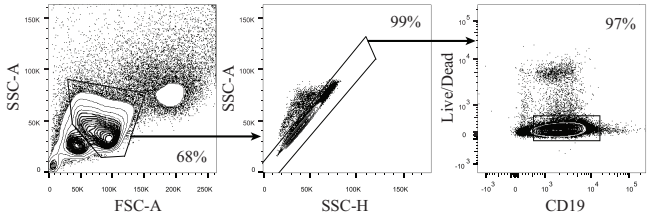

Figure S1B. Gating strategy. *Cryopreserved CD19⁺ magnetic bead isolated B cells were pre-gated to obtain singlet viable CD19⁺ cells for cell-sorting (Figure 2A).*

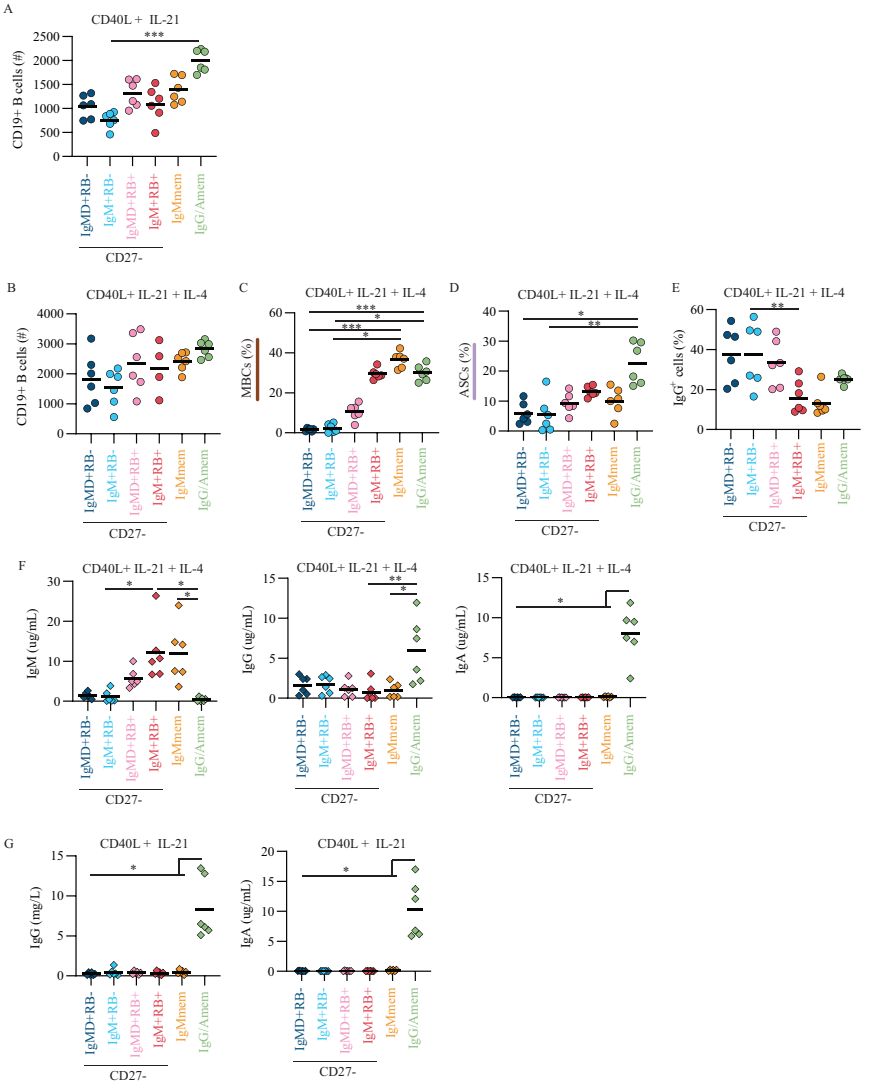

Figure S2. B cell subsets were cultured with TD stimulation for 10 days. *(**A**) Survival measured in subsets cultured with 3T3-CD40L expressing cells and IL-21 (50ng/ml) by flow cytometry (six biological replicates each consisting of two technical replicates over 2 independent experiments). B cell subsets cultured with CD40L-expressing 3T3s for 10 days in the presence of IL-21 (50ng/ml) and IL-4 (25ng/ml). (**B**) Survival, (**C**) frequencies of MBCs, (**D**) ASCs, and (**E**) IgG+ cells were measured using flow cytometry (six biological replicates each consisting of two technical replicates over 2 independent experiments). Ig secretion in TD-cultures with IL-21 and IL-4 (**F**) and IL-21 (**G**) was measured in culture supernatants by ELISA. Black lines depict mean values. Statistical differences were determined using a Friedman analysis of variance and Dunn's multiple comparison test. * $p < 0.05$, ** $p < 0.01$, *** $p < 0.001$, **** $p < 0.0001$.*

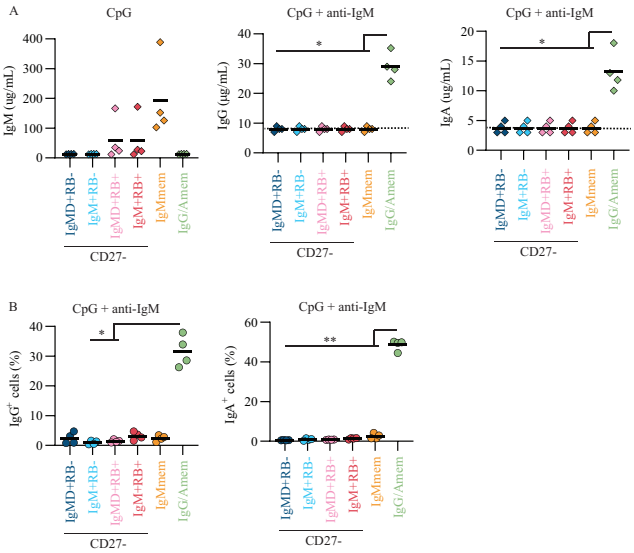

Figure S3. B cell subsets were cultured with CpG (0.1µM) and anti-IgM-F(ab')$_2$ (1µg/ml) for 7 days. *(**A**) Ig secretion was measured in culture supernatants by ELISA (four biological replicates each consisting of two technical replicates). (**B**) IgG and IgA isotype switching was measured by flow cytometry. Black lines depict mean values. Statistical differences were determined using a Friedman analysis of variance and Dunn's multiple comparison test. * $p < 0.05$, ** $p < 0.01$, *** $p < 0.001$, **** $p < 0.0001$.*

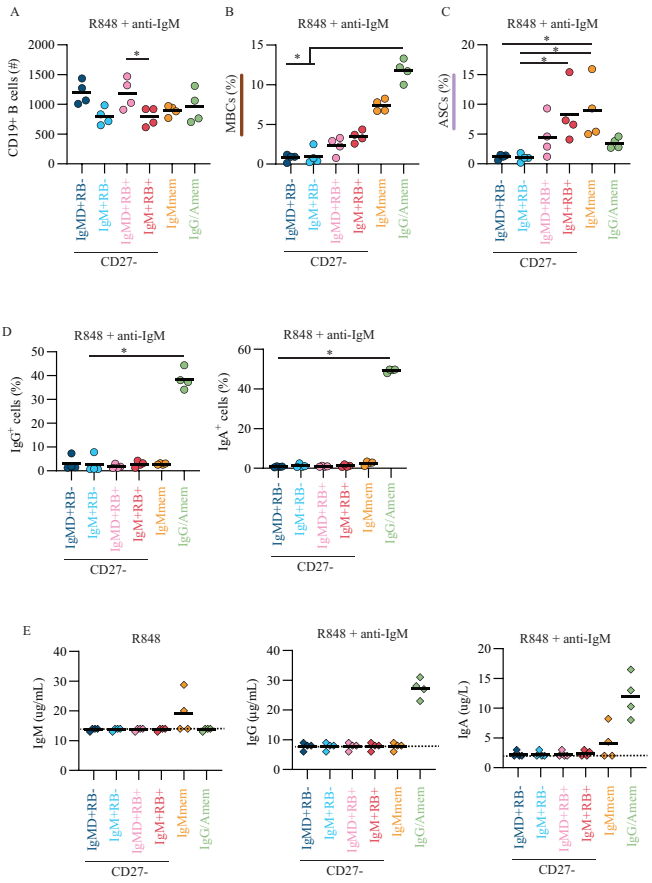

Figure S4. B cell subsets cultured with R848 (1µM) and anti-IgM-F(ab')$_2$ (1µg/ml) for 7 days. *(**A**) Survival, (**B**) frequencies of MBCs, (**C**) ASCs (**D**) and IgG$^+$ and IgA$^+$ cells were measured using flow cytometry in four biological replicates each consisting of two technical replicates. (**E**) Ig secretion was measured after 7 days by ELISA. Dashed lines represent ELISA detection limits. Black lines depict mean values. Statistical differences were determined using a Friedman analysis of variance and Dunn's multiple comparison test. * $p < 0.05$, ** $p < 0.01$, *** $p < 0.001$, **** $p < 0.0001$.*

Table SI. Repertoire analysis per sample

SAMPLE_ID	SUBSET	DONOR	Total reads	Unique reads	singletons*	Total reads excl. singletons	Unique reads excl. singletons	IGHV1**	IGHV2	IGHV3	IGHV4	IGHV5	IGHV6	IGHJ1	IGHJ2	IGHJ3	IGHJ4	IGHJ5	IGHJ6
1_naive_Jana_S882_MID18	IgMD+RB+	D1	35962	9026	7177	28785	1849	29,2	0,54	895,08	53	22,17	0	76,26	0,54	79,5	425,64	60,03	358,03
2_naive_Jana_S883_MID05	IgMD+RB-	D1	43143	7978	6271	36872	1707	13,04	2,77	643,87	338,74	1,58	0	1,98	1,19	5,53	633,2	107,51	250,59
2_naive_Jana_S883_MID02	IgM+RB+	D1	42984	10179	8156	34828	2023	68,22	1,48	730,6	179,93	19,77	0	11,37	0,99	10,87	564,51	106,77	305,49
2_naive_Jana_S883_MID03	IgM+RB-	D1	38780	9312	7488	31292	1824	93,2	0	789,47	115,68	1,64	0	4,39	85,53	8,22	470,94	99,78	331,14
2_naive_Jana_S883_MID04	IgMmem	D1	60476	13754	10897	49579	2857	75,6	0	758,14	122,16	43,05	1,05	2,8	0,7	5,25	688,13	56,7	246,41
2_naive_Jana_S883_MID01	IgA/Gmem	D1	60123	13023	10493	49630	2530	47,45	0	611,6	281,78	59,17	0	1,17	0,59	143,53	438,78	37,49	378,44
3_naive_Jana_S884_MID06	IgMD+RB+	D2	49317	10775	8577	40740	2198	12,05	0,89	677,68	256,7	52,68	0	1,34	0	25	516,07	22,77	434,82
3_naive_Jana_S884_MID08	IgMD+RB-	D2	56559	14559	11846	44713	2713	11,83	0,45	675,16	310,28	2,27	0	2,73	0,91	7,73	646,95	105,1	236,58
3_naive_Jana_S884_MID05	IgM+RB+	D2	47243	11470	9230	38013	2240	31,33	0	812,02	154,44	1,11	1,11	37,23	0	22,12	582,75	133,8	224,11
3_naive_Jana_S884_MID14	IgM+RB-	D2	47782	9805	7754	40028	2051	119,93	0	600,24	276,85	2,98	0	3,58	0,6	108	543,56	91,89	252,39
3_naive_Jana_S884_MID10	IgMmem	D2	39727	9248	7572	32155	1676	52,95	1	581,42	356,64	4	4	89,91	1	4	682,32	48,95	173,83
3_naive_Jana_S884_MID13	IgA/Gmem	D2	19611	5523	4522	15089	1001	31,2	0,49	806,92	55,58	105,31	0,49	17,06	0,49	4,88	735,74	25,84	215,99
4_naive_Jana_S885_MID15	IgMD+RB+	D3	23520	6061	4926	18594	1135	58,89	1,15	762,12	139,72	35,8	2,31	28,87	0	6,93	476,91	166,28	321,02
4_naive_Jana_S885_MID13	IgMD+RB-	D3	19045	4732	3866	15179	866	51,8	0	800,47	121,25	26,49	0	30,02	0,59	26,49	495	190,7	257,21
4_naive_Jana_S885_MID16	IgM+RB+	D3	38841	10403	8455	30386	1948	74,01	0	865,2	56,39	3,52	0,88	3,52	1,76	7,05	785,02	19,38	183,26
4_naive_Jana_S885_MID14	IgM+RB-	D3	34611	9076	7377	27234	1699	13,35	1,03	835,22	143,22	4,62	2,57	15,91	0,51	26,18	428,13	289,01	240,25
4_naive_Jana_S885_MID17	IgMmem	D3	35237	6666	5049	30188	1617	47,62	1,86	735,31	156,46	58,75	0	35,25	1,24	4,95	608,53	62,46	287,57
4_naive_Jana_S885_MID18	IgA/Gmem	D3	15384	3239	2545	12839	694	25,94	7,2	878,96	83,57	4,32	0	59,08	0	10,09	234,87	21,61	674,35

**removed from final analysis*

*** All gene expressed as percentage of unique sequences (so column H)*

CHAPTER 4

Optimized protocols for *in vitro* T cell-dependent and T cell-independent activation for B cell differentiation studies using limited cells

Casper Marsman*, Dorit Verhoeven*, Jana Koers, Theo Rispens, Anja ten Brinke, S. Marieke van Ham and Taco W. Kuijpers
*These authors contributed equally

Published in Frontiers in Immunology (2022)

ABSTRACT

For mechanistic studies, *in vitro* human B cell differentiation and generation of plasma cells are invaluable techniques. However, the heterogeneity of both T cell-dependent (TD) and T cell-independent (TI) stimuli and the disparity of culture conditions used in existing protocols makes interpretation of results challenging. The aim of the present study was to achieve the most optimal B cell differentiation conditions using isolated $CD19^+$ B cells and PBMC cultures. We addressed multiple seeding densities, different durations of culturing and various combinations of TD stimuli and TI stimuli including B cell receptor (BCR) triggering. B cell expansion, proliferation and differentiation was analyzed after 6 and 9 days by measuring B cell proliferation and expansion, plasmablast and plasma cell formation and immunoglobulin (Ig) secretion. In addition, these conditions were extrapolated using cryopreserved cells and differentiation potential was compared. This study demonstrates improved differentiation efficiency after 9 days of culturing for both B cell and PBMC cultures using CD40L and IL-21 as TD stimuli and 6 days for CpG and IL-2 as TI stimuli. We arrived at optimized protocols requiring 2500 and 25.000 B cells per culture well for TD and TI assays, respectively. The results of the PBMC cultures were highly comparable to the B cell cultures, which allows dismissal of additional B cell isolation steps prior to culturing. In these optimized TD conditions, the addition of anti-BCR showed little effect on phenotypic B cell differentiation, however it interferes with Ig secretion measurements. Addition of IL-4 to the TD stimuli showed significantly lower Ig secretion. The addition of BAFF to optimized TI conditions showed enhanced B cell differentiation and Ig secretion in B cell but not in PBMC cultures. With this approach, efficient B cell differentiation and Ig secretion was accomplished when starting from fresh or cryopreserved samples. Our methodology demonstrates optimized TD and TI stimulation protocols for more in-depth analysis of B cell differentiation in primary human B cell and PBMC cultures while requiring low amounts of B cells, making them ideally suited for future clinical and research studies on B cell differentiation of patient samples from different cohorts of B cell-mediated diseases.

INTRODUCTION

B cells are an essential arm of the adaptive immunity as their differentiation in response to foreign antigen generates protective antibodies and immunological memory[1]. The process of B cell differentiation into plasmablasts and plasma cells involves profound molecular changes in morphology, phenotype and gene expression, enabling the cells to produce and secrete large amounts of immunoglobulins (Igs). B cell differentiation is initiated by activation of B cells by exposure to antigen. Classically, B cell responses are categorized in two different B cell responses dependent on the type of antigen, known as T cell-dependent (TD) and T cell-independent (TI) responses[1,2].

In TD B cell responses, B cells are usually activated by proteinaceous antigens in the secondary lymphoid organs through recognition of their cognate antigen by the B cell receptor (BCR). Differentiation of B cells in these circumstances requires T cell help in the form of CD40-CD40L co-stimulation with T cell-derived cytokines such as IL-4 and IL-21[3-5]. Initially, this process results in the generation of memory B cells, which can rapidly differentiate into high-affinity antibody producing plasma cells during secondary antigen exposure[6,7]. Secondly, long-lived plasma cells are generated that move to bone-marrow niches from where they secrete high affinity antibodies[8]. These two compartments of humoral immunological memory are hallmarks of many vaccination strategies.

In TI B cell responses, B cells are activated without T cell help[9]. TI antigens include multimeric antigens, like bacterial capsule polysaccharides (PS) and bacterial DNA, which can activate B cells through binding of the BCR and engagement of specific Toll like receptors (TLRs) such as TLR-4 and TLR-9[10-13]. In addition to this, multiple different cytokines, produced by multiple immune cells, can interact with their respective receptor expressed on B cells and could potentially modulate the response. TI B cell responses are short-lived and do not result in selection of affinity matured antibodies. However, these TI B cell responses have been shown to result in long-lived antibody production in specific cases[14]. Although antibodies are of fundamental importance in the protection against pathogens, aberrant B cell differentiation may lead to autoimmune diseases when tolerance governed by immunological checkpoints is lost[15].

A major hurdle in the study of *in vitro* human B cell differentiation consists of the various methods described to generate *in vitro* plasmablasts and plasma cells, which often fail to exactly mimic *in vivo* responses. In these methods TD and TI antigens are often combined (**Table I**). While this is an effective method to induce B cell differentiation *in vitro* and combining TD and TI antigens could be of great importance to answer specific research questions (e.g. understanding B cell responses to specific viruses, bacteria or vaccines using adjuvants) it does not allow evaluation of the separate and distinct routes

of B cell activation that each are characterized by their own antibody output. Optimal conditions are still elusive and there are many determinant factors. Thus, this study was designed to investigate the most optimal B cell differentiation conditions with regards to several essential factors, i.e. using isolated $CD19^+$ B cells or PBMC cultures, multiple seeding densities, different durations of culturing and various combinations of TD stimuli or TI stimuli. B cell expansion, proliferation and differentiation was analyzed by flow cytometry after 6 and 9 days by measuring B cell numbers, Cell Trace Yellow (CTY) dilution, $CD27^+CD38^+$plasmablast and $CD27^+CD38^+CD138^+$ plasma cell formation and immunoglobulin (Ig) secretion in culture supernatants by Enzyme Linked Immunosorbent Assay (ELISA). In addition, these conditions were extrapolated using cryopreserved cells and differentiation potential of cryopreserved and freshly isolated cells were compared. Resulting protocols are 1-step and minimalistic, ensuring that results from different labs are comparable.

MATERIALS & METHODS

Literature review

In order to identify stimuli described in previously reported B cell differentiation protocols, a literature review was carried out using the following search terms: B cell culture, B cell expansion, B cell stimulation, B cell activation, human B cell differentiation, human plasma cell differentiation using the NCBI Pubmed database (https://www.ncbi.nlm.nih.giv/pubmed). The results of this literature review is summarized in **Table I**.

Cell lines

NIH3T3 fibroblasts expressing human CD40L ($3T3\text{-}CD40L^+$)[16] were cultured in IMDM (Lonza,Basel 4002, Switzerland) containing 10% FCS (Serana, 14641 Pessin, Germany), 100 U/mL penicillin (Invitrogen, through Thermo Fisher, 2665 NN Bleiswijk, The Netherlands), 100 µg/mL streptomycin (Invitrogen), 2 mM l-glutamine (Invitrogen), 50 µM β-mercaptoethanol (Sigma Aldrich, 3330 AA, Zwijndrecht, The Netherlands) and 500 µg/mL G418 (Life Technologies, through Thermo Fisher).

Isolation of PBMCs and B cells from human healthy donors

Buffy coats of healthy human donors were obtained from Sanquin Blood Supply. All the healthy donors provided written informed consent in accordance with the protocol of the local institutional review board, the Medical Ethics Committee of Sanquin Blood Supply, and the study conformed to the principles of the Declaration of Helsinki. The mean age of the healthy donors was 41,3 years at the time of blood withdrawal [range 27-61 years], male n=2, female n = 4. Peripheral blood mononucleated cells (PBMCs) were isolated from buffy coats using a Lymphoprep (Axis-Shield PoC AS, Dundee DD2 1XA, Scotland)

Table I. Frequently reported B cell differentiation stimuli for human naive and/or memory B cells in literature

Stimuli	Target(s)	Concentrations	Reference
Anti-IgM Anti-IgG/IgM F(ab')$_2$ Anti-IgG/IgA/IgM F(ab')$_2$	BCR	2, **5**, 10 µg/ml	(5), (17), (19), (27), (36), (37), (38), (39)
BAFF	BAFF-R. BMCA. TACI	75, **100** ng/ml	(36), (40)
aCD40, CD40L	CD40	50, 500 ng/ml 1, 5 µg/ml	(5), (17), (27), (38), (39), (41), (42), (43)
CD40L expressing L cells 3T3-CD40L fibroblasts	CD40	Various ratios of B cell : feeder cell	(3), (19), (36), (37)
CpG-ODN 2006	TLR9	1.0, 2.5, 3.2, 6.0, 10 µg/ml 0.35, **1.0** µM	(17), (27), (36), (38), (39), (40), (41), (42), (43)
IFNα	IFNAR	100, 500 U/ml	(37), (41)
IL-2	IL-2R	20, 50, 100 U/ml 25, **50** ng/ml	(3), (5), (37), (38), (39), (41), (42)
IL-4	IL-4R	10, **25**, 50, 100, 200 ng/ml	(3), (5), (17), (19), (36), (38), (41), (43)
IL-6	IL-6R	10, 50 ng/ml	(37), (41)
IL-10	IL-10R	25, 50, 200 ng/ml	(5), (36), (38), (41), (43)
IL-15	IL-15R	10 ng/ml	(36), (41)
IL-21	IL-21R	2, 20, **50**,100 ng/ml	(5), (19), (27), (36), (37), (39), (40), (42), (43)

*Abbreviations: BAFF: B cell activating factor. BCMA: B cell maturation antigen. IFN: interferon. IL: interleukin. ODN: oligodeoxynucleotide. TACI (TNFRSF13B): transmembrane activator and CAML interactor. TLR: toll like receptor. The used concentrations in this study are depicted in **bold**.*

density gradient. Afterwards, from half of the fraction of PBMCs, CD19$^+$ B cells were isolated using magnetic Dynabeads and DETACHaBEAD (Thermo Fisher) according to the manufacturer's instructions. The purity of B cells after isolation and the B cell compartment distribution at baseline was assessed by flow cytometry. All B cell isolations had a purity of >92%. Excess cells were resuspended to 20-50*10^6 cells per ml in culture medium and slowly cold freezing medium (80% DMSO / 20% FCS, Thermo Fisher) was added in a 1:1 ratio. The cell suspension was resuspended and divided over cryo-vials. Cells were frozen overnight to -80 ^{o}C in a Mr. Frosty and transferred to cryo-storage the next morning.

In vitro PBMC and B cell stimulation cultures

3T3-CD40L$^+$ were harvested, irradiated with 30 Gy and seeded in B cell medium (RPMI 1640, Gibco through Thermo Fisher) without phenol red containing 5% FCS, 100 U/mL penicillin, 100 µg/mL streptomycin, 2 mM L-glutamine, 50 µM β-mercaptoethanol and

20 µg/mL human apo-transferrin (Sigma Aldrich; depleted for human IgG with protein G sepharose (GE Healthcare, 3871MV, Hoevelaken, The Netherlands)) on 96-well flat-bottom plates (Nunc through Thermo Fisher) to allow adherence overnight. 3T3-CD40L$^+$ were seeded by adding 100 µl of 0.1*10^6 cells/ml (or 10,000) cells per well. In some experiments PMBCs were thawed from cryo-storage and washed with B cell medium. PBMCs or B cells were rested at 37 ˚C for 1h before counting. Then, 50 µl of CD19$^+$ B cells at a concentration of 0.005-, 0.05- or 0.5*10^6 cells/ml (250, 2500 or 25000 cells resp.) were co-cultured in duplicate in the presence or absence of PBMCs with the irradiated 3T3-CD40L$^+$ fibroblasts in TD settings or in 96-well U-bottom plates for TI settings. 50 µl of stimuli were added as indicated: F(ab')$_2$ fragment Goat Anti-Human IgA/G/M (5 µg/mL; Jackson Immunoresearch, Ely CB7 4EZ, UK), IL-4 (25 ng/mL; Cellgenix, 79107 Freiburg, Germany), IL-21 (50 ng/mL; Peprotech, London W6 8LL, UK), CpG ODN 2006 (1 µM, Invivogen), IL-2 (50 ng/ml, Miltenyi Biotec) and BAFF (100 ng/ml R&D) for up to 9 days. After adding the B cells to the wells, the plate was centrifuged for 1 min at 400x g to force all the cells onto the 3T3-CD40L$^+$ layer. Cryopreserved cells were thawed by agitating the tubes gently in a 37 ºC waterbath until only a small ice clump was left. The cells were transferred to a 50 ml tube and cold B cell medium was added drop-wise while the tube was constantly agitated.

CelltraceYellow labeling

CD19$^+$ B cells or PBMCs were washed with 10 ml PBS/0.1% bovine serum albumin (BSA, Sigma Aldrich) and resuspended to a concentration of 2x10^7 cells/ml in PBS/0.1%BSA. Cells and 10 µM CellTrace Yellow (Thermo Fisher Scientific) were mixed at a 1:1 ratio and incubated 20 minutes in a 37ºC waterbath in the dark, vortexing the tube every 5 minutes to ensure uniform staining. Cells were washed twice using a 10 times volume of cold culture medium to end labeling. Thereafter, B cells were cultured according to the protocol described above.

Flow cytometry

Wells were resuspended and transferred to 96-well V-bottom plates (Nunc). Cells were centrifuged 2 min at 600x g, supernatant was transferred to V-bottom plates, sealed with an ELISA sticker and stored at -20ºC. Samples were washed twice with 150 ul PBS/0.1%BSA. Cells were stained in a 25 µL staining mix with 1:1000 LIVE/DEAD Fixable Near-IR Dead cell stain kit (Invitrogen) and antibodies diluted in PBS/0.1% BSA for 20 minutes at RT in the dark (**Table II**). The samples were wash 2x with 150 ul PBS/0.1%BSA. Finally, the samples were resuspended in a volume of 140 µl, of which 90 µl was measured on a LSRII or FACSymphony flow cytometer. Samples were measured on LSRII or Symphony and analyzed using Flowjo software. The gating strategy is shown in **Figure S1**.

Table II. Antibodies used for flow cytometry.

Ab	Conjugate	Manufacturer	Clone	Catalog No.	Dilution*
CD19	BV510	BD	SJ25-C1	562947	1:100
CD20	PerCP-Cy5.5	BD	L27	332781	1:25
CD27	PE-Cy7	eBioscience	0323	25-0279-42	1:50
CD38	V450	BD	HB7	646851	1:100
CD138	FITC	BD	MI15	561703	1:50
IgG	BUV395	BD	G17-145	564229	1:100
IgM	APC	Biolegend	MHM-88	314510	1:100
CD3	PerCP	BD	SK7	345766	1:20
LIVE/DEAD	APC-Cy7	Invitrogen		L34976	1:1000

**Optimal antibody dilutions as defined for the method and staining procedure used in this paper. As the staining conditions and flow cytometer settings may differ per lab, it is advised that these dilutions are taken as guidelines and that these are validated within each individual lab.*

ELISA of culture supernatants

Supernatants of eligible conditions were tested for secreted IgG, IgA and IgM with a sandwich ELISA using polyclonal rabbit anti-human IgG, IgA and IgM reagents and a serum protein calibrator (X0908, Dako, Glostrup) all from Dako (Glostrup; product numbers A0423, Q0332 and A0425 respectively). The polyclonal rabbit anti-human IgG, IgA and IgM were diluted in coating buffer to a concentration of 5 µg/ml, then 100 µl was used to coat Nunc MaxiSorp flat bottom 96 well plates (Thermo Fisher) overnight at 4°C. Plates were washed with PBS/0.05% Tween- 20 and blocked with 100 µl PBS/1% bovine serum albumin (BSA) (Sigma Aldrich) for 1 hour at room temperature (RT). Plates were then washed and 100 µl of serum protein calibrator (X0908, Dako, Glostrup) or culture supernatant diluted in HPE buffer (M1940, Sanquin reagents) (1:25 for IgG and IgA and 1:30 for IgM) was added to each well and incubated for 1.5 hour at RT. Human serum protein low control (X0939, Dako, Glostrup) was used as reference sample on each plate. Following incubation and washing, 100 µl of detection antibody diluted in blocking buffer was added: poly rabbit anti-human IgG/HRP (1.3 g/L, 1:15,000), IgA/HRP (1.3 g/L, 1:15,000), and IgM/HRP (1.3 g/L, 1:10,000) (Dako, Glostrup; product numbers: P0214, P0215, P0216 respectively). Plates were washed and developed using TMB (00-4201-56, Invitrogen by Thermofisher), stopped using 1M H_2SO_4 stopping solution and read using the Biotek microplate reader (450-540nm) (Synergy HT, Biotek) and IgM, IgA and IgG concentrations were calculated relative to a titration curve of the serum protein calibrator.

Interference ELISA

The interference ELISA assay was developed as described in the sandwich ELISA above. Serial dilutions of $F(ab')^2$ fragment Goat Anti-Human IgA/G/M (5, 2.5, 1.25 and 0.625 µg/mL; Jackson Immunoresearch, Ely CB7 4EZ, UK) in HPE buffer (M1940, Sanquin reagents) were incubated (60 min, RT) with the standard curve dilutions of the serum protein calibrator (X0908, Dako, Glostrup). The results were plotted as titration curves.

Graphics

Schematic overviews were created using images from Servier Medical Art, which are licensed under a Creative Commons Attribution 3.0 Unported License (http://smart.servier.com).

Statistics

Statistical analysis was performed using GraphPad Prism (version 8; Graphpad Software). Data were analyzed using t tests, Repeated Measures one-way ANOVA or Repeated Measures two-way ANOVA where appropriate. Results were considered significant at $p < 0.05$. Significance was depicted as * ($p < 0.05$) or ** ($p < 0.01$), *** ($p < 0.001$) or **** ($p < 0.0001$). Correlation analyses between flow cytometry and immunoglobulin ELISA data were performed with Pearson's correlation test. *$p < 0.05$. The statistical tests performed are indicated in the figure legends.

RESULTS

Frequently reported B cell differentiation stimuli for human naive and/or memory B cells in literature

The first step in establishing optimized *in vitro* protocols for TD and TI stimulation of B cells to induce B cell differentiation was to identify frequently used and reported culture conditions by literature review (**Table I**). Following identification of a wide range of stimuli, together with consortium partner labs, standard TD and TI combinations were chosen using concentrations reflective of the publications obtained through literature review or by previous experimental work. For TD stimuli, the combination of CD40L and IL-21 was selected, a combination frequently used to mimic $CD4^+$ T cell help[5]. Although multiple methods of CD40L stimulation are reported (either soluble or using feeder cells), here a monolayer of feeder cells consisting of 3T3 mouse fibroblast expressing high levels of human CD40L was selected. For TI the combination of CpG, a well-known ligand of TLR-9, together with IL-2, a B cell survival factor, was set up[17, 18]. These combinations of stimuli were either constantly or most frequently used and therefore found to be essential.

Following the identification of CD40L and IL-21 as TD stimuli and CpG and IL-2 as TI stimuli, the effect of (1) culture duration and (2) different seeding densities (or starting B cell numbers) were determined. These experiments were performed with cells from healthy donors either using (3) purified $CD19^+$ B cells or (4) PBMC cultures corrected for B cell count, comprising of B cells and other PBMCs (mainly T cells and small fractions of monocytes and NK cells) since such cultures do not require B cell isolation and are thus more practical for routine use. For this, PBMCs from the same healthy donors were used to avoid donor variability. Additionally, the augmenting effect of (5) additional stimuli, i.e. anti-BCR and IL-4 for TD, anti-BCR and BAFF for TI, was investigated and (6) the effect of cryopreservation on B cell differentiation potential was checked. All conditions were cultured in duplicate.

Efficient *in vitro* B cell differentiation after 9 days using T cell-dependent stimulation with CD40L and IL-21 using 2500 starting B cells

In the TD assay either 25.000, 2500 or 250 starting B cells were co-cultured with CD40L-feeder cells and IL-21 enabling 3 conditions, from now on referred to as condition I, II and III (**Figure 1A**). Due to these settings, different ratios of B cell to feeder cell (1:0.4, 1:4 and 1:40 respectively) were created, resulting in different availability of CD40L during culturing. For each condition, B cell expansion and proliferation was assessed by flow cytometry after 6 and 9 days as well as plasmablast ($CD27^+CD38^+$) and plasma cell ($CD27^+CD38^+CD138^+$) formation (for gating strategy, see **Figure S1**). Additionally, the IgG, IgA and IgM secretion was measured by ELISA in culture supernatants, which acts as a second readout for B cell differentiation as B cells differentiate from surface Ig-expressing cells to Ig-secreting cells.

To assess expansion of B cells during culturing, the number of $CD19^+$ live B cells were determined. The conditions II and III showed significant more $CD19^+$ live B cells compared to its specific starting B cell numbers at day 6 and day 9 whilst a significant decline in $CD19^+$ live B cells in condition I was observed (**Figure 1B).** Condition II showed a 4-fold amplification (± 0.6; n=4) on day 6 and a 4-fold amplification (± 1.3; n=4) on day 9 compared to its starting B cell number (**Table III**). Condition III showed a 7-fold amplification (± 0.9; n=4) on day 6 and a 27-fold amplification (± 5.2; n=4) on day 9. Interestingly, in all three conditions a similar yield of $CD19^+$ live B cells was detected at day 9, but not at day 6, whilst the starting B cell numbers was different, i.e. 10-100-fold. As shown before, this suggests that the amount of available CD40L critically influences B cell survival and/or expansion during culture[19]. For further FACS analysis, we set a cut-off value at a minimum of 1000 events of $CD19^+$ live B cells. To assess proliferation, B cells were labeled with Cell Trace Yellow (CTY) prior to culturing. Proliferation was observed in all conditions at day 6 (**Figure 1C**), however conditions II and III showed a significant higher dilution of CTY in accordance with the amplification in cell numbers observed. A significant increase in the percentage of $CD27^+CD38^+$ cells between day 6 and day 9 in each condition was observed, suggesting that a 9-day culture period induced higher levels of differentiation (**Figure 1D).** However, we did not observe differences in plasma cell formation between day 6 and day 9 (**Figure 1E**) and there was no significant difference between the 3 culture conditions (statistics not shown). Measurement of secreted IgG, IgA and IgM showed a significant increase between day 6 and day 9, confirming a 9-day culture period induces higher levels of differentiation and Ig secretion (**Figure 1F**)**.** Notably, although the yield of $CD19^+$ live B cells and phenotypically differentiated plasmablasts and plasma cells was comparable in each condition at day 9, different Ig secretion patterns between the 3 conditions was observed. When we compared the 3 conditions in the flow cytometry analysis, significantly higher percentages of $CD27^-CD38^+$ B cells were observed in condition II and III (**Figure S2A and B**).

Table III. B cell survival and proliferation during different B cell differentiation conditions

Isolated CD19$^+$ B cells (TD)	**Condition I**		**Condition II**		**Condition III**	
Starting B cell number	25.000		2500		250	
3T3-CD40L cell	10.000		10.000		10.000	
Ratio B cell : 3T3-CD40L cell	1 : 0.4		1 : 4		1 : 40	
Cytokines	IL-21		IL-21		IL-21	
Mean CD19$^+$ live cells						
Day 0	25.000		2500		250	
Day 6	12438	± 3120; n=4	9736	± 1566; n=4	1656	± 224; n=4
Day 9	8012	± 2643; n=4	8899	± 3196; n=4	6769	± 1305; n=4
Mean amplification (compared to starting B cell number)						
Day 6	0.5	± 0.1; n=4	3.9	± 0.6; n=4	6.6	± 0.9; n=4
Day 9	0.3	± 0.1; n=4	3.6	± 1.3; n=4	27.1	± 5.2; n=4
PBMCs (TD)	**Condition I.2**		**Condition II.2**		**Condition III.2**	
Starting B cell number	25.000		2500		250	
3T3-CD40L cell	10.000		10.000		10.000	
Ratio B cell : 3T3-CD40L cell	1 : 0.4		1 : 4		1 : 40	
Cytokines	IL-21		IL-21		IL-21	
Mean CD19$^+$ live cells						
Day 0	25.000		2500		250	
Day 6	8601	± 1397; n=3	14487	± 4320; n=3	4139	± 311; n=3
Day 9	6019	± 695; n=3	7819	± 2713; n=3	12826	± 3750; n=3
Mean amplification (compared to starting B cell number)						
Day 6	0.3	± 0.1; n=3	5.8	± 1.7; n=3	16.6	-
Day 9	0.2	± 0.1; n=3	4.2	± 1.1; n=3	51.3	-
Isolated CD19$^+$ B cells (TI)	**Condition IV**		**Condition V**		**Condition VI**	
Starting B cell number	25.000		2500		250	
TLR ligand	CpG		CpG		CpG	
Cytokines	IL-2		IL-2		IL-2	
Mean CD19$^+$ live cells						
Day 0	25.000		2500		250	
Day 6	4751	± 1397; n=4	85	± 22.7; n=4	17	± 2.3; n=4
Day 9	1571	± 695; n=4	29	± 13.8; n=4	2	± 0.8; n=4
Mean amplification (compared to starting B cell number)						
Day 6	0.2	± 0.1; n=4	-	-	-	-
Day 9	0.1	± 0.0; n=4	-	-	-	-

PBMCs (TI)	Condition IV.2		Condition V.2		Condition VI.2	
Starting B cell number	25.000		2500		250	
TLR ligand	CpG		CpG		CpG	
Cytokines	IL-2		IL-2		IL-2	
Mean $CD19^+$ live cells						
Day 0	25.000		2500		250	
Day 6	8978	± 1985; n=3	3823	± 1983; n=3	58	± 18; n=3
Day 9	7841	± 2127; n=3	2463	± 1055; n=3	47	± 26; n=3
Mean amplification (compared to starting B cell number)						
Day 6	0.4	± 0.1; n=3	1.5	± 0.8; n=3	-	-
Day 9	0.3	± 0.1; n=3	1.0	± 0.4; n=3	-	-

Purified B cells or non-purified B cells (PBMC cultures) were cultured using a 1-step culture system for 6 and 9 days with either TD (CD40L + IL-21) or TI (CpG + IL-2) stimuli. On day 6 and day 9 cell counts and viability were determined using flow cytometry with fluorochrome-conjugated Live/Dead and anti-CD19. Results are shown as the mean ± SEM of n = 4 (B cell cultures) or n = 3 (PBMC cultures) donors. – indicates no further analysis due to <1000 $CD19^+$ live events.

In parallel experiments, PBMCs (corrected for 250, 2500 and 25.000 B cells) were cultured in similar conditions, which created conditions I.2, II.2 and III.2 (**Figure S3A**). Here, we observed again significantly more B cell expansion and proliferation in condition II.2 and III.2 with higher CD40L availability (**Figure S3B and C**, **Table III**). The number of $CD19^+$ live cells and dilution of CTY showed similar results as in condition I, II and III suggesting limited effect of the presence of PBMCs with CD40L and IL-21 stimulation. Proliferation analysis of $CD3^+$ T cells did not show any increased proliferation compared to unstimulated controls, indicating that the used stimuli did not activate T cells which would influence B cell differentiation (data not shown). Again, there was no significant difference between the 3 conditions (statistics not shown) (**Figure S3D**). No effect was observed of the presence of PBMCs on the efficacy of plasmablasts or plasma cell induction (**Figure 1D and E**, **Figure S3D and E**). Ig measurements in the supernatants of the PBMC cultures showed a significant increase in IgA and IgM secretion between day 6 and 9, indicating that a 9-day culture period induces higher levels of differentiation and Ig secretion (**Figure 3F**).

Taken together, condition I, II and III with 250, 2500, 25.000 starting B cells respectively were all suitable for generating $CD27^+CD38^+$ plasmablasts and IgG secretion at day 9, two important hallmarks of B cell differentiation. The optimal differentiation conditions for TD stimulation with limited numbers of B cells was defined here as condition II and II.2, being 2500 $CD19^+$ cells per 96-well with or without other PBMCs, which were used for further experiments.

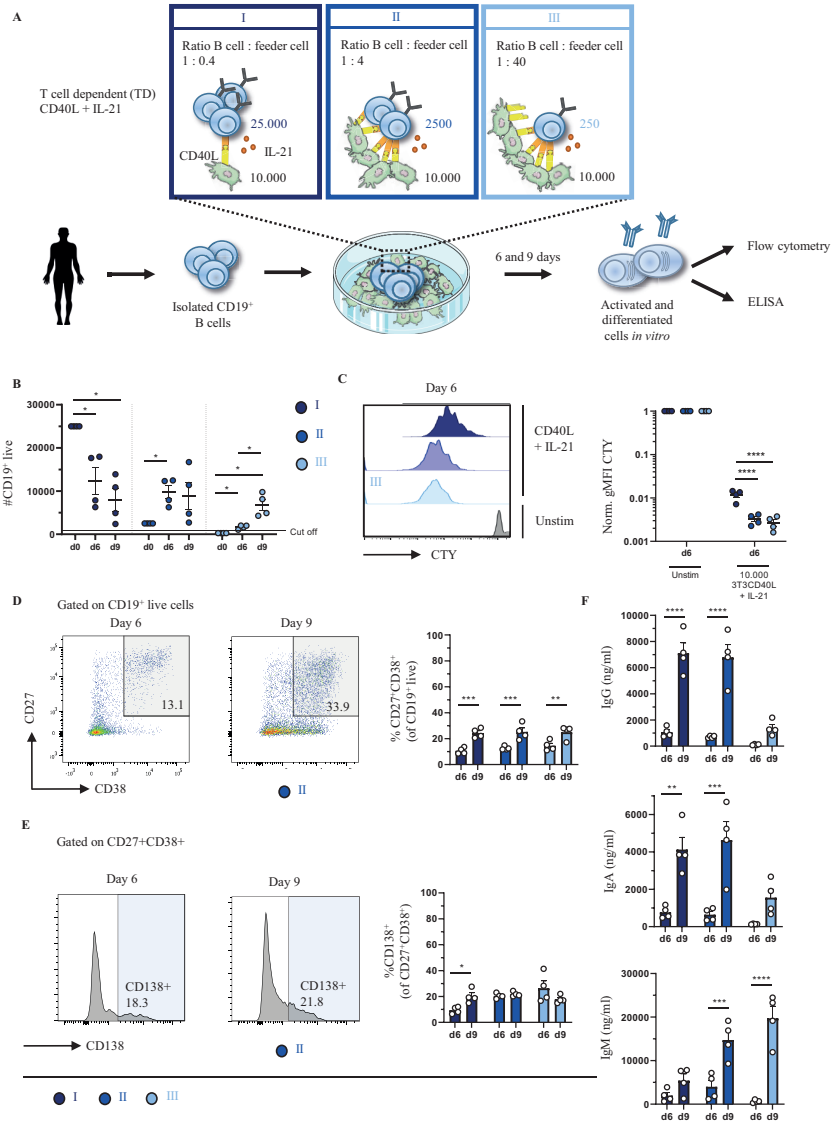

Figure 1. Proliferation, differentiation and antibody production after T cell dependent in vitro stimulation and culturing of low numbers of primary human CD19⁺ B cells. *(**A**) Schematic overview of the T cell dependent (TD) culture system to induce B cell differentiation. A total of 25000, 2500 or 250 CD19⁺ human B cells (n = 4) were stimulated with a human-CD40L-expressing 3T3 feeder layer and recombinant IL-21 (50 ng/mL) enabling condition I (dark blue), II (cobalt blue) and III (light blue). Cells were analyzed at day 6 and day 9 by flow cytometry to evaluate (**B**) number of live CD19⁺ events, (**C**) amount of proliferation by CTY dilution and frequency of (**D**) plasmablast (CD27⁺CD38⁺ B cells) and (**E**) plasma cell (CD27⁺CD38⁺CD138⁺ B cells). A cut off of 1000 events was used to proceed with further analysis. (**F**) The supernatant was collected at day 6 and day 9 to evaluate IgG, IgA and IgM production by ELISA (n = 4). Each data point represents the mean of an individual donor with duplicate culture measurements. Mean values are represented by bars and the error bars depict SEM. P values were calculated using two-way ANOVA with Sidak's multiple comparison test. * p < 0.05, ** p < 0.01, *** p < 0.001, **** p < 0.0001.*

CD40L and IL-21 stimulation in combination with anti-BCR and/or IL-4 does not increase B cell differentiation and immunoglobulin secretion

In an attempt to drive differentiation and expansion even further in our 1-step *in vitro* B cell differentiation assay, the effect of additional stimuli in our culture conditions was tested. For this purpose, the reference stimuli CD40L and IL-21 were combined with or without $F(ab)_2$ fragments targeting IgM, IgG and IgA to induce BCR signaling (also referred to as anti-BCR). Secondly, we tested whether the addition of IL-4, a cytokine important for naive B cells during the GC reactions, can augment *in vitro* B cell differentiation induced by CD40L and IL-21. In these cultures, 2500 freshly isolated $CD19^+$ B cells (condition II) or

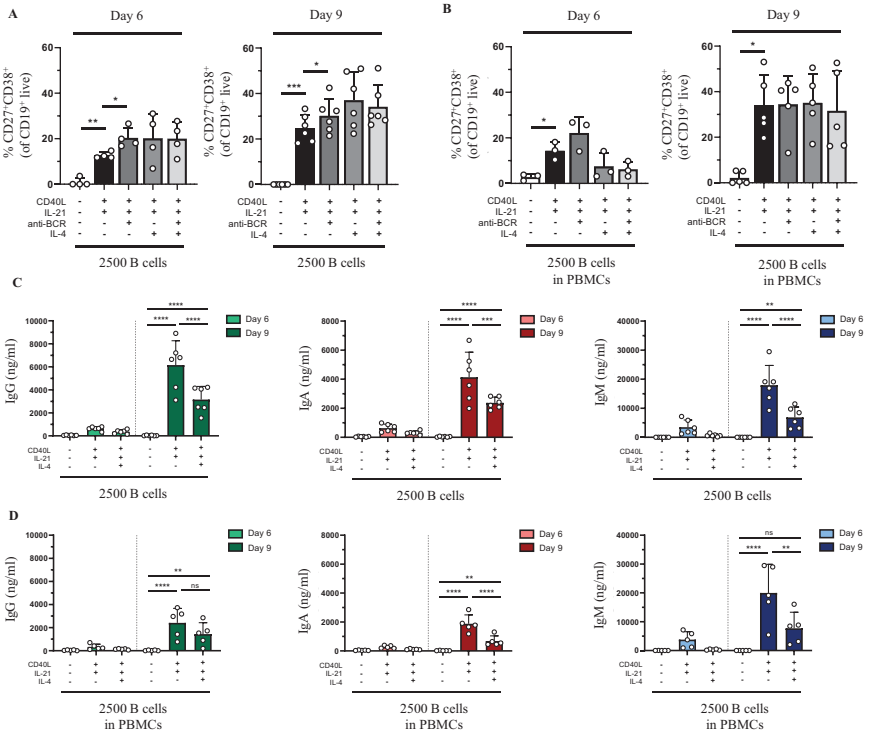

Figure 2. Addition of anti-BCR stimuli in a T cell dependent stimulation results in increased B cell differentiation while IL-4 severely inhibits antibody production. *Human primary B cells obtained from healthy donors were stimulated under conditions described in* ***Figure 1A*** *(condition II) and* ***Figure S2A*** *(condition II.2, PBMC cultures) with or without anti-BCR (anti-Ig $F(ab')_2$ mix (5 µg/mL) targeting IgM, IgG and IgA) and/or recombinant IL-4 (25 ng/mL). Frequencies of $CD27^+CD38^+$ B cells on day 6 and day 9 in (**A**) condition II and (**B**) condition II.2 (n = 4-6). (**C-D**) Total secretion of IgG, IgA and IgM measured in culture supernatants of eligible conditions after 6 and 9 days (**C**) without PBMCs (condition II) and (**D**) within PBMC cultures (condition II.2). Each data point represents the mean of an individual donor with duplicate culture measurements. Mean values are represented by bars and the error bars depict SEM. P values were calculated using one-way ANOVA with Dunnett's multiple comparison test (A-B) or two-way ANOVA with Sidak's multiple comparison test (C-D). . * p < 0.05, ** p < 0.01, *** p < 0.001, **** p < 0.0001.*

PBMCs corrected for B cell number (2500 B cells; condition II.2) were used from the same donors shown in the previous experiments. Flow cytometry was performed on day 6 and day 9 to classify $CD19^+$ cells as $CD27^+CD38^+$ plasmablasts and IgG, IgA and IgM secretion was measured in culture supernatants. In condition II we observed a significant increase in plasmablasts upon adding anti-BCR both on day 6 as on day 9 compared to CD40L and IL-21 alone (**Figure 2A**). In condition II.2 no combination of stimuli was superior to CD40L and IL-21 (**Figure 2B**). Prolonged culture to 9 days allowed a significant increase in plasmablasts in all 4 combinations of stimuli both in condition II and II.2 (statistics not shown). As addition of anti-BCR and/or IL-4 stimulation to conditions I, II or III (and PBMC culture variants of these) could also affect proliferation of $CD19^+$ cells this was investigated, showing no significant differences (**Figure S4A and B**). In the main condition with 2500 cells, significantly less cells were found when adding IL-4 to isolated $CD19^+$ cultures at day 6 but not on day 9, or in PBMC cultures (**Figure S4C and D**). As use of the mixture of $F(ab)_2$ fragments in our cultures might interfere with the IgG, IgA and IgM ELISA assay, an interference ELISA was performed. Indeed, we observed a decrease in measured IgG, IgA and IgM when $F(ab)_2$ fragments in different concentrations were added to the standard curve (**Figure S5A-C**). Therefore, samples containing anti-BCR stimulation were excluded for further analysis of secreted Ig. Although the percentages of plasmablasts on day 9 were similar (or higher) upon addition of IL-4, we observed significant lower secreted IgG, IgA and IgM in culture supernatants in the conditions where IL-4 was added (**Figure 2C and D**). In conclusion, an augmenting effect of anti-BCR on TD induced B cell differentiation was found but its use prevents Ig secretion analysis. Notably, although we observed no significant effect on plasmablast differentiation, IL-4 reduced Ig secretion under all conditions tested.

Efficient *in vitro* B cell differentiation after 6 days using TI stimulation with CpG and IL-2 with 25.000 starting B cells

In the TI assay the effect of (1) culture duration and (2) different seeding densities (or starting B cell numbers) were also determined. Again 25.000, 2500 or 250 $CD19^+$ B cells were cultured, enabling condition IV, V and VI (**Figure 3A**). We assessed B cell differentiation by flow cytometry analysis and measurements of Ig secretion on day 6 and day 9. Culturing $CD19^+$ B cells with TI stimuli resulted in a decline in $CD19^+$ B cells (**Figure 3B**, **Table III).** Flow cytometry analysis of condition V and VI showed less than 1000 events on day 6 and day 9 and these conditions were therefore excluded from further analysis. In condition IV, a significant decline in $CD19^+$ live cells was observed on day 9 compared to day 6, with two out of 4 donors not meeting the cut-off of 1000 events, thus longer culture periods under TI conditions results in lower B cell survival and/or expansion. Samples eligible for further flow cytometry analysis showed sufficient proliferation on day 6 (**Figure 3C**). There was no significant difference between day 6 and day 9 in terms of $CD27^+CD38^+$ plasmablasts, but a significant increase in $CD27^+CD38^+CD138^+$ plasma cells on day 9 (**Figure 3D and E**). Accordingly, a small increase of secreted IgG, IgA and IgM in culture supernatants was observed on day 9 (**Figure 3F**).

Extrapolation of the TI conditions to PBMC cultures enabled conditions IV.2, V.2 and VI.2 (**Figure S6A**). Consistent with condition IV, we observed a significant decrease in CD19$^+$ live B cells condition IV.2 (**Figure S6B**). Interestingly, we observed a 1.0 and 1.5-fold (± 0.8; n=3, ± 0.4; n=3) amplification of B cell numbers on day 6 and 9 in condition V.2, which provided sufficient B cell numbers for further analysis (in contrast to condition V) (**Figure S6B, Table III**). As shown before, this suggests an additional pro-survival effect of PBMCs in these culture[17]. Condition VI.2 did not meet de cut off of 1000 events and was also excluded from further analysis. Proliferation analysis by CTY dilution showed a significant difference in proliferation of CD19$^+$ live B cells at day 6 between conditions IV.2

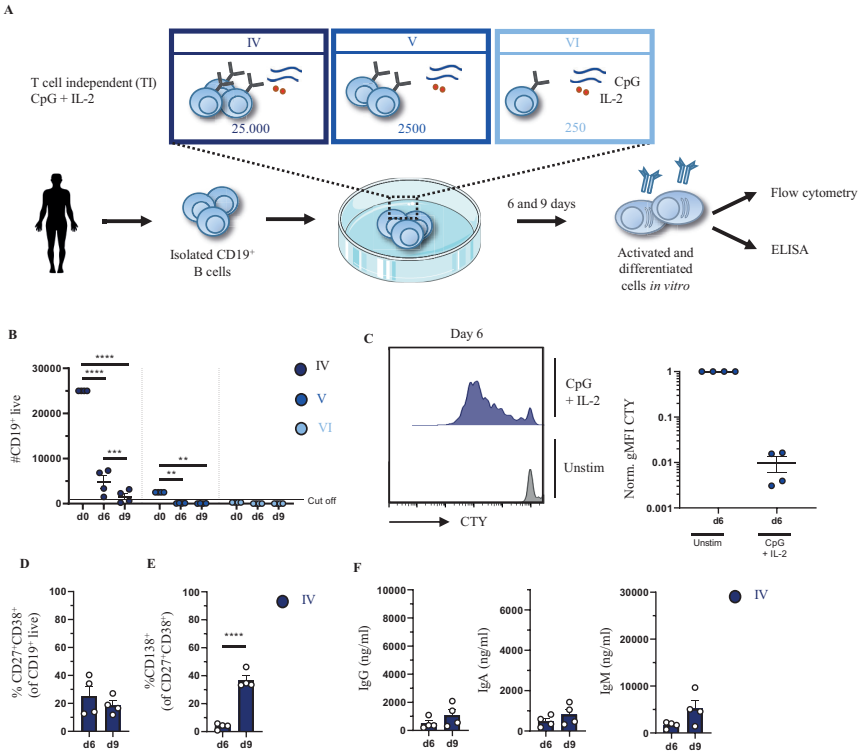

Figure 3. Proliferation, differentiation and antibody production after T cell independent in vitro stimulation and culturing of low numbers of primary human CD19$^+$ B cells. ***(A)*** *Schematic overview of the T cell independent (TI) culture system to induce B cell differentiation. A total of 25000, 2500 or 250 CD19$^+$ human B cells (n = 4) were stimulated with CpG (1 µM) and IL-2 (50 ng/ml) enabling condition IV (dark blue), V (cobalt blue) and VI (light blue). Cells were analyzed at day 6 and day 9 by flow cytometry to evaluate* ***(B)*** *number of live CD19$^+$ events,* ***(C)*** *amount of proliferation by CTY dilution and frequency of* ***(D)*** *plasmablast (CD27$^+$CD38$^+$) and* ***(E)*** *plasma cell (CD27$^+$CD38$^+$CD138$^+$) generation. A cut off of 1000 events was used to proceed with further analysis.* ***(F)*** *The supernatant was collected at day 6 and day 9 to evaluate IgG, IgA and IgM production by ELISA (n = 4). Each data point represents the mean of an individual donor with duplicate culture measurements. Mean values are represented by bars and the error bars depict SEM. P values were calculated using two-way ANOVA with Sidak's multiple comparison test (B) or unpaired t test (D-F). * p < 0.05, ** p < 0.01, *** p < 0.001, **** p < 0.0001.*

and V.2 (**Figure S6C**). Proliferation analysis of $CD3^+$ T cells showed minimal proliferation compared to unstimulated controls in the conditions IV.2 and V.2, which suggests that the used stimuli (likely IL-2) could activate the T cells in these PBMC cultures possibly influencing B cell differentiation (**Figure S6D**). Further analysis showed no significant difference between day 6 and day 9 in terms of plasmablasts and plasma cells (**Figure S6E and F**). Despite the lack of increase in the percentages of $CD27^+CD38^+$ plasmablasts and $CD27^+CD38^+$ $CD138^+$ plasma cells between day 6 and day 9, a small increase of secreted IgG, IgA and IgM was observed in culture supernatants on day 9 in condition IV.2 and V.2 (**Figure S6G**). These experiments identified condition IV and condition IV.2, being 25.000 $CD19^+$ cells per well, as most suitable for the assessment of B cell differentiation using TI stimulation.

CpG and IL-2 induced B cell differentiation can be amplified by anti-BCR and BAFF stimulation

To assess potential further assay optimization, the effect of additional stimuli to augment TI induced differentiation was investigated. For this purpose, anti-BCR stimulation with or without B cell activating factor (BAFF), another well-known survival factor and differentiation signal for B cells, were supplemented to the reference stimuli CpG and IL-2. Studies primarily done *in vitro* have shown that BAFF can be expressed by different immune cell types (including monocytes, macrophages, follicular dendritic cells), which BAFF-producing cells contribute to specific B cell responses *in vivo* is not yet understood[20-22]. In these cultures, 25.000 freshly isolated $CD19^+$ B cells (condition IV) or PBMCs corrected for B cell number (25.000 B cells; condition IV.2) were used from the same donors shown in the previous experiments. We observed a small increase in plasmablasts upon addition of anti-BCR and/or BAFF both on day 6 and day 9 in condition IV but not in IV.2 suggesting that anti-BCR, BAFF or a combination of both can amplify plasmablast formation in the cultures without the presence of other PBMCs (**Figure 4A and B**). Prolonged culture to 9 days did not result in higher percentages of plasmablasts in any 4 combinations of stimuli both in condition IV and IV.2 (statistics not shown). Analysis of samples without anti-BCR stimulation showed that in condition IV the addition of BAFF resulted in significant higher secreted IgG, IgA and IgM in culture supernatants, while this effect was not present in condition IV.2 where other PBMCs were present (**Figure 4C and D**). As addition of anti-BCR and/or BAFF stimulation to conditions IV, V or VI (and PBMC culture variants of these) could also affect proliferation of $CD19^+$ cells this was investigated, showing no significant differences (**Figure S7A andB**). In the main condition with 2500 cells, significantly more cells were found when anti-BCR stimulation was added to isolated $CD19^+$ cultures at day 6 but not on day 9 (**Figure S7C**). In PBMC cultures there is a trend towards higher $CD19^+$ counts when BAFF is present although this was not significant (**Figure S7D**). Taken together, the addition of BAFF stimulation to CpG and

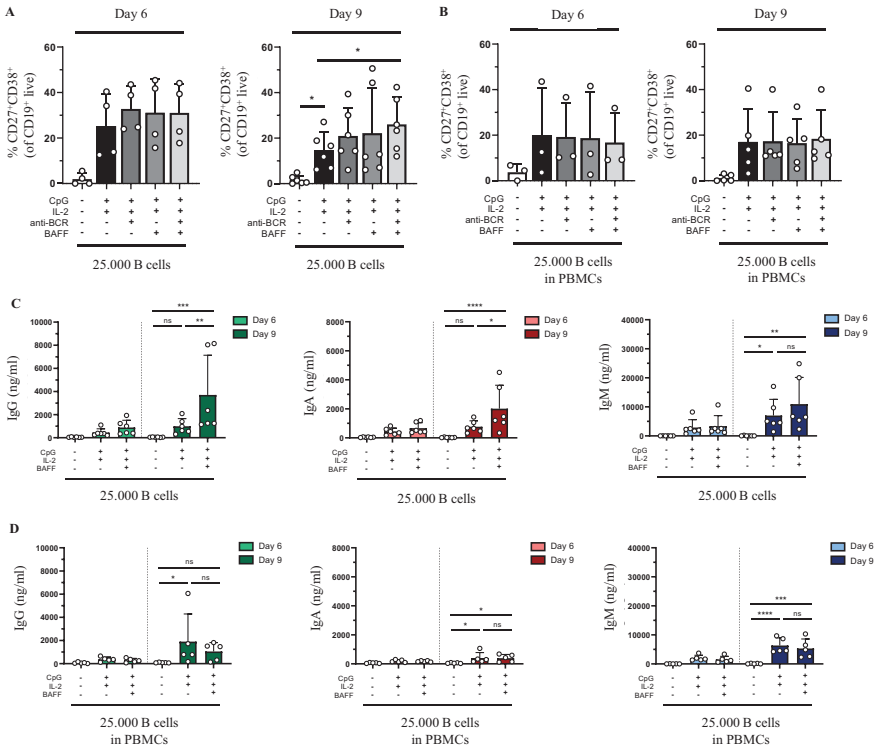

Figure 4. Addition of BAFF in a T cell independent stimulation results in increased IgG and IgA production in isolated B cell cultures. *Human primary B cells obtained from healthy donors were stimulated under conditions described in* ***Figure 3A*** *(condition IV) and* ***Figure S4A*** *(condition IV.2, PBMC cultures) with or without anti-BCR (anti-Ig F(ab')$_2$ mix (5 µg/mL) targeting IgM, IgG and IgA) and/or BAFF (100 ng/mL). Frequencies of CD27$^+$CD38$^+$ B cells on day 6 and day 9 in (**A**) condition IV and (**B**) condition IV.2 (n = 3-5). (C-D) Total secretion of IgG, IgA and IgM measured in culture supernatants of eligible conditions after 6 and 9 days (**C**) without PBMCs (condition IV) and (**D**) as PBMC culture (condition IV.2). Each data point represents the mean of an individual donor with duplicate culture measurements. Mean values are represented by bars and the error bars depict SEM. P values were calculated using one-way ANOVA with Dunnett's multiple comparison test (A-B) or two-way ANOVA with Sidak's multiple comparison test (C-D). * p < 0.05, ** p < 0.01, *** p < 0.001, **** p < 0.0001.*

IL-2 augments TI induced differentiation and Ig secretion upon culturing purified B cells, but this effect is absent in PBMC cultures.

Proportion of CD27-expressing and class-switched cells at start of culture correlate with *in vitro* induced differentiation and Ig-secretion

The ratio of naive to memory cells or the proportion of IgM or Ig-switched cells at the start of culture could be a determining factor for both TD and TI culture results. Thus, we investigated if specific B cell memory- or Ig-subsets at day 0 (**Figure S8**) correlated with culture end-points such as CD27$^+$CD38$^+$ plasmablast differentiation and IgG, IgA and IgM

secretion in culture supernatant. This analysis demonstrated that mainly the proportion of $CD27^+$ cells at the start of culture correlates with differentiation into $CD27^+CD38^+$ cells at day 6 and 9 in both TD and TI stimuli **(Table SI and SII).** Interestingly, the CD40L, IL-21 and IL-4 stimulation shows a negative correlation between the proportion of $CD27^+$ cells and differentiation (**Table SI**). This negative correlation is however again reversed when anti-BCR stimulation is also added. With regards to Ig-specific secretion, the addition of IL-4 positively correlated with day 6 IgG concentrations but negatively correlated with day 9 IgG concentrations. In TI conditions, the proportion of $CD27^+IgG^+$ and $CD27^+IgM^-$ cells positively correlated with $CD27^+CD38^+$ differentiation in all combinations of CpG, IL-2, BAFF and anti-BCR stimuli, indicating that these subsets undergo more efficient differentiation in response to these stimuli compared to other subsets. With regards to Ig-specific secretion, a higher proportion of $CD27^-$ cells at the start of culture negatively correlated with IgG and IgA secretion. Taken together, the proportion $CD27^+$ and isotype-specific subsets does significantly determine the result of TD and TI cultures.

Preserved *in vitro* B cell differentiation in cryopreserved PBMCs

The decision to use fresh PBMCs or cryopreserved PBMCs for an assay or study will depend on the assay itself as well as the logistics of handling of samples. Collection of patient samples often involves freezing of samples, therefore the effect of freezing and thawing was assessed on the B cell differentiation potential in our optimized TD and TI assays. For this purpose, the B cell differentiation experiments were repeated on frozen samples of previously used healthy donors, either total PBMCs or isolated $CD19^+$ B cells from thawed PBMCs, and assessed their B cell proliferation, differentiation potential by plasmablast formation using FACS and Ig secretion. Interestingly, the $CD19^+$ counts showed an increase in TD stimulated frozen samples compared to fresh samples, although this difference was not significant (**Figure S9A and B**). These trends were less clear in TI stimulated frozen samples (**Figure S9C and D**). Using the culturing conditions II and II.2 described above with CD40L and IL-21 stimulation, with or without IL-4, we detected a tendency to generate less $CD27^+CD38^+$ plasmablasts and subsequently lower secretion of IgG, IgA and IgM in supernatants of frozen samples after 6 and 9 days of culturing in all conditions tested, although we found no significant difference using the preferred CD40L and IL-21 stimulation (**Figure 5A and B**, **Figure S10A and B**). Using the aforementioned conditions IV and IV.2 starting with 25.000 B cells and CpG and IL-2 stimulation supplemented with or without BAFF, again, we observed lower percentages of $CD27^+CD38^+$ plasmablasts and IgG, IgA and IgM secretion in culture supernatants after 6 and 9 days of culturing when compared to their matched fresh sample (**Figure 5C and D**, **Figure S10C and D**). Thus, B cells obtained from cryopreserved PBMCs retain their ability to differentiate after *in vitro* culturing using TD and TI stimulation though we observed a small decrease in their differentiation potential.

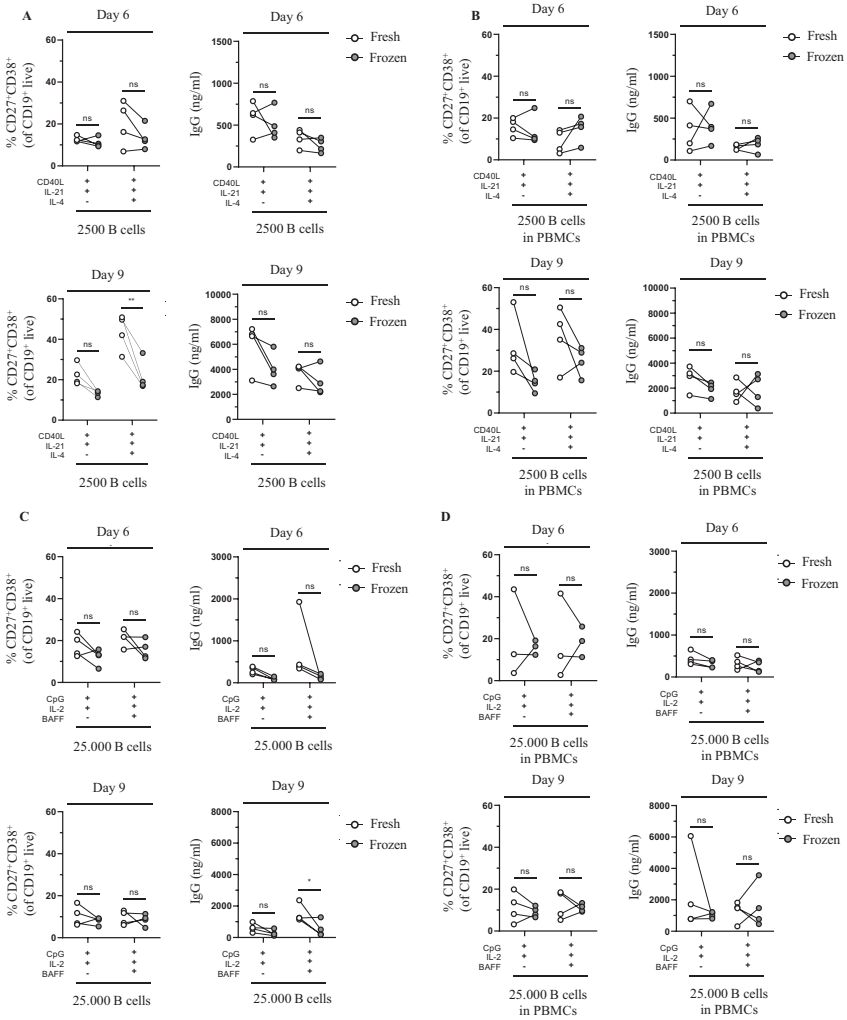

Figure 5. Cryopreserved B cells respond similarly to freshly isolated cells in T cell dependent and independent assays. *Total human B cells were isolated from fresh PBMCs (indicated in white) or frozen PBMCs (indicated in gray) and cultured for 6 and 9 days (n=4). (**A-B**) Using T cell dependent (TD) stimuli (CD40L and IL-21 with/without IL-4) 2500 B cells (fresh and frozen) were cultured under conditions described previously (**A**) without PBMCs (condition II) and (B) as PBMC culture (condition II.2). Frequencies of CD27⁺CD38⁺ B cells (left panel) and IgG production (right panel) on day 6 (upper graphs) and day 9 (lower graphs) are shown. (**C-D**) Using T cell independent (TI) stimuli (CpG and IL-2 with/without BAFF) 25000 B cells (fresh and frozen) were cultured under conditions described previously (**C**) without PBMCs (condition IV) and (**D**) with PBMCs (condition IV.2). Frequencies of CD27⁺CD38⁺ B cells (left panel) and IgG production (right panel) on day 6 (upper graphs) and day 9 (lower graphs) are shown. Each data point represents the mean of an individual donor with duplicate culture measurements. Mean values are represented by bars and the error bars depict SEM. P values were calculated using two-way ANOVA with Sidak's multiple comparison test. * $p < 0.05$.*

DISCUSSION

In this study we report optimized and efficient protocols for *in vitro* B cell differentiation using both TD and TI stimulation while requiring very low numbers of B cells. This has been accomplished by comparing several factors essential for optimal expansion, proliferation and differentiation of B cells, including stimulation duration, seeding density and combinations of activating stimuli reported in various publications for *in vitro* B cell differentiation. Here, we provide a 1-step culture system starting with isolated $CD19^+$ B cells or PBMCs corrected for B cell counts. We demonstrate successful generation of plasmablasts and plasma cells by measuring different parameters, including phenotypic markers (CD27, CD38 and CD138) combined with functional characteristics (IgG, IgA and IgM secretion). Despite the small decrease in differentiation efficiency when using cryopreserved samples, there are numerous reasons why using frozen PBMCs is favored over fresh samples. The two main reasons being that patient sampling is often done in outpatient clinics that are not in close proximity to laboratory facilities where cellular assays are performed. Secondly, patient cohorts are often sampled longitudinally and to prevent assay-to-assay variation, samples are stored for prolonged periods of time and thawed simultaneously. The loss in assay sensitivity in regards to differentiation may be minimized by narrowing down the time span in which all samples are handled or by taking along a known control. However, it should be noted that controls are preferentially also frozen PBMCs and handled in a comparable manner as the patient samples. The low number of required B cells determined here is ideal as patient samples are scarce and have value for multiple immunological assays. We believe that the conclusions and recommendations from this study will provide a base for optimized protocols that can be used to study patient related differences amongst patient cohorts of B cell mediated diseases and to screen compounds that target B cell differentiation.

To date, a plethora of different conditions for inducing B cell differentiation have been published (summarized in **Table I**). The strength of the current study is the inclusion and comparison of many variables and different stimuli. However, due to study size limitations it was not possible to include and compare all previously reported stimuli. The chosen reference stimuli for the TD assay, CD40L and IL-21, mimics the *in vivo* activation and differentiation in germinal centers (GCs), where B cells interact with CD40L and IL-21 expressing follicular T helper cells[1, 23]. In our experience, CD40L-expressing fibroblasts are the strongest activators of B cells by providing sufficient CD40 binding and crosslinking (data not shown). Interestingly, in both B cell and PBMC assay different kinetics of B cell expansion, proliferation and Ig secretion were observed when the ratio of starting B cell to 3T3-CD40L feeder cell was increased. Specifically, in condition III and III.2, starting with only 250 B cells, very high levels of IgM (but limited IgG) were observed on day 9, coinciding with an increased percentage of B cells with a $CD27^-CD38^+$ transitional-like

phenotype. It is important to note that comparing the three conditions in terms of absolute Ig production during the 6- and 9-day culture period has its limitations as the number of B cells during these culture periods differed to great extent and this could influence the height of Ig secretion (**Figure 1B**, **Figure S2B**). In our data higher availability of CD40L resulted in increased expansion of B cells and, despite cell number differences, a higher ratio of secreted IgM compared to IgA and IgG. As many facets of B cell differentiation are linked to cell division, it is possible that the timing of isotype switching or the outgrowth of specific B cell subsets occurs differently in these culture settings. Since we studied B cell differentiation in bulk B cells and PBMCs, the specific effects of CD40L on naive B cells, IgM^+- or isotype switched-memory cells cannot be distinguished. These subsets however have been shown to have different requirements for stimulation with regard to differentiation into antibody-secreting cells[24, 25]. Although we cannot make firm conclusions based on our data, it suggests and is in agreement with previous data that CD40 co-stimulation together with IL-21 regulates B cell differentiation and Ig production, and that these read-outs are driven by CD40L availability[19]. However, we acknowledge that the effect of media exhaustion could also play a role in these cultures. Refreshing the culture media could lead to increased differentiation and Ig secretion, specifically in cultures with higher starting cell numbers. This was not opted for in the current study as we sought to maintain a one-step, easy and simple culture to be used in clinical studies. Concluding from our data, we choose 2500 B cells as the optimal starting number to not preferentially outgrow specific subpopulations or isotypes. In order to mimic the *in vivo* response to cognate antigen more closely, we added an anti-BCR trigger[26]. However, we show that this hampers Ig detection. This has to be taken into account when these assays are applied for specific research questions where omitting an anti-BCR trigger is not desirable. The same holds true for adding IL-4 to the assays. Previously, we have shown that IL-4 addition is beneficial for B cell differentiation of naive B cells but only in circumstances with low CD40L stimulation[19]. In accordance with other studies using total $CD19^+$ B cells, we show that continuous IL-4 in our assay hampers Ig secretion compared to CD40L and IL-21 alone, indicating a lack of commitment to antibody secretion[5]. Because of this we do not recommend using IL-4 when the investigating induction of plasmablast differentiation. However, as IL-4 plays a major role regarding pre-GC B cell priming and promotes class-switch to IgG4 and IgE, studies focusing on e.g. IgG4-related disease or allergy might want to use IL-4 nonetheless. IgE and IgG-subclass production were however not determined in the cultures presented here.

To mimic *in vivo* TI responses, the most commonly used stimulation is TLR-9 activation through CpG, mimicking antigen activation (**Table I**). Activation with CpG induces proliferation of both human naive and memory B cells (data not shown), whilst the differentiation of naive B cells is only observed in cultures where PBMCs are present or T cell

derived cytokines such as IL-2 are supplemented[17,27]. Adding to this, *in vivo* TI stimulation has been shown to result in long-lived plasma cell generation[14]. This together indicates that though direct T-B interactions may not be required, a supportive microenvironment may be crucial to gain plasmablast fate and sustain plasma cell generation in TI responses *in vitro*. Condition IV with 25.000 starting B cells was identified as a minimum when stimulating isolated $CD19^+$ B cells with CpG and IL-2 due to limited B cell survival in this culture. Considering the significant decrease of $CD19^+$ B cells between day 6 and day 9 in condition IV, we do not recommend culturing longer than 6 days, although higher amounts of immunoglobulins can be measured with a longer culture period. Re-stimulation of cells can be opted for, but this was not investigated in this study. Finally, compared to isolated B cell cultures, PBMC TI cultures showed better survival of B cells (condition IV and V versus IV.2 and V.2 (**Table III**). Although the microenvironment provided by PBMCs may support survival there was no observation of increased differentiation.

BAFF protein is expressed by myeloid lineage cells and acts as both cell surface–associated and soluble forms[28,29]. BAFF has been shown to activate class switch recombination in human B cells, which can be enhanced by BCR crosslinking[30]. Ever since, research groups have used BAFF in B cell differentiation assays but most frequently in combinatorial use with CD40 stimulation, preventing the dissection of their individual effects. In the current study, limited effects of BAFF, in addition to anti-BCR stimulation, were found on plasmablasts formation. Interestingly, a donor-dependent effect of BAFF stimulation on the Ig secretion was observed. Healthy donors, and patients, possibly differ in their expression of BAFF-responding receptors at baseline. Furthermore, because activated monocytes and T cells can also express BAFF-responding receptors, it raises the possibility that in the PBMC cultures the addition of BAFF will stimulate the rest of the PBMCs rather than the B cells. Finally, as monocytes are known to increase BAFF secretion upon TLR-9 stimulation, it is possible that these cells were already supplying sufficient BAFF to the B cells within the PBMC TI cultures[20]. Altogether, although no detrimental effects of BAFF on B cell differentiation was observed in our assay, using BAFF should be complemented with appropriate analysis of its compliant receptors at baseline and throughout the assay.

The data presented here shows that for the TD condition stimulating as little as 2500 $CD19^+$ B cells with CD40L and IL-21 results in significant expansion, differentiation and secretion of IgM, IgA and IgG. For specific purposes, even lower cell numbers can be used. Interestingly, IL-4 did not affect differentiation but did significantly reduce antibody secretion. For studying TI responses, stimulating 25.000 $CD19^+$ B cells with CpG and IL-2 results in proliferation, differentiation and IgM, IgA and IgG production. We do not recommend using lower cell numbers for this condition. Interestingly, addition of BAFF resulted in significant increases of IgM, IgA and IgG production in TI $CD19^+$ B cell cultures. However, this effect is absent in PBMC cultures. Furthermore, we show

that both these protocols can be performed with PBMC cultures, omitting the need for B cell isolation and thus making them highly suitable for clinical research. We do however recommend that B cell numbers are corrected using measured B cell percentages, after thawing, as these percentages are variable between donors. Furthermore, monocyte and T cell involvement in these cultures could not entirely be excluded possibly explaining mixed results when comparing this and previous studies[17,27]. In addition, we recommend determining the B-cell subset and Ig-isotype composition in (patient) samples before culture as the proportion of $CD27^+$ and class-switched cells correlate with differentiation and Ig-secretion results. As healthy donor cells were used here, it will be interesting to monitor, for example, (longitudinal) auto-immune patient sample composition to determine if the same correlations are present and if these are affected during immunosuppressive treatment. Finally, we acknowledge that for specific research questions or patient samples it will be worthwhile to study additional B cell functions (e.g. pro- and anti-inflammatory cytokine production)[31] or to sort B cell subsets like naive[19], memory or MZ B cells[32,33] or IgG4-expressing cells[34]. It should be taken into consideration however how much material is available, how much material will be lost upon sorting and if instead it is possible to investigate the subset of interest within PBMC cultures.

In conclusion, it is still an active area of investigation to define how autonomous factors control TD and TI responses in healthy donors or patients with B cell mediated diseases. Future research is needed to define these autonomous factors and address signaling pathways involved in both beneficial and unwanted plasma cell development. Comparing patients and healthy donors in optimized cultures and assays that detect gene expression and post-translational modifications such as phosphorylation or ubiquitination by intracellular staining methods[35] may aid in these research questions. The TD and TI assay described here in condition II (and II.2), being 2500 $CD19^+$ B cells stimulated with CD40L and IL-21, and condition IV (and IV.2), being 25.000 $CD19^+$ B cells stimulated with CpG, IL-2 and possibly BAFF, supports efficient differentiation of human primary B cells into plasma cells, with warranted B cell expansion, proliferation and quantifiable production of IgG, IgA and IgM. Due to the minimalistic nature of the protocols, results from different labs and facilities will be highly comparable. These assays will allow in-depth dissection of B cell differentiation pathways in B cells of healthy individuals and patients.

Acknowledgements

We acknowledge the support of patient partners, private partners and active colleagues of the T2B consortium; see website: www.target-to-b.nl. We thank Simon Tol, Erik Mul, Mark Hoogenboezem and Tom Ebbes of the Sanquin Central Facility for the maintenance and calibration of the FACS machines.

Authorship contributions

J.K., C.M., D.V. designed experiments. C.M., D.V. performed experiments and analyzed data. T.R. and A.T.B. critically revised the manuscript. S.M.H. and T.W.K. devised the concept, supervised data interpretation and critically revised the manuscript. The manuscript was revised and approved by all authors.

Disclosure statement

The authors declare that this research was conducted in the absence of commercial or financial relationships that could be construed as a potential conflict of interest.

Financial support

This collaboration project is financed by the PPP Allowance made available by Top Sector Life Sciences & Health to Samenwerkende Gezondheidsfondsen (SGF) under project number LSHM18055-SGF to stimulate public-private partnerships and co-financing by health foundations that are part of the SGF. This project was also funded by the Landsteiner Foundation for Blood Transfusion Research—project grant number: LSBR 1609 and Sanquin Product and Process Development Call 2020.

REFERENCES

1. Nutt SL, Hodgkin PD, Tarlinton DM, Corcoran LM. The generation of antibody-secreting plasma cells. *Nat Rev Immunol*. 2015;15(3):160-71.
2. Allman D, Wilmore JR, Gaudette BT. The continuing story of T-cell independent antibodies. *Immunol Rev*. 2019;288(1):128-35.
3. Ding BB, Bi E, Chen H, Yu JJ, Ye BH. IL-21 and CD40L synergistically promote plasma cell differentiation through upregulation of Blimp-1 in human B cells. *J Immunol*. 2013;190(4):1827-36.
4. Shulman Z, Gitlin AD, Weinstein JS, Lainez B, Esplugues E, Flavell RA, et al. Dynamic signaling by T follicular helper cells during germinal center B cell selection. *Science*. 2014;345(6200):1058-62.
5. Ettinger R, Sims GP, Fairhurst A-M, Robbins R, da Silva YS, Spolski R, et al. IL-21 Induces Differentiation of Human Naive and Memory B Cells into Antibody-Secreting Plasma Cells. *J Immunol*. 2005;175(12):7867-79.
6. Weisel FJ, Zuccarino-Catania GV, Chikina M, Shlomchik MJ. A Temporal Switch in the Germinal Center Determines Differential Output of Memory B and Plasma Cells. *Immunity*. 2016;44(1):116-30.
7. Good KL, Tangye SG. Decreased expression of Kruppel-like factors in memory B cells induces the rapid response typical of secondary antibody responses. *Proc Natl Acad Sci U S* A. 2007;104(33):13420-5.
8. Victora GD, Nussenzweig MC. Germinal centers. Annu Rev Immunol. 2012;30:429-57.
9. Vos Q, Lees A, Wu ZQ, Snapper CM, Mond JJ. B-cell activation by T-cell-independent type 2 antigens as an integral part of the humoral immune response to pathogenic microorganisms. *Immunol Rev*. 2000;176:154-70.
10. Huggins J, Pellegrin T, Felgar RE, Wei C, Brown M, Zheng B, et al. CpG DNA activation and plasma-cell differentiation of CD27- naive human B cells. *Blood*. 2007;109(4):1611-9.
11. Pone EJ, Lou Z, Lam T, Greenberg ML, Wang R, Xu Z, et al. B cell TLR1/2, TLR4, TLR7 and TLR9 interact in induction of class switch DNA recombination: modulation by BCR and CD40, and relevance to T-independent antibody responses. *Autoimmunity*. 2015;48(1):1-12.
12. Pone EJ, Zan H, Zhang J, Al-Qahtani A, Xu Z, Casali P. Toll-like receptors and B-cell receptors synergize to induce immunoglobulin class-switch DNA recombination: relevance to microbial antibody responses. *Crit Rev Immunol*. 2010;30(1):1-29.
13. Nothelfer K, Sansonetti PJ, Phalipon A. Pathogen manipulation of B cells: the best defence is a good offence. *Nat Rev Microbiology*. 2015;13(3):173-84.
14. Bortnick A, Chernova I, Quinn WJ, 3rd, Mugnier M, Cancro MP, Allman D. Long-lived bone marrow plasma cells are induced early in response to T cell-independent or T cell-dependent antigens. *J Immunol*. 2012;188(11):5389-96.
15. DeFranco AL. Germinal centers and autoimmune disease in humans and mice. *Immunol Cell Biol*. 2016;94(10):918-24.
16. Urashima M, Chauhan D, Hatziyanni M, Ogata A, Hollenbaugh D, Aruffo A, et al. CD40 ligand triggers interleukin-6 mediated B cell differentiation. *Leuk Res*. 1996;20(6):507-15.
17. aan de Kerk DJ, Jansen MH, ten Berge IJ, van Leeuwen EM, Kuijpers TW. Identification of B cell defects using age-defined reference ranges for in vivo and in vitro B cell differentiation. *J Immunol*. 2013;190(10):5012-9.

18. Bernasconi NL, Onai N, Lanzavecchia A. A role for Toll-like receptors in acquired immunity: up-regulation of TLR9 by BCR triggering in naive B cells and constitutive expression in memory B cells. *Blood*. 2003;101(11):4500-4.

19. Unger P-PA, Verstegen NJM, Marsman C, Jorritsma T, Rispens T, ten Brinke A, et al. Minimalistic In Vitro Culture to Drive Human Naive B Cell Differentiation into Antibody-Secreting Cells. *Cells*. 2021;10(5):1183.

20. Mackay F, Schneider P. Cracking the BAFF code. Nat Rev Immunol. 2009;9(7):491-502.

21. Smulski CR, Eibel H. BAFF and BAFF-Receptor in B Cell Selection and Survival. *Front Immunol*. 2018;9:2285.

22. Giordano D, Kuley R, Draves KE, Roe K, Holder U, Giltiay NV, et al. BAFF Produced by Neutrophils and Dendritic Cells Is Regulated Differently and Has Distinct Roles in Antibody Responses and Protective Immunity against West Nile Virus. *J Immunol*. 2020;204(6):1508-20.

23. Weinstein JS, Herman EI, Lainez B, Licona-Limón P, Esplugues E, Flavell R, et al. TFH cells progressively differentiate to regulate the germinal center response. *Nat Immunol*. 2016;17(10):1197-205.

24. Deenick EK, Avery DT, Chan A, Berglund LJ, Ives ML, Moens L, et al. Naive and memory human B cells have distinct requirements for STAT3 activation to differentiate into antibody-secreting plasma cells. *J Exp Med*. 2013;210(12):2739-53.

25. Huse K, Wogsland CE, Polikowsky HG, Diggins KE, Smeland EB, Myklebust JH, et al. Human Germinal Center B Cells Differ from Naïve and Memory B Cells in CD40 Expression and CD40L-Induced Signaling Response. *Cytometry A*. 2019;95(4):442-9.

26. Cyster JG, Allen CDC. B Cell Responses: Cell Interaction Dynamics and Decisions. *Cell*. 2019;177(3):524-40.

27. Marasco E, Farroni C, Cascioli S, Marcellini V, Scarsella M, Giorda E, et al. B-cell activation with CD40L or CpG measures the function of B-cell subsets and identifies specific defects in immunodeficient patients. *Eur J Immunol*. 2017;47(1):131-43.

28. Moore PA, Belvedere O, Orr A, Pieri K, LaFleur DW, Feng P, et al. BLyS: member of the tumor necrosis factor family and B lymphocyte stimulator. *Science*. 1999;285(5425):260-3.

29. Nardelli B, Belvedere O, Roschke V, Moore PA, Olsen HS, Migone TS, et al. Synthesis and release of B-lymphocyte stimulator from myeloid cells. *Blood*. 2001;97(1):198-204.

30. Litinskiy MB, Nardelli B, Hilbert DM, He B, Schaffer A, Casali P, et al. DCs induce CD40-independent immunoglobulin class switching through BLyS and APRIL. *Nat Immunol*. 2002;3(9):822-9.

31. Lighaam LC, Unger PA, Vredevoogd DW, Verhoeven D, Vermeulen E, Turksma AW, et al. In vitro-Induced Human IL-10(+) B Cells Do Not Show a Subset-Defining Marker Signature and Plastically Co-express IL-10 With Pro-Inflammatory Cytokines. *Front Immunol*. 2018;9:1913.

32. van Asten SD, Unger PP, Marsman C, Bliss S, Jorritsma T, Thielens NM, et al. Soluble FAS Ligand Enhances Suboptimal CD40L/IL-21-Mediated Human Memory B Cell Differentiation into Antibody-Secreting Cells. *J Immunol*. 2021;207(2):449-58.

33. Budeus B, Schweigle de Reynoso S, Przekopowitz M, Hoffmann D, Seifert M, Küppers R. Complexity of the human memory B-cell compartment is determined by the versatility of clonal diversification in germinal centers. *Proc Natl Acad Sci U S A*. 2015;112(38):E5281-9.

34. Liu C, Zhang P, Zhang W. Immunological mechanism of IgG4-related disease. *J Transl Autoimmun*. 2020;3:100047.

35. Marsman C, Jorritsma T, Ten Brinke A, van Ham SM. Flow Cytometric Methods for the Detection of Intracellular Signaling Proteins and Transcription Factors Reveal Heterogeneity in Differentiating Human B Cell Subsets. *Cells*. 2020;9(12).

36. Henn AD, Rebhahn J, Brown MA, Murphy AJ, Coca MN, Hyrien O, et al. Modulation of single-cell IgG secretion frequency and rates in human memory B cells by CpG DNA, CD40L, IL-21, and cell division. *J Immunol*. 2009;183(5):3177-87.

37. Cocco M, Stephenson S, Care MA, Newton D, Barnes NA, Davison A, et al. In vitro generation of long-lived human plasma cells. *J Immunol*. 2012;189(12):5773-85.

38. Le Gallou S, Caron G, Delaloy C, Rossille D, Tarte K, Fest T. IL-2 requirement for human plasma cell generation: coupling differentiation and proliferation by enhancing MAPK-ERK signaling. *J Immunol*. 2012;189(1):161-73.

39. Tuijnenburg P, Aan de Kerk DJ, Jansen MH, Morris B, Lieftink C, Beijersbergen RL, et al. High-throughput compound screen reveals mTOR inhibitors as potential therapeutics to reduce (auto) antibody production by human plasma cells. *Eur J Immunol*. 2020;50(1):73-85.

40. Lepse N, Land J, Rutgers A, Kallenberg CG, Stegeman CA, Abdulahad WH, et al. Toll-like receptor 9 activation enhances B cell activating factor and interleukin-21 induced anti-proteinase 3 autoantibody production in vitro. *Rheumatology*. 2016;55(1):162-72.

41. Jourdan M, Caraux A, De Vos J, Fiol G, Larroque M, Cognot C, et al. An in vitro model of differentiation of memory B cells into plasmablasts and plasma cells including detailed phenotypic and molecular characterization. *Blood*. 2009;114(25):5173-81.

42. Cao Y, Gordic M, Kobold S, Lajmi N, Meyer S, Bartels K, et al. An optimized assay for the enumeration of antigen-specific memory B cells in different compartments of the human body. *J Immunol Methods*. 2010;358(1-2):56-65.

43. Sundström Y, Shang MM, Panda SK, Grönwall C, Wermeling F, Gunnarsson I, et al. Identifying novel B-cell targets for chronic inflammatory autoimmune disease by screening of chemical probes in a patient-derived cell assay. *Transl Res*. 2021;229:69-82.

SUPPLEMENTARY MATERIAL

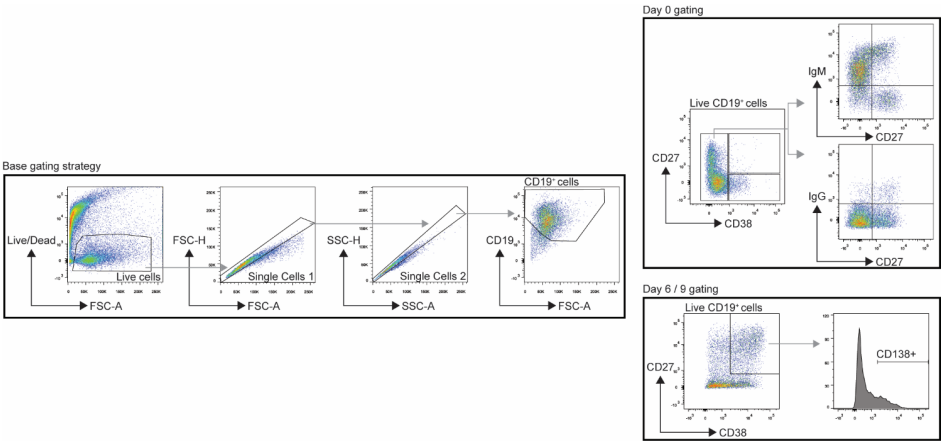

Figure S1. Flow cytometry gating strategy. *Total lymphocytes were first gated on a forward scatter (FSC-A) versus Live/Dead plot and then gated on single cells using both FSC-H/FSC-A and SSC-H/SSC-A plots. Next, CD19⁺ B cells were gated and subsets of interest were gated within the CD19⁺ B cells. On day 0 the initial characterization of the B cell compartment was performed, including pre-existing CD27⁺ CD38⁺ plasmablasts, CD27⁻ CD38⁺ and CD27⁺/⁻ CD38⁻ B cells. IgM and IgG expression within the CD27⁺/⁻ CD38⁻ B cells was used to determine the naive, non-switched memory and switched memory population at baseline. On day 6 and day 9 CD27⁺ CD38⁺ plasmablasts and CD27⁺ CD38⁺ CD138⁺ plasma cells were analyzed.*

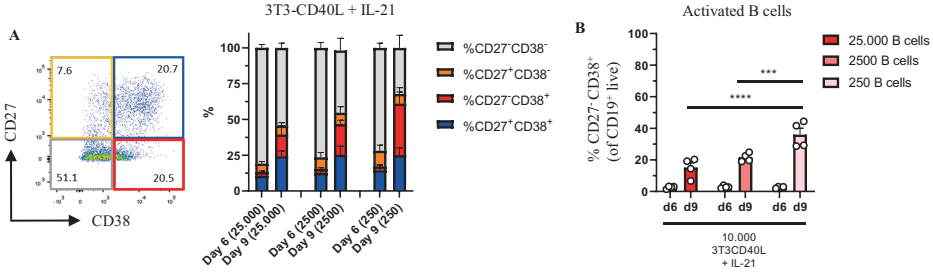

Figure S2. CD27 and CD38 expression of stimulated primary human B cells. ***(A)*** *Representative FACS plot (left panel) show gating strategy of CD27/CD38 subpopulations and quantification of the relative percentages of CD27 and CD38 subpopulations in the total CD19⁺ B cell population between 6 and 9 days of culture (n = 4). (**B**) The frequency of CD27⁻CD38⁺ B cells. Each data point represents the mean of an individual donor with duplicate culture measurements. Mean values are represented by bars and the error bars depict SEM. P values were calculated using two-way ANOVA with Tukey's multiple comparison test. *** p < 0.001, **** p < 0.0001.*

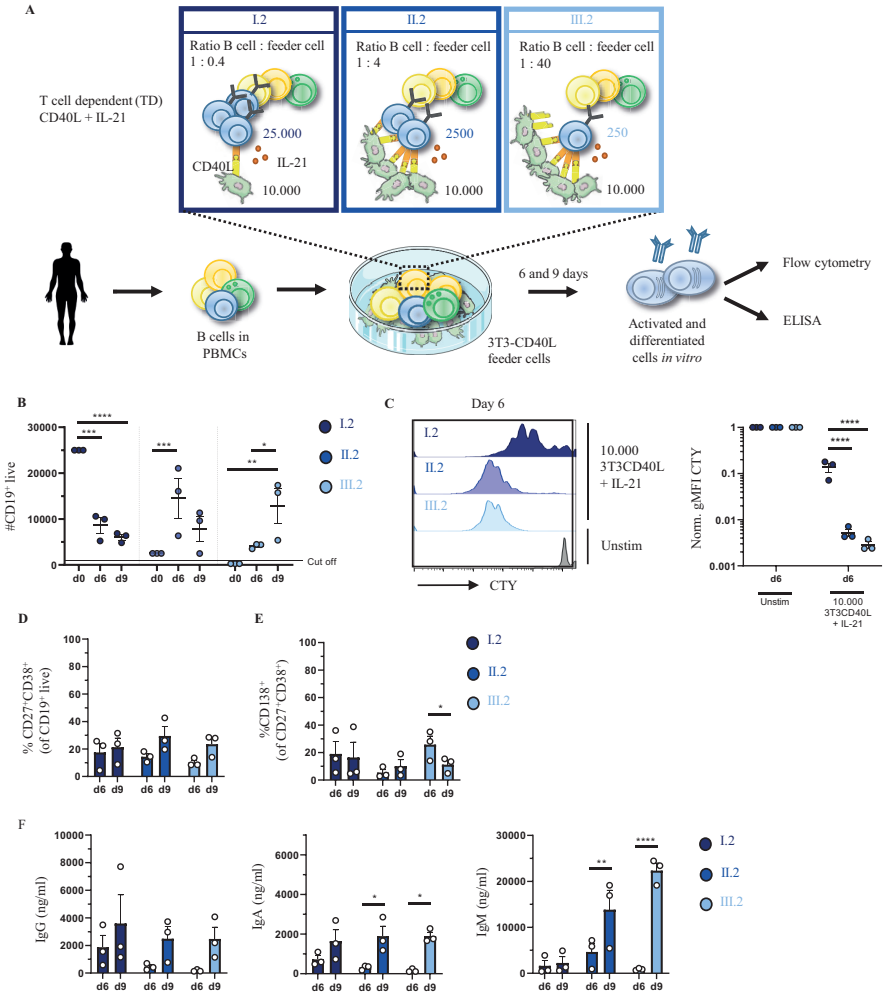

Figure S3. Proliferation, differentiation and antibody production of primary human CD19⁺ B cells after T cell dependent in vitro stimulation and culturing of PBMCs. *(**A**) Schematic overview of the T cell dependent (TD) culture system to induce B cell differentiation. A total of 25000, 2500 or 250 CD19⁺ human B cells in PBMCs (n = 3) were stimulated with a human-CD40L-expressing 3T3 feeder layer and recombinant IL-21 (50 ng/mL) enabling condition I.2 (dark blue), II.2 (cobalt blue) and III.2 (light blue). Cells were analyzed at day 6 and day 9 by flow cytometry to evaluate plasmablast and plasma cell generation. The supernatant was collected at day 6 and day 9 to evaluate IgG, IgA and IgM production by ELISA. (**B**) The number of live CD19⁺ events was analyzed using flow cytometry. A cut off of 1000 events was used to proceed with further analysis. (**C**) Representative histograms of CTY dilution (left panel) and quantification (right panel) on day 6 compared to their unstimulated condition. (**D**) The frequency of CD27⁺CD38⁺ B cells and (**E**) CD27⁺CD38⁺CD138⁺ B cells was analyzed by using flow cytometry. (**F**) IgG, IgA and IgM production in culture supernatants was evaluated by ELISA after 6 and 9 days (n = 3). Each data point represents the mean of an individual donor with duplicate culture measurements. Mean values are represented by bars and the error bars depict SEM. P values were calculated using two-way ANOVA with Sidak's multiple comparison test. * p < 0.05, ** p < 0.01, *** p < 0.001, **** p < 0.0001.*

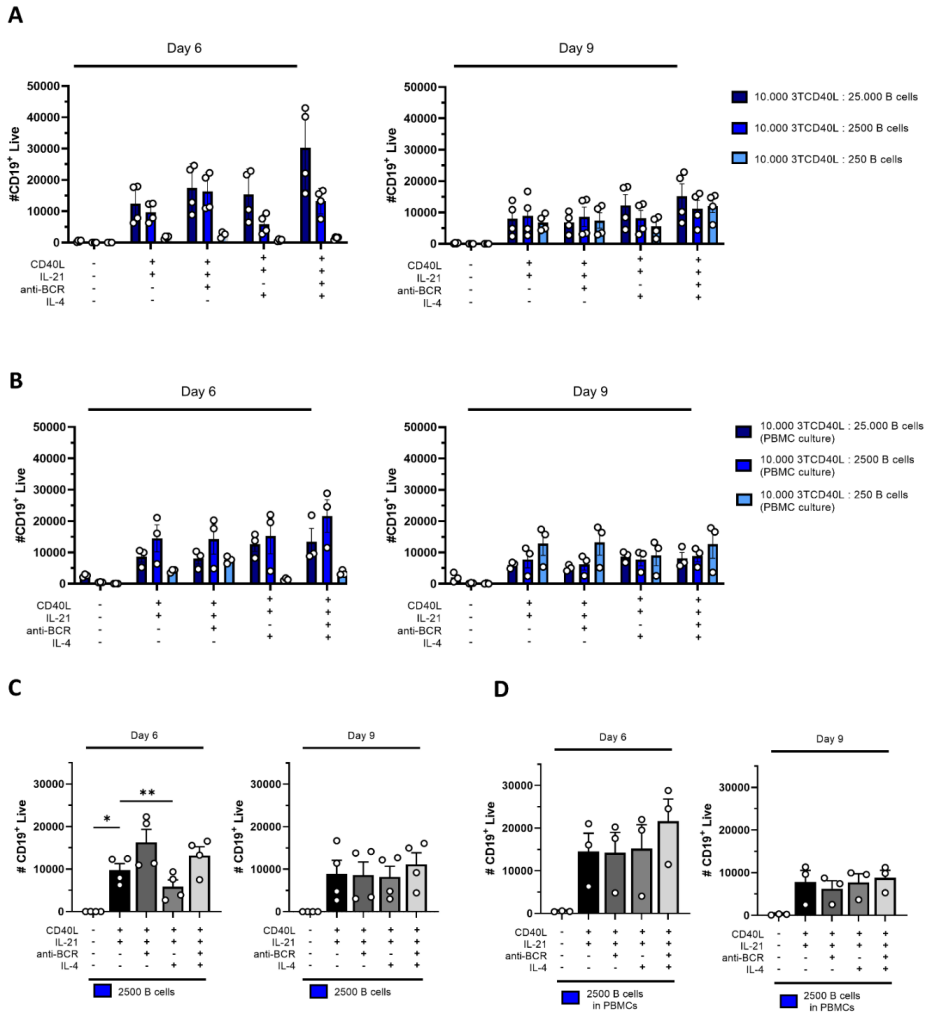

Figure S4. CD19⁺ live cells in TD cultures with anti-BCR and IL-4. ***(A – B)*** *Frequencies of CD19⁺ live cells on day 6 and day 9 in conditions described in Figure 1A (condition I, II, III) and Figure S3A (condition I.2, II.2, III.2) (PBMC cultures) with or without anti-BCR (anti-Ig F(ab')$_2$ mix (5 µg/mL) targeting IgM, IgG and IgA) and/or recombinant IL-4 (25 ng/mL). Frequencies of CD19⁺ live cells on day 6 and day 9 in* ***(C)*** *condition II (n = 4) and* ***(D)*** *condition II.2 (n = 3) including statistics. Each data point represents the mean of an individual donor with duplicate culture measurements. Mean values are represented by bars and the error bars depict SEM. P values were calculated using two-way ANOVA with Sidak's multiple comparison test. * p < 0.05, ** p < 0.01.*

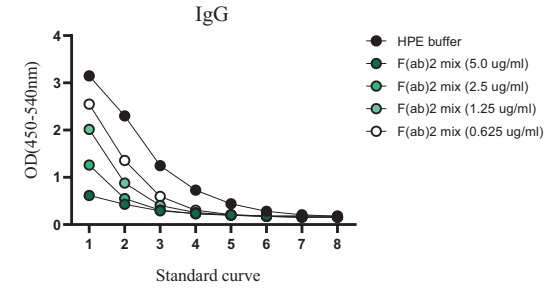

Standard Curve	Dilution (IgG)
st 1	1: 20 000
st 2	1: 40 000
st 3	1: 80 000
st 4	1: 160 000
st 5	1: 320 000
st 6	1: 640 000
st 7	1: 1 280 000
st 8	1: 2 560 000

B

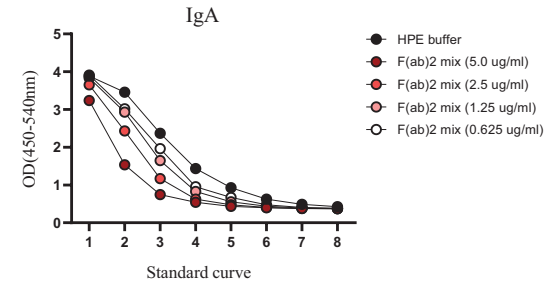

Standard Curve	Dilution (IgA)
st 1	1: 4000
st 2	1: 8000
st 3	1: 16 000
st 4	1: 32 000
st 5	1: 64 000
st 6	1: 128 000
st 7	1: 256 000
st 8	1: 512 000

C

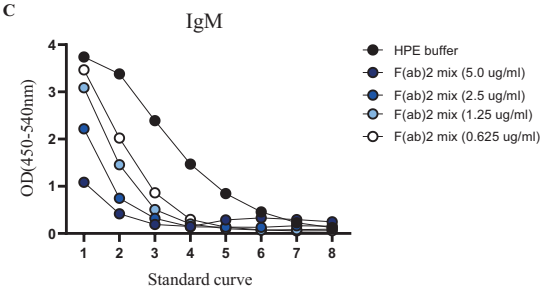

Standard Curve	Dilution (IgM)
st 1	1: 1500
st 2	1: 3000
st 3	1: 6000
st 4	1: 12 000
st 5	1: 24 000
st 6	1: 48 000
st 7	1: 96 000
st 8	1: 192 000

Figure S5. Anti-IgA/G/M F(ab')$_2$ fragments interfere with ELISA readouts. *Interference of F(ab')$_2$ fragment Goat Anti-Human IgA/G/M in (**A**) IgG, (**B**) IgA and (**C**) IgM ELISA. Serial dilutions of F(ab')$_2$ fragments (5, 2.5, 1.25 and 0.625 µg/mL) were added to the standard curve dilutions as indicated. Black lines indicate no F(ab')$_2$ fragments added.*

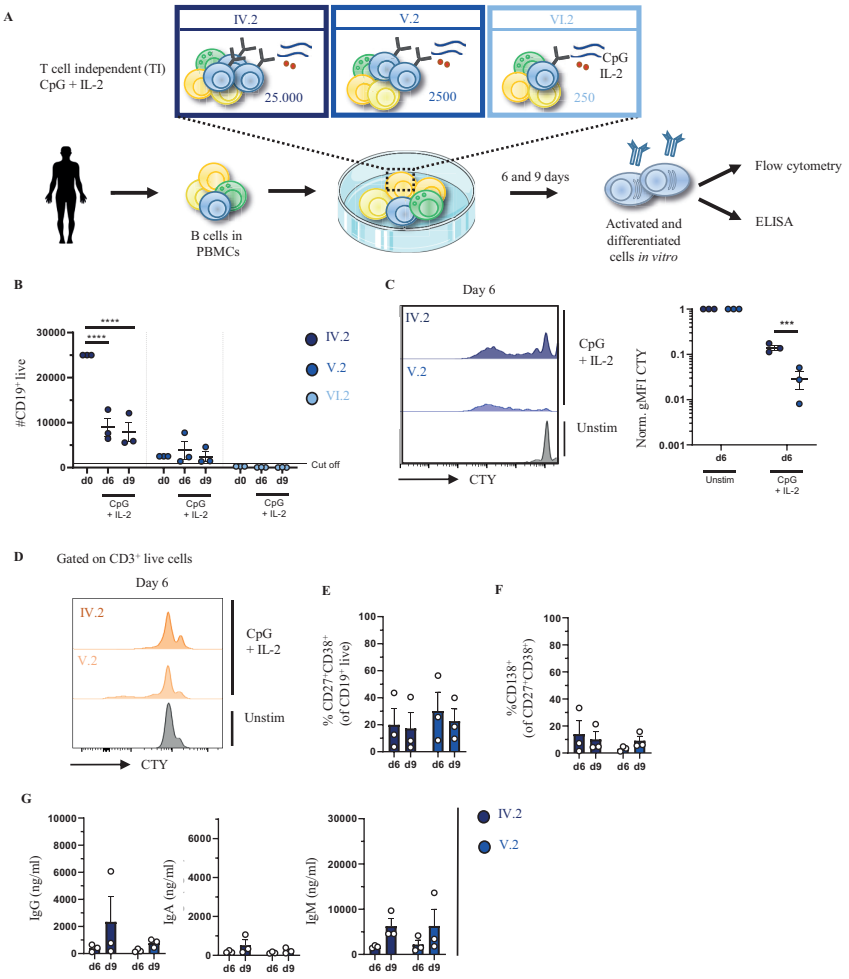

Figure S6. Proliferation, differentiation and antibody production primary human CD19⁺ B cells after T cell independent in vitro stimulation and culturing of PBMCs. *(**A**) Schematic overview of the T cell independent (TI) culture system to induce B cell differentiation. A total of 25000, 2500 or 250 CD19⁺ human B cells and PBMCs (n = 3) were stimulated with CpG (1 µM) and IL-2 (50 ng/ml) enabling condition IV.2 (dark blue), V.2 (cobalt blue) and VI.2 (light blue). Cells were analyzed at day 6 and day 9 by flow cytometry to evaluate plasmablast and plasma cell generation. The supernatant was collected at day 6 and day 9 to evaluate IgG, IgA and IgM production by ELISA. (**B**) The number of live CD19⁺ events was analyzed using flow cytometry. A cut off of 1000 events was used to proceed with further analysis. (**C**) Representative histogram of CTY dilution (left panel) and quantification (right panel) of condition IV.2 and V.2 on day 6 compared to their unstimulated condition. (**D**) Analysis of proliferation by CTY dilution of CD3⁺ T cells in condition IV.2 and V.2 on day 6. (**E**) The frequency of CD27⁺CD38⁺ B cells and (**F**) CD27⁺CD38⁺CD138⁺ B cells. (**G**) IgG, IgA and IgM production in culture supernatants was evaluated by ELISA after 6 and 9 days (n = 4). Each data point represents the mean of an individual donor with duplicate culture measurements. Mean values are represented by bars and the error bars depict SEM. P values were calculated using two-way ANOVA with Sidak's multiple comparison test. * p < 0.05, ** p < 0.01, *** p < 0.001, **** p < 0.0001.*

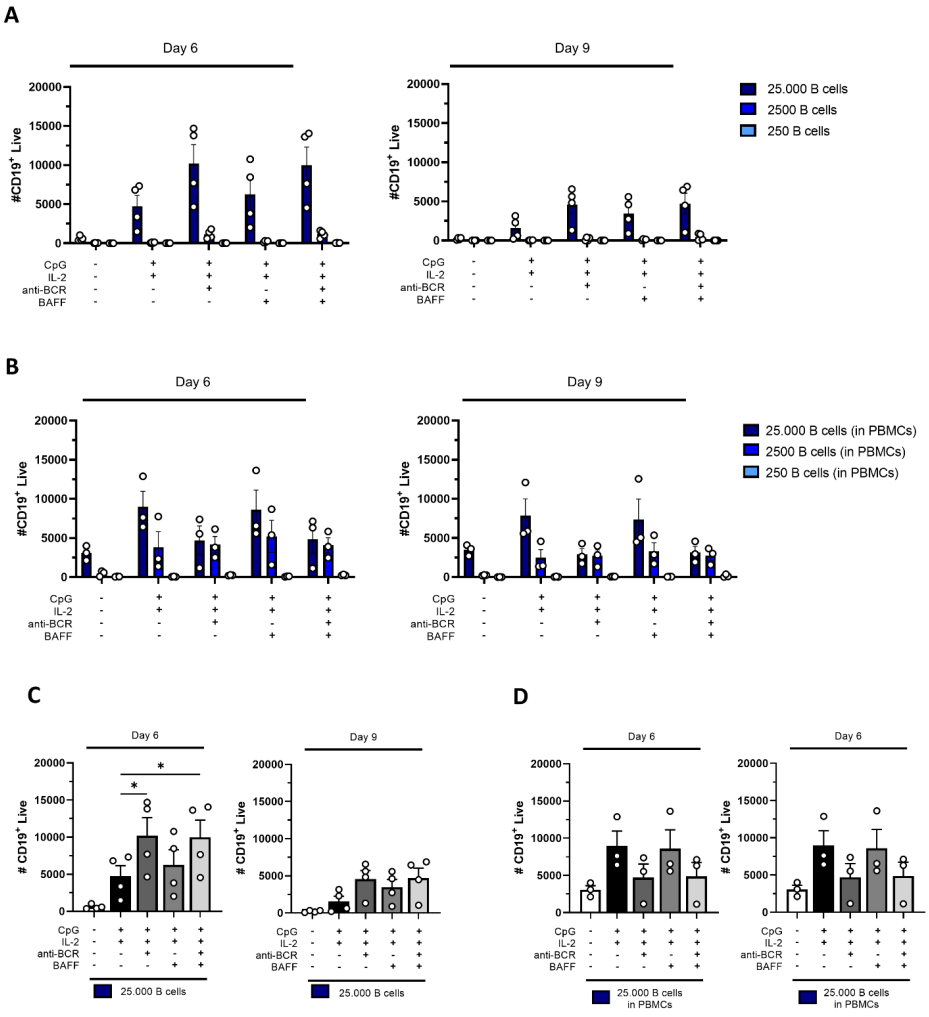

Figure S7. CD19⁺ live cells in TI cultures with anti-BCR and BAFF. *(**A – B**) Frequencies of CD19⁺ live cells on day 6 and day 9 in conditions described in **Figure 3A** (condition IV, V, VI) and **Figure S6A** (condition IV.2, V.2, VI.2) (PBMC cultures) with or without anti-BCR (anti-Ig F(ab)$_2$ mix (5 µg/mL) targeting IgM, IgG and IgA) and/or BAFF (100 ng/mL). Frequencies of CD19⁺ live cells on day 6 and day 9 in (**C**) condition IV (n=4) and (**D**) condition IV.2 (n = 3) including statistics. Each data point represents the mean of an individual donor with duplicate culture measurements. Mean values are represented by bars and the error bars depict SEM. P values were calculated using two-way ANOVA with Sidak's multiple comparison test. * $p < 0.05$.*

Donor	CD27+	CD27+IgG+	CD27+IgM+	CD27+IgM-	CD27-IgG+	CD27-IgM+	CD27-IgM-	CD27-CD38+	CD27+CD38+
A	27,066	3,688	16,117	10,884	1,732	49,383	14,219	8,676	0,881
B	10,779	1,214	7,017	3,699	1,690	55,441	19,192	10,826	0,904
C	32,601	6,886	16,463	15,582	1,574	49,220	11,932	2,669	0,294
D	22,632	3,190	13,462	8,857	0,831	56,180	14,488	3,365	0,305
E	17,830	2,855	8,827	9,047	1,933	66,667	9,750	3,206	0,439
F	29,227	2,189	23,347	5,837	1,545	60,085	4,421	3,433	0,300

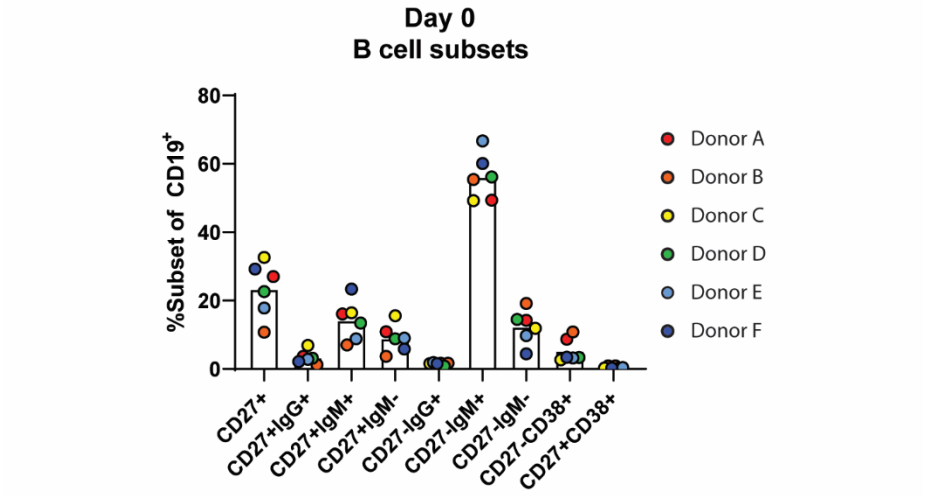

Figure S8. Characterization of the B cell compartment at day 0. *On day 0 the initial characterization of the B cell compartment of donor A-F was performed (for gating strategy see Figure S1), including pre-existing $CD27^{+}$ $CD38^{+}$ plasmablasts, $CD27^{-}$ $CD38^{+}$ and $CD27^{+/-}$ B cells. IgM and IgG expression within the $CD27^{+/-}$ $CD38^{-}$ B cells was used to determine the naive, non-switched memory and switched memory distribution at baseline. These baseline % were used for correlation analysis (see Suppl. Table 1 and 2).*

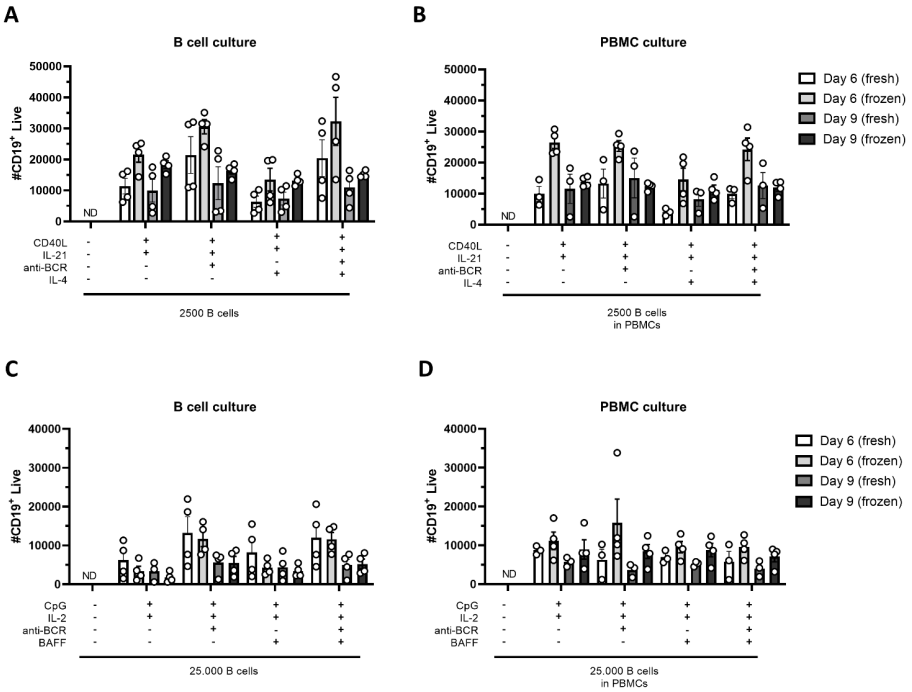

Figure S9. Frequencies of CD19⁺ live cells in TD and TI cultures using cryopreserved and freshly isolated B cells. *Frequencies of CD19⁺ live cells measured by flowcytometry from cultures with B cells isolated from fresh PBMCs or frozen PBMCs which where cultured for 6 and 9 (**A-B**) with TD stimuli with and without PBMCs (condition II and II.2) or (**C-D**) with TI stimuli (condition IV and IV.2). ND = not determined.*

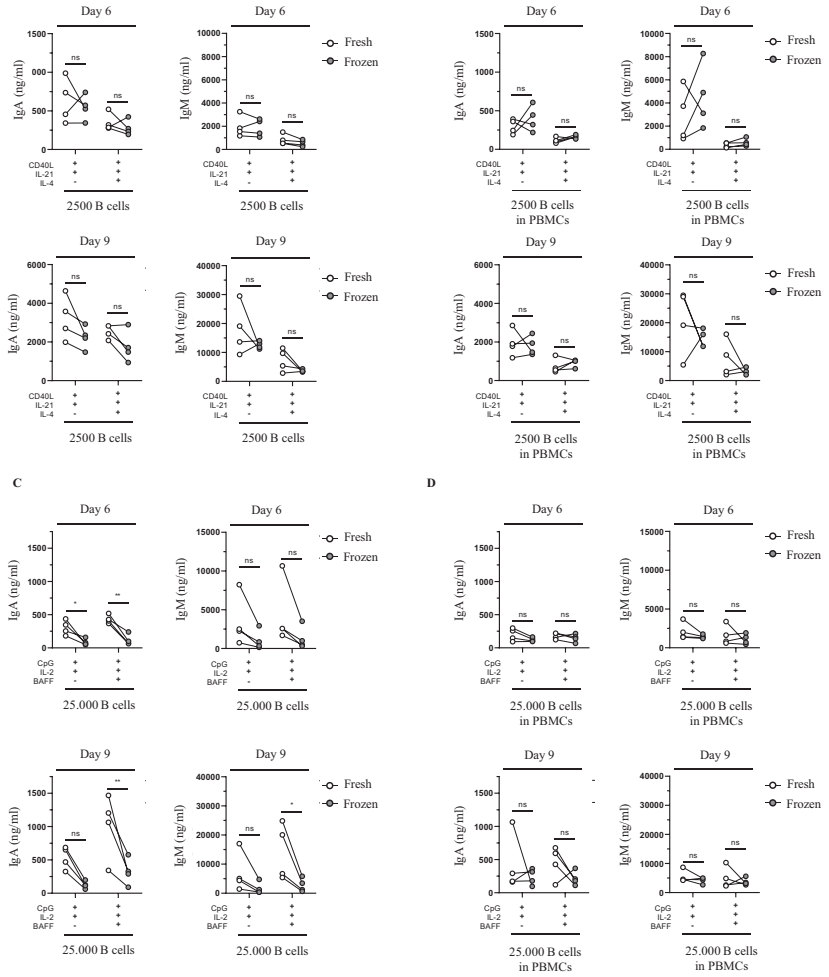

Figure S10. Cryopreserved and freshly isolated B cells produce similar amounts of antibodies in T cell dependent and independent assays. *Comparison of IgA and IgM production of B cells isolated freshly from PBMCs or from cryopreserved PBMCs obtained from the same healthy donor (n=4). Total human B cells were isolated from fresh PBMCs (indicated in white) or frozen PBMCs (indicated in gray) and cultured for 6 and 9 days. (**A-B**) Using T cell dependent (TD) stimuli (CD40L and IL-21 with/without IL-4) 2500 B cells (fresh and frozen) were cultured under conditions described previously (**A**) without PBMCs (condition II) and (**B**) with PBMCs (condition II.2). IgA (left panel) and IgM production (right panel) on day 6 (upper graphs) and day 9 (lower graphs) are shown. (**C-D**) Using T cell independent (TI) stimuli (CpG and IL-2 with/without BAFF) 25.000 B cells (fresh and frozen) were cultured under conditions described previously (**C**) without PBMCs (condition IV) and (**D**) with PBMCs (condition IV.2). IgA (left panel) and IgM production (right panel) on day 6 (upper graphs) and day 9 (lower graphs) are shown. Each data point represents the mean of an individual donor with duplicate culture measurements. Mean values are represented by bars and the error bars depict SEM. P values were calculated using two-way ANOVA with Sidak's multiple comparison test. * $p < 0.05$, ** $p < 0.01$.*

Table SI. Pearson correlations T-Dependent stimulations 2500 B cells

	Day6 %CD27+CD38+			
	CD40L + IL-21	CD40L + IL-21 + anti-BCR	CD40L + IL-21 + IL-4	CD40L + IL-21 + anti-BCR + IL-4
%CD27+	0,490	0,604	-0,218	**0,987**
%CD27+IgG+	0,766	0,838	-0,283	0,942
%CD27+IgM+	0,283	0,417	-0,165	0,949
%CD27+IgM-	0,633	0,721	-0,231	**0,986**
%CD27-IgG+	0,284	-0,094	0,899	0,125
%CD27-IgM+	-0,498	-0,356	-0,421	-0,863
%CD27-IgM-	-0,474	-0,644	0,372	**-0,951**
	Day9 %CD27+CD38+			
	CD40L + IL-21	CD40L + IL-21 + anti-BCR	CD40L + IL-21 + IL-4	CD40L + IL-21 + anti-BCR + IL-4
%CD27+	0,619	0,610	-0,322	0,465
%CD27+IgG+	0,520	0,697	-0,550	0,450
%CD27+IgM+	0,586	0,411	-0,037	0,270
%CD27+IgM-	0,329	0,557	-0,542	0,516
%CD27-IgG+	-0,400	-0,328	0,533	0,343
%CD27-IgM+	-0,343	-0,149	-0,146	-0,718
%CD27-IgM-	-0,325	-0,389	0,219	0,133
	ELISA IgG Day6		**ELISA IgG Day9**	
	CD40L + IL-21	CD40L + IL-21 + IL-4	CD40L + IL-21	CD40L + IL-21 + IL-4
%CD27+	-0,052	0,401	0,420	-0,100
%CD27+IgG+	-0,139	0,556	0,436	-0,450
%CD27+IgM+	0,103	0,215	0,356	0,223
%CD27+IgM-	-0,269	0,450	0,282	-0,485
%CD27-IgG+	-0,638	0,387	0,139	0,550
%CD27-IgM+	-0,578	-0,733	-0,774	-0,127
%CD27-IgM-	0,494	0,149	0,136	-0,047
	ELISA IgM Day6		**ELISA IgM Day9**	
%CD27+	0,409	0,156	0,348	-0,354
%CD27+IgG+	0,488	-0,356	-0,051	-0,734
%CD27+IgM+	0,251	0,548	0,585	0,119
%CD27+IgM-	0,393	-0,457	-0,157	**-0,841**
%CD27-IgG+	**-0,843**	0,365	-0,080	-0,319
%CD27-IgM+	-0,253	0,222	0,493	0,450
%CD27-IgM-	-0,030	-0,586	**-0,842**	-0,177
	ELISA IgA Day6		**ELISA IgA Day9**	
%CD27+	0,708	0,862	0,520	0,411
%CD27+IgG+	0,609	0,853	0,731	-0,317
%CD27+IgM+	0,327	0,420	0,143	0,806
%CD27+IgM-	0,638	0,716	0,577	-0,510
%CD27-IgG+	0,369	0,092	0,017	0,113
%CD27-IgM+	-0,825	-0,603	-0,165	0,266
%CD27-IgM-	0,266	-0,075	-0,214	**-0,930**

Day0 subsets

Table SI. Pearson correlations T-Dependent stimulations - 2500 B cells in PBMCs (continued)

	Day6 %CD27+CD38+			
	CD40L + IL-21	CD40L + IL-21 + anti-BCR	CD40L + IL-21 + IL-4	CD40L + IL-21 + anti-BCR + IL-4
%CD27+	0,520	0,142	0,103	**0,997**
%CD27+IgG+	0,772	0,460	-0,230	0,965
%CD27+IgM+	0,065	-0,333	0,552	0,851
%CD27+IgM-	0,650	0,299	-0,059	0,996
%CD27-IgG+	-0,204	-0,573	0,755	0,680
%CD27-IgM+	0,020	0,412	-0,621	-0,803
%CD27-IgM-	-0,790	-0,485	0,258	-0,958
	Day9 %CD27+CD38+			
%CD27+	0,649	-0,121	0,068	-0,194
%CD27+IgG+	0,108	0,044	-0,376	-0,466
%CD27+IgM+	0,764	-0,077	0,388	0,186
%CD27+IgM-	-0,085	-0,092	-0,418	-0,547
%CD27-IgG+	0,307	0,017	0,744	0,494
%CD27-IgM+	0,026	0,602	0,453	0,783
%CD27-IgM-	-0,830	-0,568	-0,851	**-0,924**
	ELISA IgG Day6		**ELISA IgG Day9**	
	CD40L + IL-21	CD40L + IL-21 + IL-4	CD40L + IL-21	CD40L + IL-21 + IL-4
%CD27+	0,491	0,410	0,876	0,130
%CD27+IgG+	0,405	-0,198	0,511	-0,480
%CD27+IgM+	0,193	0,623	0,664	0,541
%CD27+IgM-	0,493	-0,225	0,414	-0,542
%CD27-IgG+	0,138	0,659	0,445	0,603
%CD27-IgM+	-0,855	-0,057	-0,547	0,396
%CD27-IgM-	0,537	-0,584	-0,314	-0,868
	ELISA IgM Day6		**ELISA IgM Day9**	
%CD27+	0,317	0,870	-0,259	-0,164
%CD27+IgG+	0,357	0,415	-0,312	-0,696
%CD27+IgM+	0,173	0,789	0,018	0,411
%CD27+IgM-	0,201	0,211	-0,426	-0,839
%CD27-IgG+	-0,844	0,121	0,189	-0,140
%CD27-IgM+	-0,273	-0,317	0,815	0,695
%CD27-IgM-	0,178	-0,564	-0,791	-0,826
	ELISA IgA Day6		**ELISA IgA Day9**	
%CD27+	0,708	0,862	0,520	0,411
%CD27+IgG+	0,609	0,853	0,731	-0,317
%CD27+IgM+	0,327	0,420	0,143	0,806
%CD27+IgM-	0,638	0,716	0,577	-0,510
%CD27-IgG+	0,369	0,092	0,017	0,113
%CD27-IgM+	-0,825	-0,603	-0,165	0,266
%CD27-IgM-	0,266	-0,075	-0,214	**-0,930**

Day0 subsets

Table SII. Pearson correlations T-Independent stimulations - 2500 B cells

	Day6 %CD27+CD38+			
	CpG + IL-2	CpG + IL-2 + anti-BCR	CpG + IL-2 + BAFF	CpG + IL-2 + anti-BCR + BAFF
%CD27+	0,638	0,592	0,455	0,477
%CD27+IgG+	0,757	0,733	0,616	0,647
%CD27+IgM+	0,523	0,466	0,326	0,340
%CD27+IgM-	0,523	0,466	0,326	0,340
%CD27-IgG+	-0,552	-0,543	-0,616	-0,574
%CD27-IgM+	-0,118	-0,081	0,077	0,035
%CD27-IgM-	-0,738	-0,694	-0,573	-0,589
	Day9 %CD27+CD38+			
%CD27+	0,464	0,721	0,415	0,388
%CD27+IgG+	**0,826**	**0,910**	0,737	**0,819**
%CD27+IgM+	0,059	0,331	0,066	-0,079
%CD27+IgM-	0,771	**0,884**	0,662	**0,824**
%CD27-IgG+	-0,380	-0,462	-0,640	-0,421
%CD27-IgM+	-0,803	-0,531	-0,528	-0,364
%CD27-IgM-	0,378	-0,070	0,230	0,170
	ELISA IgG Day6		**ELISA IgG Day9**	
	CpG + IL-2	CpG + IL-2 + BAFF	CpG + IL-2	CpG + IL-2 + BAFF
%CD27+	0,721	0,535	0,404	0,322
%CD27+IgG+	**0,932**	0,557	0,776	0,634
%CD27+IgM+	0,373	0,271	0,035	0,022
%CD27+IgM-	**0,826**	0,636	0,690	0,545
%CD27-IgG+	-0,082	-0,135	-0,363	-0,706
%CD27-IgM+	-0,558	-0,797	-0,191	-0,420
%CD27-IgM-	-0,153	0,237	-0,056	0,226
	ELISA IgM Day6		**ELISA IgM Day9**	
%CD27+	0,243	0,252	0,237	-0,257
%CD27+IgG+	-0,320	-0,365	-0,316	-0,722
%CD27+IgM+	0,636	0,670	0,620	0,249
%CD27+IgM-	-0,420	-0,447	-0,420	**-0,830**
%CD27-IgG+	0,039	0,112	-0,410	0,076
%CD27-IgM+	0,429	0,369	0,367	0,257
%CD27-IgM-	-0,777	-0,758	-0,646	-0,207
	ELISA IgA Day6		**ELISA IgA Day9**	
%CD27+	0,270	0,406	0,503	0,402
%CD27+IgG+	0,723	0,714	0,748	0,721
%CD27+IgM+	-0,108	0,070	0,206	0,078
%CD27+IgM-	0,633	0,642	0,637	0,621
%CD27-IgG+	-0,358	-0,630	-0,459	-0,534
%CD27-IgM+	-0,203	-0,314	-0,217	-0,265
%CD27-IgM-	0,089	0,070	-0,157	0,008

Day0 subsets

Table SII. Pearson correlations T-Independent stimulations - 2500 B cells in PBMCs (continued)

	Day6 %CD27+CD38+			
	CpG + IL-2	CpG + IL-2 + anti-BCR	CpG + IL-2 + BAFF	CpG + IL-2 + anti-BCR + BAFF
%CD27+	0,780	0,887	0,774	0,894
%CD27+IgG+	0,943	0,990	0,939	0,992
%CD27+IgM+	0,402	0,572	0,393	0,586
%CD27+IgM-	0,871	0,950	0,866	0,955
%CD27-IgG+	0,143	0,332	0,133	0,348
%CD27-IgM+	-0,322	-0,500	-0,313	-0,514
%CD27-IgM-	-0,952	-0,993	-0,949	-0,995
	Day9 %CD27+CD38+			
%CD27+	0,617	0,620	0,474	0,489
%CD27+IgG+	0,735	**0,947**	0,654	**0,889**
%CD27+IgM+	0,250	0,055	0,142	-0,049
%CD27+IgM-	0,578	0,860	0,517	0,808
%CD27-IgG+	0,131	0,111	0,275	0,194
%CD27-IgM+	-0,217	-0,491	-0,041	-0,313
%CD27-IgM-	-0,217	-0,491	-0,041	-0,313
	ELISA IgG Day6		**ELISA IgG Day9**	
	CpG + IL-2	CpG + IL-2 + BAFF	CpG + IL-2	CpG + IL-2 + BAFF
%CD27+	0,594	0,654	0,544	0,278
%CD27+IgG+	0,799	0,597	**0,915**	0,340
%CD27+IgM+	0,097	0,386	-0,014	0,142
%CD27+IgM-	0,784	0,458	0,847	0,229
%CD27-IgG+	0,599	0,442	0,270	0,561
%CD27-IgM+	-0,460	-0,159	-0,390	0,270
%CD27-IgM-	-0,014	-0,487	0,046	-0,643
	ELISA IgM Day6		**ELISA IgM Day9**	
%CD27+	0,503	0,573	0,000	-0,088
%CD27+IgG+	-0,263	-0,187	-0,473	-0,718
%CD27+IgM+	0,877	**0,903**	0,414	0,511
%CD27+IgM-	-0,476	-0,409	-0,612	-0,867
%CD27-IgG+	-0,078	-0,134	-0,823	-0,295
%CD27-IgM+	0,133	0,045	0,146	0,557
%CD27-IgM-	-0,837	-0,784	-0,196	-0,736
	ELISA IgA Day6		**ELISA IgA Day9**	
%CD27+	-0,334	-0,146	0,520	-0,059
%CD27+IgG+	0,467	0,621	**0,940**	0,257
%CD27+IgM+	-0,754	-0,649	-0,055	-0,205
%CD27+IgM-	0,561	0,701	0,857	0,205
%CD27-IgG+	0,460	0,488	-0,029	0,566
%CD27-IgM+	0,227	0,050	-0,452	0,475
%CD27-IgM-	0,202	0,230	0,202	-0,509

Day0 subsets

Legend	P value <0.05 marked as BOLD

R value
-1,000
-0,800
-0,600
-0,400
-0,200
0,000
0,200
0,400
0,600
0,800
1,000

CHAPTER 5

Oxygen level is a critical regulator of human B cell differentiation and IgG class switch recombination

Jana Koers*, Casper Marsman*, Juulke Steuten*, Simon Tol, Ninotska I.L. Derksen, Anja ten Brinke, S. Marieke van Ham§ and Theo Rispens§

*/§These authors contributed equally

Published in Frontiers in Immunology (2022)

ABSTRACT

The generation of high-affinity antibodies requires an efficient germinal center (GC) response. As differentiating B cells cycle between GC dark and light zones they encounter different oxygen pressures (pO_2). However, it is essentially unknown if and how variations in pO_2 affect B cell differentiation, in particular for humans. Using optimized *in vitro* cultures together with in-depth assessment of B cell phenotype and signaling pathways, we show that oxygen is a critical regulator of human naive B cell differentiation and class switch recombination. Normoxia promotes differentiation into functional antibody secreting cells, while a population of $CD27^{++}$ B cells was uniquely generated under hypoxia. Moreover, time-dependent transitions between hypoxic and normoxic pO_2 during culture - reminiscent of *in vivo* GC cyclic re-entry - steer different human B cell differentiation trajectories and IgG class switch recombination. Taken together, we identified multiple mechanisms trough which oxygen pressure governs human B cell differentiation.

INTRODUCTION

Development of an effective long-lasting immune response implies development of high-affinity, class-switched antibodies, the result of B cell differentiation within so-called germinal centers (GC), specialized substructures in secondary lymphoid tissues. Upon initiation of the humoral immune responses, initial T cell-dependent B cell activation leads to generation of a GC response, which is preceded by a short period of extrafollicular B cell activation. During the initial extrafollicular response, an early wave of naive B cells differentiate into plasma blasts and early memory B cells. These cells display limited levels of somatic hypermutation and affinity maturation[1–4]. The GC forms approximately one week after antigen exposure and becomes organized into two histologically distinct regions; the dark zone, where B cells undergo extensive proliferation and somatic hypermutation, and the light zone, where high-affinity B cells compete for antigen in order to undergo affinity selection. Class switch recombination may occur as early as the pre-GC stages and ensues in the GC reactions[5–7]. GC B cells cycle repeatedly through the light zone and dark zone. After initial fate decision, differentiation may proceed towards affinity-matured late memory B cells or antibody secreting cells (i.e., plasmablasts and plasma cells) with accumulating affinity maturation[8–10].

Previous studies by ourselves and others using *in vitro* cultures of human or mouse B cells demonstrated that a GC-like B cell response can be faithfully reproduced, including generation of mature memory B cells and antibody secreting cells[11,12]. Similar to what has been reported *in vivo*, CD40 ligation together with the availability of Tfh-associated cytokines IL-4 and IL-21 is required to promote B cell proliferation, isotype switching and generation of antibody secreting cell *in vitro*[2,13–15]. The combined action of Tfh-derived CD40L, IL-21, and IL-4, results in activation of NFκB and JAK-STAT pathways. These are vital for, amongst others, upregulation of BLIMP1 and XBP-1s, transcription factors necessary for initiation of antibody secreting cell differentiation and antibody production[16–20], as well as C-Myc and IRF4 upregulation[18,21–23]. C-Myc is required for the survival of GC B cells and is strongly upregulated upon antigen-specific selection in the GC light zone, allowing for dark zone (re-) entry[24–27]. A central role in orchestrating these events is the transcriptional repressor BCL6, which regulates expression of amongst others c-Myc and BLIMP1[24,28,29] (For more detail, see **Figure S4A**).

The partial pressure of oxygen (pO_2) in healthy human tissues is around 3-6%,[30,31] but within lymphoid tissues, distinctive hypoxic regions exist (pO_2 ~0.5-1%), as specifically observed in GC light zone regions[32–34]. However, the role of variations in pO_2 on human B cell differentiation, and fate decision into memory B cells and antibody secreting cells has not been studied. In fact, the vast majority of *in vitro* studies is carried out at atmospheric oxygen levels ((pO_2 ~21%), which is much higher than proliferating B cells will encounter *in vivo*.

Variations in pO_2 are likely to affect the amplitude of B cell differentiation, due to profound effects of cellular metabolism as well as direct effects on transcriptional regulation[30,31,35–38]. Although, contrasting findings have been reported for the influence of hypoxia on GC responses in mice, negative effects on class switch recombination and proliferation are repeatedly described[32,34,39]. Others observed increased Tfh function induced by upregulation of HIF-1α, a major transcription factor involved in the cellular sensing of pO_2[33]. Not all previous studies have been able to confirm HIF-1α expression within GC B cells, suggesting hypoxia may regulate B cell function independent of HIF-1α[40]. Another study comparing hypoxic (1%) and venous (5%) pO_2 reported decreased class switch recombination and altered cellular metabolism upon culture at hypoxic pO_2[32]. Overall, oxygen pressure appears an important but as yet poorly understood variable in B cell differentiation.

In the present study, we systematically investigated the effect of atmospheric (21%), normoxic, tissue-associated (3%), and hypoxic (1%) pO_2 on human B cell differentiation in our highly optimized system for human primary B cell culture. Moreover, in line with varying oxygen pressures during B cell cycling in the GC dark zone and light zone, we studied time-dependent transitions in pO_2 during culture and its effects on B cell differentiation trajectories and IgG class switch recombination. We show that different oxygen pressures distinctly regulate human naive B cell differentiation and class switch recombination.

MATERIALS & METHODS

Isolation of human naive B cells

Buffy coats were obtained from anonymized healthy donors with written informed consent in accordance to the guidelines established by the Sanquin Medical Ethical Committee and in line with the Declaration of Helsinki. Human Peripheral blood mononucleated cells (PBMCs) were isolated from fresh buffy coats using Ficoll gradient centrifugation (lymphoprep; Axis-Shield PoC AS). $CD19^+$ cells were isolated by positive selection using magnetic Dynabeads (Invitrogen). Cryopreserved $CD19^+$ cells were resuspended in PBA (PBS supplemented with 0.1% bovine serum albumin) and stained for surface markers 30 minutes in the dark at 4 °C. Viable, singlet naive B cells ($CD19^+IgD^+$ $CD27^-IgG^-IgA^-$) were sorted on a FACS Aria II/III.

Human B cell cultures

3T3 mouse fibroblast cells expressing human CD40L (subtype: high), described previously [12], were harvested and irradiated with 30 Gy and seeded $10x10^3$ cells/well on 96-well plates for overnight adherence in B cell culture medium (RPMI medium supplemented with FCS (5%, Bodinco), penicillin (100 U/mL, Invitrogen), streptomycin (100 µg/mL, Invitrogen),

β-mercaptoethanol (50 μM, Sigma-Aldrich), L-glutamine (2mM, Invitrogen), human apo-transferrin (20 μg/mL, Sigma-Aldrich) depleted for IgG using protein A sepharose (GE Healthcare). The next day, naive B cells were sorted and 250 naive B cells/well were co-cultured with the seeded 3T3-CD40L expressing cells in the presence of IL-4 (25ng/ml; Peprotech) and IL-21 (50ng/ml; Peprotech) for 3 – 11 days to determine proliferation, isotype switching, GC, memory and plasma cell formation and Ig production. Cultures were maintained at 37 °C in an atmosphere with 5% pCO_2 and 21%, 3% or 1% pO_2. For some cultures after 3, 5 or 7 days cultures were moved from 1 to 3% pO_2 and vice versa.

Flow cytometry

Extracellular staining of surface markers

Cultured cells were washed with PBA and extracellular staining was performed at 4 °C for 30 minutes using the following antibody conjugates; CD19 (562947), CD38 (646851), IgD (561315), and IgM (562977), CD138 (552723), CD21 (561372 or 740395), FAS/CD95 (762346), CD80 (750440 or 558226), CD86 (748375 or 562433), CXCR4 (563924) from BD Biosciences. IgG (M1268) from Sanquin Reagents. IgA (2050-09) from SouthernBiotech. CD27 (25-0279-42) from ThermoFisher. PNA (FL-1071-5) from VectorLabs. Glut1 (FAB1418A) from R&D. LIVE/DEAD Fixable Near-IR from Invitrogen.

Intracellular staining of signaling and transcription factors

Staining procedures were performed as previously described[41]. In short, harvested and pooled cultures were kept on melting ice at all times. After washing, cultures were stained for membrane markers in a 25μl staining mix containing the Live/Dead stain, anti-CD19 and anti-CD38 antibodies. TF stain procedure also contained anti-CD27 antibodies during membrane marker staining. After staining, samples were washed once with ice-cold PBA and centrifuged. Samples were fixed with either paraformaldehyde (PFA; Sigma) or Foxp3 fixation buffer (eBioscience). PFA fixed samples were subsequently washed once and permeabilized with 90% methanol. Samples were incubated at -20°C till day of FACS analysis. Foxp3-fixed samples were washed once with Foxp3 permeabilization buffer and kept in ice-cold PBA in the dark till day of FACS analysis.

Before FACS analysis, all samples were retrieved from -20 ^{0}C or 4 ^{0}C storage and washed once with ice-cold PBA. Methanol permeabilized samples were washed once more before adding 25μl staining mix containing antibodies against STAT3 (564133, BD) , pSTAT3 (612569, BD), NFκB p65 (565446, BD), STAT6 (IC2167T, R&D), pSTAT6 (612600, BD) and C-MYC (13871S, CST), NFκB p65, HIF1α (359706, Biolegend) diluted in PBA. Samples were incubated for 45 minutes on a plate shaker at room temperature. Afterwards, samples were washed once with PBA and measured on a flow cytometer.

Foxp3 fixed samples were washed once with Foxp3 permeabilization buffer. Samples were stained in 25µl staining mix containing antibodies against PAX5 (649708, Biolegend), BCL6 (358512, Biolegend), IRF4 (646416, Biolegend) and AID (565785, BD) or PAX5, BCL6, IRF4, BLIMP1 (IC36081R-025, R&D) and XBP-1s (562820, BD) diluted in Foxp3 permeabilization buffer and incubated for 30 minutes in the fridge. Samples were washed once with Foxp3 permeabilization buffer and measured on a flow cytometer.

All antibodies used have been tested prior to experiments in target positive and negative cell lines/PMBCs/total CD19+ cells and were diluted to optimal staining concentrations. For overall population shifts the gMFI was plotted and expression frequencies were plotted when there was a particular expansion of high- or low-expressing cells. Samples were measured on the BD LSR Fortessa or BD FACSymphony and analyzed using Flowjo V10.8. For representative gating strategy, see **Figure S1**.

Proliferation assays

B cells were labelled with proliferation dye according to manufacturer's instructions. In short, sorted B cells were washed with 10 ml PBS twice and resuspended to a concentration of $2x10^7$ cells/ml in PBS. Cells and 4µM Violet Proliferation Dye 450 (VPD450, BD Biosciences) in PBS were mixed at a 1:1 ratio and incubated 15 minutes in a 37 ^{o}C water bath in the dark, vortexing the tube every 5 minutes to ensure uniform staining. Cells were washed twice using a 10 times volume of cold culture medium to end labeling. Thereafter, B cells were cultured according to the protocol described above.

Assessment of B cell metabolic status

To monitor B cell metabolic activity, cells were cultured as described and loaded with 50nM MitoTracker Red CMXRos (M7512, Invitrogen) and 25nM MitoTracker Green FM (M7514, Invitrogen), 20nM BODIPY™ FL C12 (4,4-Difluoro-5,7-Dimethyl-4-Bora-3a,4a-Diaza-s-Indacene-3-Dodecanoic Acid) (D3822, Invitrogen) or 200µM 2-NBDG (2-(N-(7-Nitrobenz-2-oxa-1,3-diazol-4-yl)Amino)-2-Deoxyglucose) (N13195, Invitrogen) for 30 minutes or 2.5uM MitoSOX (M36008, Invitrogen) for 10 minutes at 37 °C 5% CO_2 in pre-warmed Hank's Buffered Salt Solution (HBSS, 14025050, Gibco) on day 0 and 7 of culture. Cells were washed, stained for membrane markers as described above and measured on a flow cytometer. Within experiments, for each sample, cell size was determined using FSC/SCC and gMFI was corrected subsequently according to the average cell size.

Cell counts

Before FACS analysis samples were mixed with at least 10.000 CountBright Absolute counting beads (Thermo Fisher Scientific) and prepared for flow cytometry analysis as described above. Absolute B cell counts were determined according to the formula:

$$\left| \frac{\#LiveCD19+}{\#Beadsmeasured} x \#beadsadded \right.$$

Ig ELISAs of culture supernatants

IgM, IgA, IgG, and IgG1 and IgG4 expression levels were measured in culture supernatants at day 7, 11 and 14. 96-well maxisorb plates were coated with monoclonal mouse anti-human IgM (2µg/ml, MH15-1), anti-IgA (1µg/ml, MH14-01), anti-IgG (2µg/ml, MH16-1), anti-IgG1 (1µg/ml, MH161-01), and IgG4 (1µg/ml, MH164-01) in PBS all provided by Sanquin Reagents. Culture supernatants were incubated for 1h and secreted Igs were detected using 1µg/ml HRP-conjugated mouse anti-human IgM, IgA, IgG, IgG1, or IgG4 (Sanquin Reagents) in HPE (Sanquin Reagents). The ELISA was developed using TMB substrate, stopped by addition of 2M H_2SO_4 and absorbance was measured at 450 and 540 nm. OD values were normalized to values of a titration curve of a serum pool that was included in each plate.

Lactate production

L(+)-lactate production was measured in B cell culture supernatant using L-lactate Assay Kit (ab65331, Abcam) according to manufacturer's instructions. Lactate production was corrected for cell counts as measured by flow cytometry.

Real-time semi-quantitative RT-PCR

RNA isolation was performed as described elsewhere[42]. Primers were developed to span exon–intron junctions and then validated (IL-4R: 5'- CCCTGAAGTCTGGGATTTCCT -3'). Gene expression levels were measured in duplicate reactions for each sample in StepOnePlus (Applied Biosystems, Foster City, CA, USA) using the SYBR green method (Applied Biosystems, Foster City, CA, USA). Expression of housekeeping gene 16S was used for normalization.

Statistical analysis

Statistical analysis was performed using GraphPad Prism 8. Data were analyzed using Repeated Measures one-way ANOVA with Tukey's multiple comparison test, Repeated Measures two-way ANOVA with Sidak's multiple comparison test or mixed-effects analysis with Dunnett's multiple comparison test where appropriate. Results were considered significant at $p < 0.05$. Significance was depicted as *$p < 0.05$ or **$p < 0.01$, ***$p < 0.001$ or ****$p < 0.0001$. To show significance between specific datasets within a graph containing multiple datasets, the * shows the significance between the dataset matching the color of * and the dataset closest to the *.

RESULTS

Differential pO_2 controls human B cell differentiation into CD27$^+$ and antibody secreting cell compartments

The contribution of pO_2 on human naive B cell differentiation was investigated in B cell differentiation cultures while maintaining constant pCO_2. Resting naive B cells ($CD19^+IgD^+CD27^-IgG^-IgA^-$) from human peripheral blood were stimulated under atmospheric (pO_2 = 21%), normoxic (pO_2 = 3%) or hypoxic (pO_2 = 1%) conditions, using a combination of CD40L-expressing 3T3 cells[12], IL-4 and IL-21, known to facilitate class switch recombination, memory B cell and antibody secreting cell formation (**Figure 1A**)[12,43,44]. Alterations in pO_2 did not affect CD40L expression levels on 3T3 cells used for stimulation (**Figure S2I**, subtype high). Up until day 7 B cell survival was similar among pO_2 conditions, but at day 11 hypoxic cultures contained fewer cells (**Figure S2A and B**). In all cultures a rapid upregulation of activation marker CD80 was observed (**Figure S2C**). Remarkably, naive B cell differentiation, as determined by the formation of antibody secreting cells ($CD27^+CD38^+$) and $CD27^+$ ($CD27^+CD38^-$) B cells, was dramatically altered by differential pO_2. Hypoxia induced a 5 to 10-fold induction of $CD27^+$ B cells as compared to atmospheric ($p<0.0001$) and normoxic cultures ($p<0.0001$) at day 7 (**Figure 1B and C**, and absolute cell no. in **Figure S2D**), at the expense of antibody secreting cell formation at day 11. In addition, in normoxic cultures, the relative numbers of $CD138^+$ antibody secreting cells were 2 to 4-fold increased relative to atmospheric ($p<0.001$) and hypoxic cultures ($p<0.0001$, **Figure 1D**), in line with increased concentration of secreted IgM and IgG in normoxic culture supernatant at day 11 (**Figure 1E**). Naive B cells poorly survived and differentiated when cultured under extreme hypoxic conditions (pO_2 = 0.5%, **Figure S2E and F**). Furthermore, using 3T3 cells with higher or lower expression of CD40L resulted in reduced proliferation, especially at reduced oxygen pressures (resp. 'VH', and 'Low', vs 'High'; **Figure S2H and I**). The addition of anti-IgM $F(ab')_2$s to the cultures, as additional BCR stimulation, did not alter *in vitro* B cell survival and differentiation at differential pO_2s (**Figure S2J**). Next, we assessed the effect of pO_2 on antibody class switching and Ig production. Protein expression of DNA-editing enzyme AID –indispensable for class switch recombination and somatic hypermutation– were substantially elevated over time regardless of oxygen pressure, but significantly lower at low pO_2 at day 7 and 11 (**Figure 1F**), in accordance with previous studies in mice[32], reflecting the overall larger fraction of differentiated cells under these conditions (**Figure 1B and C**; **Figure S2K**). In line with AID expression levels, IgG^+ B cell frequencies were higher in atmospheric cultures ($p<0.001$, **Figure 1F**) with minimal switch to IgA^+ overall, as was expected by the IgG promoting culture conditions (CD40L + IL-21 + IL-4, **Figure S2L**). Altogether, these data illustrate a profound regulation of human naive B cell differentiation by oxygen levels and show that normoxia promotes differentiation into potent antibody secreting cells while hypoxia promotes differentiation into $CD27^+$ B cells.

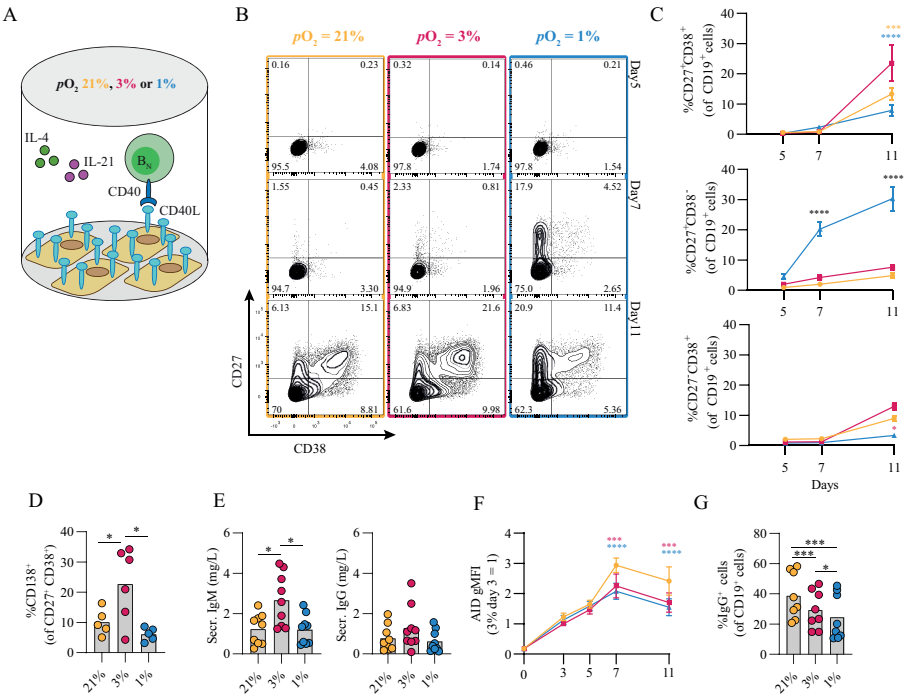

Figure 1. Differential pO_2 controls human B cell differentiation into CD27$^+$ and antibody secreting cell compartments. *(**A**) Schematic overview of B cell in vitro culture system. 250 resting human naive B cells (CD19$^+$CD27$^-$IgD$^+$) were stimulated using a human CD40L-expressing feeder cell layer (subtype 'High'[12]); recombinant human IL-4 (25ng/ml) and IL-21 (50ng/ml); and cultured at 5% pCO_2 and 21, 3, or 1% pO_2 for a maximum of 11 days. (**B**) Representative biaxial CD27/CD38 FACS plots after 5, 7, and 11 days of culture at 21, 3, or 1% pO_2. (**C**) Quantification of the percentages of CD27 and CD38 subpopulations within total CD19$^+$ B cells over time (n = 9). (**D**) CD138 expression within the CD27$^+$CD38$^+$ antibody secreting cell population (n = 6). (**E**) Cumulative secretion of IgM and IgG measured in culture supernatants after 11 days (n = 9). (**F**) gMFI of AID expression over time (n = 3). (**G**) Percentage of IgG$^+$ cells within CD19$^+$ B cells, combined surface and intracellular staining (n = 8). Bars represent means of biological replicates each composed of 2 technical replicates in (**D, F**) 2, (**E, G**) 3 or (**C**) 4 independent experiments. Statistical differences were determined using (**C, F**) mixed-effects analysis using Tukey's test for multiple comparisons (**D, E, G**) repeated measures one-way ANOVA using Tukey's test for multiple comparisons. * p<0.05, *** p<0.001, **** p<0.0001.*

Proliferative human B cells adopt glycolysis and mitochondrial-associated ROS levels are increased in hypoxic cultures

Given that cellular metabolism has been reported to be linked to gene expression and B cell differentiation[45], we assessed the metabolic status of B cells that were cultured at different pO_2s. Using flow cytometry, HIF1α levels were increased throughout hypoxic cultures compared to normoxic and atmospheric cultures (**Figure 2A**). After 7 days of *in vitro* stimulation B cells showed similar increase in cell size in all conditions compared to unstimulated cells (**Figure S3A**). Dividing lymphocytes typically rely on aerobic glycolysis, fermenting imported glucose into lactate rather than oxidizing it in the mitochondria for energy. Glycolytic activity was assessed by uptake of 2-NBDG, a fluorescent analog of

glucose, and production of lactate as an end product of glycolysis. Uptake of 2-NBDG and lactate production were not significantly different between different pO_2 culture conditions, but overall higher compared to resting naive B cells suggesting that indeed stimulated B cells require more glucose but demands did not change considerably upon differential pO_2 environments (**Figure 2B**). Also expression of GLUT1, a glucose transporter, varied minimally between culture conditions (**Figure S3B**). To asses mitochondrial oxidative metabolism we analyzed mitochondrial mass, potential and formation of reactive oxygen species (ROS) by flow cytometry at day 7. Mitochondrial mass, potential and mitochondrial ROS were higher in B cells cultured at hypoxic conditions (**Figure 2C**). Uptake of a fluorescent fatty acid probe was reduced in B cells under hypoxic conditions (**Figure 2D**), suggesting these cells rely less on oxidation of fatty acids. At day 11 metabolic markers yielded similar result among different pO_2 conditions, except for ROS levels that were significantly higher in hypoxic cultures compared to atmospheric cultures (**Figure S3C**). Taken together, these results indicate that highly proliferative B cells adopt glycolysis independent of local pO_2 levels and mitochondrial-associated ROS levels are elevated in hypoxic cultures.

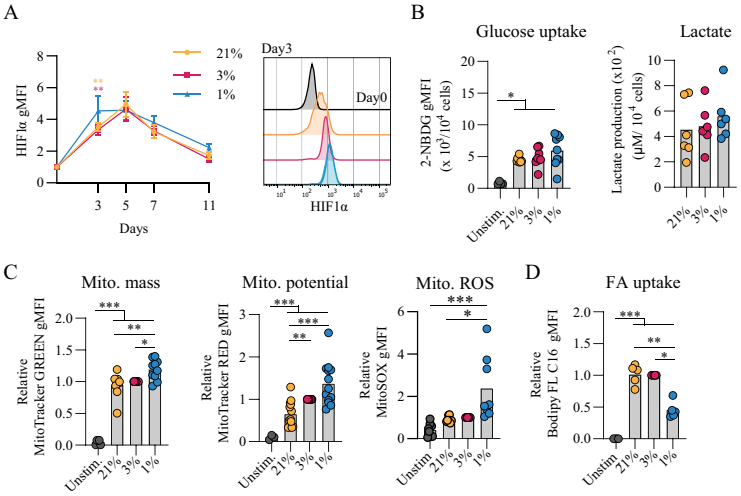

Figure 2. Proliferative human B cells adopt glycolysis and mitochondrial-associated ROS levels are increased in hypoxic cultures *(**A**) gMFI of HIF1α expression over time (n = 6) and histogram overlay at day 3. (**B**) Glucose uptake (2-NBG; (2-(N-(7-nitrobenz-2-oxa-1,3-diazol-4-yl)amino)-2-deoxyglucose) by B cells cultured for 7 days (n = 9). Lactate production measured in supernatants at day 11 in µM per 10^4 cultured B cells (n = 6). (**C**) gMFI of MitoTracker GREEN, MitoTracker RED, and MitoSOX after 7 days of culture (n = 8) indicative for mitochondrial mass, potential and ROS production, respectively. (**D**) Fatty acid (FA) uptake by B cells cultured for 7 days (n = 5). Bars represent means of biological replicates each composed of two technical replicates of (**E**) 1, (**A, C**) 2 or (**B, D**) 3 independent experiments. Statistical differences were determined using a repeated measures one-way ANOVA using Tukey's test for multiple comparisons. * p<0.05, ** p<0.01, *** p<0.001.*

pO_2 steers canonical signaling pathways that direct naive B cell differentiation pathways

The amplitude of B cell proliferation and differentiation is regulated by a complex interplay of signaling pathways induced by antigen recognition, CD40 ligation and reception of Tfh-derived cytokines IL-4 and IL-21 (summarized in **Figure S4A**)[8,46]. Upregulation of BCL6 as well as IRF4 expression suggests differentiation of cells with a GC-like phenotype (**Figure 3A and B**, respectively). In line, PNA positivity, indicative for expression of GC-specific glycans, and CD95 expression was observed early on in culture and decreased prior to the generation of $CD27^+$ B cells and antibody secreting cells (**Figure 3C and D**). PNA binding was reduced for B cells cultured at hypoxic pO_2 at day 3 and 5 potentially due to the accelerated $CD27^+$ differentiation in hypoxic cultures. Expression of CD86, an activation marker highly expressed on light zone B cells[47,48], increased rapidly during culture and remained significantly higher expressed on B cells cultured at hypoxic pO_2 (**Figure 3E**). CD40 signaling primarily shapes the magnitude of B cell expansion and survival through induction of NFκB p65 and c-Myc[22,49,50]. Moreover, NFκB p65 and c-Myc are reported to maintain cellular GC commitment[51]. B cells cultured at hypoxic pO_2 showed a reduction in NFκB p65 (**Figure 3F**) and c-Myc (**Figure 3G**) expression from day 5 onwards, supporting the concomitant differentiation into $CD27^+$ cells, and to a lesser extent antibody secreting cells, at day 7 and reduced B cells numbers observed in hypoxic cultures thereafter (**Figure S2B**).

Next, the effect of pO_2 on the IL-4R/IL-21R signaling pathways to regulate B cell and antibody secreting cell transcriptional programs was analyzed. Increased phosphorylation of STAT6 (pSTAT6), a signaling protein downstream of the IL-4R, was observed in B cells cultured at hypoxic pO_2, peaking at day 3 and 5 ($p<0.01$ at day 5) (**Figure 3H**, **Figure S4B**). This coincided with higher expression of XBP-1s, a transcription factor (TF) downstream of pSTAT6, at day 7 (**Figure 3J**, right panel), and was not the result of variable IL-4R expression levels, determined by RT-qPCR (**Figure S4C**). Peak levels of pSTAT3 on day 3 and 5, with minor differences when comparing the different pO_2 conditions (**Figure 3I**, **Figure S4D**), coincided with upregulation of BLIMP1, directly downstream of pSTAT3, and repression of PAX5, most prominently in B cells cultured at hypoxic pO_2 (**Figure 3J**, **Figure S4E**). PAX5 supports B cell identity. Consistent with this activity, B cells cultured at atmospheric pO_2 retained highest PAX5 levels throughout culture, and thus overall a lower fraction of differentiated cells under this conditions (**Figure S4E**, **Figure 1C**)[52]. Expression of BLIMP1 and XBP-1s was higher under hypoxic conditions (**Fig 3J**), and did not differ within the $CD27^-CD38^-$ population at varying pO_2 at day 7 (**Figure S4F**), suggesting elevated BLIMP1 and XBP-1s expression in B cells cultured at hypoxic pO_2 arises from the expanded $CD27^+$ compartment (**Figure 1C**). This $CD27^+$ population did not secrete more Ig at day 7 compared to cells cultured at normoxic or atmospheric pO_2 despite elevated XBP-1s expression, which is essential for the unfolded protein response in antibody secreting cells (**Figure S4G**). At day 11, naive B cells differentiation into antibody secreting

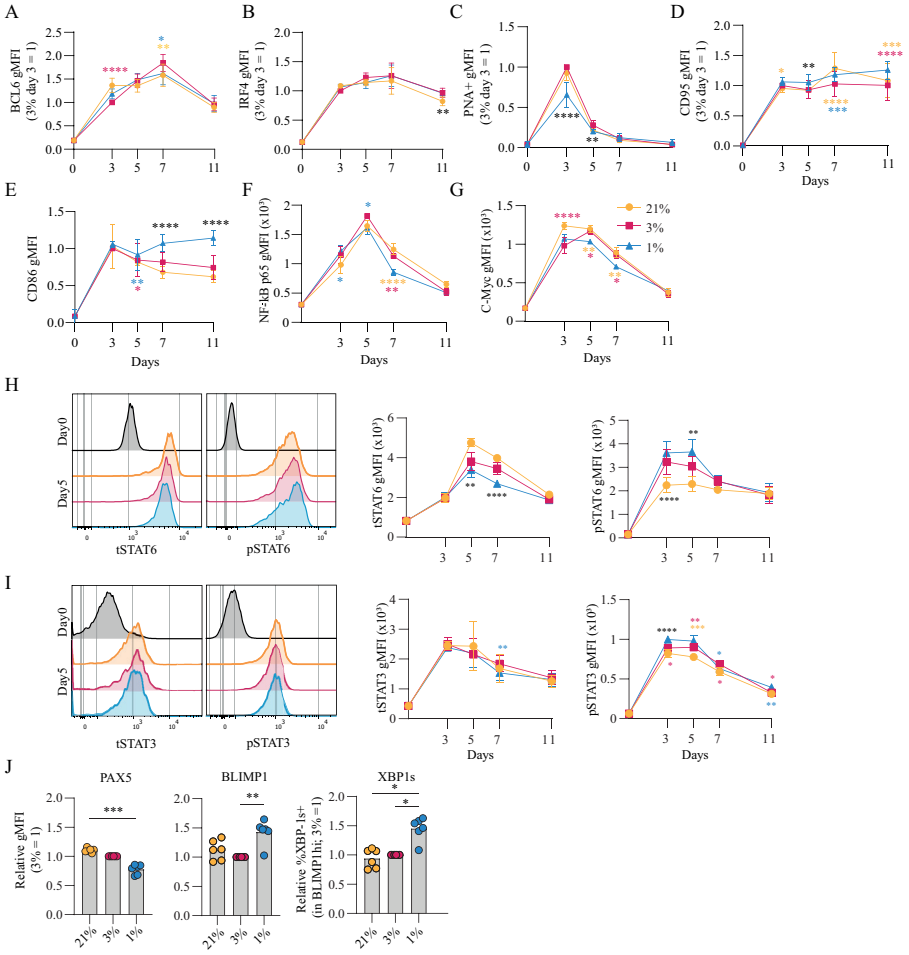

Figure 3. pO_2 steers canonical signaling pathways that direct naive B cell differentiation pathways
*(**A-D**) gMFI of (**A**) BCL-6 (n = 6) (**B**) IRF4 (n = 6) (**C**) PNA+ (n = 6) (**D**) CD95 (n = 6) (**E**) CD86 (n = 6) (**F**) NFκB active subunit p65 (n = 9) (**G**) c-Myc (n = 9) (**H-I**) gMFI of (**H**) tSTAT6 and pSTAT6 and (**F**) tSTAT3 and pSTAT3 over time in culture (n = 6) and (left panels) representative histogram overlays of pSTAT and tSTAT expression on day 5 of culture (**I**) gMFI of PAX5, BLIMP1 and %XBP-1s+ in BLIMP1hi cells (n=6) on day 7 (**A-J**) Bars represent means of biological replicates each composed of two technical replicates of 2 (**H-J**) or (**A-G**) 3 independent experiments (**A-I**) Differences in gMFI were determined using mixed-effects analysis using Tukey's test for multiple comparisons. (**J**) Differences in gMFI were determined using repeated measures one-way ANOVA using Tukey's tests for multiple comparisons. * p<0.05, ** p<0.01, *** p<0.001, **** p<0.0001.*

cells in normoxic cultures outperformed atmospheric cultures in which B cells retained higher PAX5 levels and repression of BLIMP1 and XBP-1s (**Figure S4H**). Furthermore, cells in normoxic cultures had highest XBP-1s levels in line with higher Ig production observed in these cultures ($p<0.05$) (**Figure 1G**). Overall, B cell culture at different pO_2 affects CD40-, IL-21R- and IL-4R-dependent signaling pathways essential for efficient B cell survival and differentiation. Expression dynamics of B differentiation-associated TFs PAX5, BLIMP1 and XBP1 were influenced by local pO_2, skewing the formation of $CD27^+$ and/or antibody secreting cell populations at hypoxic or normoxic pO_2, respectively.

Hypoxic pO_2 drives generation of a unique $CD27^{++}$ B cell population, with enhanced antibody secreting cell differentiation capacity and Ig production upon restimulation

Culturing B cells at hypoxic pO_2 resulted in a remarkable increase in $CD27^+$ B cells which emerged earlier as compared to atmospheric and normoxic cultures (**Figure 1C**). Interestingly, there was not only enlargement of this compartment but also formation of a population of $CD27^{++}$ cells (4.4% of CD19+ population), absent in normoxic and atmospheric cultures at day 7 ($p<0.05$) (**Figure 4A**, **Figure S5**) To assess the phenotype of these $CD27^{++}$ B cells, transcription factor profiles directing B cell differentiation were compared between $CD27^-$, $CD27^{+/-}$, $CD27^{+/+}$ and $CD27^{++}CD38^{++}$ populations that developed under hypoxic pO_2 at day 7 (**Figure 4B**). PAX5 expression was lower and BLIMP1 expression higher in $CD27^{+/++}$ cells compared to $CD27^-CD38^-$ B cells, with PAX5 and BLIMP1 expression being similar between $CD27^{++}$ and $CD27^{++}CD38^{++}$ populations (**Figure 4C**, upper and middle panel). Expression of XBP-1s increased as differentiation progressed, being highest in the $CD27^{++}CD38^{++}$ population (**Figure 4C**, lower panel). Moreover, a rise in the frequency of IgG^+ B cells coincided with increasing CD27 expression, being highest in the $CD27^{++}$ population (**Figure 4D**).

As the $CD27^{++}$ showed a distinct transcriptional profile compared to $CD27^{+/-}$ and $CD27^-$ B cells, we assessed whether this translated into functional differences with regard to antibody secreting cell differentiation and Ig production. To this end naive B cells were cultured for 7 days under hypoxia, after which different CD27 expressing populations were sorted and subsequently cultured at antibody secreting cell-promoting normoxic pO_2 for an additional 4 or 7 days (**Figure 4E**). $CD27^{++}$ cells showed a significant increase in antibody secreting cell differentiation and antibody production as compared to the $CD27^{+/-}$ and $CD27^-$ subsets ($p<0.05$) (**Figure 4F**), indicating that with the same level of stimulation the $CD27^{++}$ cells had enhanced capacity to differentiate towards functional antibody secreting cells. In summary, a population of $CD27^{++}$ B cells emerged exclusively in hypoxic cultures, with the potential to rapidly differentiate into antibody secreting cells and produce Ig after restimulation.

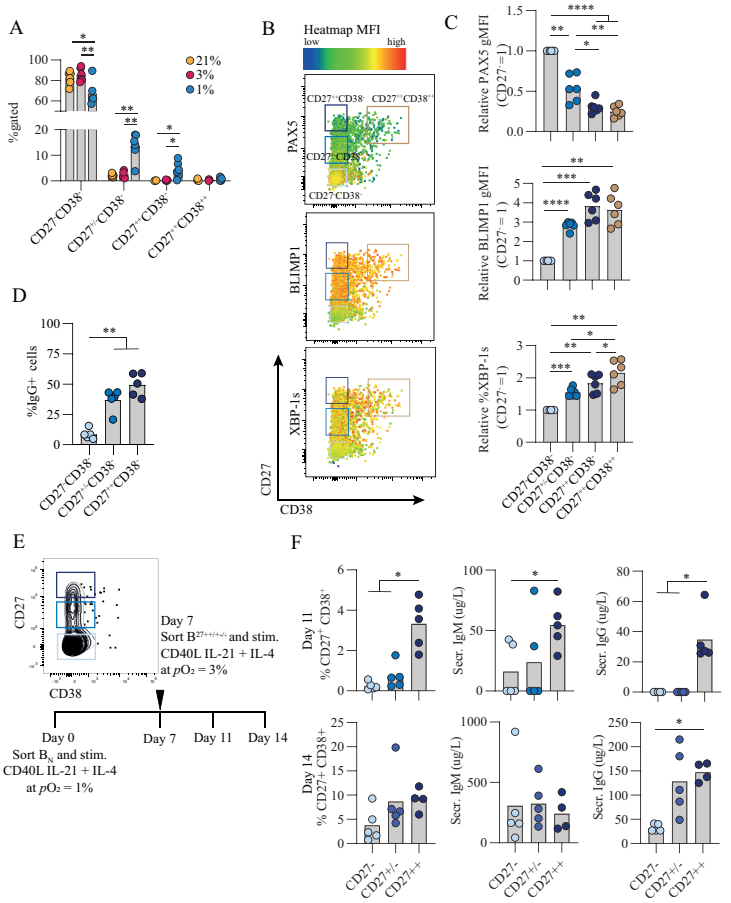

Figure 4. Hypoxic pO_2 drives generation of a unique CD27^{++} B cell population, with enhanced antibody secreting cell differentiation capacity and Ig production upon restimulation *(**A**) Quantification of percentage of CD27$^-$CD38$^-$, CD27$^{+/-}$CD38$^-$, CD27^{++}CD38$^-$ and CD27^{++}CD38^{++} cells on day 7 of culture (n = 5) (**B**) Representative biaxial flow cytometry plot of CD27 and CD38 expression, with heatmap depicting MFI expression of PAX5, BLIMP1 and XBP-1s on day 7. (**C**) gMFI of PAX5, BLIMP1 and XBP-1s in respective populations of CD27$^-$CD38$^-$, CD27$^{+/-}$CD38$^-$, CD27^{++}CD38$^-$ and CD27^{++}CD38^{++} cells on day 7 (n = 6) (**D**) Percentage of IgG+ B cells on day 7 of of culture at 1% pO_2 within CD27^{++} CD38$^-$, CD27$^{+/-}$ CD38$^-$ or CD27$^-$ CD38$^-$ populations. (n = 5) (**E**) Representative example of FACS sort gating strategy on day 7 to isolate CD27^{++} CD38$^-$, CD27$^{+/-}$ CD38$^-$ or CD27$^-$ CD38$^-$ B cells with schematic experimental time line. (**F**) Quantification of %CD27$^+$CD38$^+$ cells by flow cytometry and IgG and IgM secretion by ELISA, 4 or 7 days after sort (day 11 or 14 of culture) (n = 5). (**A-F**) Bars represent means of biological replicates each composed of two technical replicates of (**A, C, D**) 2 or (**F**) 1 independent experiment (**A**) Differences in %gated cells were determined using mixed-effects analysis using Tukey's test for multiple comparisons. (**C, D, F**) Differences in gMFI and % gated cells were determined using repeated measures one-way ANOVA using Tukey's test for multiple comparisons. * p<0.05, ** p<0.01, *** p<0.001, **** p<0.0001.*

Time-dependent pO_2 transitions alter B cell differentiation dynamics and promote class switch recombination to IgG

Given that during an *in vivo* GC reaction B cells cycle between the hypoxic light zone and normoxic dark zone, we assessed the effect of a pO_2 transition on B cell differentiation and class switch recombination *in vitro*. To this end, naive B cells were cultured at either hypoxic or normoxic pO_2 and transferred at stated time points to normoxic or hypoxic pO_2, respectively. Independent of timing, a transition from hypoxic to normoxic pO_2 increased antibody secreting cell differentiation concomitant with decreased $CD27^+$ cell formation (**Figure 5A and B**). Transition from hypoxic to normoxic pO_2 at day 3 of culture enhanced antibody secreting cell differentiation at day 11 compared to continued culture at hypoxic pO_2 and was similar to continuous culture under normoxic pO_2 (**Figure 5A and B**), with BLIMP1 expression lower compared to hypoxic cultures and similar to levels observed in normoxic cultures (**Figure 5C**). A transition from 1 to 3% pO_2 at day 5 led to a moderate generation of $CD27^+$ B cells and reduced antibody secreting cells formation in line with continuous hypoxic cultures. When hypoxic cultures were transitioned to normoxic pO_2 at day 7, this induced an efficient formation of antibody secreting cells at day 11. Different from cultures at hypoxic pO_2 on day 3 and 5, at day 7 hypoxic cultures consist for a significant proportion (~20%) of $CD27^{+/++}$ B cells, which efficiently differentiate to antibody secreting cells upon restimulation and transition to normoxic pO_2 as was shown in **Figure 4F**. Overall this suggests time-dependent transitions in pO_2 steer B cell differentiation, where early (day 3) transitions from hypoxic to normoxic pO_2 lead to antibody secreting cell formation comparable to continuous normoxic cultures whereas a pO_2 transition later on during culture (day 7) induces antibody secreting cell formation - in part - via the $CD27^{++}$ compartment. These data show that *in vitro* B cell differentiation can occur via distinct trajectories steered by differential pO_2, where hypoxia drives differentiation via a $CD27^{++}$ population and atmospheric and normoxic pO_2 via $CD38^+$ or directly towards antibody secreting cells (**Figure S6A**). Remarkably, transitions from hypoxic to normoxic pO_2 at day 3 and 5 enhanced class switch recombination to IgG^+ B cells concomitant with a reduction in IgM^+ B cells (**Figure 5D**). Even though the percentage of $CD138^+$ antibody secreting cells was similar (**Figure 5E**) and lower compared to continuous normoxic cultures (**Figure 1D**), transition of hypoxic to normoxic pO_2 at day 3 and 5 resulted in higher quantities of secreted IgM and IgG in culture supernatants (**Figure 5F**). Enhanced IgG class switch recombination and Ig production were no longer observed when the pO_2 transition was made at day 7.

Vice versa, transition from normoxic to hypoxic pO_2 at day 3 and 5 enhanced $CD27^+$ B cell formation and BLIMP1 expression compared to continuous normoxic cultures and was more similar to continuous hypoxic cultures (**Figure S6B, C and D**). A transition at day 7 from normoxic to hypoxic pO_2 was deleterious for both $CD27^+$ B cell and antibody secreting cell differentiation. class switch recombination to IgG^+ B cells and Ig production levels ranged between those found in continuous normoxic and hypoxic cultures (**Figure S6E, F and G**).

Overall, time-dependent transitions between hypoxic and normoxic pO_2 during culture govern different human B cell differentiation trajectories and IgG class switch recombination *in vitro*.

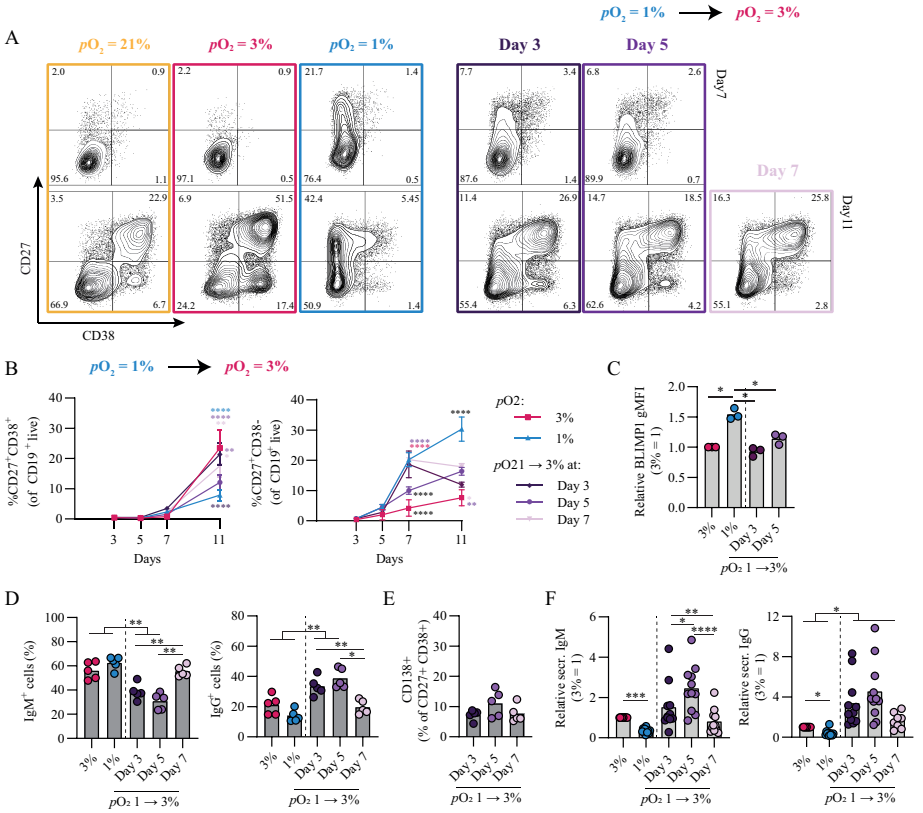

Figure 5. Time-dependent pO_2 transitions alter naive B cell differentiation and IgG class switch recombination. *(**A**) Representative biaxial CD27/CD38 FACS plots of 21, 3, 1% pO2 cultures and 1 – 3% pO_2 transition cultures at day 3, 5 or 7 shown for day 7 and 11 of culture. (**B**) Quantification of $CD27^+CD38^+$ and $CD27^+CD38^-$ B cells over time in culture (n = 11) (**C**) gMFI of BLIMP1 on day 7 (n = 3) (**D**) Frequency of IgM^+ and IgG^+ B cells on day 11 (n = 5). (**E**) CD138 expression within the $CD27^+CD38^+$ population (n = 5). (**F**) IgM and IgG levels were measured by ELISA in culture supernantant after 11 days (n = 11). Bars represent means of biological replicates each composed of two technical replicates of (**B, F**) 3, (**D**) 2 or (**C, E**) 1 independent experiment. (**B**) Statistical differences were determined using mixed-effects analysis using Tukey's test for multiple comparisons (**C-F**) Differences in gMFI, % gated cells and Ig production were determined using repeated measures one-way ANOVA using Tukey's test for multiple comparisons. * $p<0.05$, ** $p<0.01$, *** $p<0.001$, **** $p<0.0001$.*

DISCUSSION

The GC reaction is at the heart of the humoral immune response. Both extrafollicular and GC B cell responses take place within human tissues where oxygen pressure may range from 0.5-6% pO_2 with hypoxic regions (0.5-1% pO_2) described within GC light zone regions. Preciously little information is available about the potential role of local pO_2 on human B cell fate decision during their cycling between dark zone and light zone, typically characterized by dissimilar oxygen pressures. Here we studied the effect of atmospheric (21%), tissue associated (normoxia, 3%) and hypoxic (1%) pO_2 on human B cell differentiation. We observe profound differences in B cell differentiation, dynamics of emergence of various cell populations, class switch, and Ig production under these different oxygen pressures. **Figure 6** summarizes our key findings on the contribution of pO_2 on human naive B cell differentiation. In both hypoxic and normoxic cultures, naive B cells differentiated into a GC-like phenotype as evidenced by the expression of BCL6 and IRF4, as well as increased expression of CD95 and PNA binding. Similar to light zone B cell phenotype and function *in vivo*[8], B cells cultured at hypoxic pO_2 showed high expression of CD86 and differentiated rapidly into $CD27^+$ B cells. Moreover, culture at hypoxic pO_2 generated a unique population of $CD27^{++}$ B cells efficient in antibody secreting cell differentiation and Ig production upon restimulation. In normoxic cultures, naive B cells predominantly differentiated into antibody secreting cells, which occurred less rapidly compared to $CD27^+$ B cell formation at hypoxic pO_2 in line with time-dependent waves of memory B cell and antibody secreting cell formation *in vivo*[2]. Finally, time-dependent transitions from hypoxic to normoxic pO_2 during culture changes B cell differentiation trajectories and promotes IgG class switch recombination and Ig production. This indicates during *in vivo* B cell cycling between GC light zone and GC dark zone, the dynamic variation in pO_2 is also likely to form another regulatory layer for human B cell differentiation. Overall, our results identify oxygen as a critical factor in dictating human B cell differentiation and demonstrate the necessity of incorporating GC-like physiological pO_2 variations rather than continuous atmospheric pO_2 to study human B cell responses *in vitro*.

In vivo, antigen-specific triggering of the BCR is required for the generation of an efficient GC response. We did not observe an effect on B cell survival or differentiation by addition of a BCR stimulus to the B cell cultures at different pO_2, in line with previous reports showing limited additional effects of BCR triggers in *in vitro* cultures[12]. Despite the absence of a BCR trigger, we saw a clear upregulation of c-Myc expression which is normally upregulated upon positive selection in the GC, in line with previous reports indicating CD40L ligation to be sufficient to induce c-Myc expression[53]. We observed a reduction of c-Myc and NFκB expression in cells cultured at hypoxic pO_2 after an initial surge upon culture initiation. c-Myc and NFκB signaling play a major role in transcriptional regulation of GC B cell proliferation and cell survival, thereby correlating with our observations

regarding reduced cell numbers towards the end of cultures at hypoxic pO_2. Naive B cell survival was abrogated upon culture at 0.5% pO_2 and upon higher CD40L co-stimulation (subtype VH) at low pO_2, but not atmospheric pO_2, due to impaired proliferation. Hence, the level of CD40L co-stimulation impacts B cell survival at physiological pO_2.

Highly proliferative lymphocytes have been described to adopt glycolysis[54], which -although not comprehensively studied- is in line with the increase in glycolysis-associated metabolic traits observed in our cultures independent of *in vitro* pO_2. B cells cultured under

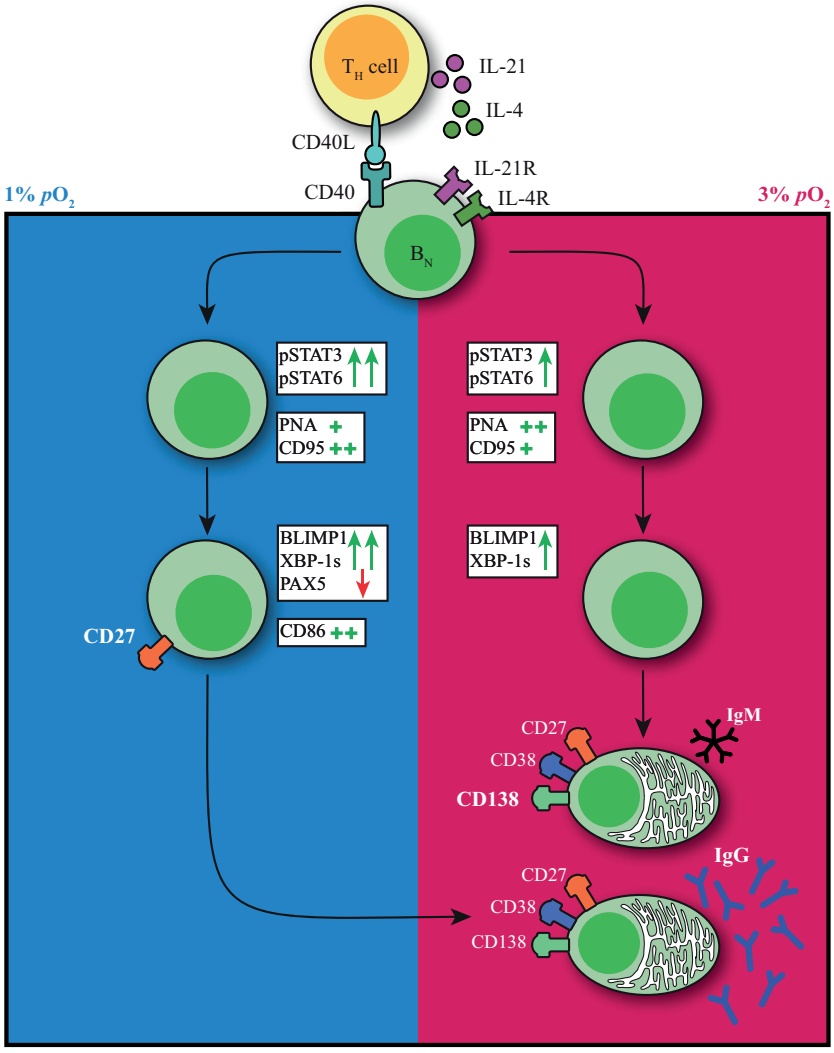

Figure 6. pO_2 as a critical driver of B cell differentiation *in vitro*. *Schematic representation of the effect of differential pO_2 on B cell differentiation and underlying signaling pathways.*

hypoxic pO_2 carried out mitochondrial oxidative metabolism, in addition to glycolysis. The difference in B cell differentiation trajectories and expansion of the $CD27^+$ compartment in hypoxic cultures may explain the expanded metabolic program towards mitochondrial oxidative metabolism at day 7. Much of the research on crosstalk between immune responses and pO_2 has focused on the TF HIF1α. We observe upregulation of HIF1α expression throughout all culture conditions not only at hypoxic pO_2. HIF1α can also be induced by signaling through CD40L, BCRs as well as TLR ligands, probably explaining the increase in HIF1α also in non-hypoxic cultures[55]. Furthermore, a recent study could not identify expression of hypoxia-induced genes in *ex vivo* analyzed mouse GC B cells[40], indicating HIF1α is not the sole regulator of hypoxia-associated responses.

Clear differences were observed in the expansion of $CD27^+$ B cell and/or antibody secreting cell compartments in human naive B cells cultures at hypoxic and normoxic pO_2, respectively, driven by differences in the underlying molecular pathways regulating B cell survival and differentiation. It has been shown that there is a time-dependent developmental switch in the output of the GCs, such that it first dedicates itself to memory B cell generation and later switches to mainly producing antibody secreting cells[2]. During culture of naive B cells at hypoxic pO_2 a hypoxia-dependent $CD27^{++}$ population emerged early during culture. The question arises whether these $CD27^{++}$ cells may resemble memory B cell generated early within a GC response. Albeit unanswered in this study, it did become clear that these $CD27^{++}$ cells did not secrete Igs, whereas upon restimulation they swiftly differentiated into antibody secreting cells and exhibited efficient Ig secretion, in line with functionalities of memory B cells[56]. Nevertheless, these cells clearly expressed a transcription factor signature of increased BLIMP1 and XBP-1s expression concomitant with a reduction of the B cell identity TF PAX5, similar to antibody secreting cells and different from memory B cells[16,19]. In line with varying pO_2 during a GC response, where B cells cycle between hypoxic light zone to normoxic dark zone, we observed time-dependent effects of pO_2 transitions on human B cell differentiation trajectories. Taken together, hypoxic pO_2 primes B cells for efficient antibody secreting cell differentiation from a $CD27^+$ phenotype that, in order to occur, favors a transition to a normoxic environment. Besides B cell differentiation trajectories, also IgG class switch recombination was influenced by pO_2 transitions. When cultured at continuous pO_2, atmospheric pO_2 yielded the highest proportion of IgG^+ B cells (albeit not corroborated with equally elevated levels of IgG antibody production). Similar numbers of IgG^+ B cells could be generated in cultures that transitioned from hypoxic to normoxic pO_2 at day 3 or 5. Overall, our *in vitro* studies demonstrate the necessity of incorporating GC-like physiological pO_2 variations rather than continuous atmospheric pO_2 to study human B cell responses *in vitro*, as it more closely resembles the *in vivo* GC microenvironment and recapitulates time-dependent regulation of B cell fate decisions.

Besides local pO_2, other factors such as availability of nutrients, migratory and physical signals such as shear stress are also likely to contribute to B cell fate decision during both extrafollicular and GC B cell responses, warranting the need for 3D culture systems or organoids that more closely resemble the GC microenvironment to facilitate human *in vitro* B cell differentiation studies. In addition, several pathological conditions have been described to be related to hypoxia, such as myocardial ischemia[57], metabolic diseases[58], chronic heart and kidney diseases[59], and reproductive diseases[60]. Moreover, pO_2 has been measured and found to be significantly reduced in the majority of tumors, and sensitivity to chemotherapeutic agents changed dramatically under hypoxic conditions[61–63], highlighting the importance to adopt hypoxic cultures also for other avenues such as cancer-related drug testing and *in vitro* disease models.

In summary, we demonstrate that oxygen is an important regulator of human naive B cell differentiation by promoting oxygen-dependent differentiation trajectories and IgG class switch recombination.

Authors contributions

JK, CM, JS, ST, AB, MH and TR designed research. JK, CM, JS, ST and ND performed research. JK, CM and JS analyzed data. JK, CM, JS, AB, MH and TR wrote the paper. All authors critically reviewed the manuscript, gave final approval of the version to be published, and agreed to be accountable for all aspects of the work ensuring that questions related to the accuracy or integrity of any part of the work are appropriately investigated and resolved.

Financial support

This study was supported by Landsteiner Foundation for Blood Transfusion (Grants 1626 and 1609) and Sanquin Product and Process Development Call 2020

Disclosure statement

There are no commercial or financial conflicts of interest.

Ethics approval

The studies involving human participants were reviewed and approved by Sanquin Medical Ethical Committee. The patients/participants provided their written informed consent to participate in this study.

REFERENCES

1. Elsner RA, Shlomchik MJ. Germinal Center and Extrafollicular B Cell Responses in vaccination, immunity and autoimmunity. *Immunity*. 2020;53(6):1136-1150. doi:10.1016/j.immuni.2020.11.006.
2. Weisel FJ, Zuccarino-Catania G V., Chikina M, Shlomchik MJ. A Temporal Switch in the Germinal Center Determines Differential Output of Memory B and Plasma Cells. *Immunity*. 2016;44(1):116-130. doi:10.1016/j.immuni.2015.12.004
3. Laidlaw BJ, Cyster JG. Transcriptional regulation of memory B cell differentiation. *Nat Rev Immunol*. 2021;21(4):209-220. doi:10.1038/s41577-020-00446-2
4. Suan D, Kräutler NJ, Maag JLV, et al. CCR6 Defines Memory B Cell Precursors in Mouse and Human Germinal Centers, Revealing Light-Zone Location and Predominant Low Antigen Affinity. *Immunity*. 2017;47(6):1142-1153.e4. doi:10.1016/j.immuni.2017.11.022
5. Cunningham AF, Gaspal F, Serre K, et al. Salmonella induces a switched antibody response without germinal centers that impedes the extracellular spread of infection. *J Immunol*. 2007;178(10):6200-6207. doi:10.4049/jimmunol.178.10.6200
6. Marshall JL, Zhang Y, Pallan L, et al. Early B blasts acquire a capacity for Ig class switch recombination that is lost as they become plasmablasts. *Eur J Immunol*. 2011;41(12):3506-3512. doi:10.1002/eji.201141762
7. Roco JA, Mesin L, Binder SC, et al. Class Switch Recombination Occurs Infrequently in Germinal Centers. *Immunity*. 2019;51(2):337-350. doi:10.1016/j.immuni.2019.07.001.Class
8. Victora GD, Nussenzweig MC. Germinal centers. *Immunol Rev*. 2022;247(1):5-10. doi:10.1111/j.1600-065X.2012.01125.x
9. Shinnakasu R, Inoue T, Kometani K, et al. Regulated selection of germinal-center cells into the memory B cell compartment. *Nat Immunol*. 2016;17(7):861-869. doi:10.1038/ni.3460
10. Laidlaw BJ, Schmidt TH, Green JA, Allen CDC, Okada T, Cyster JG. The Eph-related tyrosine kinase ligand Ephrin-B1 marks germinal center and memory precursor B cells. *J Exp Med*. 2017;214(3):639-649. doi:10.1084/jem.20161461
11. Takahashi Y, Dutta PR, Cerasoli DM, Kelsoe G. *In Situ Studies of the Primary Immune Response to (4-Hydroxy-3-Nitrophenyl)Acetyl. V. Affinity Maturation Develops in Two Stages of Clonal Selection*. Vol 187.; 1998.
12. Unger PPA, Verstegen NJM, Marsman C, et al. Minimalistic In Vitro Culture to Drive Human Naive B Cell Differentiation into Antibody-Secreting Cells. *Cells*. 2021;10(5). doi:10.3390/cells10051183
13. Linterman MA, Beaton L, Yu D, et al. IL-21 acts directly on B cells to regulate Bcl-6 expression and germinal center responses. *J Exp Med*. 2010;207(2):353-363. doi:10.1084/jem.20091738
14. Tangye SG, Ferguson A, Avery DT, Ma CS, Hodgkin PD. Isotype Switching by Human B Cells Is Division-Associated and Regulated by Cytokines. *J Immunol*. 2002;169(8):4298-4306. doi:10.4049/jimmunol.169.8.4298
15. Zotos D, Coquet JM, Zhang Y, et al. IL-21 regulates germinal center B cell differentiation and proliferation through a B cell-intrinsic mechanism. *J Exp Med*. 2010;207(2):365-378. doi:10.1084/jem.20091777
16. Tellier J, Nutt SL. Plasma cells: The programming of an antibody-secreting machine. *Eur J Immunol*. 2019;49(1):30-37. doi:10.1002/eji.201847517

17. Nutt SL, Hodgkin PD, Tarlinton DM, Corcoran LM. The generation of antibody-secreting plasma cells. *Nat Rev Immunol*. 2015;15(3):160-171. doi:10.1038/nri3795

18. Klein U, Casola S, Cattoretti G, et al. Transcription factor IRF4 controls plasma cell differentiation and class-switch recombination. *Nat Immunol*. 2006;7(7):773-782. doi:10.1038/ni1357

19. Ding BB, Bi E, Chen H, Yu JJ, Ye BH. IL-21 and CD40L Synergistically Promote Plasma Cell Differentiation through Upregulation of Blimp-1 in Human B Cells. *J Immunol*. 2013;190(4):1827-1836. doi:10.4049/jimmunol.1201678

20. Avery DT, Deenick EK, Ma CS, et al. B cell-intrinsic signaling through IL-21 receptor and STAT3 is required for establishing long-lived antibody responses in humans. *J Exp Med*. 2010;207(1):155-171. doi:10.1084/jem.20091706

21. Craxton A, Shu G, Graves JD, Saklatvala J, Krebs EG, Clark EA. p38 MAPK is required for CD40-induced gene expression and proliferation in B lymphocytes. *J Immunol*. 1998;161(7):3225-3236.

22. Sun SC. The non-canonical NF-κB pathway in immunity and inflammation. *Nat Rev Immunol*. 2017;17(9):545-558. doi:10.1038/nri.2017.52

23. Chen D, Ireland SJ, Remington G, et al. CD40-Mediated NF-κB Activation in B Cells Is Increased in Multiple Sclerosis and Modulated by Therapeutics. *J Immunol*. 2016;197(11):4257-4265. doi:10.4049/jimmunol.1600782

24. Finkin S, Hartweger H, Oliveira TY, Kara EE, Nussenzweig MC. Protein Amounts of the MYC Transcription Factor Determine Germinal Center B Cell Division Capacity. *Immunity*. 2019;51(2):324-336.e5. doi:10.1016/j.immuni.2019.06.013

25. Luo W, Weisel F, Shlomchik MJ. B Cell Receptor and CD40 Signaling Are Rewired for Synergistic Induction of the c-Myc Transcription Factor in Germinal Center B Cells. *Immunity*. 2018;48(2):313-326.e5. doi:10.1016/j.immuni.2018.01.008

26. Calado DP, Sasaki Y, Godinho SA, et al. The cell-cycle regulator c-Myc is essential for the formation and maintenance of germinal centers. *Nat Immunol*. 2012;13(11):1092-1100. doi:10.1038/ni.2418

27. Dominguez-Sola D, Victora GD, Ying CY, et al. The proto-oncogene MYC is required for selection in the germinal center and cyclic reentry. *Nat Immunol*. 2012;13(11):1083-1091. doi:10.1038/ni.2428

28. Kitano M, Moriyama S, Ando Y, et al. Bcl6 Protein Expression Shapes Pre-Germinal Center B Cell Dynamics and Follicular Helper T Cell Heterogeneity. *Immunity*. 2011;34(6):961-972. doi:10.1016/j.immuni.2011.03.025

29. Harris MB, Chang C-C, Berton MT, et al. Transcriptional Repression of Stat6-Dependent Interleukin-4-Induced Genes by BCL-6: Specific Regulation of Iε Transcription and Immunoglobulin E Switching. *Mol Cell Biol*. 1999;19(10):7264-7275. doi:10.1128/mcb.19.10.7264

30. Atkuri KR, Herzenberg LA, Herzenberg LA. Culturing at atmospheric oxygen levels impacts lymphocyte function. *Proc Natl Acad Sci U S A*. 2005;102(10):3756-3759. doi:10.1073/pnas.0409910102

31. Burrows N, Maxwell PH. Hypoxia and B cells. *Exp Cell Res*. 2017;356(2):197-203. doi:10.1016/j.yexcr.2017.03.019

32. Cho SH, Raybuck AL, Stengel K, et al. Germinal centre hypoxia and regulation of antibody qualities by a hypoxia response system. *Nature*. 2016;537(7619):234-238. doi:10.1038/nature19334

33. Cho SH, Raybuck AL, Blagih J, et al. Hypoxia-inducible factors in CD4+ T cells promote metabolism, switch cytokine secretion, and T cell help in humoral immunity. *Proc Natl Acad Sci U S A*. 2019;116(18):8975-8984. doi:10.1073/pnas.1811702116

34. Abbott RK, Thayer M, Labuda J, et al. Germinal Center Hypoxia Potentiates Immunoglobulin Class Switch Recombination. *J Immunol*. 2016;197(10):4014-4020. doi:10.4049/jimmunol.1601401

35. Burrows N, Bashford-Rogers RJM, Bhute VJ, et al. Dynamic regulation of hypoxia-inducible factor-1α activity is essential for normal B cell development. *Nat Immunol*. 2020;21(11):1408-1420. doi:10.1038/s41590-020-0772-8

36. Jellusova J, Cato MH, Apgar JR, et al. Gsk3 is a metabolic checkpoint regulator in B cells. *Nat Immunol*. 2017;18(3):303-312. doi:10.1038/ni.3664

37. Halligan DN, Murphy SJE, Taylor CT. The hypoxia-inducible factor (HIF) couples immunity with metabolism. *Semin Immunol*. 2016;28(5):469-477. doi:10.1016/j.smim.2016.09.004

38. Li L, Feng C, Qin J, et al. Regulation of humoral immune response by HIF-1α-dependent metabolic reprogramming of the germinal center reaction. *Cell Immunol*. 2021;367. doi:10.1016/j.cellimm.2021.104409

39. Firmino NS, Cederberg RA, Lee C-M, et al. Germinal center hypoxia in tumor-draining lymph nodes negatively regulates tumor-induced humoral immune responses in mouse models of breast cancer. *Oncoimmunology*. 2021;10(1):1959978. doi:10.1080/2162402X.2021.1959978

40. Weisel FJ, Mullett SJ, Elsner RA, et al. Germinal center B cells selectively oxidize fatty acids for energy while conducting minimal glycolysis. *Nat Immunol*. 2020;21(3):331-342. doi:10.1038/s41590-020-0598-4

41. Marsman C, Jorritsma T, Ten Brinke A, van Ham SM. Flow Cytometric Methods for the Detection of Intracellular Signaling Proteins and Transcription Factors Reveal Heterogeneity in Differentiating Human B Cell Subsets. *Cells 2020, Vol 9, Page 2633*. 2020;9(12):2633. doi:10.3390/CELLS9122633

42. Souwer Y, Chamuleau MED, Van De Loosdrecht AA, et al. Detection of aberrant transcription of major histocompatibility complex class II antigen presentation genes in chronic lymphocytic leukaemia identifies HLA-DOA mRNA as a prognostic factor for survival. *Br J Haematol*. 2009;145(3):334-343. doi:https://doi.org/10.1111/j.1365-2141.2009.07625.x

43. Koers J, Pollastro S, Tol S, et al. CD45RB Glycosylation and Ig Isotype Define Maturation of Functionally Distinct B Cell Subsets in Human Peripheral Blood. *Front Immunol*. 2022;13(April):1-8. doi:10.3389/fimmu.2022.891316

44. Marsman C, Verhoeven D, Koers J, Rispens T. Optimized protocols for in vitro T cell-dependent and T cell- independent activation for B cell differentiation studies using limited cells. Published online 2022. doi:10.20944/preprints202111.0365.v2

45. Pearce EL, Pearce EJ. Metabolic pathways in immune cell activation and quiescence. *Immunity*. 2013;38(4):633-643. doi:10.1016/j.immuni.2013.04.005

46. Verstegen NJM, Ubels V, Westerhoff H V., van Ham SM, Barberis M. System-Level Scenarios for the Elucidation of T Cell-Mediated Germinal Center B Cell Differentiation. *Front Immunol*. 2021;12:1-19. doi:10.3389/fimmu.2021.734282

47. Victora GD, Schwickert TA, Fooksman DR, et al. Germinal center dynamics revealed by multiphoton microscopy with a photoactivatable fluorescent reporter. *Cell*. 2010;143(4):592-605. doi:10.1016/j.cell.2010.10.032

48. Allen CDC, Ansel KM, Low C, et al. Germinal center dark and light zone organization is mediated by CXCR4 and CXCR5. *Nat Immunol*. 2004;5(9):943-952. doi:10.1038/ni1100

49. Craxton A, Shu G, Graves JD, Saklatvala J, Krebs EG, Clark EA. p38 MAPK is required for CD40-induced gene expression and proliferation in B lymphocytes. *J Immunol*. 1998;161(7):3225-3236. http://www.ncbi.nlm.nih.gov/pubmed/9759836

50. Chen D, Ireland SJ, Remington G, et al. CD40-Mediated NF-κB Activation in B Cells Is Increased in Multiple Sclerosis and Modulated by Therapeutics. *J Immunol*. 2016;197(11):4257-4265. doi:10.4049/jimmunol.1600782

51. Heise N, De Silva NS, Silva K, et al. Germinal center B cell maintenance and differentiation are controlled by distinct NF-κB transcription factor subunits. *J Exp Med*. 2014;211(10):2103-2118. doi:10.1084/jem.20132613

52. Cobaleda C, Schebesta A, Delogu A, Busslinger M. Pax5: The guardian of B cell identity and function. *Nat Immunol*. 2007;8(5):463-470. doi:10.1038/ni1454

53. Luo W, Weisel F, Shlomchik MJ. B Cell Receptor and CD40 Signaling Are Rewired for Synergistic Induction of the c-Myc Transcription Factor in Germinal Center B Cells. *Immunity*. 2018;48(2):313-326.e5. doi:10.1016/j.immuni.2018.01.008

54. Vander Heiden MG, Cantley LC, Thompson CB. Understanding the Warburg effect: the metabolic requirements of cell proliferation. *Science*. 2009;324(5930):1029-1033. doi:10.1126/science.1160809

55. Halligan DN, Murphy SJE, Taylor CT. The hypoxia-inducible factor (HIF) couples immunity with metabolism. *Semin Immunol*. 2016;28(5):469-477. doi:10.1016/j.smim.2016.09.004

56. Deenick EK, Avery DT, Chan A, et al. Naive and memory human B cells have distinct requirements for STAT3 activation to differentiate into antibody-secreting plasma cells. *J Exp Med*. 2013;210(12):2739-2753. doi:10.1084/jem.20130323

57. Abe H, Semba H, Takeda N. The Roles of Hypoxia Signaling in the Pathogenesis of Cardiovascular Diseases. *J Atheroscler Thromb*. 2017;24(9):884-894. doi:10.5551/jat.RV17009

58. Trayhurn P, Wang B, Wood IS. Hypoxia in adipose tissue: a basis for the dysregulation of tissue function in obesity? *Br J Nutr*. 2008;100(2):227-235. doi:10.1017/S0007114508971282

59. Sun K, Zhang Y, D'Alessandro A, et al. Sphingosine-1-phosphate promotes erythrocyte glycolysis and oxygen release for adaptation to high-altitude hypoxia. *Nat Commun*. 2016;7:12086. doi:10.1038/ncomms12086

60. Zamudio S, Borges M, Echalar L, et al. Maternal and fetoplacental hypoxia do not alter circulating angiogenic growth effectors during human pregnancy. *Biol Reprod*. 2014;90(2):42. doi:10.1095/biolreprod.113.115592

61. Carreau A, El Hafny-Rahbi B, Matejuk A, Grillon C, Kieda C. Why is the partial oxygen pressure of human tissues a crucial parameter? Small molecules and hypoxia. *J Cell Mol Med*. 2011;15(6):1239-1253. doi:10.1111/j.1582-4934.2011.01258.x

62. Schito L, Semenza GL. Hypoxia-Inducible Factors: Master Regulators of Cancer Progression. *Trends in cancer*. 2016;2(12):758-770. doi:10.1016/j.trecan.2016.10.016

63. Brown JM. Exploiting tumour hypoxia and overcoming mutant p53 with tirapazamine. *Br J Cancer*. 1998;77 (4):12-14. doi:10.1038/bjc.1998.430

SUPPLEMENTARY MATERIAL

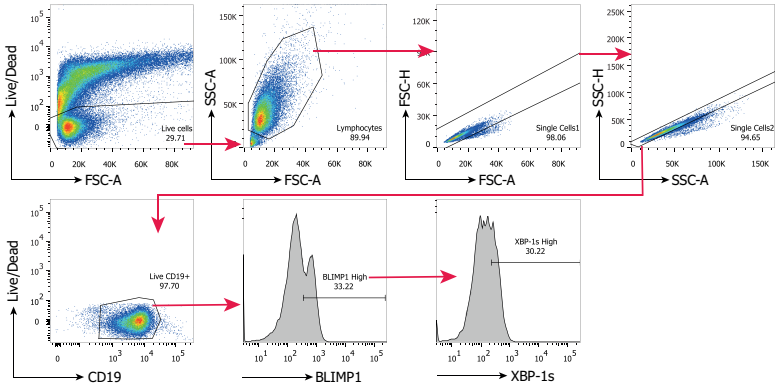

Figure S1. Representative gating strategy of B cells after culture. *First, live cells are gated based on viability dye and FSC-A, subsequently lymphocytes are gated using FSC-A and SSC-A, two gates to select singles, based on FSC and SSC A and H parameters. Finally cells were gated as live, CD19⁺ whereupon specific phenotyping and transcription factor markers were gated. Example gating strategy for BLIMP1 and XBP-1s gates.*

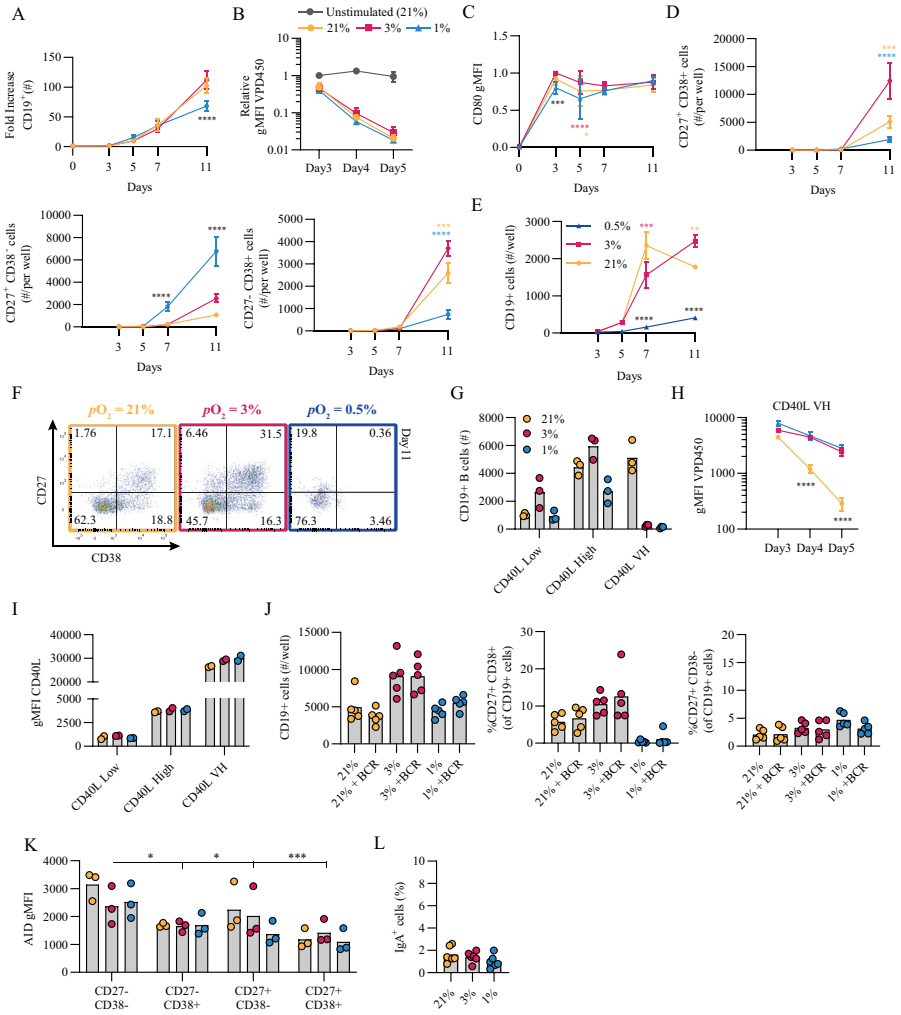

Figure S2. Hypoxia promotes human B cell differentiation *in vitro.* ***(A)*** *Fold increase in number of CD19+ cells over the course of the culture compared to day 0 (250 cells/well, n = 9).* ***(B)*** *Proliferation (n = 3).* ***(C)*** *gMFI CD80 (n = 6).* ***(D)*** *The number of CD19$^+$ cells retrieved per well within the CD27/CD38 quadrants (n = 9).* ***(E)*** *Number of live CD19$^+$ cells present in cultures using 0.5, 3 and 21 % pO_2 (n = 3).* ***(F)*** *Representative CD27/CD38 biaxial plot showing the differentiation of naive B cells at 0.5, 3 and 21% pO_2 at day 11 of culture.* ***(G)*** *Number of live CD19$^+$ cells in cultures stimulated with IL-4 + IL-21 and human CD40L low, high or very high (VH) co-stimulation cultured at 21, 3 and 1% pO_2 for 11 days (n = 3).* ***(H)*** *As in (G) for proliferation at day 3, 4 and 5 (n = 3). (I) Expression levels of human CD40L low, high and very high (VH) expressed on mice 3T3 fibroblast cells cultured at 21, 3 and 1% pO_2 for 5 days (n = 2).* ***(J)*** *Number of live CD19$^+$ cells, percentage of CD27$^+$CD38$^+$ and CD27+CD38- cells in cultures with and without 1µg/ml anti-IgM F(ab')$_2$ cultured for 11 days (n = 5).* ***(K)*** *AID expression within the different CD27/CD38 quadrants (n = 3).* ***(L)*** *IgA$^+$ B cells after 11 days of culture (n = 6). Bars represent means of biological replicates each composed of two technical replicates of (F-I, K) 1, (A, B, J, L) 2 or (C- E) 3 independent experiments. Statistical differences were determined using (B-F) mixed effects model using Tukey's test for multiple comparisons. (H-J) repeated measures one-way ANOVA using Tukey's test for multiple comparisons. * $p < 0.05$, ** $p < 0.01$, *** $p < 0.001$, **** $p < 0.0001$.*

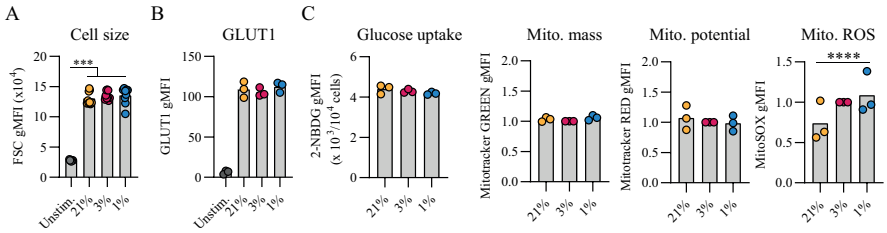

Figure S3. B cell cultured at hypoxic pO_2 alter their metabolic program. *At day 7 of culture (**A**) Cell size determined as gMFI of the forward scatter (FSC, n =14), (**B**) gMFI of GLUT1 expression, and (**C**) gMFI of 2-NBDG, MitoTracker GREEN, MitoTracker RED, and MitoSOX in cells cultured at differential pO_2 for 11 days (n = 3). Bars represent means of biological replicates each composed of two technical replicates of (A) 2 (B-C) or 1 independent experiments. Statistical differences were determined using repeated measures one-way ANOVA using Tukey's test for multiple comparisons. *** $p < 0.001$, **** $p < 0.0001$.*

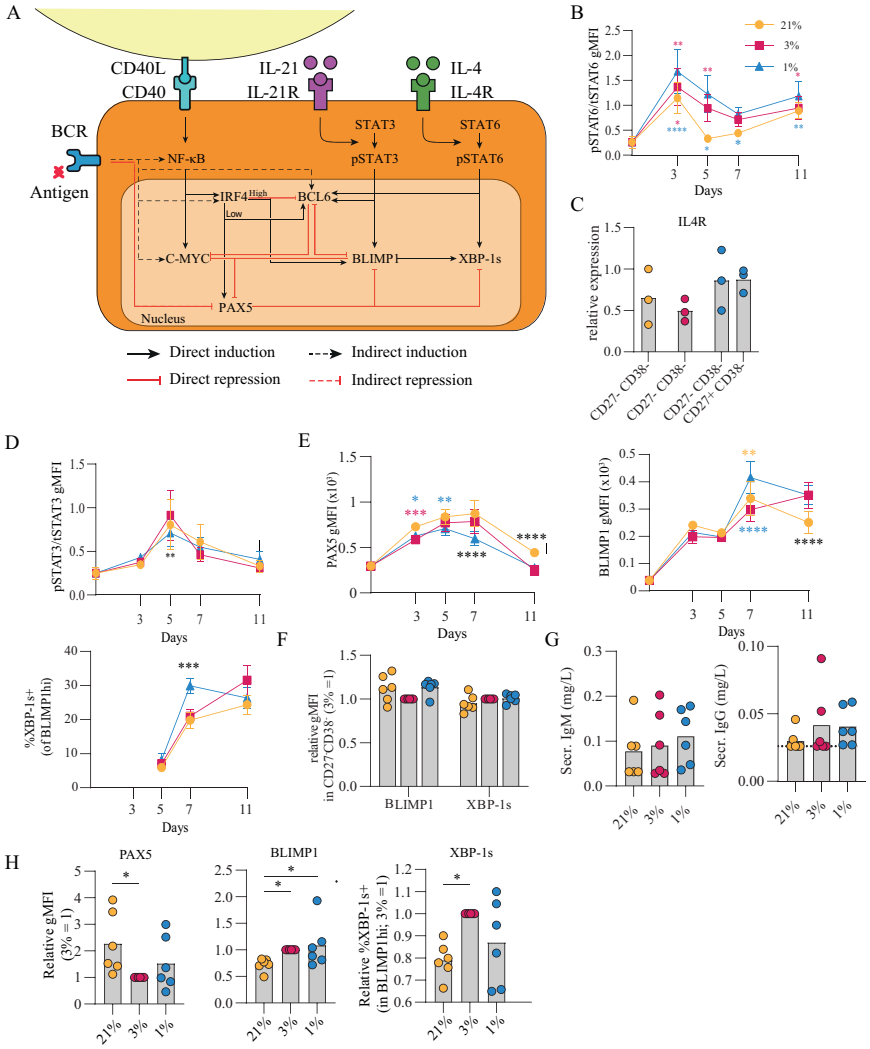

Figure S4. pO_2 steers molecular signaling underlying B cell differentiation. *(**A**) Schematic representation of intracellular signaling events leading to TF expression regulation upon B cell stimulation with typical Tfh signals including CD40L, IL-21 and IL-4. (**B**) ratio of pSTAT6/tSTAT6 gMFI (n = 6). (**C**) Relative expression of IL-4R mRNA as determined by RT-qPCR (n = 3). (**D**) ratio of pSTAT3/tSTAT3 gMFI (n = 6) (**E**) gMFI of PAX5, BLIMP1 and %XBP-1s over time (n = 6) (**F**) gMFI of BLIMP1 and XBP-1s within CD27⁻CD38⁻ population. (n = 6) (G) secreted IgM and IgG as measured by ELISA on day 7 of culture (n = 6) (**H**) gMFI of PAX5, BLIMP1 and %XBP-1s at day 11 (n = 6). Bars represent means of biological replicates each composed of two technical replicates of (B, D-H) 2 or (C) 1 independent experiments. Statistical differences were determined using (B, D-E) mixed-effects analysis using Tukey's test for multiple comparisons or (C, F-H) using repeated measures one-way ANOVA using Tukey's test for multiple comparisons.* p < 0.05, ** p < 0.01, *** p < 0.001, **** p < 0.0001.*

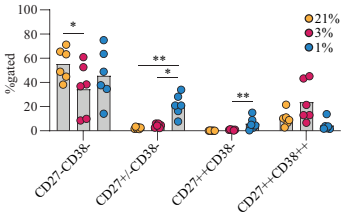

Figure S5. Hypoxic pO_2 leads to generation of pre-ASC CD27^{++} B cell subset. *Quantification of cells in CD27^{-}CD38^{-}, CD27$^{+/-}$CD38^{-}, CD27^{++}CD38^{-}, CD27^{++}CD38^{++} gates on day 11 of culture (n = 6) (n = 5) Bars represent means of biological replicates each composed of two technical replicates of 1 independent experiment. Statistical differences were determined using mixed effects analysis using Tukey's test for multiple comparisons * $p < 0.05$, ** $p < 0.01$, *** $p < 0.001$, **** $p < 0.0001$.*

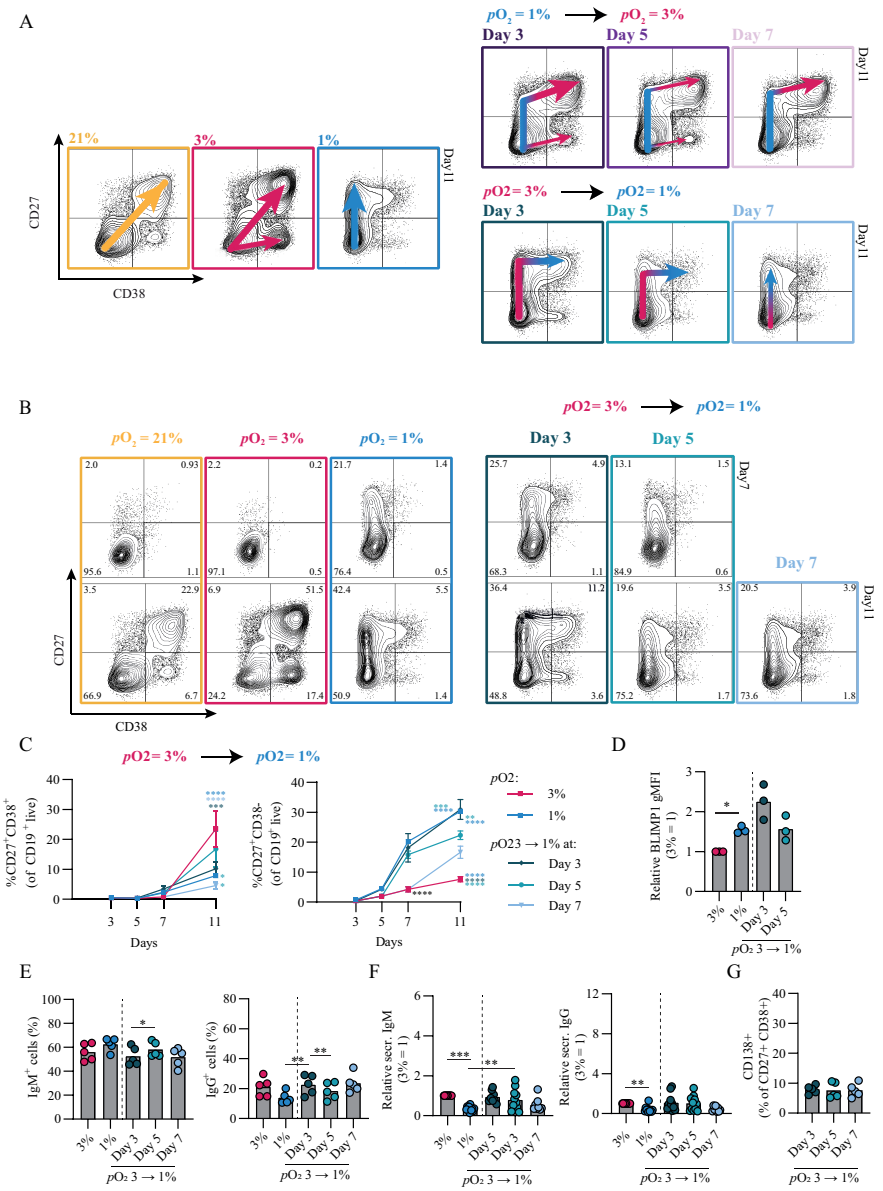

Figure S6. Time-dependent pO_2 transitions alter B cell differentiation dynamics and promote CSR to IgG. *(**A**) Schematic representation of CD27/CD38 differentiation trajectories of human naive B cells in vitro (**B**) Representative biaxial CD27/CD38 FACS plots of 21, 3 and 1% pO_2 cultures and 3 - 1% pO_2 transition cultures at day 3, 5 and 7 shown for day 7 and 11 of culture. (**C**) Quantification of $CD27^+CD38^+$ and $CD27^+CD38^-$ B cell formation (n = 11) (**D**) gMFI of BLIMP1 at day 7 (n = 3) (**E**) Frequency of IgM^+ and IgG^+ cells determined by intracellular flow cytometry (n = 5) (**F**) and cumulative IgM and IgG secretion in culture supernatants at day 11 in 3 and 1% pO_2 cultures and 3 - 1% pO_2 transition cultures (n = 11). (**G**) CD138 expression within the $CD27^+CD38^+$ ASC population (n = 5). Bars represent means of biological replicates each composed of two technical replicates of (C, F) 3, (E, G) 2, or (D) 1 independent experiment. Statistical differences were determined using mixed-effects analysis using Tukey's test for multiple comparisons. * $p < 0.05$, ** $p < 0.01$, *** $p < 0.001$, **** $p < 0.0001$.*

CHAPTER 6

Biased *N*-glycosylation site distribution and acquisition across the antibody V region during B cell maturation

Jana Koers, Ninotska I.L. Derksen, Pleuni Ooijevaar-de Heer P,
Benjamin Nota, Fleur S. van de Bovenkamp,
Gestur Vidarsson and Theo Rispens

Published in the Journal of Immunology (2019)

ABSTRACT

Antibodies can acquire *N*-linked glycans in their variable regions during antigen-specific B cell responses. Amongst others, these *N*-linked glycans can affect antigen binding and antibody stability. Elevated *N*-linked glycosylation has furthermore been associated with several B cell-associated pathologies. Basic knowledge about patterns of variable region glycosylation at different stages of B cell development is scarce. The aim of the current study is to establish patterns of *N*-glycosylation sites in antibody variable regions of naive and memory B cell subsets. We analyzed the distribution and acquisition of *N*-glycosylation sites within antibody variable regions of peripheral blood and bone marrow B cells of 12 healthy individuals, 8 myasthenia gravis patients, and 6 systemic lupus erythematosus patients, obtained by next-generation sequencing. *N*-glycosylation sites are clustered around complementarity-determining regions (CDRs) and the DE loop for both heavy and light chains, with similar frequencies for healthy donors and patients. No evidence was found for an overall selection bias against acquiring an *N*-glycosylation site, except for the CDR3 of the heavy chain. Interestingly, both IgE and IgG4 subsets have a 2-fold higher propensity to acquire Fab glycans compared to IgG1 or IgA. When expressed as recombinant monoclonal antibody, 35 out of 38 (92%) non-germline *N*-glycosylation sites became occupied. These results point towards a differential selection pressure of *N*-glycosylation site acquisition during affinity maturation of B cells, which depends on the location within the variable region, and is isotype- and subclass-dependent. Elevated Fab glycosylation represents an additional hallmark of T_H2-like IgG4/IgE responses.

INTRODUCTION

B cells are essential in adaptive immunity by recognizing and neutralizing a large variety of pathogen-associated antigens via membrane-bound receptors or secreted antibodies. In order to generate a diverse repertoire of antibodies, structural diversity is initially generated by the rearrangement of variable (V), diversity (D), and joining (J) genes, followed by somatic hypermutation (SHM) and class switch recombination. SHM is critical for antibody maturation by optimizing antigen recognition via accumulation of point mutations in the variable regions (V(D)J genes) of both heavy and light chains. An additional layer of antibody diversification arises from the glycosylation of *N*-glycosylation sites. *N*-glycosylation sites are consensus tripeptides consisting of asparagine, followed by any amino acid except proline, and either serine or threonine (N-X-S/T; X - P). The presence of such a motif does not guarantee its glycosylation, and is therefore usually referred to as potential *N*-glycosylation site. Here we will use the term *N*-glycosylation site to indicate these motifs, unless indicated otherwise. Since approximately 15% of serum IgG has variable regions that carry *N*-linked glycans[1,2], and only few germline alleles carry *N*-glycosylation consensus tripeptides[3], the majority of variable region glycosylation is therefore the result of SHM.

Glycosylation can have profound effects on protein function. In particular, IgG Fc glycosylation can directly modulate C1q and FcγR binding[4–8], and associations between glycosylation status and autoimmune disease have been demonstrated[9]. Antigen-specific IgG-responses also have been shown to result in skewing towards altered fucosylation and galactosylation in certain infectious- and alloimmune diseases[10–13]. Less is known about the variable region glycans, so-called Fab glycans, but several studies have reported a role for Fab glycans not only in modulating antigen binding[14–19] but also in increasing antibody stability[20], or extending *in vivo* antibody half-life[15,21]. Recently, evidence was provided for differential positive or negative selection for Fab glycosylation during antigen-specific antibody responses[19], which could in part be attributed to a direct effect of Fab glycans on antigen binding. Furthermore, altered levels of Fab glycosylation have been associated with pregnancy[1] as well as with several pathophysiological conditions, including follicular lymphoma[22], rheumatoid arthritis (RA) [23–25], primary Sjögren's syndrome (SS)[26,27], and suggested for systemic lupus erythematosus (SLE) [28]. In other words, differential selection pressure towards accumulation of Fab glycans is observed during various immune responses. However, the mechanisms behind these different layers of selection for or against Fab glycosylation and the extent of possible functional consequences are currently not known.

We previously showed that the distribution of *N*-glycosylation sites within the heavy chain variable regions of memory B cells is not random, but is largely dependent on the biased

distribution of positions where a single nucleotide mutation would suffice to introduce an *N*-glycosylation site, so-called 'progenitor sites' (**Figure 1A** and **Table I**)[19]. Further insights in the regulation of loss and gain of *N*-glycosylation sites in antibody variable regions may aid in understanding the selection for Fab glycosylated antibodies during antibody responses in various (patho)physiological conditions. Herein, we expand previous investigation of patterns and acquisition tendencies of *N*-glycosylation sites within heavy and light chain antibody variable regions during B cell maturation of healthy individuals, and two B cell associated diseases, SLE and myasthenia gravis (MG).

Table I. Description of variable region *N*-glycosylation site subsets

Subset	Description
Germline site	*N*-glycosylation site present in germline arrangement of a V gene allele.
Non-germline site	All *N*-glycosylation sites not corresponding to germline sites. These are the result of somatic hypermutation, or, within the CDR3, can also result from junctional diversity
Progenitor site	Sequon in the germline that can become an *N*-glycosylation site with a single nucleotide mutation (see Fig. 4C). Most glycosylation sites in the memory repertoire correspond to these; and resulted from somatic hypermutation
Non-progenitor site	Other non-germline *N*-glycosylation sites. These include those within the CDR3 that resulted from junctional diversity, as well as those that resulted from two or more mutations during somatic hypermutation.

METHODS

Data sets

For this study we included data sets from three open source efforts. From the first data set (SRA: PRJNA338795)[29] non-processed sequence reads from peripheral blood (PB) memory B cells ($CD19^+CD27^+$/reads from IgM, IgG, IgA, kappa, lambda) and naive B cells ($CD19^+CD27^-$/reads from IgM) of 4 healthy donors and 9 myasthenia gravis (MG) patients were collected. From the second data set (SRA: PRJEB18926)[30] non-processed sequence reads from PB and bone marrow (BM) mononuclear cells (reads from IgG1-4, IgA, IgM, IgE) of 6 allergic but otherwise healthy donors were obtained. In case of seasonal allergens, samples were taken out of season, and in all cases, subjects were free of symptoms at the time of sample collection. From the third data set (SRA: SRP057017)[31] non-processed sequence reads from PB memory B cells ($CD19^+IgD^-CD27^+$/reads from IgM, IgG, IgA) and naive B cells ($CD19^+IgD^+CD27^-$/reads from IgM) of 2 healthy donors and 7 SLE patients were collected.

Data processing

A total of 13 million raw paired end reads were assembled, quality trimmed, and filtered using Pandaseq[32] and in-house Perl and Awk scripts (sequences with a Q-value <30 or unidentified (N) nucleotides were excluded from further analysis). Isotypes were assigned using constant region primer matching (primers sequences are previously described[29–31]) and a random subset of ca. 20.000 sequences per isotype per sample were used for variable region germline alignment and mutation analysis of unique productive reads using IMGT/HiV-QUEST (http://www.imgt.org/HighV-Quest/)[33]. IgM sequences were subdivided into naive IgM with zero mutation in the V gene of the heavy chain (V_H), thus corresponding to the germline sequence, and memory IgM with ≥1 mutation(s) in the V_H. The memory B cell repertoire was represented by PB memory IgM, IgG and IgA and BM IgG and IgA. Biological replicates of PB and BM memory IgM, IgG and IgA and BM IgE sequences were similar, however, this was not the case for PB IgE[30]. The latter were therefore excluded from most analyses and IgE sequences were not included in the combined memory repertoire analysis. Very few sequences of PB IgE were available for one of six donors and these were therefore excluded from the analysis. Sequences of the four IgG subclasses were processed as described above. Sequences from two biological replicates for 5 healthy donors were available from both PB and BM IgG1-4 B cells. One of six donors had essentially no IgG4 sequences and was excluded from the analysis. In one of the studies next-generation sequencing was carried out using unique molecular identifiers (UMIs)[29]. When using UMI-guided read processing, as described previously[29], error rates decreased with approximately 1 error/sequence, illustrating the improved sequence quality when using UMI-adopted sequencing approaches. However, there was no appreciable difference in frequency distributions of *N*-glycosylation sites between the different types of processing.

Analysis of *N*-glycosylation sites

N-glycosylation site (N-X-S/T, X-P) mapping and matching to variable region progenitor sites was carried out essentially as previously described using either a combination of custom VB scripts and SQL queries in Microsoft Access[19], or custom R scripts. Additional data processing was also carried out using custom R scripts. *N*-glycosylation sites within the CDR3 region of the heavy chain (H-CDR3) were subdivided according to their position in either the left junction (position 105 – start D gene), the D gene (nonameric sequon of IMGT D3-REGION) or the right junction (D gene terminus – position 117). Sequences missing the D gene were excluded from further analysis. To analyze mutation propensities at progenitor sites, we subdivided progenitor sites as being Type I, IIa, and IIb, as described in the main text. In brief, for each type of progenitor site one or two of the three possible mutations at a specific nucleotide position result in a glycosylation site and those can be compared to the other one or two possible mutations at that same nucleotide position that do not result in a *N*-glycosylation site. For each unique progenitor site, frequencies of each of the three possible mutations were determined and compared. *N*-glycosylation sites

that emerged through multiple mutations within the triplet were excluded and therefore potential cases of co-dependent mutations were not considered in this analysis. In addition, framework region (FR) 1 was excluded from the analysis as most 5' primers annealed to this region. Only progenitor sites for which >1500 sequence reads were available were included in the analysis.

Antibody production and purification

Recombinant monoclonal antibodies were produced and purified as previously described[19]. In brief, synthetic V_H and V_L gene constructs were separately cloned into pcDNA3.1 expression vectors containing the corresponding constant (C) genes, and cotransfected in HEK293F cells. After a 5-day incubation at 37°C in humidified 8% CO_2 antibodies were purified from culture supernatant using protein G sepharose. For the generation of antibodies with germline *N*-glycosylation sites we used clone mAb63 for IGHV4-34. For IGHV1-8 we expressed an IGHV1-2 clone (anti-ADL 1.2) with and without a D81N mutation, which makes the clone homologous to an IGHV1-8 gene (i.e., ..TSTR(**N/D) TS**ISTA.. vs ..TMTR**DTS**ISTA..). Similarly, for IGHV5-10-1, we expressed guselkumab (IGHV5-51) with and without a R66N mutation, making the sequence homologous to IGHV5-10-1 (i.e., ...DSDT(**N/R)YS**PSFQ… vs …DSYT **RYS**PSFQ…).

Detection of *N*-linked glycans at variable regions of monoclonal antibodies

Detection of *N*-glycosylation site occupancy was performed as described previously[19]. In brief, glycosylation of recombinant antibodies was analyzed by SDS-PAGE and lectin ELISAs, using *Sambucus nigra* agglutinin (SNA, Vector Laboratories) for the detection of sialic acid. All monoclonal antibodies that showed increased molecular weight by SDS-PAGE also scored positive in the SNA lectin ELISA.

Statistical tests

Statistical comparisons were performed using two-tailed Student's *t* test, one-way analysis of variance (ANOVA) or Wilcoxon signed rank test. Measures for correlation used Pearson or Spearman's *r* test. Differences were considered statistically significant when the *P* values <0.05 (*P<0.05, ** P<0.01, *** P<0.001). Statistical analyses were performed using Graphpad Prism 7.04.

RESULTS

Distributions but not frequencies of non-germline *N*-glycosylation sites are similar amongst the different memory B cell repertoires

The frequency distributions of non-germline *N*-glycosylation sites (**Table I**) in naive and memory B cell populations were evaluated for 12 healthy individuals (ca. 1.5 million

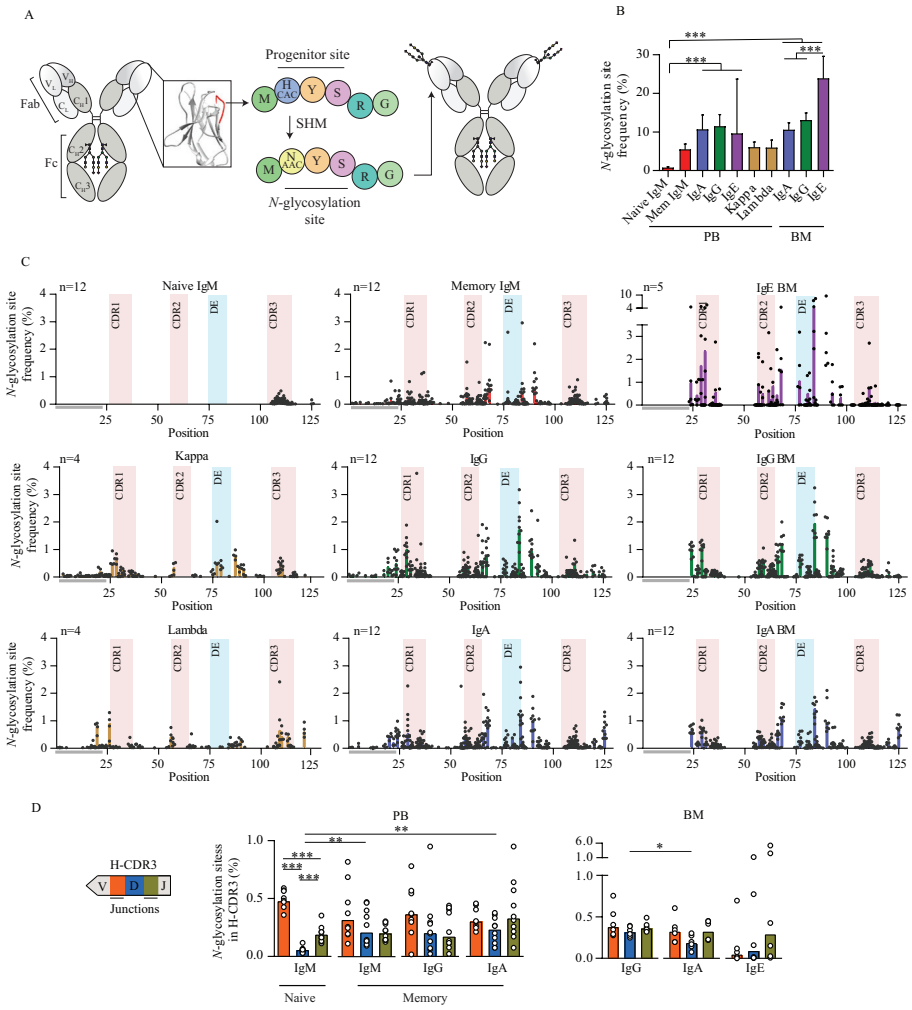

Figure 1. Frequency distribution of non-germline N-glycosylation sites across antibody variable region sequences for healthy individuals. ***(A)*** *Schematic representation of N-glycosylation site acquisition by SHM at a progenitor site in the antibody variable region.* ***(B)*** *The frequency of N-glycosylation sites (%) per isotype in PB and BM B cells. Bars indicate medians, error bars ± S.D., with the number of individuals indicated in (C).* ***(C)*** *The frequency (%) distributions of non-germline N-glycosylation sites across the variable region are shown for naive (IgM) and memory PB B cells (IgM, IgG, IgA, Kappa and Lambda) and switched memory BM B cells (IgG, IgA, IgE). The number of individuals is indicated in the upper left corner of each frequency distribution. Each dot represents a single donor; bars represent medians. Horizontal grey bars indicate FR1, for which coverage is incomplete (see M&M). Sites within the CDR3 at positions 111.1 – 112.1 are collapsed into position 111.* ***(D)*** *Frequency (%) of N-glycosylation sites across junctions and D genes in the H-CDR3 for PB and BM B cells. Each dot represents a single donor, bars represent median. B and D, one-way ANOVA, *** p <0.001; ** p <0.01 * p <0.05.*

sequence reads, **Table SI**). The frequencies of *N*-glycosylation sites were lowest for naive IgM, followed by IgM memory, Kappa and Lambda light chains, and highest for switched memory B cells (**Figure 1B**). Interestingly, the frequency of sites was similar for IgG and IgA, but significantly higher in BM IgE. The biological replicates of PB IgE yielded completely dissimilar results[30], hence the large S.D., and were therefore not taken into account for subsequent analyses. Despite differences in absolute frequencies, the **overall distribution of non-germline N-glycosylation sites across the heavy chain variable regions was fairly similar** for the different PB and BM memory B cell populations and clustered around the CDRs and the DE loop (**Figure 1C**). The main exception are *N*-glycosylation sites within FR4 position 125 that were significantly more frequent in IgA compared to the other memory repertoires. *N*-glycosylation sites found in variable regions of memory B cell light chain sequences (n=4), showed similar clustering of *N*-glycosylation sites around the CDRs and DE loop as observed for heavy chain sequences (**Figure 1C**, Kappa and Lambda). Of note, between individual donors, the frequency of sites found at a specific position varies considerably for all repertoires.

Non-progenitor sites found within and outside of the CDR3

In the V and J genes, the majority of *N*-glycosylation sites within memory rearranged sequences correspond to 'progenitor sites'[19] (**Table I**) ranging from 77 – 88% for heavy chains and 79 and 88% for kappa and lambda light chains, respectively. The remaining non-progenitor sites can be subdivided as either randomly introduced within the CDR3 V-D and D-J / V-J junctions during V(D)J recombination or is the result of two or more mutations. Non-progenitor sites found in the heavy chains also have the tendency, although less pronounced, to clustered around the CDRs and DE loop (**Figure S1A**). Naive B cells, carry besides germline sites (not shown in **Figure 1**, see below), *N*-glycosylation sites within V-D and D-J junctions of the H-CDR3 (**Figure 1C**, naive IgM), with significantly higher tendency within V-D junctions (**Figure 1D**). The frequency of *N*-glycosylation sites within the D genes is low in the naive repertoire but increases significantly in memory B cells. Despite these changes, the total frequency of sites within the H-CDR3 does not increase upon B cell maturation (see below). Of class switched B cells found in bone marrow, IgA expressing B cells have fewer *N*-glycosylation sites within the D gene compared to IgG.

Negative selection for germline *N*-glycosylation sites in the memory repertoire

Three *N*-glycosylation sites are encoded in the germline IGVH repertoire (alleles IGHV1-8, IGHV4-34, and IGHV5-10-1). These were analyzed separately for their frequency in both the naive and memory repertoires (**Figure 2A**). In memory B cells, the frequencies of germline sites at position 81 (IGHV1-8) and position 57 (IGHV4-34) are significantly lower than those in naive IgM B cells, both because the V_H gene allele frequencies are lower, and furthermore because a substantial part of the germline sites is reverted to non-

glycosylation sites by SHM. This trend was less pronounced for position 66 in the less prevalent allele IGHV5-10-1 (which was observed in only 4 out of 12 donors). Similar patterns were observed for bone marrow derived switched memory B cells (**Figure 2B**). Interestingly, germline site IGHV1-8 was retained in most cases for BM IgE (although the allele frequency did decrease compared to naive IgM B cells), whereas the site disappeared due to mutations in at least 40% of the cases for IgG or IgA. V_L alleles containing germline sites (IGKV5-2, IGLV3-12, IGLV3-22, IGLV5-37) were observed infrequently (≤0.06%) and were not further analyzed.

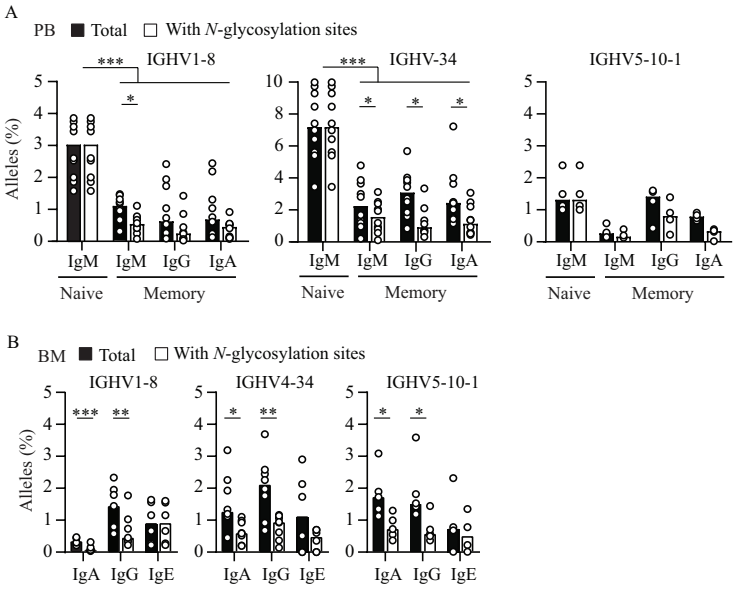

Figure 2. Loss of germline *N*-glycosylation sites in memory B cell repertoires. ***(A)*** *Germline site and corresponding allele frequencies (%) in naive and memory PB B cells for 12 healthy individuals. The three germline sites correspond to positions 81, 57, and 66 in IGHV1-8, IGHV4-34, an IGHV5-10-1, respectively. The latter allele was only observed in 4/12 donors.* ***(B)*** *Germline site and corresponding allele frequencies (%) in memory BM B cells for 6 healthy individuals. Bars represent medians, each dot represents 1 donor. One-way ANOVA, *** p <0.001, ** p <0.01, * p <0.05.*

Signs of negative selection for acquisition of *N*-glycosylation sites in the H-CDR3

Next, we evaluated the relationship between acquiring *N*-glycosylation sites and the accumulation of non-silent somatic mutations in the heavy chain variable regions (**Figure 3A**). The percentage of sequences that carry non-germline *N*-glycosylation sites was highly dependent on the number of mutations, and increases rapidly up to 15 mutations, after which a plateau is established (**Figure 3B and C**). Furthermore, non-progenitor sites within V_H and J_H genes accumulate steadily but more slowly with increasing number of mutations (**Figure 3D**). By contrast, the percentage of sequences carrying *N*-glycosylation

sites within the H-CDR3 is essentially invariant with respect to the number of somatic mutations (**Figure 3D**). This implies a negative selection bias for glycosylation sites within the H-CDR3 compared to the overall variable region.

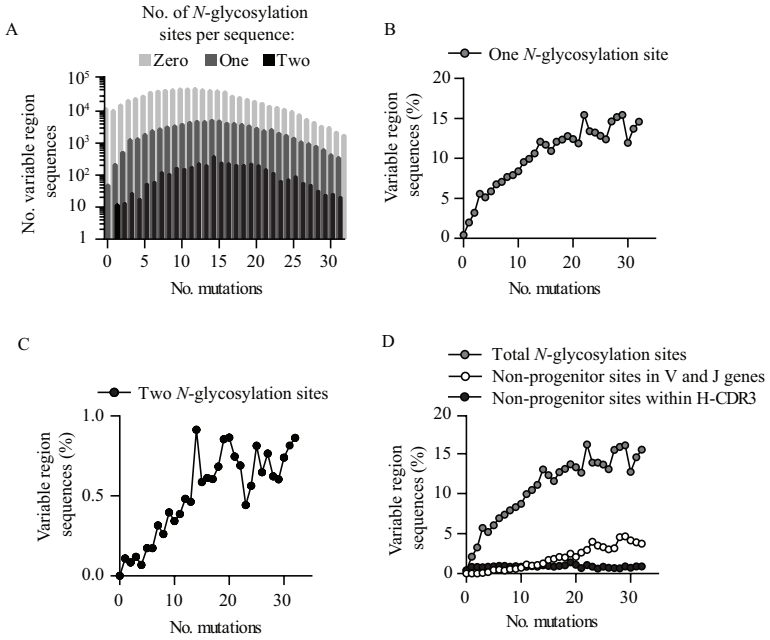

Figure 3. Negative selection pressure for non-germline *N*-glycosylation sites in H-CDR3. ***(A)*** *Number of V_H sequences containing zero, one, or two N-glycosylation sites versus the number of non-silent mutations found in the sequence. Sequences of 12 healthy individuals for memory IgM, IgG, IgA were collapsed as their individual patterns showed high resemblance.* ***(B,C)*** *Percentage of V_H sequences acquiring one (B) or two (C) N-glycosylation sites in the variable region versus the number of non-silent mutations.* ***(D)*** *Percentages of sequences with, non-germline N-glycosylation sites in the complete variable region, non-progenitor sites across V and J genes, and within the H-CDR3 versus the number of non-silent somatic mutations.*

Progenitor site and mutation propensity dictate the *N*-glycosylation sites present in the memory repertoire

Next, we examined to which extent the frequency of acquired *N*-glycosylation sites at progenitor site positions depends on the frequency of the progenitor sites. **Figure 4A** shows frequencies of progenitor sites, grouped per position for most commonly used V_H gene families, with corresponding *N*-glycosylation sites found in the memory repertoire. Certain progenitor sites are frequent but rarely mutate into an actual *N*-glycosylation site (e.g. position 56 in IGHV3) or the other way around (less common progenitor sites that relatively frequent mutate into actual *N*-glycosylation sites e.g. position 86 in IGHV4). For other positions both the progenitor site and the *N*-glycosylation site are frequently found (e.g. position 90 in IGHV4). In other words, acquiring *N*-glycosylation sites during SHM is not solely dictated by the presence of a progenitor site, since the observed mutation

frequencies differ substantially between positions. Nevertheless, a moderate correlation was found between the number of progenitor sites (i.e., allele frequency) and the number of *N*-glycosylation sites (**Figure 4B**; Pearson $r = 0.55$, $p < 0.001$).

In order to analyze the propensity for mutation towards *N*-glycosylation sites in more detail, we compared progenitor site mutations resulting in *N*-glycosylation sites to the other two possible mutations at the same nucleotide position. For the majority of progenitor sites (designated 'Type I'; an example is shown in **Figure 4C**), only one specific replacement mutation results in an *N*-glycosylation site (Rglyc), whereas the two other possible mutations correspond to other non-silent or 'replacement' mutations (Ro). Analysis of all unique Type I nonameric progenitor sites across V_H gene families revealed a large variation in mutation frequencies for both glycan-introducing and other replacement mutations across progenitor

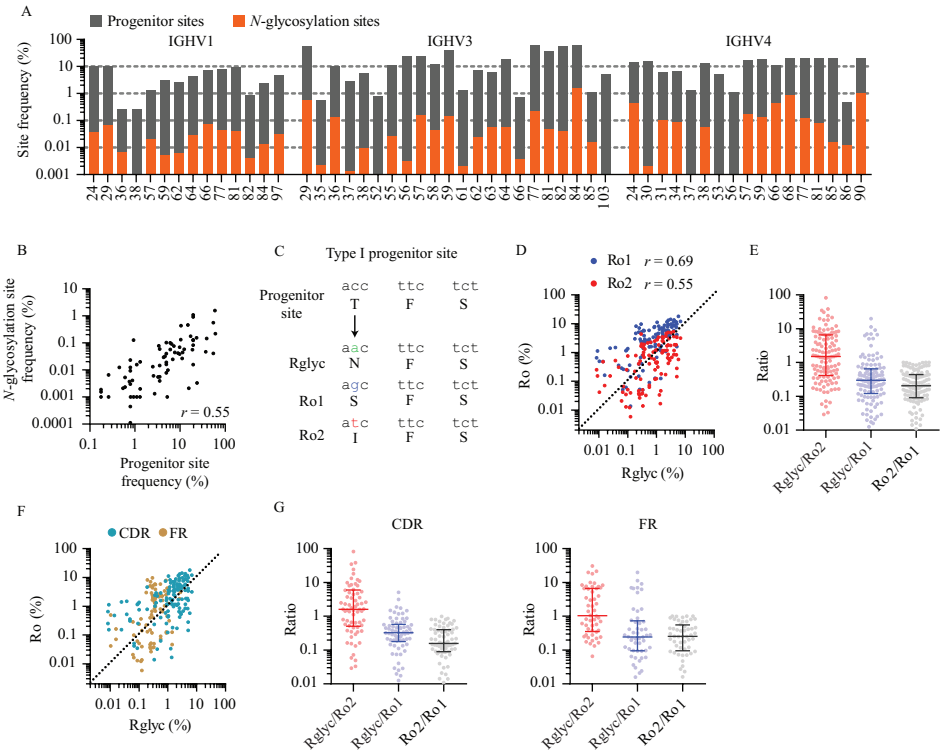

Figure 4. The *N*-glycosylation site repertoire is dictated by progenitor site frequency and site-specific mutation propensities. ***(A)*** *Frequencies (%) of progenitor sites (grey) versus acquired N-glycosylation sites (orange), grouped according to V_H family for 12 healthy individuals (less frequently used V_H families are not shown; non-matched sites and progenitor sites with a frequency <0.2% are excluded).* ***(B)*** *Correlation between progenitor site and N-glycosylation site frequencies (%).* ***(C)*** *Example of a – Type I – germline nonameric progenitor site nucleotide motif.* ***(D, E)*** *Scatterplot and ratios of glycan-introducing mutations (Rglyc) stratified to either of the two other replacement mutations (Ro1 and Ro2, the most and least frequent other mutation, respectively) for all Type I progenitor sites. Spearman's r and Wilcoxon signed rank test.* ***(F, G)*** *As D and E, but stratified according to the progenitor site being in the CDR or FR.*

sites (**Figure 4D**). A moderate to strong correlation was observed between either the Rglyc and the most frequent other mutation (Ro1; r_s = 0.69, p <0.0001) and the least frequent other mutation (Ro2; r_s = 0.55, p <0.0001) at each particular site. On average, the Rglyc mutation was slightly more frequent than Ro2 (**Figure 4E**, median = 1.51, p <0.0001), and about three times less frequent as Ro1 (median = 0.30, p <0.0001). This means that the overall propensity to acquire a glycan-introducing mutation falls within the range of acquiring another replacement mutation at that position, but with a wide range of ca. 0.01 to 100-fold for individual positions. Furthermore, the relative propensity for glycan-introducing mutations (relative to the other mutations, i.e., Ro1 and Ro2) observed for the CDRs is similar for the FRs, despite a higher overall mutation frequency for the CDRs (**Figure 4F and G**). Similar trends were observed for two other, less frequent groups of progenitor sites Type IIa/b mutations (examples are shown in **Figure S1B**), for which two out of three mutations at a single nucleotide position result in a glycosylation site (**Figure S1C**). Taken together, these results indicate that there is no pronounced selection pressure against acquiring *N*-glycosylation sites within the variable region during B cell maturation.

T_H2 associated antibodies have increased levels of *N*-glycosylation sites

Since we observed a 2-fold higher frequency of non-germline *N*-glycosylation sites for IgE in comparison to the other switched isotypes, we also examined *N*-glycosylation site frequencies for the IgG subclasses including IgG4, which is also associated with T_H2-like antibody responses. We previously observed an increased frequency of *N*-glycosylation sites in PB IgG4 variable region sequences, albeit in a small dataset[19]. Here, we confirm and extend this observation for 5 individuals for which IgG subclass-specific sequences were available for both PB and BM IgG B cells. Both PB and BM IgG4 antibodies have significantly higher frequencies of *N*-glycosylation sites in comparison to the other IgG subclasses (**Figure 5A**) and similar to BM IgE. The elevated number of *N*-glycosylation sites in IgG4 and IgE could not be explained by elevated levels of SHM (**Figure 5B**).

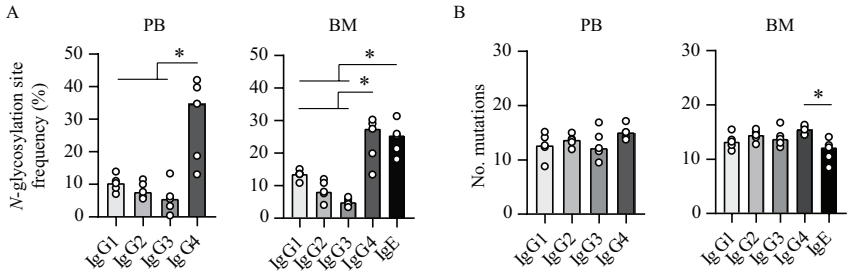

Figure 5. Enrichment of non-germline *N*-glycosylation sites in T_H2 associated antibodies IgG4 and IgE. ***(A)*** *Frequency (%) of V_H sequences containing N-glycosylation sites for PB and BM IgG subclasses and BM IgE sequences for 5 healthy individuals. Each dot represents a single donor, bars represent medians. One-way ANOVA, * p <0.05.* ***(B)*** *The number of replacement mutations within the sequences described in (A). Each dot represents a single donor (n=5), bars represent medians. One-way ANOVA, * p <0.05.*

Furthermore, there were no obvious differences in V_H allele usage that could clarify these differences in *N*-glycosylation site frequencies (data not shown). Taken together, the elevated levels of *N*-glycosylation sites for both IgE and IgG4 indicate an altered selection pressure for the variable region antibody repertoire for T_H2-like antibody responses.

Bulk B cell *N*-glycosylation patterns in autoimmune patients resembles those of healthy individuals

Next, we assessed the acquisition of variable region *N*-glycosylation sites in the general antibody repertoire of patients with autoantibody-mediated immune diseases, i.e. systemic lupus erythematosus (SLE, n=7) and myasthenia gravis (MG, n=9). *N*-glycosylation site frequency, distribution, and repertoire composition of bulk memory B cell repertoires of these patients were very similar to those of healthy individuals (Distributions not shown; **Figure S2A-D**). In other words, there does not appear to be gross alterations in Fab glycosylation patterns in these B cell-associated autoimmune diseases.

Antibodies with *N*-glycosylation sites at progenitor sites are frequently glycosylated

The presence of an *N*-glycosylation site does not guarantee that sites become occupied with glycans, since this is also influenced by the nature of the core amino acid (X), adjacent amino acids, and the overall folding of the protein[34–36]. Here we examined the actual glycosylation tendencies for both germline and non-germline variable region *N*-glycosylation sites. First, to investigate if the negative selection for germline sites in the memory repertoire may be attributed to glycosylation of these sites, antibodies corresponding to germline alleles IGHV1-8, IGHV4-34, and IGHV5-10-1 were expressed and glycosylation of the three germline *N*-glycosylation sites was analyzed using gel electrophoresis. Antibodies with Fab glycans exhibit an increased molecular weight compared to their non-glycosylated counterparts (**Figure 6A**). We observed that the germline site at position 57 in IGHV4-34 is not glycosylated, whereas germline sites at position 81 in IGHV1-8 and 66 in IGHV5-10-1 do become fully and partially glycosylated, respectively.

Next, we investigated the glycosylation of 38 non-germline *N*-glycosylation sites located at progenitor site positions in 27 different recombinant expressed monoclonal antibodies (including previously described[18,19,34,35,37] and newly examined – for details see **Table SII**). From these *N*-glycosylation sites 35 out of 38 (92.1%) become at least partially occupied by glycans as confirmed by gel electrophoresis, lectin ELISA, or Mass Spectrometry (**Figure 6B**, **Figure S2E and F**). In addition, we did not observe preferential glycosylation of monoclonal antibodies that carry the N-X-S sequon compared to N-X-T, 90.5% and 94.1% respectively. These results suggest that in general, the acquisition of *N*-glycosylation sites located on progenitor sites during SHM will lead to expression of antibodies with variable region glycans. A major exception are the progenitor sites at position 57 in V_H family IGHV4, that

are homologous to the germline site in IGHV4-34. Introduction of this *N*-glycosylation site into two different IGHV4 alleles (IGHV4-4 and IGHV4-39) did not lead to the introduction of a glycan (**Figure 6C**). In summary, although not every position across the variable region has been tested, these results suggest that the majority of the *N*-glycosylation sites introduced by SHM during B cell maturation have the potential to become glycosylated.

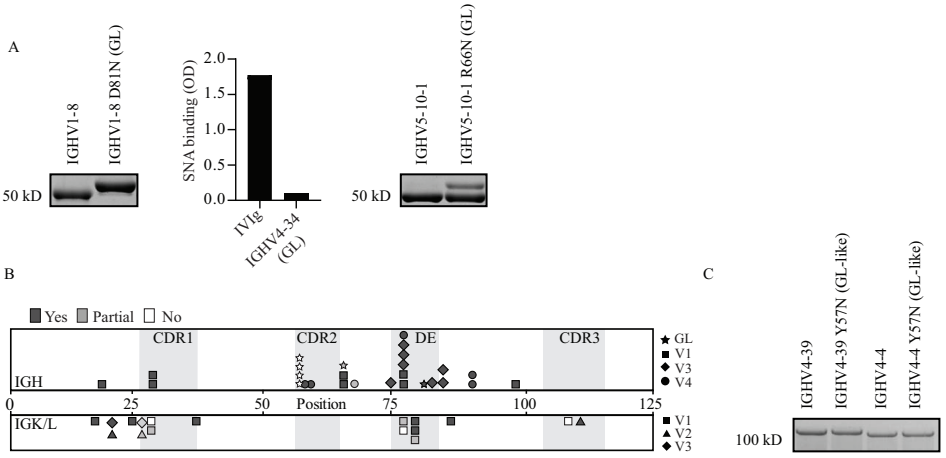

Figure 6. Glycosylation of *N*-glycosylation sites in monoclonal antibodies. ***(A)*** *Gel-electrophoresis of germline (GL) N-glycosylation sites. Left, reduced SDS-PAGE of full length IgG1 IGHV1-8, heavy chain at 50 kD. Middle, lectin ELISA of F(ab')$_2$ IGHV4-34. Right, reduced SDS-PAGE of full length IgG1 IGHV5-10-1, heavy chain at 50 kD.* ***(B)*** *Schematic overview of the glycosylation of 38 N-glycosylation sites (in 27 different monoclonal antibodies) at various progenitor site positions. Glycosylation was confirmed by gel-electrophoresis, lectin ELISA or Mass Spectrometry as detailed in* ***Table SII****.* ***(C)*** *Gel electrophoresis of IGHV4-34 GL site replacement in IGHV4-39 and IGHV4-4. Non-reduced SDS-PAGE of F(ab')$_2$ fragments, at 100 kD.*

DISCUSSION

Glycosylation of antibody variable regions stands out as an additional layer of repertoire diversification, being dependent on the primary amino acid structure as well as subsequent events resulting in attachment and further processing of glycans. Here, we analyzed in detail the patterns and biases of *N*-glycosylation sites across naive and memory B cell subsets. With the exception of the H-CDR3, we did not find evidence for an overall selection bias against the introduction of *N*-glycosylation sites in the variable region. This is noteworthy given that introduction of a large bulky glycan may be a disruptive event in terms of folding or antigen binding.

Interestingly, we observed an almost 2-fold higher propensity for both IgE and IgG4 to acquire glycans compared to IgG1 or IgA, indicating that T_H2-like responses develop a skewed variable region repertoire.

The 2-fold increase of acquired *N*-glycosylation sites for IgE and IgG4 could not be explained by increased levels of somatic mutations in these isotypes nor by a biased V gene usage. IgG4 and IgE responses have in common that they are often produced during so called T_H2 responses, characterized by IL-4 and IL-5, the former of which is known to induce class switching to both IgG4 and IgE[36]. Although glycans can positively contribute to antigen binding[14–18], it is unlikely that antigens that provoke a T_H2-like response would generally be better recognized by antibodies carrying glycans. Alternatively, there may be (endogenous) sugar binding lectins involved in T_H2-skewed responses that pose a selective survival advantage to B cells with Fab glycosylated B cell receptors. For IgE, there are indications for impaired GC responses[38,39], which tentatively might provide the environment that positively selects for enhanced levels of Fab glycosylation. IgG4 antibody responses are associated with tolerance which make it feasible that Fab glycans contribute to a tolerogenic phenotype by dampening antigen binding or interaction with lectins on other immune cells and thereby exerting immune modulatory properties. Of note, we have recently observed elevated levels of Fab glycosylation on serum IgG4 from patients with IgG4-related disease[40]. A disease characterized – amongst others – by abnormally high levels of infiltrating $IgG4^+$ plasma cells into one or more affected organs. The potential consequences of elevated Fab glycosylation levels of IgG4 and IgE remain to be investigated.

It is relevant to point out that the biases observed in this study do not solely reflect selection. First, the non-random clustering of progenitor sites in the germline repertoire[19] already pre-determines to a substantial degree at which positions *N*-glycosylation sites are introduced. Second, the intrinsic mutability of a germline gene varies substantially depending on its sequence, and the distribution of so-called 'mutation hot- and cold-spot motifs' influence overall mutation patterns during somatic hypermutation[41,42]. Furthermore, since the overall patterns for acquiring *N*-glycosylation sites at particular positions reflect the average of a multitude of individual, antigen-specific B cell responses, it is not possible to directly link such patterns to antigen-driven selection, similar to other amino acid substitution profiles[43]. For example, the negative bias for *N*-glycosylation site acquisition in the H-CDR3 in general, does not exclude the occasional positive contribution of a H-CDR3 glycan to antigen binding. On the other hand, it is feasible that alterations in glycosylation patterns may, for example, associate with certain physiological or pathological conditions. In this regard, the hyper Fab glycosylation observed for RA-specific autoantibodies (>90%)[34], or the increased frequencies of *N*-glycosylation sites in parotid gland-derived B cells of primary SS patients[26] represent an important research topic. Nevertheless, bulk serum IgG in RA patients does not appear to be aberrantly Fab glycosylated. Here we show that this is also true for the bulk memory repertoire of SLE and MG patients. Thus, despite the presence of relatively large amounts of autoantibodies in some patients, most of the circulating antibodies are not autoreactive. Therefore, differential glycosylation pattern of these autoantibodies cannot be revealed from bulk repertoire analysis. Elevated

levels of Fab glycosylation have been suggested as a general feature of autoimmunity[28]. However, the observed frequencies of *N*-glycosylation sites within bulk B cell repertoires of autoimmune disease patients fall well within the range of those observed here for healthy individuals. Therefore, aberrant Fab glycosylation may be mostly restricted to disease-specific autoreactive B cells, for reasons yet to be unraveled. Altered autoreactivity of Fab glycosylated antibodies poses a potential mechanism. A recent paper described positive selection for Fab glycosylated autoantibodies in SS patients due to enhanced autoantigen binding[44]. However, both enhanced and diminished binding was observed for autoantibodies associated with RA[34] and Fab glycans have also been suggested to contribute to redemption of autoreactivity[45].

Bulky glycan structures in suboptimal positions may interfere with antibody folding and function. Therefore, one might expect that the introduction of *N*-glycosylation sites is restricted. We observed that *N*-glycosylation sites readily emerge throughout the variable region with similar distributions of sites amongst the different antibody classes that clustered around the antigen binding regions. A striking exception was an IgA-restrictive site at position 125. It would be of interest to find out if this site becomes glycosylated and whether it serves a purpose in IgA physiology. IgA antibodies associated with the intestinal lumen may benefit from extensive glycosylation as it can offer protection for the many residing proteases[46]. For one region in particular, the CDR3 of the heavy chain, we observed that relatively few sequences acquired *N*-glycosylation sites, irrespective of the accumulation of mutations. Interestingly, of all CDRs H-CDR3 is most important for antigen recognition and is the epicenter of most antigen-antibody contacts[47]. It is therefore likely that introduction of a glycan in the H-CDR3 is a highly unfavorable event, which can explain the local negative selection for *N*-glycosylation sites.

Somatic mutations can introduce but also remove *N*-glycosylation sites. For germline *N*-glycosylation sites the preservation of the sites in the memory repertoire was an unfavorable event, both in terms of selection against V_H alleles carrying germline sites, as well as substantial loss of sites due to somatic hypermutation. In case of IGHV1-8, it is possible that the occurring negative selection is attributed to the presence of a glycan on the germline *N*-glycosylation site. By contrast, the germline site in IGHV4-34 is not glycosylated, thus glycosylation can therefore not account for the negative selection pressure. However, the IGHV4-34 allele has been associated with autoreactivity and is therefore negatively selected in general[48]. The main contribution of germline sites to the comprehensive variable region *N*-linked glycan repertoire of the memory B cell population derives from IGHV1-8. With taking into account the infrequent occurrence of IGHV5-10-1, we estimate that germline sites account for approximately 5% of the glycans found on serum IgG and IgA.

It should be kept in mind that beyond the presence or absence of a glycan, its structural profile can vary substantially from one *N*-linked glycan to another[49]. The essential first event during glycosylation is the attachment of a high-mannose structure to the asparagine residue of the *N*-glycosylation site during antibody translation and folding in the ER. The presence of any glycan – regardless of its precise structure – depends on this first step. Hereafter, substantial multi-step glycan trimming and build-up takes place in the Golgi, with a wealth of possible outcomes[9]. Transfer of *N*-linked glycans to prototypic *N*-glycosylation sites does not always occur and is amongst others constrained by the accessibility of the *N*-glycosylation site for glycan attaching enzymes. Here, we show that the majority of *N*-glycosylation sites introduced at progenitor sites by SHM are glycosylated (**Figure 6**) which suggest that progenitor sites in general are located at positions that allow facile glycosylation. In summary, this study identified additional factors that shape the antibody variable region *N*-glycosylation repertoire. These results indicate that there exists differential selection pressure for glycans during B cell responses, with a profound skewing during T_H2-like responses.

Author contributions

JK and TR designed research. JK and TR collected data used in this study. JK, ND, PO performed research. JK, BN and TR analyzed data. JK, FB, GV and TR wrote the paper. All authors critically reviewed the manuscript, gave final approval of the version to be published, and agreed to be accountable for all aspects of the work ensuring that questions related to the accuracy or integrity of any part of the work are appropriately investigated and resolved.

Financial support

This study was supported by Landsteiner Foundation for Blood Transfusion (Grant1626).

Disclosure statement

There are no commercial or financial conflicts of interest.

REFERENCES

1. Bondt A, Rombouts Y, Selman MHJ, et al. Immunoglobulin G (IgG) Fab Glycosylation Analysis Using a New Mass Spectrometric High-throughput Profiling Method Reveals Pregnancy-associated Changes. 2014:3029-3039. doi:10.1074/mcp.M114.039537
2. van de Bovenkamp FS, Hafkenscheid L, Rispens T, Rombouts Y. The Emerging Importance of IgG Fab Glycosylation in Immunity. *J Immunol*. 2016;196(4):1435-1441. doi:10.4049/jimmunol.1502136
3. Lefranc M. IMGT, the International ImMunoGeneTics Information System. *Cold Spring Harb Protoc*. 2011(6):595-603.
4. Sondermann P, Huber R, Oosthuizen V, Jacob U. The 3.2-A crystal structure of the human IgG1 Fc fragment-Fc g RIII complex. *Nature*. 2000;406(July):267-273.
5. Ferrara C, Grau S, Jäger C, Sondermann P, Brünker P, Waldhauer I. Unique carbohydrate – carbohydrate interactions are required for high affinity binding between Fc γ RIII and antibodies lacking core fucose. *Proc Natl Acad Sci U S A*. 2011;108(31):12669-12674. doi:10.1073/pnas.1108455108
6. Quast I, Keller CW, Maurer MA, et al. Sialylation of IgG Fc domain impairs complement-dependent cytotoxicity. *J Clin Invest*. 2015;125(11). doi:10.1172/JCI82695.of
7. Peschke B, Keller CW, Weber P, Quast I, Lünemann JD. Fc-galactosylation of human immunoglobulin gamma isotypes improves c1q Binding and enhances complement-Dependent cytotoxicity. *Front Immunol*. 2017;8(June). doi:10.3389/fimmu.2017.00646
8. Dekkers G, Treffers L, Plomp R, et al. Decoding the Human Immunoglobulin G-Glycan Repertoire Reveals a Spectrum of Fc-Receptor- and Complement- Mediated-Effector Activities. *Front Immunol*. 2017;8(August). doi:10.3389/fimmu.2017.00877
9. Dekkers G, Rispens T, Vidarsson G. Novel Concepts of Altered Immunoglobulin G Galactosylation in Autoimmune Diseases. *Front Immunol*. 2018;9:553. doi:10.3389/fimmu.2018.00553
10. Kapur R, Kustiawan I, Vestrheim A, et al. A prominent lack of IgG1-Fc fucosylation of platelet alloantibodies in pregnancy. *Blood*. 2018;123(4):471-481. doi:10.1182/blood-2013-09-527978.
11. Kapur R, Valle L Della, Sonneveld M, et al. Low anti-RhD IgG-Fc-fucosylation in pregnancy : a new variable predicting severity in haemolytic disease of the fetus and newborn. *Br J Haematol*. 2014;(June):936-945. doi:10.1111/bjh.12965
12. Wang TT, Sewatanon J, Memoli MJ, et al. IgG antibodies to dengue enhanced for FcγRIIIA binding determine disease severity. *Science*. 2017;355(6323):395-398. doi:10.1126/science.aai8128.IgG
13. Ackerman ME, Crispin M, Yu X, et al. Natural variation in Fc glycosylation of HIV-specific antibodies impacts antiviral activity. *J Clin Invest*. 2013;123(5):2183-2192. doi:10.1172/JCI65708DS1
14. Wright A, Tao M, Kabat EA, Morrison SL. Antibody variable region glycosylation : position effects on antigen binding and carbohydrate structure. *EMBO*. 1991;10(10):2717-2723.
15. Coloma MJ, Trinh RK, Martinez AR, Morrison SL. Position Effects of Variable Region Carbohydrate on the Affinity and In Vivo Behavior of an Anti-(1 → 6) Dextran Antibody. Published online 2018.
16. Wallick BYSC, Kabat EA, Morrison SL. Glycosylation of a VH residue of a monoclonal antibody against alpha (1----6) dextran increases its affinity for antigen. *JEM*. 1988;168:1099-1109.
17. Tachibana H, Kim J, Shirahata S. Building high affinity human antibodies by altering the glycosylation on the light chain variable region in N -acetylglucosamine-supplemented hybridoma cultures. *Cytotechnology*. 1997;23(1-3):151-159.
18. Leibiger H, Wu D, Stigler R, Marx U. Variable domain-linked oligosaccharides of human monoclonal IgG: structure and influence on antigen binding. *Biochem J*. 1999;538:529-538.

19. van de Bovenkamp FS, Derksen NIL, Ooievaar-de Heer P, et al. Adaptive antibody diversification through N -linked glycosylation of the immunoglobulin variable region. *Proc Natl Acad Sci U S A*. 2018;115(8):1901-1906. doi:10.1073/pnas.1711720115

20. van de Bovenkamp F, Derksen N, van Breemen M, et al. Variable Domain N -linked glycans acquired During antigen-specific immune responses can contribute to immunoglobulin g antibody stability. *Front Immunol*. 2018;9:1-9. doi:10.3389/fimmu.2018.00740

21. Goletz, SA, Czyk, D, Stoeckl L. Fab-glycosylated antibodies. Patent WO 2012/020065. Published online 2012.

22. Radcliffe CM, Arnold JN, Suter DM, et al. Human Follicular Lymphoma Cells Contain Oligomannose Glycans in the Antigen-binding Site of the B-cell Receptor. *J Biol Chem*. 2007;282(10):7405-7415. doi:10.1074/jbc.M602690200

23. Youings A, Chang S, Dwek RA, Scragg IG. Site-specific glycosylation of human immunoglobulin G is altered in four rheumatoid arthritis patients. *bio*. 1996;630:621-630.

24. Vergoessen R, Slot L, Hafkenscheid L, et al. B-cell receptor sequencing of anti-citrullinated protein antibody (ACPA) IgG-expressing B cells indicates a selective advantage for the introduction of N-glycosylation sites during somatic hypermutation. *Ann Rheum Dis*. 2018;77(6):955-958.

25. Lloyd KA, Steen J, Amara K, et al. Variable domain N-linked glycosylation and negative surface charge are key features of monoclonal ACPA: Implications for B-cell selection. *Eur J Immunol*. 2018;48(6):1030-1045. doi:10.1002/eji.201747446

26. Hamza N, Hershberg U, Kallenberg CGM, et al. Ig Gene Analysis Reveals Altered Selective Pressures on Ig-Producing Cells in Parotid Glands of Primary Sjögren's Syndrome Patients. *J Immunol*. 2015;194(2):514-521. doi:10.4049/jimmunol.1302644

27. Visser A, Doorenspleet M, de Vries N, et al. Acquisition of N-glycosylation sites in immunoglobulin heavy chain genes During local expansion in Parotid salivary glands of Primary sjögren Patients. *Front Immunol*. 2018;9(March):1-12. doi:10.3389/fimmu.2018.00491

28. Visser A, Hamza N, Kroese FGM, Bos N. Acquiring new N-glycosylation sites in variable regions of immunoglobulin genes by somatic hypermutation is a common feature of autoimmune diseases. *Ann Rheum Dis*. 2018;77(10):1-2. doi:10.1136/annrheumdis-2017-212568

29. Heiden JA Vander, Stathopoulos P, Julian Q, et al. Dysregulation of B Cell Repertoire Formation in Myasthenia Gravis Patients Revealed through Deep Sequencing. *J Immunol*. 2017;198(4):1460-1473. doi:10.4049/jimmunol.1601415

30. Levin M, Levander F, Palmason R, Greiff L, Ohlin M. Antibody-encoding repertoires of bone marrow and peripheral blood—a focus on IgE. *J Allergy Clin Immunol*. 2017;139(3):1026-1030. doi:10.1016/j.jaci.2016.06.040

31. Tipton CM, Fucile CF, Darce J, et al. Diversity , cellular origin and autoreactivity of antibody-secreting cell population expansions in acute systemic lupus erythematosus. *Nat Immunol*. 2015;16(7):755-765. doi:10.1038/ni.3175

32. Masella AP, Bartram AK, Truszkowski JM, Brown DG, Neufeld JD. PANDAseq : PAired-eND Assembler for Illumina sequences. *BMC Bioinformatics*. 2012;13(1):31. doi:10.1186/1471-2105-13-31

33. Brochet X, Lefranc M, Giuidicelli V. IMGT / V-QUEST : the highly customized and integrated system for IG and TR standardized V-J and V-D-J sequence analysis. *Nucleic Acids Res*. 2008;36:503-508. doi:10.1093/nar/gkn316

34. Rombouts Y, Willemze A, Van Beers JJBC, et al. Extensive glycosylation of ACPA-IgG variable domains modulates binding to citrullinated antigens in rheumatoid arthritis. *Ann Rheum Dis*. 2016;75(3):578-585. doi:10.1136/annrheumdis-2014-206598

35. Tachibana H, Seki K, Murakami H. Identification of hybrid-type carbohydrate chains on the light chain of human monoclonal antibody specific to lung adenocarcinoma. *Biochim Biophys Acta*. 1993;1182(3):257-263.

36. Ishizaka A, Sakiyama Y, Nakanishi M, et al. The inductive effect of interleukin-4 on IgG4 and IgE synthesis in human peripheral blood lymphocytes. *Clin Exp Immunol*. 1990;79(3):392-396.

37. Harindranath N, Goldfarb IS, Ikematsu H, et al. Complete sequence of the genes encoding the VH and VL regions of low- and high-affinity monoclonal IgM and IgA1 rheumatoid factors produced by CD5+ B cells from a rheumatoid arthritis patient. *Int Immunol*. 1991;3(9):865-875. doi:10.1093/intimm/3.9.865

38. Aalberse RC, Lupinek C, Siroux V, et al. sIgE and sIgG to airborne atopic allergens : Coupled rather than inversely related responses. *Eur J Allergy Clin Immunol*. Published online 2018:4-7. doi:10.1111/all.13548

39. Yang Z, Robinson MJ, Chen X, et al. Regulation of B cell fate by chronic activity of the IgE B cell receptor. *Elife*. Published online 2016:1-31. doi:10.7554/eLife.21238

40. Culver EL, van de Bovenkamp FS, Derksen NIL, et al. Unique patterns of glycosylation in immunoglobulin subclass G4-related disease and primary sclerosing cholangitis. *J Gastroenterol Hepatol*. 2019;34(10). doi:10.1111/jgh.14512

41. Wei L, Chahwan R, Wang S, Wang X, Pham PT, Goodman MF. Overlapping hotspots in CDRs are critical sites for V region diversification. *Proc Natl Acad Sci U S A*. 2015;112(7):728-737. doi:10.1073/pnas.1500788112

42. Saini J, Hershberg U. B cell Variable genes have evolved their codon usage to focus the targeted patterns of somatic mutation on the complementarity determining regions. *Mol Immunol*. 2015;65(1):157-167. doi:10.1016/j.molimm.2015.01.001.B

43. Sheng Z, Schramm CA, Kong R, et al. Gene-specific substitution Profiles describe the types and Frequencies of Amino Acid Changes during Antibody somatic hypermutation. *Front Immunol*. 2017;8:1-14. doi:10.3389/fimmu.2017.00537

44. Koelsch KA, Cavett J, Smith K, et al. Evidence of Alternative Modes of B Cell Activation Involving Acquired Fab Regions of N -Glycosylation in Antibody-Secreting Cells Infiltrating the Labial Salivary Glands of Patients With € gren ' s Syndrome Sj o. *Arthritis Rheumatol*. 2018;70(7):1102-1113. doi:10.1002/art.40458

45. Sabouri Z, Schofield P, Horikawa K, et al. Redemption of autoantibodies on anergic B cells by variable-region glycosylation and mutation away from self-reactivity. *Proc Natl Acad Sci U S A*. 2014;111(25):E2567-75. doi:10.1073/pnas.1406974111

46. Kilian M, Reinholdt J, Lomholt H, Poulsen K, Frandsen E. Biological significance of IgAl proteases i n bacterial colonization and pathogenesis : critical evaluation of experimental evidence. *AMPIS*. 1996;104(5):321-338.

47. Xu JL, Davis MM. Diversity in the CDR3 Region of V H Is Sufficient for Most Antibody Specificities. *Immunity*. 2000;13(1):37-45.

48. Pugh-bernard AE, Silverman GJ, Cappione AJ, et al. Regulation of inherently autoreactive VH4-34 B cells in the maintenance of human B cell tolerance. *J Clin Invest*. 2001;108(7):1061-1070. doi:10.1172/JCI200112462.Introduction

49. Anumula KR. Quantitative glycan profiling of normal human plasma derived immunoglobulin and its fragments Fab and Fc. *J Immunol Methods*. 2012;382(1-2):167-176. doi:10.1016/j.jim.2012.05.022

SUPPLEMENTARY MATERIAL

Table SI. Overview of total read counts after data processing per donor per antibody isotype

Ref	B cell source	Isotype	Samples per isotype	No. reads
Van der Heiden[29]	PB	IgM n	HD07_M ; HD09_M ; HD10_M ; HD13_M	1786 ; 4509 ; 2812 ; 2324
	PB	IgM m	HD07_M ; HD09_M ; HD10_M ; HD13_M	10226; 8511 ; 6845 ; 7759
	PB	IgG	HD07_M ; HD09_M ; HD10_M ; HD13_M	4503 ; 3978 ; 5191 ; 9570
	PB	IgA	HD07_M ; HD09_M ; HD10_M ; HD13_M	10914 ; 7740 ; 6189 ; 10613
	PB	Kappa	HD07_M ; HD09_M ; HD10_M ; HD13_M	9023 ; 9366 ; 8876; 10258
	PB	Lambda	HD07_M ; HD09_M ; HD10_M ; HD13_M	8582 ; 6668 ; 6833 ; 6725
	PB	IgG	MK08_M ; MK02_M ; MK03_M ; AR03_M ; AR04_M ; AR02_M ; AR05_M ; MK04_M ;	3340 ; 5140 ; 1379 ; 5366 ; 5010 ; 7722 ; 4287 ; 1512
	PB	IgA	MK08_M ; MK02_M ; MK03_M ; AR03_M ; AR04_M ; AR02_M ; AR05_M ; MK04_M ; MK05_M	6927 ; 9039 ; 4394 ; 8848; 12289 ; 10166 ; 15470 ; 4951 ; 6568
Levin[30]	PB	IgM n	Donor 1 – 6 PB sample 1	7069 ; 8011 ; 4693 ; 8911 ; 3406 ; 6492
	PB	IgM n	Donor 1 – 6 PB sample 2	7786 ; 8847 ; 5561 ; 8025 ; 3194 ; 7156
	PB	IgM m	Donor 1 – 6 PB sample 1	8184 ; 7561 ; 11541 ; 7801 ; 14804 ; 9454
	PB	IgM m	Donor 1 – 6 PB sample 2	8062 ; 8748 ; 13114 ; 7045 ; 13979 ; 10800
	PB	IgG	Donor 1 – 6 PB sample 1	12936 ; 11704 ; 13400 ; 14515 ; 13399 ; 11144
	PB	IgG	Donor 1 – 6 PB sample 2	14200 ; 14268 ; 11433 ; 11473 ; 12273 ; 12598
	PB	IgA	Donor 1 – 6 PB sample 1	11836 ; 11111 ; 13272 ; 12409 ; 13533 ; 10667
	PB	IgA	Donor 1 – 6 PB sample 2	12974 ; 10491 ; 12791 ; 11433 ; 13256 ; 16633
	PB	IgE	Donor 1 – 5 PB sample 1	9144 ; 3803 ; 4822 ; 2463 ; 8312
	PB	IgE	Donor 1 – 5 PB sample 2	10296 ; 7436 ; 9218 ; 6914 ; 6456
	BM	IgG	Donor 1 – 6 BM sample 1	16475 ; 15642 ; 16572 ; 15687 ; 15763 ; 17338
	BM	IgG	Donor 1 – 6 BM sample 2	15979 ; 15624 ; 17693 ; 16377 ; 17374 ; 16019

Table SI. Overview of total read counts after data processing per donor per antibody isotype (continued)

Ref	B cell source	Isotype	Samples per isotype	No. reads
Tipton[31]	BM	IgA	Donor 1 – 6 BM sample 1	12128 ; 11732 ; 11315 ; 12516 ; 12145 ; 11256
	BM	IgA	Donor 1 – 6 BM sample 2	12441 ; 12569 ; 11427 ; 12867 ; 12586 : 13631
	BM	IgE	Donor 1 – 6 BM sample 1	13241 ; 12477 ; 11765 ;9620 ; 12638 ; 10802
	BM	IgE	Donor 1 – 6 BM sample 2	13114 ; 13609 ; 12454 ; 8462 ; 11743 ; 10835
	PB	IgG	SLE1-126 ; SLE2-178 ; SLE3-292 ; SLE4-2037; SLE5-262 ; SLE7-730 ; SLE6-161	13190 ; 12187 ; 14998 ; 14904 ; 15388 ; 14763; 12006
	PB	IgA	SLE1-126 ; SLE2-178 ; SLE3-292 ; SLE4-2037; SLE5-262 ; SLE7-730 ; SLE6-161	13939 ; 11689 ; 12702 ; 14379 ; 13133 ; 12723; 12715
	BM	IgA	D1 ; D2	9213 ; 11663
	BM	IgG	D1 ; D2	10805 ; 11734

PB, peripheral blood; BM, bone marrow; IgM n, IgM naive; IgM m, IgM memory

Table SII. Glycosylation of non-germline *N*-glycosylation sites corresponding to progenitor sites in the variable domain of monoclonal antibodies.

	Position	Allele	Occupied	Clone	*N*-glycosylation site
Heavy chain	20	IGHV1-69*01	Yes	RA10[34]	NVS
	29	IGHV1-18*01	Yes	α-IFX 1.3[19]	NFT
	29	IGHV1-2*02	Yes	α-cFib 1.2[34]	NVT
	58	IGHV3-21*02	Yes	RA11[34]	NRS
	59	IGHV3-9*01	Yes	ADL G63S[19]	NSS
	66	IGHV1-69*01	Yes	α-IFX 2.1[19]	NYT
	66	IGHV1-18*01	Yes	α-ADL 1.3[19]	NYT
	68	IGHV4-39*01	Partial	RF065	NYT
	75	IGHV3	Yes	CBGA1[18]	NNS
	77	IGHV1-3*01	Yes	α-ADL 2.1[19]	NFT
	77	IGHV3-53*03	Yes	RA8[34]	NIS
	77	IGHV3-9*01	Yes	ADL T77N[19]	NIS
	77	IGHV4-39*01	Yes	α-ADL 2.6[19]	NIS
	77	IGHV1-3*01	Yes	α-ADL 2.10[19]	NIT
	77	IGHV3-30*01	Yes	α-D T77N	NIS
	82	IGHV3-9*01	Yes	ADL K84T[19]	NAT
	84	IGHV3-30*01	Yes	α-IFX 2.3[19]	NNT
	84	IGHV3-9*01	Yes	ADL K84N[19]	NNS
	90	IGHV4-38-2*02	Yes	RF063	NLT
	90	IGHV4-34*01	Yes	α-ADL 2.7[19]	NLT
	97	IGHV1-2*02	Yes	α-cFib 1.2[34]	NDT
Light chain	18	IGLV1-51*01	Yes	α-cFib 1.1[34]	NVT
	22	IGLV3-25*02	Yes	RA8[34]	NCS
	22	IGKV4-1*01	Yes	RA14[34]	NCT
	25	IGLV1-51*01	Yes	mAb-C5[35]	NSS
	26	IGKV3-20*01	Partial	α-ADL 2.10[19]	NRS
	26	IGKV2-28*01	Yes	RA15[34]	NQS
	28	IGKV1-33*01	Partial	α-ADL 2.9[19]	NIS
	28	IGKV1-33*01	No	α-NTZ 2.2	NIS
	37	IGKV1-27*01	Yes	ADL L39S[19]	NYS
	77	IGKV1-33*01	Partial	α-ADL 2.9[19]	NGS
	77	IGKV1-33*01	No	α-NTZ 2.2	NGS
	79	IGKV1-33*01	Yes	α-ADL 2.2[19]	NGS
	79	IGKV1-27*01	Yes	ADL S79N[19]	NGS
	79	IGKV1-39*01	Partial	α-D S79N	NGS
	86	IGKV1-27*01	Yes	ADL D86N[19]	NFT
	108	IGKV1-27*01	No	ADL A114T[19]	NRT
	110	IGLV2-23*02	Yes	α-IFX 1.4[19]	NIT

ADL, Adalimumab; IFX, Infliximab; NTZ, Natalizumab; RF, Rheumatoid Factor; GSK, Guselkumab; RA, Rheumatoid arthritis; cFib, citrullinated fibrinogen; H, heavy chain; L, light chain

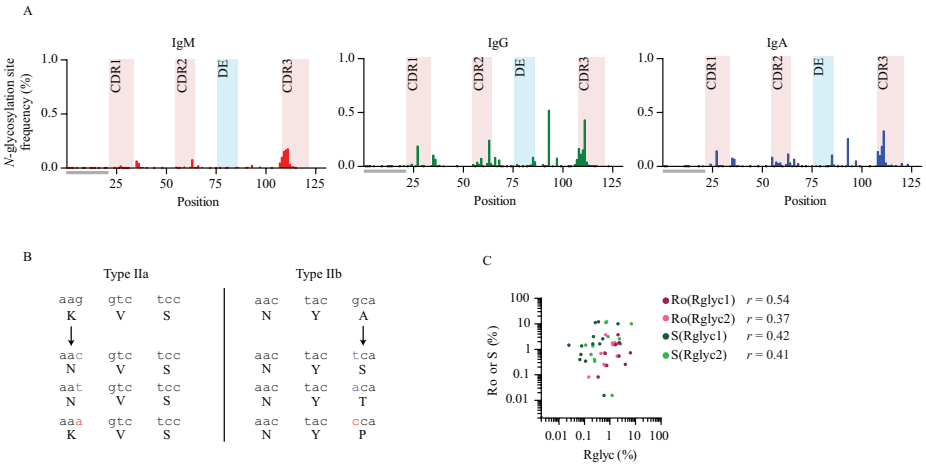

Figure S1. Frequency distribution of non-progenitor sites across antibody variable region for healthy individuals. *(**A**) Distributions are shown for memory PB B cells (IgM, IgG and IgA). Bars represent medians from multiple donors (n=12). Horizontal grey bars indicates FWR1, for which coverage is incomplete. Sites within the H-CDR3 at positions 111.1 – 112.1 are collapsed into position 111. (**B**) Mutation propensities in Type IIa and IIb progenitor sites. Examples of a Type IIa and IIb germline nonameric progenitor site nucleotide motif (**C**) Scatterplot of the glycan-introducing mutations (Rglyc1, Rglyc2) versus either the silent (S) or replacement (Ro) mutation. Correlations were observed both between Rglyc mutations and silent (S) mutations (rs= 0.75, p = 0.003) and non-silent (Ro) mutations (rs = 0.56, p = 0.007). The propensity for Rglyc mutations over S mutations was 4-fold lower (median = 0.22, p <0.0001), and slightly higher for Ro mutations (median Rg/Ro = 1.29, p <0.04). Spearman's r, p <0.0001 and Wilcoxon signed rank test.*

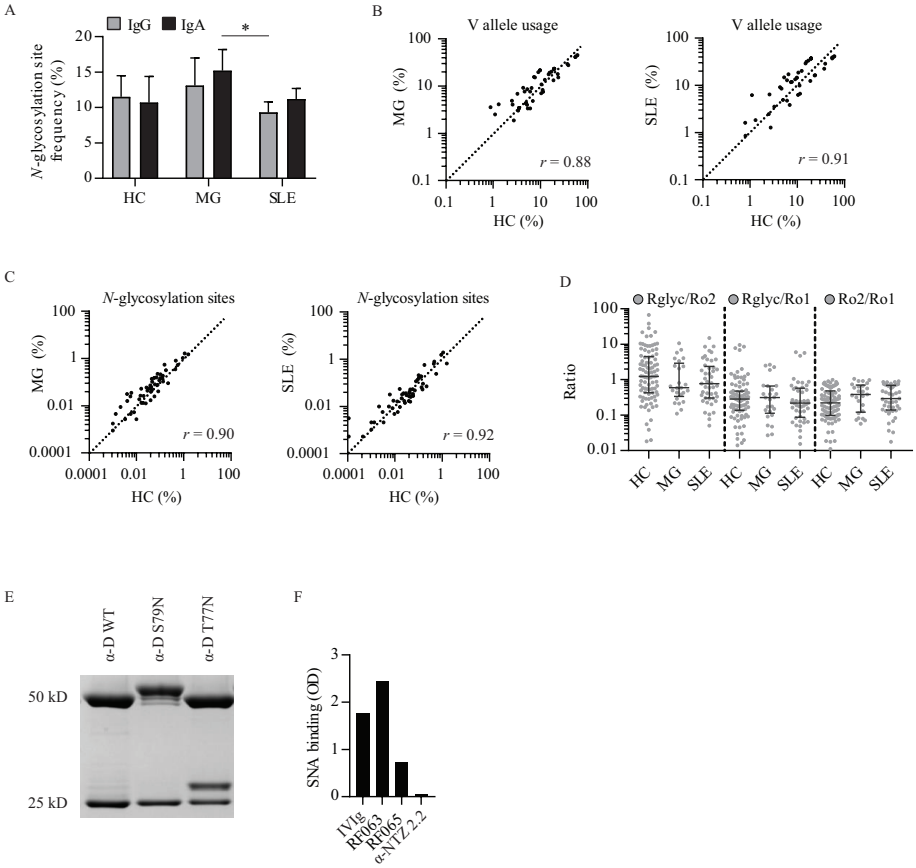

Figure S2. Frequency distribution of non-germline *N*-glycosylation sites across antibody variable region sequences for MG and SLE patients. *(**A**) The frequency of N-glycosylation sites (%) for IgG and IgA PB B cells of healthy individuals (HC; n=12) and disease subjects (MG; n=9, SLE; n=7). Bars indicate medians, error bars ± S.D. (**B**,**C**) Correlation of progenitor sites and acquired glycosylation sites between HC and disease subjects for PB derived memory B cells. (**D**) Ratios of Rglyc versus Ro mutations compared for HC and disease subjects. (**E**) Glycosylation assessment of five monoclonal antibodies with N-glycosylation sites. Gel-electrophoresis of α-D monoclonal antibodies. (**F**) Lectin ELISA for IVIg, two rheumatoid factor (RF) monoclonal antibodies RF063 and RF065 and α- natalizumab (NTZ) 2.2*

CHAPTER 7

Differences in IgG autoantibody Fab glycosylation across autoimmune diseases

Jana Koers, Rocco Sciarrillo, Ninotska I.L. Derksen,
Esther M. Vletter, Yvonne E. Fillié-Grijpma,
Elisabeth Raveling-Eelsing, Nuno A. G. Graça, Thiemo Leijser,
Hendri H. Pas, L. Laura van Nijen-Vos, Maaike V.J. Braham,
Anne-Marie Buisman, Jan de Jong, Angela I. Schriek,
Anne P. Tio-Gillen, Y.K. Onno Teng, Maurice Steenhuis,
Francis H. Swaneveld, Steven W. de Taeye, Marit J. van Gils,
Jan J.G.M.Verschuuren, Bram Rutgers, Peter Heeringa, Barbara Horváth,
Bart C. Jacobs, Karina de Leeuw, Casper F.M. Franssen,
Agnès Veyradier, Paul Coppo, Kyra A. Gelderman, S. Marieke van Ham,
Cécile A.C.M. van Els, Diane van der Woude, Ruth Huizinga,
Maartje G. Huijbers, Taco W. Kuijpers, Rene E.M. Toes,
Nicolaas A. Bos, Theo Rispens, on behalf of the T2B consortium

Published in the Journal of Allergy and Clinical Immunology (2023)

ABSTRACT

Increased prevalence of autoantibody Fab glycosylation has been demonstrated for several autoimmune diseases. To study if elevated Fab glycosylation is a common feature of autoimmunity, we investigated Fab glycosylation levels on serum IgG and its subclasses for autoantibodies associated with a range of different B cell-mediated autoimmune diseases, including rheumatoid arthritis, myasthenia gravis subtypes, pemphigus vulgaris, ANCA-associated vasculitis, systemic lupus erythematosus, anti-GBM glomerulonephritis, thrombotic thrombocytopenic purpura and Guillain-Barré syndrome. The level of Fab glycosylated IgG antibodies was assessed by lectin affinity chromatography and autoantigen-specific immunoassays. In six out of ten autoantibody responses, in five out of eight diseases, we found increased levels of Fab glycosylation on IgG autoantibodies that varied from 86% in RA to 26% in SLE. Elevated autoantibody Fab glycosylation was not restricted to IgG4, which is known to be prone to Fab glycosylation, but also present in IgG1. When autoimmune diseases with a chronic disease course were compared with more acute autoimmune illnesses, increased Fab glycosylation was restricted to the chronic diseases. As a proxy for chronic autoantigen exposure, we determined Fab glycosylation levels on antibodies to common latent herpes viruses, as well as to gp120 in chronically HIV-1-infected individuals. Immunity to these viral antigens was not associated with increased Fab glycosylation levels, indicating that chronic antigen-stimulation as such does not lead to increased Fab glycosylation levels. Our data indicate that in chronic but not acute B cell-mediated autoimmune diseases disease-specific autoantibodies are enriched for Fab glycans.

INTRODUCTION

A central role of the immune system is to protect the host from invading pathogens, while maintaining tolerance to self. Failure to distinguish self from non-self is at the basis of autoimmunity and if improperly regulated this can lead to pathology and disease[1]. To date nearly 100 distinct autoimmune diseases are described that collectively affect 3-5% of the general population, with ever rising incidence. Autoimmune diseases are highly diverse and diseases differ in severity, affected tissue(s) and effector mechanism that cause damage. Although incompletely understood, autoimmunity is thought to result from a combination of loss of tolerance mechanisms, genetic susceptibility, and environmental factors[2].

The presence of autoantibodies is a common feature of many autoimmune diseases, and for some diseases these can be useful for diagnosis and classification and for others may correlate with the disease status or predict further clinical evolution of the disease[3]. Autoantibodies can be directed against a variety of molecules, such as nucleic acids, lipids or proteins and mediate both systemic inflammation and tissue damage[4]. For several IgG autoantibody responses, an increased prevalence of antibody variable region (Fab) glycosylation has been observed[5], such as anti-CCP in rheumatoid arthritis (RA)[6,7] and anti-MPO in ANCA-associated vasculitis (AAV)[8,9]. Fab glycans are attached to consensus *N*-glycosylation sites (N-X-S/T) that are mainly introduced via the process of somatic hypermutation during antigen-specific immune responses, as they are largely absent in the naive B cell repertoire[10]. In healthy individuals, about 10-14% of serum IgG is Fab glycosylated[11–15] with IgG4 antibodies showing higher levels of Fab glycosylation (44%) compared to the other IgG subclasses (IgG1:12%, IgG2:11%, IgG3:15%)[15]. Furthermore, mass spectrometry glycan analysis revealed that most Fab glycans have a complex-type biantennary structure with high levels (>90%) of terminal sialic acid residues[13,16,17].

The role of Fab glycans in autoimmunity, as for immunity in general, is poorly understood. Fab glycans can affect antigen binding[18–20]. Therefore, it has been postulated that Fab glycans may reduce autoimmunity by masking the autoantigen binding sites of autoantibodies[21]. Likewise, Fab glycans expressed by autoreactive B cell receptors (BCRs) have been shown to enhance BCR-signaling and to prolong its expression on the cell-surface after antigenic triggering[22]. In certain B cell lymphoma, such as follicular or diffuse large B cell lymphoma, the introduction of Fab glycans on the BCR might allow for interaction with lectins in the germinal center and thereby provide survival signals to sustain tumor growth[23,24]. In addition, Fab glycans may also arise upon chronic antigen exposure since elevated Fab glycosylation levels are found on IgG4 and IgE antibodies which are associated with repeated or chronic antigen exposure[10,15,25,26]. Furthermore, anti-hinge autoantibodies in both RA patients and healthy individuals were extensively Fab glycosylated suggesting that

elevated Fab glycosylation may develop in response to an inflammatory microenvironment not per se restricted to autoimmunity[27].

Although several IgG autoantibody responses have been characterized with increased levels of Fab glycans, it is not known whether this is a general characteristic acquired by autoantibodies that develop in the context of autoimmunity. Therefore, characterization of Fab glycosylation levels on a broad spectrum of autoantibody responses is important as it may provide a more detailed understanding of the role of Fab glycans in pathological conditions.

METHODS

Patients and healthy controls were included at the various collaborating teams at the University Medical Centers in Amsterdam, Leiden, Rotterdam, Groningen, and Paris according to the approved study protocols and with written consent of the patients according to the Declaration of Helsinki. In this study cross-sectional samples were included prior to (B cell targeted) therapy or more than 6 months after immunosuppressive treatment. For samples, lectin (SNA) affinity chromatography, total and specific IgG immunoassays, and gel filtration chromatography, see details in **Supplementary material**.

Statistical analysis

Differences between two groups were analyzed using a paired or unpaired t-test and between multiple groups using a Kruskal-Wallis ANOVA and a Dunn posttest for multiple comparisons. Non-parametric correlations were analyzed with a Spearman rank correlation test. A p value <0.05 was considered significant. The statistical analyses were carried out using GraphPad Prism 9.1.1.

RESULTS

Variable levels of autoantibody Fab glycosylation across multiple autoimmune diseases

To investigate if elevated levels of Fab glycosylation are a general characteristic acquired by antibodies that develop in the context of autoimmunity, we analyzed the level of Fab glycosylation for ten autoimmune disease-associated IgG autoantibody responses in cross-sectional serum samples taken before B cell targeted therapy across eight different autoimmune diseases (**Table I**). To do so, we fractionated sera of autoimmune patients (n = 101) and healthy controls (n = 15) using *Sambucus nigra agglutinin* (SNA, sialic acid binding lectin) affinity chromatography (**Figure 1A**). SNA affinity chromatography of

serum results in an SNA+ fraction (enriched for sialylated antibodies) and an SNA- fraction (devoid of sialylated antibodies). Total and specific IgG is measured in the initial serum and in SNA+ and SNA- fractions by quantitative ELISA, RIA, Luminex, FEIA or MIA. The percentage of Fab sialylated antibodies is calculated by dividing the amount of (antigen-specific) IgG detected in the SNA+ fraction by the combined amount of (antigen-specific) IgG detected in the SNA+ and SNA- fractions (amount refers to arbitrary units measured in each fraction, **Supplementary material**). This technique allows for the enrichment of Fab sialylated antibodies, but not for Fc glycans, and provides a good estimate for the level of Fab glycosylation as over 90% of Fab glycans carry terminal sialic acid residues[12,13,28].

Table I. Description of included autoimmune diseases for determination of autoantibody Fab glycosylation levels

Disease	Autoantigen(s)	Autoantibody subclass(es)	Organ(s) affected	No. patients included
Rheumatoid Arthritis	CCP2, CarP	IgG1-4	Joints, lungs, heart, skin, eyes and others	12
Myasthenia Gravis	MuSK, AChR	IgG1, IgG4	Muscle	24
Pemphigus Vulgaris	Dsg3	IgG1, IgG4	Oral mucosa, skin	9
ANCA-Associated Vasculitis	PR3	IgG1, IgG3	Blood vessel walls	21
Systemic Lupus Erythematosus	dsDNA	IgG1, IgG3	Skin, joints, kidneys, lungs, heart, others	10
Anti-Glomerular Basement Membrane disease	α3(VI) NC1	IgG1, IgG4	Kidneys & lungs	8
Guillain-Barré Syndrome	Gangliosides	IgG1, IgG3, IgG4	Peripheral nervous system	8
Thrombotic Thrombocytopenic Purpura	ADAMTS13	IgG1, (IgG4)	Central nervous system, kidneys, and others	9

In line with previous studies[6,15,29], for ACPA in RA, we found high levels of Fab glycosylation (anti-CCP2, 86% [IQR 71-90]) that were significantly elevated compared with those of total IgG (14% [IQR 12-16], p <0.0001, **Figure 1B**). For the subset of samples with quantifiable anti-CarP antibody levels, we also found high levels of Fab glycosylation for anti-CarP antibodies (51% [IQR 42-77]), but significantly lower than for anti-CCP2 antibodies (p = 0.05). Significantly increased levels of autoantibody Fab glycosylation were also observed for anti-Dsg3 antibodies found in patients with PV (49% [IQR 37-55], p <0.0001), anti-PR3 antibodies found in patients with AAV (31% [IQR 15-40], p <0.0001) and anti-dsDNA (26% [IQR 19-34] p = 0.02) antibodies found in patients with SLE when compared to Fab glycosylation levels on their total IgG (**Figure 1C**). In contrast, Fab glycosylation levels on autoantibody responses found in patients with anti-GBM glomerulonephritis, GBS and TTP, anti-alpha3(IV)NC1 antibodies (10% [IQR 2-23]), anti-gangliosides antibodies (<3%

[IQR 2-4]) and anti-ADAMTS13 antibodies (3% [IQR 1-10]), respectively were found to be similar or decreased compared with that of their total IgG (GBM: 14%, p = 0.07; GBS: 11%, p <0.0001 and TTP: 12%, p = 0.05) (**Figure 1D**). Remarkably, in patients with MG we found high levels of Fab glycosylation for anti-MuSK antibodies (46% [IQR 29-64], p = 0.0001) but levels comparable to those of total IgG (11% [IQR 11-17]) for anti-AChR antibodies

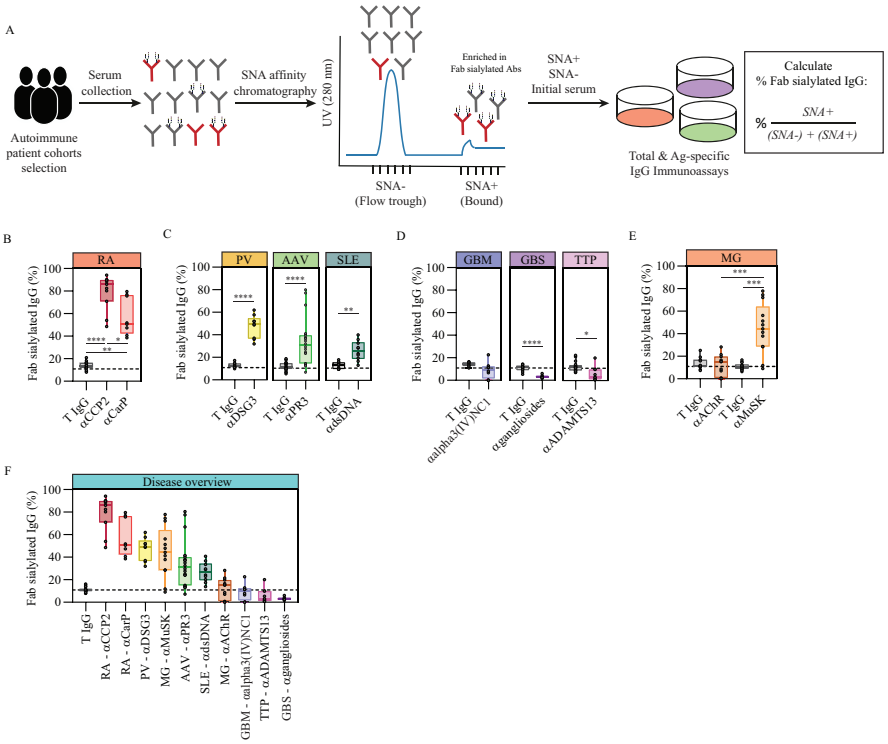

Figure 1. Prevalence of IgG autoantibody Fab glycosylation across multiple autoimmune diseases. ***(A)*** *Schematic overview of methodology. Cross-sectional serum samples taken before B cell targeted therapy or more than 6 months after immunosuppressive treatment from eight different autoimmune patients cohorts were fractionated using SNA affinity chromatography generating a sialic acid enriched (SNA+) and depleted (SNA-) pool of serum proteins. Total and antigen-specific IgG is determined for both fractions. The percentage of Fab glycosylated antibodies was calculated by dividing the amount of IgG in SNA+ by the amount of IgG in the combined SNA+ and SNA-fractions (i.e., arbitrary units measured in each fraction). Percentage of Fab sialylated total (T) IgG, (**B**) anti-CCP2 (n = 11) and anti-CarP (n = 8) in rheumatoid arthritis (RA), (**C**) anti-Dsg3 (n = 9) in pemphigus vulgaris (PV), anti-PR3 (n = 21) in ANCA-associated vasculitis (AAV), anti-dsDNA (n = 10) in systemic lupus erythematosus (SLE), (**D**) anti-alpha3(IV)NC1 (n = 8) in anti-GBM glomerulonephritis (GBM), anti-gangliosides (n = 8) in Guillain-Barré syndrome (GBS), and anti-ADAMTS13 (n = 9) in Thrombotic thrombocytopenic purpura (TTP), and (**E**) anti-MuSK (n = 13) and anti-AChR (n = 11) in myasthenia gravis (MG). (**F**) Overview of Fab glycosylation levels of total IgG in healthy controls and ten IgG autoantibody responses across eight different autoimmune diseases. Dashed lines represent the median for Fab glycosylation of T IgG in healthy donor sera (11%, IQR 11-14%, n = 18). Box-plots show median and IQR. Statistical differences were determined using a paired or unpaired t-test or Kruskal-Wallis ANOVA and Dunn's multiple comparison test. * p < 0.05, ** p < 0.01, *** p < 0.001, **** p < 0.0001.*

(15% [IQR 1-20], p = 0.63). Contrary to anti-CCP2 and anti-CarP antibodies in RA, anti-MuSK and anti-AChR antibodies in MG were not measured in the same individuals as these rarely co-exist. Because anti-dsDNA autoantibodies in SLE patients revealed elevated Fab glycosylation, we additionally analyzed two other autoantibody responses in the same patients. For anti-Sm antibodies, which are specifically associated with SLE, Fab glycosylation levels were elevated (n = 6 (23% [IQR 15-31] p = 0.04), contrary to the less disease-specific anti-Ro52 antibodies (14% [IQR 12-19] p = 0.38, n = 7) (**Figure S2**, panel A). **Figure 1F** provides an overview of Fab glycosylation levels on total IgG in healthy individuals and disease-associated autoantibody responses ordered by decreasing median Fab glycosylation levels. SNA+/SNA- antigen detection values of quantitative immunoassays are reported in the supporting information. Size-exclusion chromatography was performed to confirm the presence of Fab glycans on antigen-specific autoantibodies (larger hydrodynamic volume) for anti-PR3 and anti-MuSK antibodies (**Figure S1**, panel B), as previously described for anti-CCP2 and anti-hinge antibodies in RA[6,27]. For anti-MuSK IgG4 antibodies the size shift was less pronounced probably due to the fact that most IgG4 molecules carry only a single Fab glycosylated Fab arm due to half-molecule exchange[30]. Autoantibody levels did not correlate with total IgG levels (**Figure S2B**) nor with Fab glycosylation levels (**Figure S3**) for any of the diseases, which suggests that high or low level of Fab glycosylation are not the result of the level of antibodies produced, in line with earlier studies[27,31].

IgG autoantibody subclass distribution and Fab glycosylation levels

Next, we determined Fab glycosylation levels of IgG subclasses in autoantibody responses that showed elevated levels of Fab glycosylation. In healthy individuals IgG4 Fab glycosylation levels are increased (43% [IQR 40-48]) compared with that of other IgG subclasses (IgG1; 12% [IQR 11-17], IgG3; 15% [IQR 12-16]), and of total IgG (11% [IQR 9-14], **Figure 2A**), of which IgG4 antibodies are only a minor fraction[10,15]. Within anti-MuSK and anti-Dsg3 autoantibody responses, a large fraction is of the IgG4 subclass[32,33]. Therefore, we investigated whether the increased Fab glycosylation levels observed for these responses could be explained by a high proportion of IgG4 antibodies, that have elevated levels of Fab glycans in general. For MusK MG we found that levels of Fab glycosylation of anti-MuSK IgG4 antibodies (66% [IQR 58-73]) were significantly higher than that of total IgG4 (31% [IQR 19-41], p <0.0001) and anti-MuSK IgG (46% [IQR 29-64], p = 0.005), whereas Fab glycosylation levels of anti-MuSK IgG1 antibodies (3% [IQR 2-15]) were not elevated compared to total IgG (11% [IQR 8-14], p = 0.99) or IgG1 (12% [IQR 9-14], p = 0.99). This indicates a subclass-specific increased selection for Fab glycosylation of anti-MuSK antibodies, restricted to the IgG4 subclass (**Figure 2B**). Fab glycosylation for PV-associated anti-Dsg3 followed a different pattern (**Figure 2C**). Fab glycosylation levels on anti-Dsg3 IgG1 antibodies (30% [IQR 21-52]) were significantly higher than total IgG1 (12% [IQR 11-15], p = 0.003) but not different from anti-Dsg3 IgG (49% [IQR 37-55], p =

0.39). Anti-Dsg3 IgG4 antibodies (56% [IQR 36-68]) were not different from total IgG4 (45% [IQR 29-47], p = 0.32) nor from anti-Dsg3 IgG (49% [IQR 37-55], p = 0.98). Anti-Dsg3 IgG3 antibodies were only detectable in a small fraction of patients (n = 3) and presented variable levels of Fab glycosylation levels with high interpatient variation (26% [IQR 11-56], **Figure S4A**) not significantly different from total IgG3 (10% [IQR 8-12], p = 0.25). Fab glycosylation levels for anti-PR3 antibodies in AAV, a response dominant in IgG1 and IgG3, were elevated for anti-PR3 IgG1 (21% [IQR 10-34]) and anti-PR3 IgG4 antibodies (40% [IQR 31-49]), and low for anti-PR3 IgG3 antibodies (5% [IQR 0-16], **Figure 2D**). Fab glycosylation of total IgG4 (35% [IQR 21-44]) and anti-PR3 IgG4 antibodies (40% [IQR 31-49], p = 0.93) were not significantly different. Here, although not significant overall, some individuals showed a remarkable increase in anti-PR3 IgG1 Fab glycosylation compared to total IgG1 (14% [IQR 11-15], p = 0.14). Six AAV patients were included at first onset of disease and 15 patients during relapse. Interestingly, the median Fab glycosylation level of anti-PR3 IgG, and thus IgG subclasses, was significantly lower in patients at first onset of disease (14% [IQR 12-27], p = 0.009) than those in relapse (36% [IQR 26-41]) and not different from total IgG (12% [IQR 10-17], p = 0.91, **Figure S4B**). Anti-Dsg3 and anti-PR3 IgG1 Fab glycosylation levels were significantly higher than those of anti-MuSK IgG1 whereas Fab glycosylation levels for anti-MuSK IgG4 were higher compared to anti-PR3 IgG4 but not anti-Dsg3 IgG4 (**Figure S4C**). For RA, no reliable data were obtained for IgG2-4. This is in line with the observation that the ACPA subclass composition is dominated by IgG1, with a minor contribution of other subclasses, including IgG4, which is estimated to contribute, on average, 5% to the overall ACPA IgG composition[34,35]. Assays for reliable measurements of anti-dsDNA IgG subclasses were lacking and therefore not included in this study.

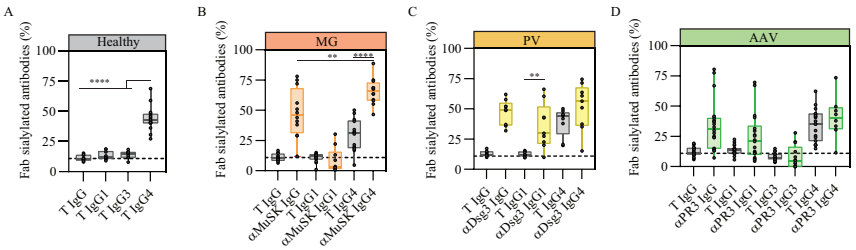

Figure 2. Fab glycosylation levels of IgG autoantibody subclasses. *(**A**) Percentage of sialylated antibodies for total (T) IgG and IgG1, IgG3, and IgG4 in healthy donor sera (n = 18). (**B**) Fab sialylated antibody levels for total and specific anti-MuSK IgG (n = 12), IgG1 (n = 10), and IgG4 (n = 12) in MG patients. (**C**) Fab sialylated antibody levels for total and specific anti-Dsg3 IgG, IgG1 and IgG4 (n = 9) in PV patients. (**D**) Fab glycosylation levels for total and specific anti-PR3 IgG (n = 22), IgG1 (n = 18), IgG3 (n = 15) and IgG4 (n = 11) in AAV patients. Box-plots show median and IQR. Statistical differences were determined using a Kruskal-Wallis ANOVA and Dunn's multiple comparison test. * p < 0.05, ** p < 0.01, *** p < 0.001, **** p < 0.0001.*

Chronic viral antigen stimulation or repeated tetanus toxoid immunization does not lead to increased levels of antigen-specific IgG Fab glycosylation

To investigate if elevated levels of Fab glycosylation are characteristic of situations of chronic antigen exposure, we analyzed Fab glycosylation levels on antibodies targeting several different herpes viruses in the same patient groups and in healthy controls. Infection with a single or multiple of these herpesviruses is common in the general adult population. Once infected, individuals establish a lifelong latency with repeated periods of viral reactivation and exposure[36]. Fab glycosylation levels were determined on IgG antibodies specific for Human cytomegalovirus (CMV), Epstein-Barr virus (EBV) and Varicella-zoster virus (VZV) in autoimmune patients (n = 69) and healthy controls (n = 15) that tested seropositive for one or multiple of these viruses. The prevalence of CMV/EBV/VZV infections amongst the included autoimmune patients and healthy controls were fairly similar (**Figure S5A**). Fab glycosylation levels for IgG antibodies against CMV (9% [IQR 4-16]) in patients and healthy controls were comparable to total IgG levels (12% [IQR 10-15], p = 0.18, **Figure 3A**). Interestingly, Fab glycosylation levels on anti-EBV (3% [IQR 2-5]) and anti-VZV antibodies (8% [IQR 5-11]) were significantly lower compared to total IgG (12%, EBV: p <0.0001, VZV: p = 0.02). Furthermore, Fab glycosylation levels were also evaluated for anti-gp120 antibodies in treatment-naive chronic HIV-1-infected individuals. Altered Fc glycosylation levels as well as specific Fab glycans on broadly neutralizing antibodies were previously reported[37,38]. However, also in this case, we observed that Fab glycosylation levels were lower rather than elevated (0.5% [IQR 0.2-1.1]) compared to total IgG (13% [9-17], p = 0.0001; **Figure 3B**). Fab glycosylation levels for antibodies to tetanus toxoid (TT, 12% [IQR 8-18]), a typical vaccine antigen that mainly induces IgG1, were similar to those of total IgG (12% [IQR 10-15], p = 0.84) across all autoimmune diseases and comparable to those of healthy individuals (13% [IQR 8-23], p = 0.5), and to those hyper-immunized with TT (HI-Healthy, 11% [IQR 10-15], p = 0.99, **Figure 3C**). There were no significant differences in Fab glycosylation levels of CMV/EBV/VZV/TT antibody responses when separated per disease (**Figure S5B**). IgG Fab glycosylation levels were also studied in individuals that recently underwent an acute primary viral infection. Fab glycosylation levels on anti-spike (S, 5% [IQR 5-14]), anti-spike protein receptor-binding domain (RBD, 4% [IQR 2-5]) and anti-nucleocapsid protein (N, 8% [IQR 4-10]) IgG antibodies in SARS-CoV-2 infected individuals were found to be significantly lower compared to those of total IgG (13% [IQR 11-14], p <0.0001) (**Figure 3D**). Taken together, antibodies developed during both chronic and acute viral antigen exposure show normal to low levels of Fab glycosylation.

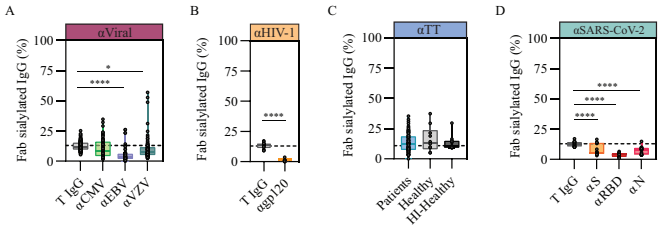

Figure 3. IgG Fab glycosylation levels after chronic and acute viral antigen exposure. *(**A**) Percentage of Fab sialylated antibodies for total (T) IgG, anti-CMV, anti-EBV, and anti-VZV in serum of autoimmune patients (including RA, PV, AAV, SLE, TTP and GBS, CMV; n = 41, EBV; n = 44, VZV; n = 53) and healthy controls (CMV; n = 6, EBV; n = 9, VZV; n = 13). (**B**) Percentage of Fab sialylated antibodies for total (T) IgG and anti-gp120 antibodies in serum of chronic HIV-1-infected individuals (n = 14). (**C**) Percentage of Fab sialylated IgG for anti-tetanus toxoid (TT) in autoimmune patients (including RA, MG, PV, AAV, SLE, TTP and GBS, n = 110), healthy controls (n = 10), and TT hyper-immunized (n = 11). (**D**) Fab sialylated antibodies for T IgG, anti-S, anti-RBD and anti-N IgG in healthy individuals previously infected with SARS-CoV-2 (S; n = 19, RBD; n = 19, N; n = 18). Box-plots show median and IQR. Statistical differences were determined using a paired t-test or Kruskal-Wallis ANOVA and Dunn's multiple comparison test. * $p < 0.05$, **** $p < 0.0001$.*

DISCUSSION

In this disease-overarching study, we compared IgG autoantibody Fab glycosylation levels between ten different disease-associated IgG autoantibody responses across eight different autoimmune diseases. We observed elevated levels of autoantibody Fab glycosylation in a number of chronic B cell mediated autoimmune diseases, including, for the first time, anti-Dsg3, anti-MuSK, anti-PR3, anti-dsDNA IgG autoantibody responses, but not for autoantibody responses found in acute B cell mediated autoimmune diseases. Hence, chronic B cell mediated autoimmune diseases may share a common pathophysiological mechanism of immune dysregulation hallmarked by elevated Fab glycosylation levels. Furthermore, within autoantibody responses we observed subclass-specific increases of Fab glycosylation and no enhanced Fab glycosylation levels were found on antibodies directed against viral antigens, including antigens from common latent herpes viruses, indicating that chronic or repeated antigen exposure in itself does not necessarily lead to increased antibody Fab glycan levels and is context-dependent.

In recent years it has become increasingly clear that Fab glycans play a role in antibody function but also in immune function. Besides diversification of the antibody repertoire several functional attributes have been demtonstrated to involve Fab glycans, including impact on antigen binding[15,18–20,39], antibody half-life and stability[40–44], and engagement of (endogenous) lectins[23,45], such as SIGLEC CD22[46]. The level of Fab glycosylation for any given IgG autoantibody response is the result of the subclass distribution and their individual level of Fab glycosylation. Functional characteristics of the different IgG subclasses are major determinants in the differences between IgG1/IgG3-, and IgG4-

dominant autoimmune diseases in the way they contribute to inflammation and damage[47–49]. The level of Fab glycosylation on anti-MuSK IgG4 antibodies significantly exceeded levels of total IgG4 whereas Fab glycosylation on anti-MuSK IgG1 antibodies was low. This indicates a subclass-specific increased selection for Fab glycosylation of anti-MuSK, being in this case restricted to the IgG4 subclass. In PV, another archetypical IgG4-dominated autoimmune disease, Fab glycosylation levels of anti-Dsg3 IgG4 antibodies were high, but not significantly elevated compared to total IgG4. In both these diseases, an association between high levels of Fab glycans and the presence of pathogenic IgG4 autoantibodies is observed. The presence of Fab glycans may create an additional layer that can contribute to the pathogenicity of these autoantibodies. Of note, altered *N*-glycosylation of anti-PLA2R1 IgG4 in patients with membranous nephropathy has been reported to result in local activation of complement via the lectin pathway thereby contributing to pathogenicity[50]. Fab glycosylation of anti-PLA2R IgG4 was not assessed specifically in this study. Different from MuSK MG though, the Fab glycosylation levels of anti-Dsg3 IgG1 antibodies in PV were significantly increased compared to total IgG1. Hence, high levels of autoantibody Fab glycosylation in PV are not exclusive to IgG4 when determined in the same individuals. IgG1 Fab glycosylation levels were also elevated for anti-PR3 antibodies in a fraction of AAV patients and was previously observed for total IgG1 in patients with IgG4-related disease[51]. Fab glycosylation levels on antigen-specific IgG3 was generally low. However for anti-Dsg3 IgG3, we observed several cases with elevated levels of Fab glycosylation, whereas anti-PR3 IgG3 antibody Fab glycosylation levels were low. Autoantibody responses thus widely differ in the preferred subclass expression and the level of Fab glycosylation on these antibodies. Subclass-specific enrichment of Fab glycans may occur under conditions where Fab glycans are functionally relevant.

A commonality among several autoantibody responses is a skewing towards the IgG4 isotype, a subclass that has elevated levels of Fab glycans in general and is elicited upon T_H2 type responses, associated with chronic antigen exposure and sometimes tolerance build-up. Chronic or relapsed viral infections are not associated with an IgG4 skewing. Hence, chronic antigen exposure, within specific contexts, could still result in elevated Fab glycosylation.

For AAV patients at first onset of disease Fab glycosylation levels were significantly lower than those who suffered from a relapse, suggesting that Fab glycans are positively selected during the course of the disease. In RA, selection in favor of Fab glycans was also observed in a longitudinal study into ACPA response development[31,52]. Accumulation of Fab glycans as a natural byproduct of ongoing B cell responses is unlikely. For ACPA the number of variable region mutations did not correlate with the frequency of *N*-glycosylation sites[29]. Furthermore, both IgG4 and IgE antibodies have elevated levels of Fab glycans despite having similar or even fewer variable region mutation levels as other isotypes[10,25,53]. It

remains unclear how selection for Fab glycans takes place. There might be a role for the antigen or the context of the antigen to drive Fab glycosylation. However, binding of antibodies or BCRs to antigens is not consistently enhanced or decreased by Fab glycans[18–20,22,39,40]. Alternatively, Fab glycans on BCRs may interact with lectins as indicated for B cell lymphomas[23,24], and thereby acquire a survival advantage compared to non-Fab glycosylated BCRs. Further evidence is needed to support this hypothesis.

Autoantibodies in chronic progressive autoimmune diseases all, but anti-AChR, displayed elevated levels of Fab glycosylation. Autoantibodies in TTP, anti-GBM glomerulonephritis and GBS had normal or even decreased levels of Fab glycosylation. These diseases generally run a relapsing-remitting or acute monophasic disease course instead of being chronic. Possible discrepancies between monophasic and chronic disease states is a prolonged exposure to antigen, ongoing inflammation, evolving B cell responses (see above), and epitope spreading. As a proxy for chronic antigen exposure we examined antibodies to common latent herpes viruses and HIV. Fab glycosylation levels were not elevated, indicating that chronic antigen stimulation as such does not lead to increased Fab glycosylation levels. By contrast, antibodies formed against therapeutic proteins, another setting with prolonged antigen exposure, were previously found to display elevated Fab glycosylation levels[15,27]. Possibly, antibodies against microbes may evolve in a microbe-specific context in which Fab glycans are not favorable. As most enveloped viruses have an overall negative charge due to the phospholipids on the cell surface[54,55], the potentially hampered antibody binding due to charge repulsion by antibodies carrying negatively charged sialylated Fab glycans[12,13] may result in negative selection for the introduction of these glycans, even upon repeated exposure. In line with this hypothesis, IgG autoantibodies against Rhesus D, present on the negatively charged surface of red blood cells, were also characterized by low level of Fab glycans[15]. The AChR antigen has also been described to have a negative surface charge[56] different from the MuSK antigen which is largely positively charged[57], potentially explaining the non-elevated levels of Fab glycans for anti-AChR antibodies in MG. Moreover, the majority of GBS, TTP, and anti-GBM glomerulonephritis patients report a viral or bacterial infection before disease onset. The immune system generates antibodies to fight infection, that coincidently trigger autoimmunity in genetically susceptible individuals due to cross-reactivity with self-antigens[58–60]. The low levels of Fab glycans observed on autoantibodies in GBS, TTP and anti-GBM glomerulonephritis might stem from these antibodies originating from cross-reactive anti-microbe immune responses. In line, recent studies further strengthen the link between EBV infection and multiple sclerosis (MS) etiology[61]. It will be interesting to study if autoantibodies in MS originate from cross-reactive EBV antibodies and display low levels of Fab glycans.

Although the included number of patients per disease is limited the strength of the current study lies in the determination of autoantibody Fab glycosylation levels on a broad spectrum

of autoimmune diseases. To determine the clinical prognostic value of Fab glycans, it will be of interest to study longitudinal Fab glycosylation levels and profiles on disease-associated autoantibody responses in more individuals and correlate these with clinically relevant parameters such as disease severity or remission versus active disease, and treatment status. Whether alterations in autoantibody Fab glycosylation levels will affect the course of the disease or change upon immunosuppressive treatment needs yet to be determined. For RA, Fab glycans are described to predict progression to RA and thereafter stabilizes once disease is established[31,52].

Thus, considering the importance of the autoantibody subclass and glycosylation status for the pathogenic potential of a specific-autoantibody response, it might be helpful to include these parameters for diagnostic purposes. Taken together, the variable emerging autoantibody Fab glycosylation levels indicates that Fab glycosylation on autoantibodies is not a random process but is, rather, subject to context-dependent selection mechanisms during autoimmune responses.

Acknowledgments

We acknowledge the support of patient partners, private partners and active colleagues of the T2B consortium; see website: www.target-to-b.nl.

Author contributions

JK, RS, NB, TK, and TR designed research. JK, RS, ND, TL, YF, ER, EV, HP, MB, LN, JJ and NG performed research. JK, RS, ND, YF, ER, EV, HP, NG and TR analyzed data. JK, NB, TK, DW, RT, RH, CE, MH, and TR wrote the paper. All authors critically reviewed the manuscript, gave final approval of the version to be published, and agreed to be accountable for all aspects of the work ensuring that questions related to the accuracy or integrity of any part of the work are appropriately investigated and resolved.

Disclosure statement

MGH and JJV are coinventors on patent applications based on MuSK-related research. The LUMC, MGH and JJV receive royalties from these patents. LUMC receives royalties for a MuSK ELISA. NAGG is an inventor of a patent application regarding autoantibody-resistant ADAMTS13 variants. The remaining authors declare that this research was conducted in the absence of commercial or financial relationships that could be construed as a potential conflict of interest.

Financial support

This collaboration project is financed by the PPP Allowance made available by Top Sector Life Sciences & Health to Samenwerkende Gezondheidsfondsen (SGF) under projectnumber LSHM18055-SGF to stimulate public-private partnerships and co-financing by health

foundations that are part of the SGF. This study was supported by ReumaNederland. This study was supported by a research grant from the Landsteiner Foundation for Blood Transfusion (Grant1626) to TR. MGH receives financial support from the LUMC (Gisela Their Fellowship 2021), Top Sector Life Sciences & Health to Samenwerkende Gezondheidsfondsen (LSHM18055-SGF and LSHM19130), Prinses Beatrix Spierfonds (W.OR-19.13) and the Dutch Science Organization NWO (VENI 0915016181 0040). This study was supported by a research grant from the Vasculitis Foundation to PH (2016) (http://www.vasculitisfoundation.org/research/research-program/).

Ethics approval

Patients and healthy controls were included at the various collaborating teams at the University Medical Centers in Amsterdam, Leiden, Rotterdam, Groningen, and Paris according to the approved study protocols and with written consent of the patients according to the Declaration of Helsinki.

REFERENCES

1. Meffre E, O'Connor KC. Impaired B-cell tolerance checkpoints promote the development of autoimmune diseases and pathogenic autoantibodies. *Immunol Rev*. 2019;292(1):90-101. doi:10.1111/imr.12821
2. Rosenblum MD, Remedios KA, Abbas AK. Mechanisms of human autoimmunity. *J Clin Invest*. 2015;125(6):2228-2233. doi:10.1172/JCI78088
3. Damoiseaux J, Andrade LE, Fritzler MJ, Shoenfeld Y. Autoantibodies 2015: From diagnostic biomarkers toward prediction, prognosis and prevention. *Autoimmun Rev*. 2015;14(6):555-563. doi:10.1016/j.autrev.2015.01.017
4. Mackay IR. Travels and travails of autoimmunity: A historical journey from discovery to rediscovery. *Autoimmun Rev*. 2010;9(5):A251-A258. doi:10.1016/j.autrev.2009.10.007
5. Biermann MHC, Griffante G, Podolska MJ, et al. Sweet but dangerous - The role of immunoglobulin G glycosylation in autoimmunity and inflammation. *Lupus*. 2016;25(8):934-942. doi:10.1177/0961203316640368
6. Rombouts Y, Willemze A, Beers JJBC Van, et al. Extensive glycosylation of ACPA-IgG variable domains modulates binding to citrullinated antigens in rheumatoid arthritis. *Ann Rheum Dis*. 2016;75(3):578-585. doi:10.1136/annrheumdis-2014-206598
7. Hafkenscheid L, Bondt A, Scherer HU, et al. Structural analysis of variable domain glycosylation of anti-citrullinated protein antibodies in rheumatoid arthritis reveals the presence of highly sialylated glycans. *Mol Cell Proteomics*. 2017;16(2):278-287. doi:10.1074/mcp.M116.062919
8. Lardinoisid OM, Deterding LJ, Hess JJ, et al. Immunoglobulins g from patients with anca-associated vasculitis are atypically glycosylated in both the fc and fab regions and the relation to disease activity. *PLoS One*. 2019;14(2):1-25. doi:10.1371/journal.pone.0213215
9. Holland M, Yagi H, Takahashi N, et al. Differential glycosylation of polyclonal IgG, IgG-Fc and IgG-Fab isolated from the sera of patients with ANCA-associated systemic vasculitis. *Biochim Biophys Acta - Gen Subj*. 2006;1760(4):669-677. doi:10.1016/j.bbagen.2005.11.021
10. Koers J, Derksen NIL, Ooijevaar-de Heer P, et al. Biased N -Glycosylation Site Distribution and Acquisition across the Antibody V Region during B Cell Maturation . *J Immunol*. 2019;202(8):2220-2228. doi:10.4049/jimmunol.1801622
11. Käsermann F, Boerema DJ, Rüegsegger M, et al. Analysis and functional consequences of increased Fab-sialylation of intravenous immunoglobulin (IVIG) after lectin fractionation. *PLoS One*. 2012;7(6):e37243. doi:10.1371/journal.pone.0037243
12. Bondt A, Rombouts Y, Selman MHJ, et al. Immunoglobulin G (IgG) Fab Glycosylation Analysis Using a New Mass Spectrometric High-throughput Profiling Method Reveals Pregnancy-associated Changes. 2014:3029-3039. doi:10.1074/mcp.M114.039537
13. Anumula KR. Quantitative glycan profiling of normal human plasma derived immunoglobulin and its fragments Fab and Fc. *J Immunol Methods*. 2012;382(1-2):167-176. doi:10.1016/j.jim.2012.05.022
14. Stadlmann J, Pabst M, Altmann F. Analytical and functional aspects of antibody sialylation. *J Clin Immunol*. 2010;30(1):15-19. doi:10.1007/s10875-010-9409-2
15. van de Bovenkamp FS, Derksen NIL, Ooievaar-de Heer P, et al. Adaptive antibody diversification through N -linked glycosylation of the immunoglobulin variable region. *Proc Natl Acad Sci U S A*. 2018;115(8):1901-1906. doi:10.1073/pnas.1711720115

16. Stadlmann J, Weber A, Pabst M, et al. A close look at human IgG sialylation and subclass distribution after lectin fractionation. *Proteomics*. 2009;9(17):4143-4153. doi:10.1002/pmic.200800931

17. Bondt A, Wuhrer M, Kuijper TM, Hazes JMW, Dolhain RJEM. Fab glycosylation of immunoglobulin G does not associate with improvement of rheumatoid arthritis during pregnancy. *Arthritis Res Ther*. 2016;18(1):1-6. doi:10.1186/s13075-016-1172-1

18. Wallick BYSC, Kabat EA, Morrison SL. Glycosylation of a VH residue of a monoclonal antibody against alpha (1----6) dextran increases its affinity for antigen. *JEM*. 1988;168:1099-1109.

19. Tachibana H, Kim J, Shirahata S. Building high affinity human antibodies by altering the glycosylation on the light chain variable region in N -acetylglucosamine-supplemented hybridoma cultures. *Cytotechnology*. 1997;23(1-3):151-159.

20. Leibiger H, Wu D, Stigler R, Marx U. Variable domain-linked oligosaccharides of human monoclonal IgG: structure and influence on antigen binding. *Biochem J*. 1999;538:529-538.

21. Sabouri Z, Schofield P, Horikawa K, et al. Redemption of autoantibodies on anergic B cells by variable-region glycosylation and mutation away from self-reactivity. *Proc Natl Acad Sci*. 2014;111(25):E2567-E2575. doi:10.1073/pnas.1406974111

22. Kissel T, Ge C, Hafkenscheid L, et al. Surface Ig variable domain glycosylation affects autoantigen binding and acts as threshold for human autoreactive B cell activation. 2022;1759:1-22.

23. Coelho V, Krysov S, Ghaemmaghami AM, et al. Glycosylation of surface Ig creates a functional bridge between human follicular lymphoma and microenvironmental lectins. *Proc Natl Acad Sci U S A*. 2010;107(43):18587-18592. doi:10.1073/pnas.1009388107

24. Chiodin G, Allen JD, Bryant DJ, et al. Insertion of atypical glycans into the tumor antigen-binding site identifies DLBCLs with distinct origin and behavior. *Blood*. 2021;138(17):1570-1582. doi:10.1182/blood.2021012052

25. Koning MT, Trollmann IJM, Van Bergen CAM, et al. Peripheral IgE repertoires of healthy donors carry moderate mutation loads and do not overlap with other isotypes. *Front Immunol*. 2019;10(JULY):1-8. doi:10.3389/fimmu.2019.01543

26. Levin M, Levander F, Palmason R, Greiff L, Ohlin M. Antibody-encoding repertoires of bone marrow and peripheral blood- a focus on IgE. *J Allergy Clin Immunol*. 2017;3(139):1026-1030.

27. Koers J, Derksen N, Falkenburg W, et al. Elevated Fab glycosylation of anti-hinge antibodies. *Scand J Rheumatol*. 2021;00(00):1-8. doi:10.1080/03009742.2021.1986959

28. van de Bovenkamp FS, Hafkenscheid L, Rispens T, Rombouts Y. The Emerging Importance of IgG Fab Glycosylation in Immunity. *J Immunol*. 2016;196(4):1435-1441. doi:10.4049/jimmunol.1502136

29. Vergoessen R, Slot L, Hafkenscheid L, et al. B-cell receptor sequencing of anti-citrullinated protein antibody (ACPA) IgG-expressing B cells indicates a selective advantage for the introduction of N-glycosylation sites during somatic hypermutation. *Ann Rheum Dis*. 2018;77(6):955-958.

30. Koneczny I, Stevens JAA, De Rosa A, et al. IgG4 autoantibodies against muscle-specific kinase undergo Fab-arm exchange in myasthenia gravis patients. *J Autoimmun*. 2017;77:104-115. doi:10.1016/j.jaut.2016.11.005

31. Kissel T, Hafkenscheid L, Wesemael TJ, et al. ACPA-IgG variable domain glycosylation increases before the onset of rheumatoid arthritis and stabilizes thereafter; a cross-sectional study encompassing over 1500 samples. 2021.

32. Borges LS, Richman DP. Muscle-Specific Kinase Myasthenia Gravis. *Front Immunol*. 2020;11(May):1-11. doi:10.3389/fimmu.2020.00707

33. Futei Y, Amagai M, Ishii K, Kuroda-Kinoshita K, Ohya K, Nishikawa T. Predominant IgG4 subclass in autoantibodies of pemphigus vulgaris and foliaceus. *J Dermatol Sci*. 2001;26(1):55-61. doi:10.1016/S0923-1811(00)00158-4

34. Lundström SL, Fernes-Cerqueira C, Ytterberg AJ, et al. IgG antibodies to cyclic citrullinated peptides exhibit profiles specific in terms of IgG subclasses, Fc-glycans and a fab- Peptide sequence. *PLoS One*. 2014;9(11):1-22. doi:10.1371/journal.pone.0113924

35. Chapuy-Regaud S, Nogueira L, Clavel C, Sebbag M, Vincent C, Serre G. IgG subclass distribution of the rheumatoid arthritis-specific autoantibodies to citrullinated fibrin. *Clin Exp Immunol*. 2005;139(3):542-550. doi:10.1111/j.1365-2249.2004.02708.x

36. Grinde B. Herpesviruses: latency and reactivation ? viral strategies and host response. *J Oral Microbiol*. 2013;(5).

37. Scheid JF, Mouquet H, Ueberheide B, et al. Sequence and structural convergence of broad and potent HIV antibodies that mimic CD4 binding. *Science*. 2011;333(6049):1633-1637. doi:10.1126/science.1207227

38. Chuang GY, Asokan M, Ivleva VB, et al. Removal of variable domain N-linked glycosylation as a means to improve the homogeneity of HIV-1 broadly neutralizing antibodies. *MAbs*. 2020;12(1):1-12. doi:10.1080/19420862.2020.1836719

39. Wright A, Tao M, Kabat EA, Morrison SL. Antibody variable region glycosylation : position effects on antigen binding and carbohydrate structure. *EMBO*. 1991;10(10):2717-2723.

40. Coloma MJ, Trinh RK, Martinez AR, Morrison SL. Position Effects of Variable Region Carbohydrate on the Affinity and In Vivo Behavior of an Anti-(1 → 6) Dextran Antibody. 2018.

41. Goletz, SA, Czyk, D, Stoeckl L. Fab-glycosylated antibodies. Patent WO 2012/020065. 2012.

42. Courtois F, Agrawal NJ, Lauer TM, Trout BL. Rational design of therapeutic mAbs against aggregation through protein engineering and incorporation of glycosylation motifs applied to bevacizumab. *MAbs*. 2016;8(1):99-112. doi:10.1080/19420862.2015.1112477

43. Middaugh CR, Litman GW. Atypical glycosylation of an IgG monoclonal cryoimmunoglobulin. *J Biol Chem*. 1987;262(8):3671-3673.

44. van de Bovenkamp F, Derksen N, van Breemen M, et al. Variable Domain N -linked glycans acquired During antigen-specific immune responses can contribute to immunoglobulin g antibody stability. *Front Immunol*. 2018;9(April):1-9. doi:10.3389/fimmu.2018.00740

45. Schneider D, Dühren-von Minden M, Alkhatib A, et al. Lectins from opportunistic bacteria interact with acquired variable-region glycans of surface immunoglobulin in follicular lymphoma. *Blood*. 2015;125(21):3287-3296. doi:10.1182/blood-2014-11-609404

46. Wong KL, Li Z, Ma F, et al. SM03, an Anti-CD22 Antibody, Converts Cis-to-Trans Ligand Binding of CD22 against α2,6-Linked Sialic Acid Glycans and Immunomodulates Systemic Autoimmune Diseases. *J Immunol*. 2022. doi:10.4049/jimmunol.2100820

47. Koneczny I. Update on IgG4-mediated autoimmune diseases: New insights and new family members. *Autoimmun Rev*. 2020;19(10):102646. doi:10.1016/j.autrev.2020.102646

48. Huijbers MG, Plomp JJ, van der Maarel SM, Verschuuren JJ. IgG4-mediated autoimmune diseases: a niche of antibody-mediated disorders. *Ann N Y Acad Sci*. 2018;1413(1):92-103. doi:10.1111/nyas.13561

49. Ludwig RJ, Vanhoorelbeke K, Leypoldt F, et al. Mechanisms of autoantibody-induced pathology. *Front Immunol*. 2017;8(MAY). doi:10.3389/fimmu.2017.00603

50. Haddad G, Lorenzen JM, Ma H, et al. Altered glycosylation of IgG4 promotes lectin complement pathway activation in anti-PLA2R1-associated membranous nephropathy. *J Clin Invest*. 2021;131(5):1-16. doi:10.1172/JCI140453

51. Culver EL, van de Bovenkamp FS, Derksen NIL, et al. Unique patterns of glycosylation in IgG4-related disease and primary sclerosing cholangitis. *J gastroentol Hepatol*. 2018. doi:10.1111/jgh.14512

52. Hafkenscheid L, de Moel E, Smolik I, et al. N-Linked Glycans in the Variable Domain of IgG Anti–Citrullinated Protein Antibodies Predict the Development of Rheumatoid Arthritis. *Arthritis Rheumatol*. 2019;71(10):1626-1633. doi:10.1002/art.40920

53. Levin M, Levander F, Palmason R, Greiff L, Ohlin M. Antibody-encoding repertoires of bone marrow and peripheral blood—a focus on IgE. *J Allergy Clin Immunol*. 2017;139(3):1026-1030. doi:10.1016/j.jaci.2016.06.040

54. Robb NC, Taylor JM, Kent A, et al. Rapid functionalisation and detection of viruses via a novel Ca2+-mediated virus-DNA interaction. *Sci Rep*. 2019;9(1):1-13. doi:10.1038/s41598-019-52759-5

55. Joonaki E, Hassanpouryouzband A, Heldt CL, Oluwatoyin A. Surface Chemistry Can Unlock Drivers of Surface Stability of SARS-CoV-2 in a Variety of Environmental Conditions. *Ann Oncol*. 2020;19-21.

56. Meltzer RH, Thompson E, Soman K V., et al. Electrostatic steering at acetylcholine binding sites. *Biophys J*. 2006;91(4):1302-1314. doi:10.1529/biophysj.106.081463

57. Fichtner ML, Vieni C, Redler RL, et al. Affinity maturation is required for pathogenic monovalent IgG4 autoantibody development in myasthenia gravis. *J Exp Med*. 2020;217(12). doi:10.1084/JEM.20200513

58. Jacobs BC, Rothbarth PH, van der Meché FGA, et al. The spectrum of antecedent infections in Guillain-Barré syndrome. *Neurology*. 1998;51(4):1110 LP - 1115. doi:10.1212/WNL.51.4.1110

59. Aminov R. Editorial : Microbial and Environmental Factors in autoimmune and inflammatory diseases. 2017;8(March):6-8. doi:10.3389/fimmu.2017.00243

60. Smatti MK, Cyprian FS, Gheyath KN, Almishal RO, Yassine HM. Viruses and Autoimmunity: A Review on the Potential Interaction and Molecular Mechanisms Maria. 2019;(Figure 1):1-18.

61. Bjornevik K, Cortese M, Healy BC, et al. Longitudinal analysis reveals high prevalence of Epstein-Barr virus associated with multiple sclerosis. *Science (80-).* 2022;375(6578):296-301. doi:10.1126/science.abj8222

SUPPLEMENTARY MATERIAL

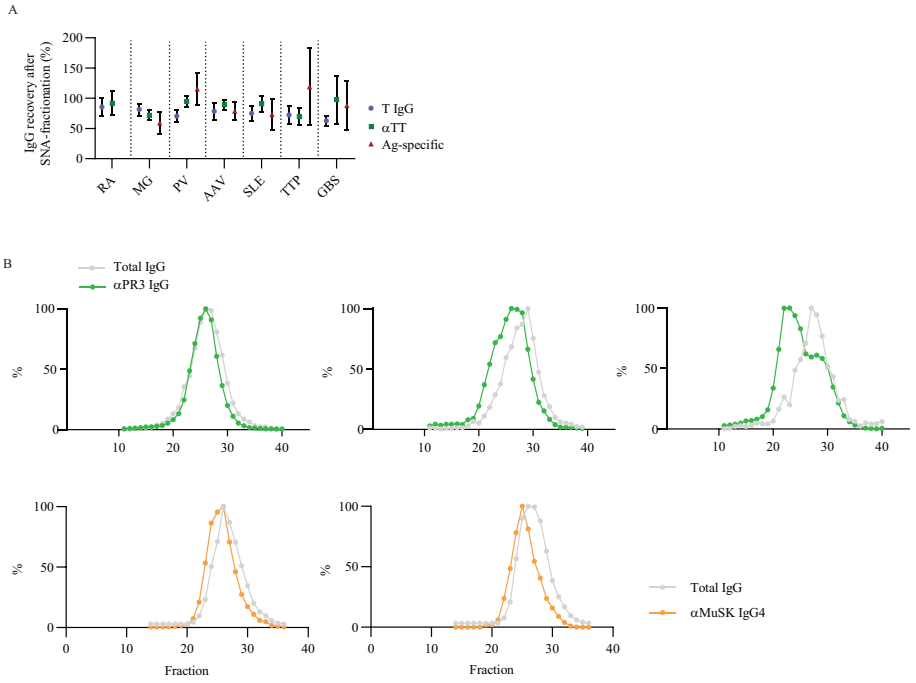

Figure S1. ***(A)*** *Recovery of IgG after SNA fractionation. Graph shows the recovered percentage of IgG in T IgG ELISAs, TT ABTs and antigen-specific assays per disease. The recovery was calculated as the percentage of IgG found by adding up the level of IgG detected in the SNA- and SNA+ fractions and comparing that to the level of IgG detected in the non-fractionated sera. The average recovery across the disease cohorts was about 75% for T IgG, 87% for TT ABT, and 89% for the antigen-specific assays.* ***(B)*** *Size-exclusion chromatography confirmed the presence of (differentially) Fab glycosylated disease-associated autoantibodies in AAV (αPR3, Green) and MuSK MG (αMuSK, Orange). Patient serum fractionation by gel filtration chromatography, followed by ELISA detection, shows that ag-specific IgG from patients with high and moderate SNA binding profiles elute earlier than the bulk of total IgG molecules seen as a shift to the left. IgG autoantibodies with low SNA binding profiles do not show this shift and co-elute with total IgG.*

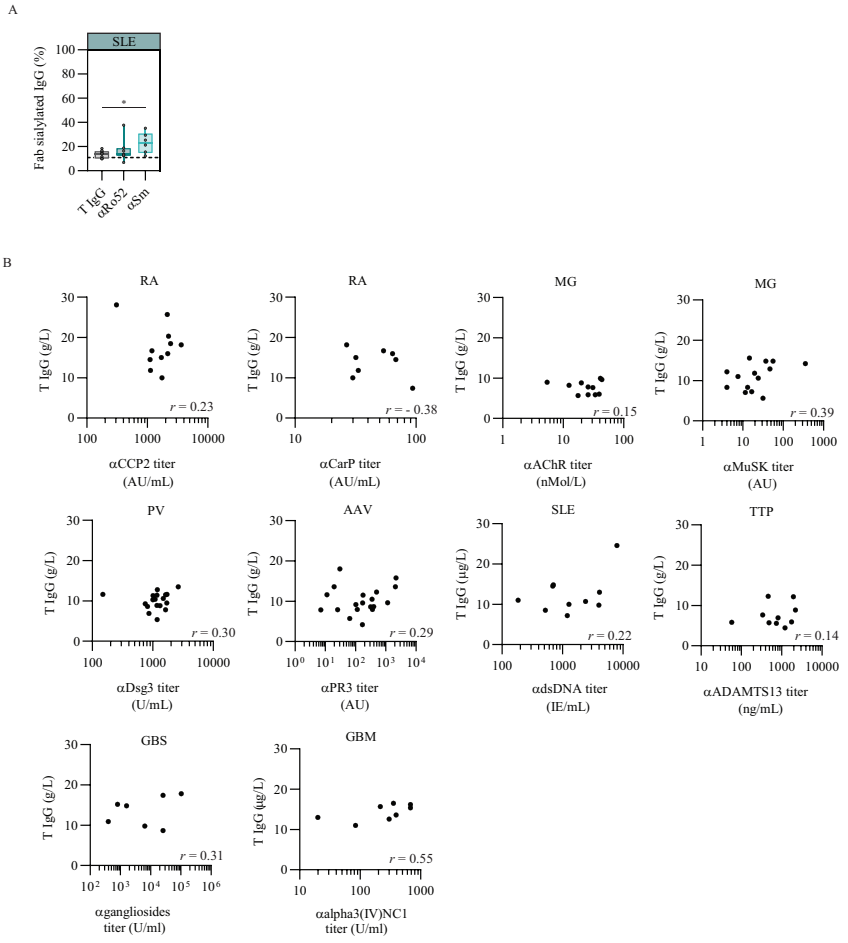

Figure S2. ***(A)*** *Percentage of Fab sialylated total (T) IgG, anti-Ro52 (n = 7) and anti-Sm (n = 6) antibodies in anti-dsDNA seropositive systemic lupus erythematosus (SLE) patients shown in figure 1C. Dashed line represents the median for Fab glycosylation of T IgG in healthy donor sera (11%, IQR 11-14%, n = 18). Box-plots show median and IQR. Statistical differences were determined using a paired t-test. * p < 0.05.* ***(B)*** *Correlation between total IgG and antigen-specific IgG titers. Spearman rank correlation coefficients (r) are represented at the right side of each graph. None of the correlations showed to be significant.*

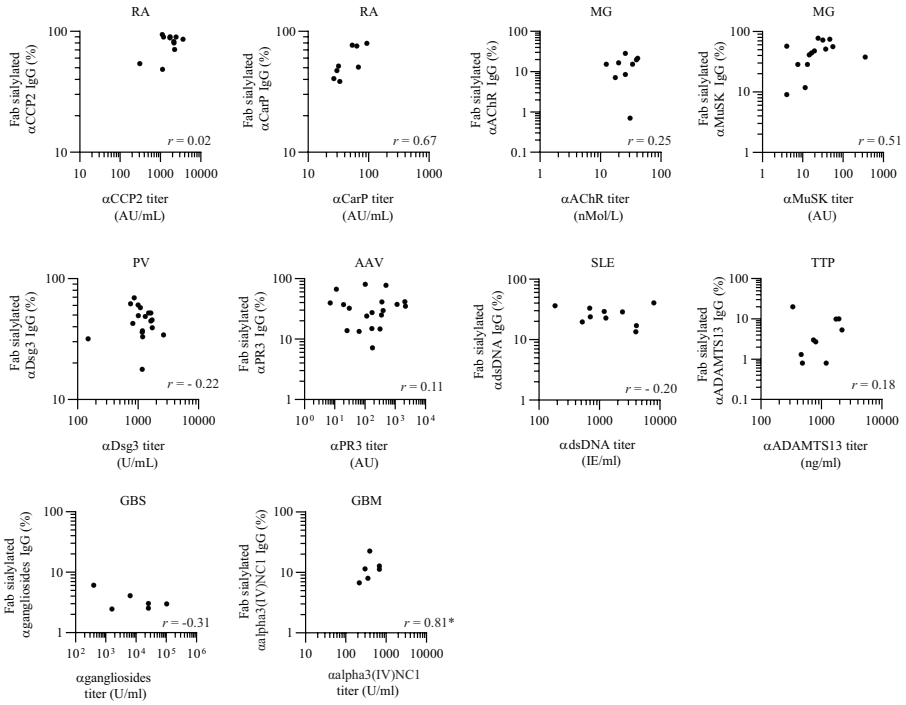

Figure S3. Correlation between the percentage of antigen-specific Fab glycosylated IgG and antigen-specific IgG titers. *Spearman rank correlation coefficients (r) are represented at the right side of each graph. None of the correlations, except for GBM, showed to be significant.*

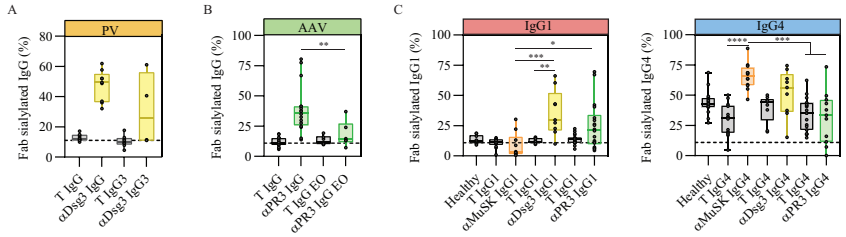

Figure S4. ***(A)*** *Fab glycosylation levels for anti-Dsg3 IgG3 in PV (n = 3).* ***(B)*** *Fab glycosylation levels for anti-PR3 in early onset AAV patients (EO, n = 6) versus established AAV patients (n = 16).* ***(C)*** *Comparison of Fab glycosylation levels for anti-MuSK, anti-Dsg3 and anti-PR3 IgG1 and IgG4. Box-plots show median and IQR. Statistical differences were determined using a Kruskal-Wallis ANOVA and Dunn's multiple comparison test. * p < 0.05, ** p < 0.01, *** p < 0.001, **** p < 0.0001.*

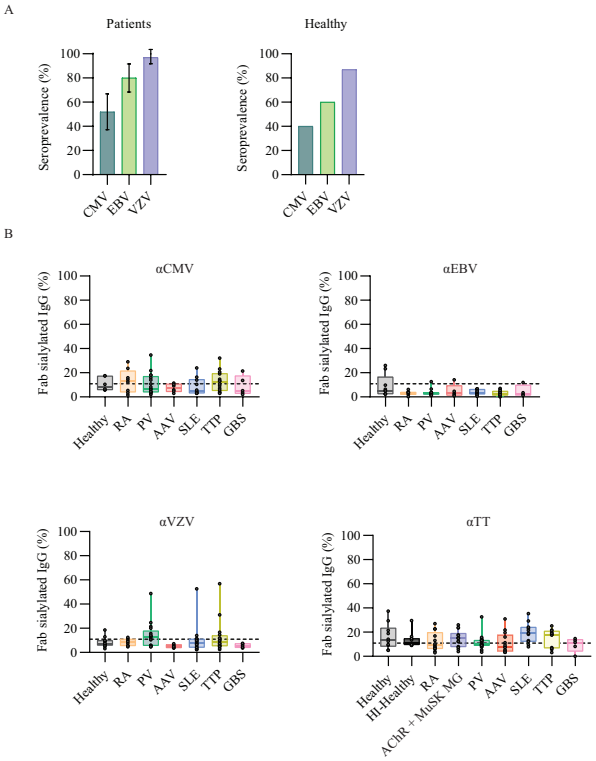

Figure S5. IgG Fab glycosylation levels after chronic and acute viral antigen exposure. *(**A**) Seroprevalence of CMV/EBV/VZV infections amongst the included autoimmune patients (n = 69) and healthy controls (n = 15). (**B**) Percentage of Fab sialylated antigen-specific IgG for TT, CMV, EBV, and VZV shown for healthy controls and separately for each autoimmune disease. Box-plots show median and IQR. Statistical differences were determined using a Kruskal-Wallis ANOVA and Dunn's multiple comparison test.*

METHODS

Patients with rheumatoid arthritis (RA)

This study included twelve patients with RA refractory to disease-modifying antirheumatic drugs that were also included in a previous study[1]. All patients had active disease at baseline (median at baseline 3.60 DAS [range 2.17–5.23]) and a median disease duration of 14 years (IQR 3-53). All patients were confirmed ACPA IgG positive. The study protocol was approved by the Ethics Committee of the Leiden University Medical Center.

Patients with AChR and MuSK myasthenia gravis (MG)

The patients with AChR MG participated in a single-center, prospective, placebo-controlled tetanus toxoid vaccination study at the Leiden University Medical Centre. Inclusion criteria were a confirmed diagnosis of MG or LEMS, age between 18 and 65 years and stable disease during 3 months before participation. Patients continued their medication during the study. A maximum daily dose of 30 mg of prednisolone (+/- 5 mg) was allowed as well as the use of other immunosuppressive medication[2]. Baseline samples, thus pre-treatment, were included in this study. The MuSK MG patients participated in a Biobank study and donated serum at the moment of consultations for regular care at the Neurology outpatient clinic. Both studies were approved by Medical Ethics Committee of the Leiden University Medical Centre.

Patients with pemphigus vulgaris (PV)

Patients' sera were obtained from the diagnostic biobank of the Center for Blistering diseases in the University Medical Center of Groningen, a tertiary referral center in the Netherlands. Diagnosis of pemphigus vulgaris was made according to the golden standard; classical clinical and histological features and deposition of IgG, complement component 3, or both on the epidermal cell surface[3]. Sera of nine patients with active disease were included. Clinical endpoints were defined according international consensus[4]. The Medical Research Involving Human Subjects Act does not apply to this type of non-interventional study with leftover materials for diagnostic purposes.

Patients with PR3-ANCA-associated vasculitis (AAV)

Twenty-two active AAV patients were included (54.5% female, median age 56 year [IQR 22-77]) and one patient was included twice during two consecutive relapses with 3.4 years in between. All patients were confirmed anti-PR3 IgG positive. Six patients were included at first onset of disease and 15 patients during a first or second relapse. Median disease duration of relapsing patients was 14,6 years [IQR 2.2–24.5]. The study was approved by the METc of the University Medical Center Groningen (METc 2012/151).

Patients with systemic lupus erythematosus (SLE)

Ten active SLE patients (70% female, median age 41 years [IQR 21-53]) were included that were previously collected at the UMCG. All patients had active disease at baseline (median SLEDAI of 11 [IQR 6–20]) and a median disease duration of 110 months [IQR 0–556]. Nine patients had increased anti-dsDNA antibodies, and seven decreased complement. Five patients did not use any medication, one patient only hydroxychloroquine, three patients the combination of mycofenolate mofetil, prednisolone and hydroxychloroquine and one patient used azathioprine, prednisolone and hydroxychloroquine. The Medical Research Involving Human Subjects Act does not apply to this type of non-interventional study with leftover materials for diagnostic purposes. The study was locally registered (UMCG research register 201600591).

Patients with thrombotic thrombocytopenic purpura (TTP)

Patients' sera were obtained from the French Reference Center for Thrombotic Microangiopathies, CNR-MAT (Paris, France), from nine patients in the acute phase of iTTP disease onset (first bout of disease), before treatments. All patients were initially clinically diagnosed with a Microangiopathic Hemolytic Anemia without any apparent cause, and all had a profound thrombocytopenia (< 30 G/L) and mild renal involvement (serum creatinine < 2.25 mg/dL) (French Clinical Score[5] = 2). All patients had ADAMTS13 < 10% (FRETS-VWF73) and detectable autoantibodies against ADAMTS13 in varying titers (> 15 IU/ml), confirming the iTTP diagnosis. These patients were described previously[6]. The study was approved by the Ethics Committee of Hôpital Pitié-Salpêtrière and Hôpital Saint-Antoine (Assistance Publique-Hôpitaux de Paris, France).

Patients with Guillain-Barré syndrome (GBS)

The GBS patients included in this study participated in the multicenter and randomized-controlled Second Immunoglobulin Dose (SID)-GBS trial[7]. Ten patients were selected for the presence of anti-ganglioside antibodies and availability of serum samples before treatment with intravenous immunoglobulins (IVIg). These patients had active disease (median GBS disability score 4 [IQR 1-4]) and serum samples were taken within two weeks after the onset of weakness. After SNA fractionation, two patients had non-detectible anti-ganglioside levels and were excluded. The study was approved by the IRB of the Erasmus MC (MEC-2009-368) and the local participating centers.

Patients with anti-glomerular basement membrane (anti-GBM) glomerulonephritis

Eight patients with acute anti-GBM GN were included. Median age was 49 years [IQR 30-65] and 37.5% was female. This is a monophasic illness, therefore all patients were at start of disease. The study was approved by the METc of the University Medical Center Groningen (METc 2015/088).

Individuals infected with HIV

Serum samples were obtained from HIV seropositive individuals who enrolled in the Amsterdam Cohort Studies (ACS). Included individuals were infected with HIV for >2 years and treatment-naive at the time of serum collection. The Medical Research Involving Human Subjects Act does not apply to this type of non-interventional study with anonymized leftover materials.

Individuals infected with SARS-CoV-2

Plasma samples were obtained from RT-PCR-positive SARS-CoV-2 recovered adults who enrolled in the convalescent plasma (CCP) program at Sanquin Blood Bank (Amsterdam, the Netherlands)[8]. Donors were included if tested positive in a SARS-CoV-2 PCR, which during this period was only provided to individuals presenting COVID-19-related symptoms, and were symptom-free for at least 2 weeks. These donors were infected with the original Wuhan-Hu-1 strain of the SARS-CoV-2 virus and were not previously vaccinated. Approval was granted by the Ethics Advisory Council of Sanquin Blood Supply Foundation.

Healthy controls

Healthy donor serum samples were collected as part of a previous study from anonymous, healthy volunteers[9].

Lectin (SNA) affinity chromatography

SNA affinity chromatography was performed as described previously[10]. Serum samples (~30µl) were diluted 8.6x in Tris-buffered saline (TBS, 10 mM Tris, 140 mM NaCl, pH 7.4) and applied over a column containing 1 ml of Sambucus nigra agglutinin (SNA) agarose (Vector Laboratories) using the ÄKTAprime plus system (GE Healthcare) at 0.2 ml/min. Flow through with unbound proteins (SNA depleted) in TBS and eluted bound protein (SNA enriched) in 0.5 M lactose in 0.2 M acetic acid were collected in 0.5 ml fractions at 0.8 ml/min. SNA- and SNA+ fraction were pooled separately and dialyzed against PBS overnight at 4°C. After SNA affinity chromatography serum was diluted ~330x in SNA+ fractions (end volume ~10mL) and ~150x in SNA- fractions (end volume ~4.5mL). For some antigen-specific assays, described in more detail below, it was necessary to concentrate the SNA fractions by ultrafiltration prior to measurements. Immunoassay detection values were corrected for the dilution (and concentration) factors. Samples that after concentration had values still below the assays detection limit were excluded from the study. The antibody recovery after SNA fractionation was on average 75% (**Figure S1A**). Using this method, we found 11% [IQR:10-14%] Fab glycosylation for IgG in healthy donors, which is consistent with previously described percentages obtained by using the same[10–13] or other methods[14].

Calculation of percentage of Fab sialylation

To determine the level of Fab glycosylation, SNA+ and SNA- fractions were measured in total IgG and autoantigen-specific assays, described below. The percentage of Fab sialylated antibodies was calculated by dividing the amount of (antigen-specific) IgG detected in the SNA+ fraction by the combined amount of (antigen-specific) IgG detected in the SNA+ and SNA- fractions (formula depicted in **Figure 1A**).

Antigen-specific Immunoassays

Disease-associated autoantibodies were measured in previously established quantitative antigen-specific assays, each described in more detail below. If necessary, antigen-specific immunoassay were optimized to facilitate measurements of SNA fraction. Autoantibodies were first measured in the non-fractionated sera to provide insight in the dilution range that needed to be tested per patient for both SNA fractions. For all selected samples, parallelism to the calibrator was investigated by testing multiple dilutions. No substantial non-parallelism was observed and autoantibody levels were calculated relative to a calibrator of a reference serum/monoclonal antibody present on every plate.

Detection of CCP2 antibodies

CCP2 IgG was determined by ELISA as described previously[15]. In short, Microcoat streptavidin microplates-high capacity plates were coated with biotinylated CCP-2 citrullin peptide (1µg/ml) diluted in PBS supplemented with 0.1% bovine serum albumin (BSA) for 1 h at RT. Next, serum samples diluted 50-fold in PBS/1% BSA/0.05% Tween 20 were incubated for 1 h at 37°C. CCP2 IgG was detected using rabbit anti-human IgG-HRP (diluted 1:5000, P0214; Dako, Glostrup, Denmark). Plates were developed using 2,2'-azino-bis(3-ethylbenothiazoline-6-sulfonicacid) (ABTS) mixed with 0.05% H2O2. OD values were measured using an ELISA reader at 415 nm. CCP2 IgG subclasses were measured as described previously[16–18], with minor adaptations. Briefly, plates were coated with CCP2-cittruline or CCP2-arginine (1 µg/ml) for 1 h at RT and serum samples were incubated for 1 h at 37 °C. For detection of CCP2 IgG1 mouse-anti-human (MAH)-IgG1-HRP (Life Technologies, A10648, Clone HP6069) was used and CCP2 IgG4 was detected using MAH-IgG4 (Life Technologies, A10654, Clone HP6025) and CCP2 IgG3 was detected using MAH-IgG3 (Nordic MUbio, Clone HP6080) followed by HRP-conjugated GAM-Ig (DAKO, P0447) and rabbit-anti-goat (RAG)-Ig (DAKO, P0449). Plate development and absorbance measurements were performed similar to CCP2 IgG.

Detection of CarP antibodies

Detection of CarP IgG antibodies was performed as described previously[19], with minor adaptions. In short, carbamylated fetal calf serum (CaFCS; 10 µg/ml) or non-modified FCS was coated on plates overnight at 4 °C. After blocking the plates for 6 hours on ice with PBA, serum samples were incubated overnight at 4°C. Serum was diluted in PTB and

incubated overnight on ice. CCP2 IgG was detected using rabbit anti-human IgG antibody (Dako) diluted in PTB incubated for 3.5 hours on ice. Antibodies were detected with goat anti-rabbit IgG-HRP (Dako) after incubation for 3.5 hours on ice. HRP enzyme activity was visualized using 2,2'-azino-bis(3-ethylbenothiazoline-6-sulfonicacid) (ABTS) mixed with 0.05% H2O2. OD values were measured using an ELISA reader at 415 nm. A pool of CarP positive sera were used as a reference and was included in each plate. CarP IgG subclasses were measured by ELISA as described previously[16,19], with minor adaptations. Coating and serum incubation steps were similar as described for CarP IgG. Detection of CarP IgG1 and IgG4 was performed using mouse anti-human (MAH)-IgG1-HRP (Life Technologies, A10648, Clone HP6069) or MAH-IgG4 (Life Technologies, A10654, Clone HP6025), followed by goat-anti-mouse (GAM)-Ig-HRP (DAKO, P0447). CarP IgG3 was detected using MAH-IgG3 (Nordic MUbio, Clone HP6080) followed by GAM-Ig-HRP (DAKO, P0447) and continued with rabbit-anti-goat (RAG)-Ig (DAKO, P0449). Plate development and absorbance measurements were performed similar to CarP IgG.

Detection of MuSK antibodies

MuSK antibodies were quantified using a MuSK ELISA as described previously[20] with some additional variations. Briefly, MaxiSorp plates (Thermo Fisher) were coated with recombinant MuSK (3µg/ml, full length extracellular protein) and MuSK specific IgG1, IgG4 or IgG were detected using mouse anti-human IgG1 (PeliClass), mouse anti-human IgG4 (Nordic MUbio) or rabbit-a-human IgG/AP (Jackson) respectively and a rabbit anti-mouse-AP (Dako) as secondary antibody. A standardized positive control was taken along for quantification. Plates were developed with pNPP (VWR). Samples were quantified using SoftMax pro (version 7.0.3, Molecular Devices).

Detection of AChR autoantibodies

AChR antibodies were measured using the AChRAb RIA kit (RSR limited, UK) according to the instructions of the manufacturer at the clinical chemical lab of the LUMC. This assay uses radiolabeled (125I-)AChR receptors to capture AChR antibodies.

Detection of Dsg3 autoantibodies

Dsg3 IgG antibodies were measured using the MESACUP™-2 TEST Desmoglein 3 ELISA kit (MBL, Tokyo, Japan). Samples were measured diluted 1:100, and adjusted if necessary to fall within the linear range for detection. Dsg3 IgG was detected using the anti-IgG conjugate provided by the ELISA kit according to manufacturer's instructions. For anti-Dsg3 subclass measurements we used HRP-conjugated monoclonal antibodies for IgG1 (HP6069), IgG3 (HP6050) and IgG4 (HP6025).

Detection of anti-PR3 antibodies

Levels of anti-PR3 IgG and subclasses were measured using an in-house ELISA as previously described[21,22] with minor alterations. Briefly, 96-well plates (Greiner Bio-One) were coated with goat anti-mouse IgG-Fc (1.3µg/ml, Jackson ImmunoResearch Laboratories Inc., West Grove, PA, USA) in 0.1M carbonate buffer pH 9.6 and incubated for at least 24 hrs at 4 °C. After washing, mouse anti-human PR3 (0.624µg/ml, Hycult Biotech) was added to the plates in 0.1M TRIS/HCL pH 8.0 containing 0.05% Tween-20, 0.3M NaC1, 2% BSA and 1% normal goat serum (incubation buffer) and incubated for 2hr at RT. After washing, plates were incubated overnight at 4 °C with an extract of azurophilic granules of normal human neutrophils in incubation buffer. Subsequently, plates were washed and serum or SNA fractions were diluted in PBT and incubated for 2hrs at RT. As standard a pool of positive patient sera was used. After washing, plates were blocked with 0.5% normal mouse serum in incubation buffer and incubated for 30 minutes at RT. Plates were washed and conjugates were added, for IgG goat anti-human IgG Fc-AP (1:1000), for IgG1 mouse anti-human IgG1 Fc-AP (1:1000), for IgG2 mouse anti-human IgG2 Fc-AP (1:500), for IgG3 mouse anti-human IgG3 Hinge-AP (1:1000) and for IgG4 mouse anti-human IgG4 Fc-AP (1:1000) (all from Southern Biotec) were diluted in incubation buffer and incubated for 1hr at RT. After washing, bound antibodies were detected with p-nitrophenyl-phosphate disodium and the reaction was stopped with 5M NaOH. The optical densities (OD) were read at 405 nm.

Detection of anti-dsDNA autoantibodies

Anti-dsDNA antibodies levels were determined in serum and SNA fractions by the Phadia200 using EliA dsDNA Well reagents (Thermo Fisher) that uses double-stranded plasmid DNA as antigen. Anti-dsDNA antibody levels were measured according to the manufactures protocol.

Detection of anti-Ro52 and anti-Sm autoantibodies

Anti-Ro52 and anti-SM antibodies levels were determined in serum and SNA fractions using the Milliplex human autoimmune autoantibody panel (Merck) in the Luminex platform using Ro52 and Sm antigen coupled beads. Anti-Ro52 and anti-SM antibody levels were measured according to the manufactures protocol.

Detection of ADAMTS13 autoantibodies

The ADAMTS13 antigen specific assay was performed as described previously[6]. Briefly, an in-house sandwich ELISA was developed where ADAMTS13 is captured using a mouse monoclonal antibody against the metalloprotease domain (antibody 3H9[23]), and the patient samples incubated against a recombinant wild-type ADAMTS13 in adequate dilutions. In parallel, a dilution curve is included within the plate as an internal control, using the human monoclonal antibody II-1 (anti-Spacer[24]). The signal for the sample is detected by means

of a 1:10000 mix of anti-human-IgG1-, 2-, 3- and 4-HRP conjugated antibodies (Sanquin Reagents, The Netherlands) followed by incubation with a TMB solution and the reaction was stopped using H2SO4 and absorbance was measured at 450 nm and 540 nm.

Detection of ganglioside antibodies

Anti-ganglioside antibodies were determined as previously described[25], with minor modifications. Half-area 96-well plates (Corning Life Sciences, Amsterdam, The Netherlands) were coated with 150 pmol glycolipid in ethanol per well. SNA fractions were tested 1:2 diluted in PBS supplemented with 1% BSA. For each sample the ΔOD490 nm was calculated by subtracting the OD of uncoated (i.e. ethanol only) wells from the glycolipid-coated wells. ΔOD490 nm were subsequently normalized to a positive control serum.

Detection of anti-GBM autoantibodies

anti-GBM antibody levels were determined by the Phadia ImmunoCAP 250 analyzer using EliA GBM Well reagents (Thermo Fisher) that uses the human recombinant α3 chain of collagen IV as antigen. Anti-GBM antibody levels were measured according to the manufactures protocol.

Tetanus Toxoid antigen binding test

Tetanus Toxoid (TT) antigen binding tests were performed as described previously[26]. In short, samples were diluted and antibodies were captured using protein G Sepharose (Thermo Fisher). TT specific antibodies were detected using radiolabeled (125I) TT and anti-TT antibody concentration was determined along a titration curve using a reference sample.

Detection of CMV, EBV, and VZV antibodies

Immunoglobulin G antibodies against CMV and EBV, and VZV were quantified in plasma by a multiplex immunoassay developed in-house[27–29]. CMV, strain AD 169, (40 µg/ml, Meridian Life Science), EBV-VCA (10 µg/ml, Microbix Biosystems), EBV-EBNA-1, (5 µg/ml, Meridian Life Science) and VZV strain VZ-10 (55 µg/ml, GenWay) were coupled to differently labeled carboxylated beads (12.5 × 106/ml; Luminex) that were chosen so that they were not directly adjacent to each other. Beads were incubated for 2 h at RT in the dark under constant rotation at 25 rpm and subsequently washed 3 times with PBS. The reference serum and control sera were prediluted in PBS containing 0.1% (vol/vol) Tween 20 and 3% (wt/vol) BSA). The reference, controls, and blanks were included on each plate. The reference was 3-fold serially diluted over 10 wells, and samples were measured in two dilutions (undiluted and 1/200 and 1/4,000). After the final washing step, beads were resuspended in 100 µl PBS and shaken before analysis in a Bio-Plex 200 instrument (Bio-Rad Laboratories) using Bio-Plex Manager (version 4.1.1) software (Bio-Rad) with

a 5-parameter fit. All data were transformed into international units per milliliter (IU/ml) using the international standard for every antigen. Seropositivity thresholds were adapted from previous studies[27,28,30], CMV >7.5 AU/ml, EBV ≥ 22 RU/ml, and VZV > 0.26 IU/ml.

HIV-1 envelop ELISA

Quantification of gp120 specific IgG responses was described previously and for the current study adopted to human serum samples. JRCSF gp120 protein production was performed as described previously[31–33]. In short, 96-well half-area microtiter plates (Greiner) were coated overnight with 2µg/ml recombinant JRCSF gp120 protein in PBS. After washing two times with 1x Tris-buffered saline (TBS, 20 mM Tris, 150 mM NaCl, pH 7.5) plates were blocked with 1% Casein in TBS (Thermo Fischer) and subsequently washed three times with TBS. Serum samples and SNA fractions were serially diluted in Casein/20% sheep sera and incubated for 2 h at RT. After washing three times with TBS, plates were incubated with 3.3µg/ml goat-anti-human-HRP in Casein for 1 h at RT and subsequently washed five times with TBS/0.05% Tween-20. Plates were developed using 0,1M NaAc + 0,1M citric acid + 1% TMB + 0,01% H_2O and the reaction was stopped using 0.8M H_2SO_4 and absorbance was measured at 450 nm. Signals were quantified using a serially diluted calibrator consisting of pooled convalescent plasma (ARP-3957, HIV reagent program) that was included on each plate.

SARS-CoV-2 S, RBD and N bridging assays

SARS-CoV-2 bridging assays are described elsewhere[8,34]. In brief, 96-well microtiter plates were coated overnight with recombinant S (1µg/ml), RBD (1µg/ml) or N (1µg/ml) in PBS at 4°C. Recombinant proteins were produced as described previously[35]. After washing five times with PBS-T, plasma samples were diluted 1200-fold in PBS-T supplemented with 0.2% gelatin (PTG) and incubated for 1 h at RT. Following washing, anti-human IgG MH16-1-HRP (0.5µg/ml, Sanquin) in PTG was incubated for 30 min at RT. Plates were developed using 75% 1-Step Ultra TMB-ELISA substrate (Thermo Fisher) in MilliQ, stopped with 0.2 M H2SO4 and absorbance was measured at 450 nm and 540 nm. Signals were quantified using a serially diluted calibrator consisting of pooled convalescent plasma that was included on each plate. This calibrator was arbitrarily assigned a value of 100 AU/ml.

Gel filtration chromatography

Gel filtration chromatography was performed on ~50ul serum of PR3 and MuSK seropositive AAV and MG patients using fast liquid chromatography (ÄKTA, GE Helthcare) equipped with a Superdex 200 10/300 column (GE Healthcare). For each disease three serum samples were included with a low, moderate or high SNA binding profile established by SNA chromatography and ELISA. Sera were diluted in PBS and filtered using a 0.2uM filter and injected onto the FPLC system running at a flow rate of 1.0ml/min. Fractions of 250ul were

collected spanning the protein peak, detected by the UV detector at a wavelength of 280 nm. Chromatography fractions were analyzed by ELISA to determine total IgG (described below) and anti-PR3 IgG or anti-MuSK IgG4 levels (described above).

IgG ELISA

Total serum IgG was quantified using enzyme-linked immunosorbent assays as described previously[10]. Briefly, 96-well microtiter plates (MaxiSorp, Nunc, Roskilde) were coated overnight with 2µg/ml monoclonal mouse anti-human IgG (MH16-1, Sanquin reagents) diluted in PBS. After washing with 0.02% PBS/Tween 20, samples, diluted in HPE buffer (Sanquin reagents), were incubated for 1h and washed with PBS-T. IgG was detected using 1µg/ml HRP-labeled MH16-1 (Sanquin reagents) in HPE buffer. Plates were developed using TMB substrate solution (Interchim, Montlucon Cedex) diluted in H_2O, stopped with 0.2M H_2SO_4. Absorbance was measured at 450 and 540 nm.

IgG1, IgG3 and IgG4 subclass ELISAs

Serum IgG1, IgG3 and IgG4 was quantified using 96-well microtiter plates coated overnight with monoclonal mouse anti-human IgG1 (2µg/ml, MH161-1, Sanquin reagents), IgG3 (2 µg/ml, MH163-1) or IgG4 (3.3µg/ml, MH164-4) diluted in PBS. After washing, serum was incubated for 1h and detected using 100µl/well HRP-conjugated polyclonal rabbit anti-human IgG (A18903, Novex) diluted 1:20.000 in HPE buffer containing 1% normal mouse serum. Subsequent steps of assay development and quantification were performed as described above for total IgG.

REFERENCES

1. Arthritis Rheumatism - 2007 - Teng - Immunohistochemical analysis as a means to predict responsiveness to rituximab (1).pdf.
2. Strijbos E, Huijbers MG, van Es IE, Alleman I, van Ostaijen-ten Dam MM, Bakker J, et al. A prospective, placebo controlled study on the humoral immune response to and safety of tetanus revaccination in myasthenia gravis. Vaccine [Internet]. 2017;35(46):6290–6. Available from: https://doi.org/10.1016/j.vaccine.2017.09.078
3. Acad Dermatol Venereol - 2020 - Joly - Updated S2K guidelines on the management of pemphigus vulgaris and foliaceus (1).pdf.
4. Murrell DF, Dick S, Ahmed AR, Amagia M, Barnadas MA, Borradori L, et al. Consensus statement on definitions of disease, end points, and therapeutic response for pemphigus. J Am Acad Dermatol. 2008;58(6):1043–6.
5. Coppo P, Schwarzinger M, Buffet M, Wynckel A, Clabault K, Presne C, et al. Predictive features of severe acquired ADAMTS13 deficiency in idiopathic thrombotic microangiopathies: The French TMA reference center experience. PLoS One. 2010;5(4).
6. Graça NAG, Ercig B, Pereira LCV, Kangro K, Kaijen P, Nicolaes GAF, et al. Modifying ADAMTS13 to modulate binding of pathogenic autoantibodies of patients with acquired thrombotic thrombocytopenic purpura. Haematologica. 2020;105(11):2619–30.
7. Walgaard C, Jacobs BC, Lingsma HF, Steyerberg EW, Van den Berg B, Doets AY, et al. Second intravenous immunoglobulin dose in patients with Guillain-Barré syndrome with poor prognosis (SID-GBS): a double-blind, randomised, placebo-controlled trial. Lancet Neurol. 2021;20(4):275–83.
8. Steenhuis M, van Mierlo G, Derksen NIL, Ooijevaar-de Heer P, Kruithof S, Loeff FL, et al. Dynamics of antibodies to SARS-CoV-2 in convalescent plasma donors. Clin Transl Immunol. 2021;10(5).
9. Pouw RB, Brouwer MC, Geissler J, Van Herpen L V., Zeerleder SS, Wuillemin WA, et al. Complement factor H-related protein 3 serum levels are low compared to factor H and mainly determined by gene copy number variation in CFHR3. PLoS One. 2016;11(3):1–13.
10. van de Bovenkamp FS, Derksen NIL, Ooievaar-de Heer P, van Schie KA, Kruithof S, Berkowska M, et al. Adaptive antibody diversification through N -linked glycosylation of the immunoglobulin variable region. Proc Natl Acad Sci U S A. 2018;115(8):1901–6.
11. Käsermann F, Boerema DJ, Rüegsegger M, Hofmann A, Wymann S, Zuercher AW, et al. Analysis and functional consequences of increased Fab-sialylation of intravenous immunoglobulin (IVIG) after lectin fractionation. PLoS One [Internet]. 2012 [cited 2017 Jan 26];7(6):e37243. Available from: http://www.ncbi.nlm.nih.gov/pubmed/22675478
12. Guhr T, Bloem J, Derksen NIL, Wuhrer M, Koenderman AHL, Aalberse RC, et al. Enrichment of sialylated IgG by lectin fractionation does not enhance the efficacy of immunoglobulin G in a murine model of immune thrombocytopenia. PLoS One. 2011;6(6):1–8.
13. Stadlmann J, Weber A, Pabst M, Anderle H, Kunert R, Ehrlich HJ, et al. A close look at human IgG sialylation and subclass distribution after lectin fractionation. Proteomics. 2009;9(17):4143–53.
14. Anumula KR. Quantitative glycan profiling of normal human plasma derived immunoglobulin and its fragments Fab and Fc. J Immunol Methods [Internet]. 2012;382(1–2):167–76. Available from: http://dx.doi.org/10.1016/j.jim.2012.05.022
15. Arthritis Rheumatism - 2007 - Verpoort - Fine specificity of the anti citrullinated protein antibody response is.pdf.

16. van Delft MAM, Verheul MK, Burgers LE, Derksen VFAM, van der Helm-van Mil AHM, van der Woude D, et al. The isotype and IgG subclass distribution of anti-carbamylated protein antibodies in rheumatoid arthritis patients. Arthritis Res Ther. 2017;19(1):1–12.

17. Arthritis Rheumatism - 2006 - Verpoort - Isotype distribution of ANTI CYCLIC citrullinated peptide antibodies in.pdf.

18. Van Der Woude D, Syversen SW, Van Der Voort EIH, Verpoort KN, Goll GL, Van Der Linden MPM, et al. The ACPA isotype profile reflects long-term radiographic progression in rheumatoid arthritis. Ann Rheum Dis. 2010;69(6):1110–6.

19. Shi J, Knevel R, Suwannalai P, Van Der Linden MP, Janssen GMC, Van Veelen PA, et al. Autoantibodies recognizing carbamylated proteins are present in sera of patients with rheumatoid arthritis and predict joint damage. Proc Natl Acad Sci U S A. 2011;108(42):17372–7.

20. Huijbers MG, Vink AFD, Niks EH, Westhuis RH, van Zwet EW, de Meel RH, et al. Longitudinal epitope mapping in MuSK myasthenia gravis: Implications for disease severity. J Neuroimmunol [Internet]. 2016;291:82–8. Available from: http://dx.doi.org/10.1016/j.jneuroim.2015.12.016

21. Vanderlocht J, van Beers JJBC, Limburg PC, Damoiseaux J, Roozendaal C. Antigen-specific detection of autoantibodies against myeloperoxidase (MPO) and proteinase 3 (PR3). Methods Mol Biol. 2019;1901:153–76.

22. Gueirard P, Delpech A, Gilbert D, Godin M, Loet X Le, Tron F. Anti-myeloperoxidase antibodies: Immunological characteristics and clinical associations. J Autoimmun. 1991;4(3):517–27.

23. Feys HB, Roodt J, Vandeputte N, Pareyn I, Lamprecht S, Van Rensburg WJ, et al. Thrombotic thrombocytopenic purpura directly linked with ADAMTS13 inhibition in the baboon (Papio ursinus). Blood. 2010;116(12):2005–10.

24. POS W, LUKEN BM, KREMER HOVINGA JA, TURENHOUT EAM, SCHEIFLINGER F, DONG JF, et al. VH1-69 germline encoded antibodies directed towards ADAMTS13 in patients with acquired thrombotic thrombocytopenic purpura. J Thromb Haemost. 2009;7:421–8.

25. Kuijf ML, Van Doorn PA, Tio-Gillen AP, Geleijns K, Ang CW, Hooijkaas H, et al. Diagnostic value of anti-GM1 ganglioside serology and validation of the INCAT-ELISA. J Neurol Sci. 2005;239(1):37–44.

26. van Schouwenburg PA, Bartelds GM, Hart MH, Aarden L, Wolbink GJ, Wouters D. A novel method for the detection of antibodies to adalimumab in the presence of drug reveals "hidden" immunogenicity in rheumatoid arthritis patients. J Immunol Methods [Internet]. 2010;362(1–2):82–8. Available from: http://dx.doi.org/10.1016/j.jim.2010.09.005

27. Tcherniaeva I, den Hartog G, Berbers G, van der Klis F. The development of a bead-based multiplex immunoassay for the detection of IgG antibodies to CMV and EBV. J Immunol Methods [Internet]. 2018;462(May):1–8. Available from: https://doi.org/10.1016/j.jim.2018.07.003

28. Samson LD, van den Berg SPH, Engelfriet P, Boots AMH, Hendriks M, de Rond LGH, et al. Limited effect of duration of CMV infection on adaptive immunity and frailty: insights from a 27-year-long longitudinal study. Clin Transl Immunol. 2020;9(10).

29. Smits GP, Van Gageldonk PG, Schouls LM, Van Der Klis FRM, Berbers GAM. Development of a bead-based multiplex immunoassay for simultaneous quantitative detection of IgG serum antibodies against measles, mumps, rubella, and varicella-zoster virus. Clin Vaccine Immunol. 2012;19(3):396–400.

30. Van Lier A, Smits G, Mollema L, Waaijenborg S, Berbers G, Van Der Klis F, et al. Varicella zoster virus infection occurs at a relatively young age in the Netherlands. Vaccine [Internet]. 2013;31(44):5127–33. Available from: http://dx.doi.org/10.1016/j.vaccine.2013.08.029

31. Sanders RW, van Gils MJ, Derking R, Sok D, Ketas TJ, Burger JA, et al. HIV-1 VACCINES. HIV-1 neutralizing antibodies induced by native-like envelope trimers. Science. 2015 Jul;349(6244):aac4223.

32. Sanders RW, Derking R, Cupo A, Julien J-P, Yasmeen A, de Val N, et al. A next-generation cleaved, soluble HIV-1 Env trimer, BG505 SOSIP.664 gp140, expresses multiple epitopes for broadly neutralizing but not non-neutralizing antibodies. PLoS Pathog. 2013 Sep;9(9):e1003618.

33. Torrents de la Peña A, de Taeye SW, Sliepen K, LaBranche CC, Burger JA, Schermer EE, et al. Immunogenicity in Rabbits of HIV-1 SOSIP Trimers from Clades A, B, and C, Given Individually, Sequentially, or in Combination. J Virol. 2018 Apr;92(8).

34. Vogelzang EH, Loeff FC, Derksen NIL, Kruithof S, Ooijevaar-de Heer P, van Mierlo G, et al. Development of a SARS-CoV-2 Total Antibody Assay and the Dynamics of Antibody Response over Time in Hospitalized and Nonhospitalized Patients with COVID-19. J Immunol. 2020;205(12):3491–9.

35. Larsen MD, de Graaf EL, Sonneveld ME, Plomp HR, Nouta J, Hoepel W, et al. Afucosylated IgG characterizes enveloped viral responses and correlates with COVID-19 severity. Science (80-). 2021;371(6532).

CHAPTER 8

Elevated Fab glycosylation of anti-hinge antibodies

Jana Koers, Ninotska I.L. Derksen, Willem J.J. Falkenburg, Pleuni Ooijevaar-de Heer, Michael T. Nurmohamed, Gerrit Jan Wolbink and Theo Rispens

Published in the Scandinavian Journal of Rheumatology (2021)

ABSTRACT

Rheumatoid arthritis (RA) is characterized by systemic inflammation and the presence of anti-citrullinated protein antibodies (ACPAs), which contain remarkably high levels of Fab glycosylation. Anti-hinge antibodies (AHAs) recognize IgG hinge neo-epitopes exposed following cleavage by inflammation-associated proteases, and are also frequently observed in RA, and with higher levels compared to healthy controls (HCs). Here, we investigated AHA specificity and levels of Fab glycosylation as potential immunological markers for RA. AHA serum levels, specificity and Fab glycosylation were determined for the IgG1/4-hinge cleaved by matrix metalloproteinase 3, cathepsin G, pepsin, or IdeS using ELISA and lectin affinity chromatography in patients with early active RA (n = 69) and HCs (n = 97). AHAs reactivity was detected for all hinge neo-epitopes in both RA and HCs. Reactivity against CatG-IgG1-F(ab')$_2$s and pepsin-IgG4-F(ab')$_2$s was more prevalent in RA. Moreover, all AHA responses showed increased Fab glycosylation levels in both RA and HCs. AHA responses are characterized by elevated levels of Fab glycosylation and highly specific neo-epitope recognition, not just in RA but also in HCs. These results suggest that extensive Fab glycosylation may develop in response to an inflammatory proteolytic microenvironment, but is not restricted to RA.

INTRODUCTION

Rheumatoid arthritis (RA) is a chronic inflammatory disorder marked by joint erosions. This state of chronic inflammation generates a plethora of neo-epitopes derived from inflammation-associated post-translational protein modifications that can be targeted by an assembly of autoantibodies known as the anti-modified protein antibodies (AMPAs). Of these, the anti-citrullinated protein antibodies (ACPAs) have been characterized extensively and are indicative for disease course, disease activity and treatment strategy[1]. ACPAs show cross-reactivity between different citrullinated proteins and peptides and a striking increase in Fab glycosylation (>90% versus 15-25% on total IgG)[2,3]. During inflammation and infection, endogenous (e.g. matrix-metalloproteinases (MMPs) and cathepsins) or exogenous proteases (e.g. IdeS, produced by infectious microbes) are abundantly expressed and able to cleave IgG at protease-specific locations within the hinge region into a $F(ab')_2$ and a Fc fragment[4,5]. Another AMPA, the anti-hinge antibodies (AHAs) specifically recognize neo-epitopes exposed in the hinge of proteolytically cleaved IgG molecules, which are absent in intact IgG[5,6]. AHAs are found more frequently in RA patients compared to HCs[7]. In particular, a predominant, subclass-specific reactivity for the pepsin/MMP7-cleaved IgG4 hinge was observed in a subset of RA patients, which was essentially absent in HCs[8,9]. Increased levels of several MMPs and cathepsins have been demonstrated in the synovial fluid of RA patients. However, AHA responses against IgG cleaved by RA-associated proteases MMP3 or cathepsin G have not been studied in RA. Furthermore, whether AHAs, like ACPAs, also have aberrant Fab glycosylation levels is unclear. Here, we studied AHA responses that may play a role in RA pathology and investigate their potential as immunological markers for RA. Therefore, levels and specificity of AHAs directed against inflammation (MMP3, Cathepsin G, pepsin) and infection (IdeS) related IgG hinge neo-epitopes and their levels of IgG Fab glycosylation were studied in patients with early active RA.

MATERIALS AND METHODS

Patients

In this study we included 69 baseline serum samples from individuals diagnosed with active early rheumatoid arthritis (RA) that were included in the "COBRA-light" trial[10]. These patients had not been treated with disease-modifying anti-rheumatic drugs during baseline sample collection. RA was diagnosed according to the 1987 criteria of the American College for Rheumatism[11]. To validate the increased reactivity for CatG-IgG1-$F(ab')_2$ in RA (**Figure 1C**) an additional RA cohort was measured composed of 100 baseline serum samples from consecutive RA patients with established disease with a median disease duration of 8 years (IQR, 3-16) and a mean disease activity score (DAS28) of 5.2[12]. These patients have not been treated with biologics but, in most cases, have been treated with

conventional anti-rheumatic drugs, such as methotrexate. Serum samples from 97 randomly selected healthy individuals were included in all measurements except for **Figure 1C**. Here, another 100 HCs were measured to validate CatG-IgG1-F(ab')$_2$ reactivity.

Ethical approval

RA patients gave written informed consent for use of serum samples and clinical data. No informed consent was obtained for the samples from the healthy controls, because materials used for this study were leftovers from samples taken for routine diagnostic purposes. HC materials were used anonymously without any connection to clinical or person-specific data.

Antibodies

The anti-biotin IgG1/IgG2/IgG3/IgG4 were generated in-house as described previously[13]. In brief, synthetic V_H and V_L DNA constructs were separately cloned into pcDNA3.1 expression vectors containing the corresponding constant domain gene segments, and cotransfected in HEK293F cells. After a 5-day incubation at 37°C in humidified 8% CO_2 antibodies were purified from culture supernatant using protein G Sepharose (ThermoFisher). For inhibition experiments we made use of therapeutic Abs adalimumab (IgG1, Humira, AbbVie) and natalizumab (IgG4, Tysabri, Biogen Idec International).

Generation of proteolytic cleaved F(ab')$_2$ fragments

IgG1 and IgG4 F(ab')$_2$ fragments yielded by proteolysis with either pepsin (isolated from porcine gastric mucosa, Sigma-Aldrich) or IdeS (*Streptococcus pyogenes*, FabRICATOR, Genovis) were generated as described previously[1]. Non-digested IgG was removed with a HiTrap protein G or A column. Purified F(ab')$_2$ fragments were dialyzed against PBS.

Generation of recombinant F(ab')$_2$ fragments

Besides proteolytic cleaved F(ab')$_2$ fragments also recombinant F(ab')$_2$ fragments were produced. Synthetic V_H and V_L DNA constructs were separately cloned into pcDNA3.1 expression vectors containing the corresponding constant CH1 and κ (light chain) domain gene segment, and cotransfected in HEK293F cells. After a 5-day incubation at 37°C in humidified 8% CO_2 F(ab')$_2$ fragments were purified from culture supernatant using α-κ Sepharose (Capture select, ThermoFisher). Fab byproducts were extracted from the purified F(ab')$_2$ fragments by use of size-exclusion chromatography (**Figure S1A**). Size and purity of all proteolytic cleaved and recombinant expressed F(ab')$_2$s were evaluated by gel electrophoresis (SDS-PAGE, **Figure S1B**) by loading 5 µg F(ab')$_2$s on precast 4-12% Bis-Tris gels (NuPAGE, ThermoFisher) and visualized with Coomassie Blue. When AHA reactivity for proteolytically cleaved IgG1-F(ab')$_2$s versus recombinantly expressed IgG1-F(ab')$_2$s of the same protease was compared in a group of 86 HCs reactivity was highly similar (**Figure S2**).

Synthetic peptides

Synthetic peptide analogs (pep) of the IgG1/4 lower hinge were designed from the C-terminal amino acids exposed by the protease (MMP3, CatG, pepsin or IdeS) up to 14 amino acids upstream. Synthetic peptides were ordered and produced at Genscript (**Table SI**) and dissolved in ultrapure H_2O and pH-adjusted to pH 7-8 using 4 M NaOH. In inhibition experiments peptides were pre-incubated with the serum samples for 1 hour before testing in the AHA ELISA or peptides were used as coating antigen in the AHA peptide ELISA.

AHA ELISA

Levels of serum AHAs in RA patients and HCs were measured as described previously[9]. To reduce assay background reactivity PBS/0.02% Tween-20 was replaced for High Performance ELISA (HPE) buffer (Sanquin Reagents) in the $F(ab')_2$, serum, and IgG-HRP incubation steps. Briefly, 96-well plates were coated with biotinylated human serum albumin (HSA-biotin) washed, and opsonized with either proteolytic cleaved or recombinant expressed anti-biotin $F(ab')_2$ fragments. After washing, plates were incubated with serum samples (diluted 1:400), washed and AHAs were detected using mouse anti-human IgG-HRP (MH16-1, Sanquin) and developed using TMB substrate. The reaction was stopped by addition of 0.2 M H_2SO_4 and absorbance was measured at 450 and 540 nm. AHA concentrations were calculated relative to a calibration curve of a reference serum showing high reactivity for pepsin-IgG1-$F(ab')_2$s (defined to contain 200 AU/ml[8]) present on every plate. This calibration curve was used for the AHA concentration determination of all studied AHA reactivities as we observed that all reactivities diluted equally. As calculated values are non-proportional they were expressed in arbitrary units per milliliter (AU/ml). For most subjects tested, a serum dilution of 1:400 gave AHA levels within the dynamic range of the assays. When necessary, samples were tested at higher dilutions to reach the dynamic range. The cut-off for AHA positivity was determined by inhibition experiments using a selection of sera including both positive and negative for a specific AHA reactivity as described before[9]. Cut-offs were set at the level where all positive sera were negative after inhibition. AHA ELISAs for the different AHAs had similar background reactivities, as expected, since $F(ab')_2$ targets are highly similar and only differ by a few amino acids. This resulted in a consistent cut-off value across all $F(ab')_2$ targets of 4 AU/ml. Individuals that showed high reactivity to the HSA-biotin coat were excluded from the data set (HC 1 sample; RA 4 samples). Reproducibility of the AHA ELISA is shown in **Figure S3** as example for anti-CatG-IgG1-$F(ab')_2$ reactivity in RA patients (r = 0.87****).

AHA peptide ELISA

To improve the specificity of the AHA ELISA we exchanged the anti-biotin $F(ab')_2$ fragments with biotinylated synthetic peptides (**Table SI**, Genscript). Streptavidin-coated ELISA plates (ThermoFisher) were pre-washed and opsonized with 0.1µg/ml biotinylated

synthetic peptide in PBS for 1 hour and washed. Subsequent sample incubation and detection are performed identical as described for the AHA ELISA above. For CatG-IgG1 and pepsin-IgG4 peptide ELISAs shown in **Figures 2B and C**, samples were diluted 1:400 in HPE enriched with 25µg/ml pepsin-cleaved adalimumab (IgG1) to prevent detection of cross-reactive pepsin-IgG1-AHAs. Detection and quantification were performed as described for the AHA ELISA above.

Detection of Fab glycosylation on AHAs

We analyzed the AHA Fab glycosylation levels for individuals that showed a moderate to high AHA level. Fab glycosylated AHAs were purified from serum as described previously[14], using *Sambucus nigra* agglutinin (SNA) affinity chromatography, which makes use of the fact that the SNA lectin enriches for Fab glycans, but not for Fc glycans, through their terminal 2,6-linked sialic acid residues. SNA affinity chromatography provides a good estimate for the level of Fab glycosylation as more than 90% of Fab glycans carry terminal sialic acid residues[14-18]. In brief, RA patient and HC serum samples were applied over a SNA column. The bound fraction of sialic acid containing proteins were eluted with 0.5 M lactose in 0.2 M acetic acid and dialyzed against PBS. In the AHA ELISA set-up, the percentages of Fab glycosylated AHAs were calculated by dividing the amount of AHAs in the SNA-enriched fraction by the amount of AHAs in the combined SNA-depleted and -enriched fractions. AHA concentrations in both SNA depleted and enriched fractions were determined using the calibration curve as described above for the AHA ELISA. As reference measurements also the levels of IgG Fab glycosylation for total IgG (pan-IgG) and anti-tetanus toxoid (TT), a typical vaccine antigen often detectable in the general population, were determined for all samples. To confirm the presence of Fab glycans size-exclusion chromatography was performed on sera that showed normal, moderate and high SNA-binding. Sera were fractionated using a HPLC (Agilent 1260 Infinity II) equipped with a Superdex 200 (GE Healthcare), and analyzed by ELISA to detect total IgG and AHAs using in-house protocols as described above and previously[14].

Statistical analysis

Differences between groups were analyzed with a Mann-Whitney U test or a Kruskal-Wallis test, and (non-parametric) correlations were analyzed with a Spearman rank correlation test. A p value < 0.05 was considered significant. The statistical analysis was carried out using Graphpad Prism 8.

RESULTS

Anti-hinge antibodies that target cathepsin G-IgG1-F(ab')$_2$s are more frequent and have higher levels in RA

We evaluated the level of AHA reactivity for a panel of IgG hinge neo-epitopes in baseline serum samples from 69 treatment-naïve consecutive RA patients with active disease (< 2 years)[10] and 97 HCs. To obtain a homogeneous fraction of F(ab')$_2$s with defined C termini, F(ab')$_2$s were recombinantly expressed with truncated hinge regions, representing IgG1 or IgG4 proteolytically cleaved by MMP3, CatG, pepsin, or IdeS (**Figure 1A**; **Figure S1A and B**)[5]. AHA reactivity for the RA-associated proteases MMP3- and CatG-IgG1-F(ab')$_2$s could be detected in both RA patients and HCs (**Figure 1B**). AHA reactivity was also observed for pepsin- and IdeS-IgG1/4-F(ab')$_2$s in line with previous results[9]. Reactivity against CatG-IgG1-F(ab')$_2$s was most frequent for both, but more prevalent in RA compared with HCs (57% vs 44%, fold diff. 1.3), and with significantly higher levels (p = 0.03). Pepsin-IgG4-

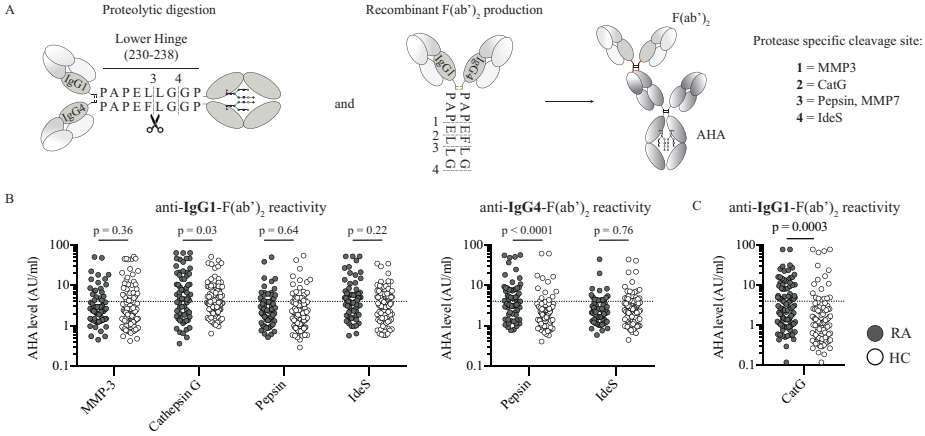

anti-**IgG1**-F(ab')$_2$ reactivity

AHA Reactivity	Cut-off 4 AU/ml % pos. RA	% pos. HC
MMP3	29	36
CatG	57	44
Pepsin	30	26
IdeS	51	44

anti-**IgG4**-F(ab')$_2$ reactivity

AHA Reactivity	Cut-off 4 AU/ml % pos. RA	% pos. HC
Pepsin	46	13
IdeS	23	25

anti-**IgG1**-F(ab')$_2$ reactivity

AHA Reactivity	Cut-off 4 AU/ml % pos. RA	% pos. HC
CatG validation	43	18

Figure 1. Presence and levels of anti-hinge reactivity in RA patients and HCs. *(**A**) Schematic representation of two alternative methods for F(ab')$_2$ generation. Amino acid sequences of IgG1 and IgG4 lower hinge regions with assigned cleavage sites for MMP3 (1), cathepsin G (2), pepsin/MMP-7 (3), and IdeS (4). (**B**) Scatterplots show levels of AHA reactivity against six different F(ab')$_2$ targets generated by four different proteases: MMP3-, CatG-, pepsin-, and IdeS-IgG1-F(ab')$_2$s and pepsin- and IdeS-IgG4-F(ab')$_2$s determined using the AHA ELISA in early RA patients (n = 69) and HCs (n = 97). (**C**) Scatter plot shows CatG-IgG1-F(ab')$_2$ reactivity in additional validation cohorts of established RA patients (n=100) and HCs (n=100). Dashed lines represent cut-off levels at 4 AU/ml for positivity. Differences in AHA levels between RA and HC were analyzed with a Mann-Whitney U test. Tables show the frequency of AHA positivity (% pos.) in early RA and HCs for the six different F(ab')$_2$ targets and for the CatG-IgG1 validation cohorts at a cut-off of 4 AU/ml.*

F(ab')$_2$ reactivity was also more prevalent in RA, as was observed previously. The increased AHA level and frequency for CatG-IgG1-F(ab')$_2$s in RA were validated in an additional cohort of established RA patients[11] and HCs (**Figure 1C**; $p = 0.0003$; fold diff. 2.4).

Anti-hinge antibodies are predominantly 'protease-restricted'

Next, we evaluated the specificity of AHAs targeting IgG hinge neo-epitopes. Pairwise comparisons of all AHA reactivities revealed that single positivity was found more frequently than double positivity (**Figure S4**).

Inhibition experiments were performed to more extensively evaluate the specificity of AHA responses in RA and HCs. With few exceptions, little to no inhibition of AHA binding was observed using either excess amounts of F(ab')$_2$s or single-chain hinge peptides with a non-identical C-terminus (**Figure 2A**, **Figure S5**, **Table SI**). By contrast, identity inhibitor(s) invariably showed strong inhibition. In some cases, cross-reactivity was observed between AHAs recognizing MMP3- and CatG-IgG1-F(ab')$_2$s, as well as between pepsin- and CatG-IgG1-F(ab')$_2$s. Also, some cross-reactivity was observed for the AHA response against pepsin-IgG1-F(ab')$_2$s versus pepsin-IgG4-F(ab')$_2$s in HCs.

As both CatG-IgG1 and pepsin-IgG4 reactivities are more prevalent in RA, we examined if a more RA-specific subset of these reactivities may be detected by performing the AHA ELISAs for both targets while including a pepsin-IgG1-F(ab')$_2$ inhibitor in a larger panel of subjects. For CatG-IgG1-F(ab')$_2$ reactivity (**Figure 2B**) we found little evidence for cross-reactivity in both HC and RA. On the other hand, for pepsin-IgG4-F(ab')$_2$s, we observed cross-reactivity in most HCs (5 out of 9) versus fewer in RA (5 out of 24; **Figure 2C**). We also compared neo-epitope reactivity to single-chain peptide versus double-chain F(ab')$_2$. We observed a moderate correlation for AHA binding to the peptide versus the F(ab')$_2$ in RA (CatG-IgG1: $r = 0.67$, $p < 0.0001$; pepsin-IgG4: $r = 0.61$, $p < 0.0001$; **Figure 2D and E**), and for HCs, correlation was weaker (CatG-IgG1: $r = 0.49$, $p < 0.0001$) or absent (pepsin-IgG4: $r = 0.17$, $p = 0.086$), indicating a qualitative difference in pepsin-IgG4 AHAs between HC and RA in addition to a quantitative difference.

Elevated levels of Fab glycosylation on anti-hinge antibodies

To estimate IgG Fab glycosylation levels on AHAs we fractionated sera from RA patients and HCs using *Sambucus nigra* agglutinin (SNA) affinity chromatography, making use of the fact that SNA enriches for Fab glycans, but not for Fc glycans, through their terminal 2,6-linked sialic acid residues found in >90% of Fab glycans[14-18], and determined the AHA IgG SNA-bound fraction by ELISA. A significant increase in IgG sialylation was observed across all AHA responses compared to reference total IgG (pan-IgG, RA 14%, HC 11%) and anti-tetanus toxoid (TT, RA 16%, HC 14%) with high inter-patient variability for most IgG hinge neo-epitopes (**Figure 3**). No significant difference was observed when AHA responses were compared between RA patients and HCs and AHA levels and IgG sialylation levels did not

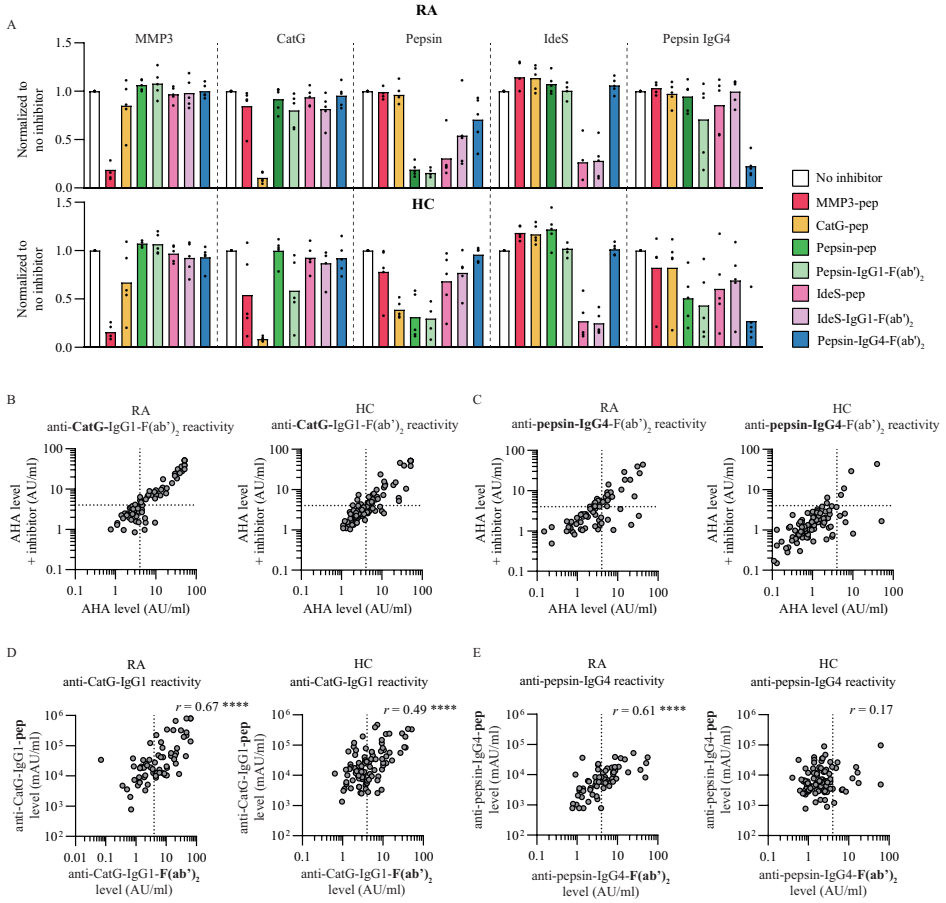

Figure 2. Specificity of anti-hinge antibody responses in RA and HCs. *(A) Specificity is determined for each reactivity (indicated above each panel) in 5 early RA patients (upper graph) and 5 HCs (bottom graph) with established positivity for the tested F(ab')$_2$ target. Serum is pre-incubated with excess amounts of synthetic peptides (pep, **Table SI**) or F(ab')$_2$s (generated by cleaving therapeutic antibodies [adalimumab, IgG1; natalizumab, IgG4] with pepsin or IdeS) and tested in the AHA ELISA. Obtained OD values were normalized to the situation without inhibitor. Bars indicate means of five samples. Inhibitors are generated from the IgG1 sequence unless stated otherwise in the legend. (**B**) Inhibition of AHA reactivity against CatG-IgG1-F(ab')$_2$ using pepsin-cleaved adalimumab (IgG1) in early RA patients (n = 69) and HCs (n = 97). (**C**) As in (B) but for pepsin-IgG4-F(ab')$_2$s reactivity. (**D**) AHA reactivity for CatG-IgG1-F(ab')$_2$s versus CatG-IgG1-pep in early RA patients (n = 69) and HCs (n = 97). (**E**) As in (D) but for anti-pepsin-IgG4 reactivity. Similarity for F(ab')$_2$ versus peptide reactivity was determined using the Spearman rank correlation coefficient (r); **** p < 0.0001.*

correlate (**Figure S6**). The presence of Fab glycans on AHAs was confirmed by size-exclusion chromatography and subsequent ELISA (**Figure S7**). Thus, elevated IgG Fab glycosylation is a hallmark of AHAs in both RA and HCs and was found to be increased for infection (IdeS) as well as for inflammation (MMP3, CatG, and pepsin) associated AHA responses.

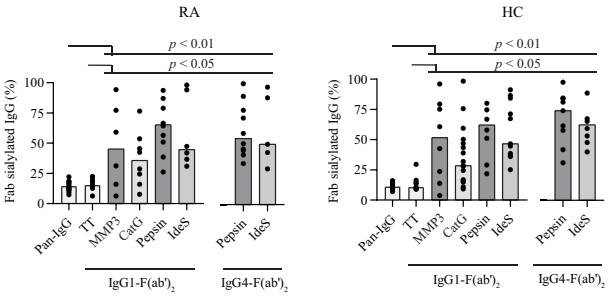

Figure 3. Levels of Fab glycosylation on anti-hinge antibodies in RA and HCs. *Graphs show the percentage of IgG Fab glycosylated antibodies for total IgG (pan-IgG), anti-tetanus toxoid (TT), and AHAs directed against the six different IgG1/4-F(ab')$_2$ targets for a total of 24 early RA patients and 27 HCs that tested seropositive for the respective F(ab')$_2$ target. SNA (lectin) affinity chromatography of serum results in a sialic acid positive fraction (enriched for Fab glycosylated IgG) and a sialic acid negative fraction (almost devoid of Fab glycosylated IgG)[14]. Specific and total IgG is measured in both fractions by AHA ELISA (Materials and Methods), TT antigen binding test, and IgG ELISA (as described previously[14]). For each reactivity >5 subjects were included and bars indicate medians. A Kruskal-Wallis test was performed for pan-IgG or TT versus all AHA reactivities.*

DISCUSSION

Here we explored the molecular characteristics of AHAs from RA patients compared with HCs. We found that both RA patients and HCs showed reactivity against all evaluated IgG-F(ab')$_2$s with rather restricted specificity and limited cross-reactivity with F(ab')$_2$s generated by different proteases. Reactivity against CatG-IgG1-F(ab')$_2$s and pepsin-IgG4-F(ab')$_2$s was found more frequently and with higher levels in RA. Strikingly, all AHA responses were characterized by elevated Fab glycosylation, not only in RA but also in HCs.

The higher frequency of CatG-IgG1-F(ab')$_2$s reactivity in RA might be explained by increased levels and activity of cathepsin G in the synovial fluid of these patients resulting in high levels of immunogenic CatG-cleaved IgG[19]. However, this was not observed for MMP3 of which levels and activity are also increased in RA. Differential AHA levels might be caused by a difference in immunogenicity towards the exposed hinge neo-epitope or the context in which these autoantibodies develop (e.g. severity of inflammation). To study the relation between AHA levels and disease activity (DAS28), associations with other autoantibodies or inflammation (CRP levels) and to differentiate patient subgroups a larger group of subjects will be necessary.

Besides higher frequencies and levels for both CatG-IgG1-F(ab')$_2$s and pepsin-IgG4-F(ab')$_2$s in RA, AHAs in RA also recognized these neo-epitopes with higher specificity as they showed less cross-reactivity with pepsin-IgG1-F(ab')$_2$s and were more efficient in recognizing the single-chain peptide, compared to AHAs in HCs. This suggests that AHAs in HCs do not solely recognize the neo-epitope and/or that the double-chain

conformation of the antibody C-terminus is crucial for epitope recognition. Thus, the AHAs produced by RA patients and HCs differ both quantitatively and qualitatively. Importantly, specific recognition of pepsin-IgG4-F(ab')$_2$s is rare in HCs which implies its potential as immunological marker for RA.

All AHA responses show elevated Fab glycosylation levels, albeit with high inter-patients variability and less elevated on average (55%) than observed for ACPAs, a prevalent autoantibody in RA with high levels of Fab glycans (>90%)[3]. For another prevalent autoantibody in RA, the rheumatoid factors (RFs), Fab glycosylation levels have not been determined. However, analysis of rheumatoid factor variable region sequences[20] revealed that most non-isotype switched sequences displayed few *N*-glycosylation sites and, although in limited number of sequences, also the switched sequences did not show aberrant levels of *N*-glycosylation sites (unpublished data). Importantly, elevation of AHA Fab glycosylation levels was not exclusively found in RA but to a similar degree in HCs. This suggests that selection for Fab glycosylated AHAs can occur in (chronic) inflammatory states independent of it being induced by infection or autoimmunity. As antibody responses can persist over time, elevated AHA Fab glycosylation can be a sign of active but also of previous inflammation, which would explain the observed elevation in HCs. The reason for certain (auto)antibody responses to acquire (elevated) Fab glycosylation remains incompletely understood. A proposed mechanism for selection of Fab glycan-expressing B cells involves the engagement of Fab glycosylated B cell receptors with glycan binding molecules, e.g. CD22 on the B cell surface which may modify the activation threshold of these B cells, leading to a selection advantage[21].

For most studied parameters we did not observe large differences between RA patients and HCs. Presumably, AHAs develop in response to IgG cleaved by proteases, which may be of bacterial or endogenous origin. In particular, (chronic) inflammation may induce a proteolytic microenvironment and one might speculate elevated Fab glycosylation to be a characteristic thereof, rather than an autoantibody-specific feature.

In conclusion, we have expanded the molecular characterization of the AHA repertoires in RA patients and HCs. Both Cathepsin G-cleaved IgG1 and pepsin-cleaved IgG4 anti-hinge responses were found more frequently and with higher levels in RA and since pepsin-cleaved IgG4 recognition was also more specific in RA, this response has the potential for being a immunological marker for disease. Furthermore, elevated IgG Fab glycosylation is a hallmark of anti-hinge antibodies in both RA patients and healthy controls. Future research should provide more insights in the contribution of the serological AHA status, combined with the presence of other AMPAs and disease activity, to provide the best information regarding diagnosis, prognosis and therapy efficacy in RA.

Author contributions

JK, WF, GW and TR designed research. JK, ND, PO and WF performed research. JK, ND, WF and TR analyzed data. JK, TR, GW and MN wrote the paper. All authors critically reviewed the manuscript, gave final approval of the version to be published, and agreed to be accountable for all aspects of the work ensuring that questions related to the accuracy or integrity of any part of the work are appropriately investigated and resolved.

Financial support

This study was supported by Landsteiner Foundation for Blood Transfusion (Grant1626).

Disclosure statement

The authors declare no commercial or financial conflicts of interest.

REFERENCES

1. Bugatti S, Manzo A, Montecucco C, Caporali R. The clinical value of autoantibodies in rheumatoid arthritis. *Front Med*. 2018;5:339.
2. Lloyd KA, Steen J, Amara K, Titcombe PJ, Israelsson L, Lundström SL, *et al*. Variable domain N-linked glycosylation and negative surface charge are key features of monoclonal ACPA: Implications for B-cell selection. *Eur J Immunol*. 2018;48:1030-45.
3. Rombouts Y, Willemze A, van Beers JJ, Shi J, Kerkman PF, van Toorn L, *et al*. Extensive glycosylation of ACPA-IgG variable domains modulates binding to citrullinated antigens in rheumatoid arthritis. *Ann Rheum Dis*. 2016;75:578-85.
4. Ribbens C, Martin y Porras M, Franchimont N, Kaiser MJ, Jaspar JM, Damas P, *et al*. Increased matrix metalloproteinase-3 serum levels in rheumatic diseases: Relationship with synovitis and steroid treatment. *Ann Rheum Dis*. 2002;61:161-6.
5. Ryan MH, Petrone D, Nemeth JF, Barnathan E, Björk L, Jordan RE. Proteolysis of purified IgGs by human and bacterial enzymes in vitro and the detection of specific proteolytic fragments of endogenous IgG in rheumatoid synovial fluid. *Mol Immunol*. 2008;45:1837-46.
6. Brezski RJ, Knight DM, Jordan RE. The Origins, Specificity, and Potential Biological Relevance of Human Anti-IgG Hinge Autoantibodies. *Sci World J*. 2011;11:1153-67.
7. Birdsall HH, Lidsky MD, Rossen RD. Anti-Fab' antibodies in rheumatoid arthritis. Measurements of the relative quantities incorporated in soluble immune complexes in sera and supernatants from cultured peripheral blood lymphocytes. *Arthritis Rheum*. 1983;26:1481-92.
8. Van De Stadt LA, De Vrieze H, Derksen NIL, Brouwer M, Wouters D, van Schaardenburg D, *et al*. Antibodies to IgG4 hinge can be found in rheumatoid arthritis patients during all stages of disease and may exacerbate chronic antibody-mediated inflammation. *Arthritis Rheumatol*. 2014;66:1133-40.
9. Falkenburg WJJ, van Schaardenburg D, Ooijevaar-de Heer P, Tsang-A-Sjoe MW, Bultink IE, Voskuyl AE, *et al*. Anti-Hinge Antibodies Recognize IgG Subclass– and Protease-Restricted Neoepitopes. *J Immunol*. 2017;198:82-93.
10. Den Uyl D, Ter Wee M, Boers M, Kerstens P, Voskuyl A, Nurmohamed M, *et al*. A non-inferiority trial of an attenuated combination strategy ('COBRA-light') compared to the original COBRA strategy: Clinical results after 26 weeks. *Ann Rheum Dis*. 2014;73:1071-78.
11. Arnett FC, Edwothy SM, Bloch DA, McShane DJ, Fries JF, Cooper NS, *et al*. Classification criteria: The 1987 American Rheumatism Association revised criteria for the classification of rheumatoid arthritis. *Arthritis Rheum*. 1988; 31, 315-24.
12. Jamnitski A, Krieckaert CL, Nurmohamed MT, Hart MH, Dijkmans BA, Aarden L, *et al*. Patients non-responding to etanercept obtain lower etanercept concentrations compared with responding patients. *Ann Rheum Dis*. 2012;71:88-91.
13. Kohen F, Bagci H, Barnard G, Bayer EA, Gayer B, Schindler DG, *et al*. Preparation and properties of anti-biotin antibodies. *Methods Enzym*. 1997; 279, 451-63.
14. van de Bovenkamp FS, Derksen NIL, Ooijevaar-de Heer P, van Schie KA, Kruithof S, Berkowska MA, *et al*. Adaptive antibody diversification through N-linked glycosylation of the immunoglobulin variable region. *Proc Natl Acad Sci U S A*. 2018;115:1901-06.
15. Stadlmann J, Weber A, Pabst M, Anderle H, Kunert R, J. Ehrlich, H, *et al*. A close look at human IgG sialylation and subclass distribution after lectin fractionation. *Proteomics*. 2009; 9:4143–4153.

16. Guhr T, Bloem J, Derksen NIL, Wuhrer M, Koenderman AHL, Aalberse RC, *et al.* Enrichment of sialylated IgG by lectin fractionation does not enhance the efficacy of immunoglobulin G in a murine model of immune thrombocytopenia. *PLoS One*. 2011;6:e21246

17. Käsermann F, Boerema DJ, Rüegsegger M, Hofmann A, Wymann S, Zuercher AW, *et al.* Analysis and functional consequences of increased Fab-sialylation of intravenous immunoglobulin (IVIG) after lectin fractionation. *PLoS One.* 2012;7:e37243.

18. Bondt A, Rombouts Y, Selman MHJ, Hensbergen PJ, Reiding KR, Hazes JM, *et al*. Immunoglobulin G (IgG) Fab Glycosylation Analysis Using a New Mass Spectrometric High-throughput Profiling Method Reveals Pregnancy-associated Changes. *Mol Cell Proteomics*. 2014;13:3029-39.

19. Gao S, Zhu H, Zuo X, Luo H. Cathepsin g and its role in inflammation and autoimmune diseases. *Arch Rheumatol*. 2018;33:498-504.

20. Falkenburg WJJ, von Richthofen HJ, Rispens T. On the origin of rheumatoid factors: Insights from analyses of variable region sequences. *Semin Arthritis Rheum*. 2019;48:603-610.

21. Vletter EM, Koning MT, Scherer HU, Veelken H, Toes REM. A Comparison of Immunoglobulin Variable Region N-Linked Glycosylation in Healthy Donors, Autoimmune Disease and Lymphoma. *Front Immunol*. 2020;11:241.

SUPPLEMENTARY MATERIAL

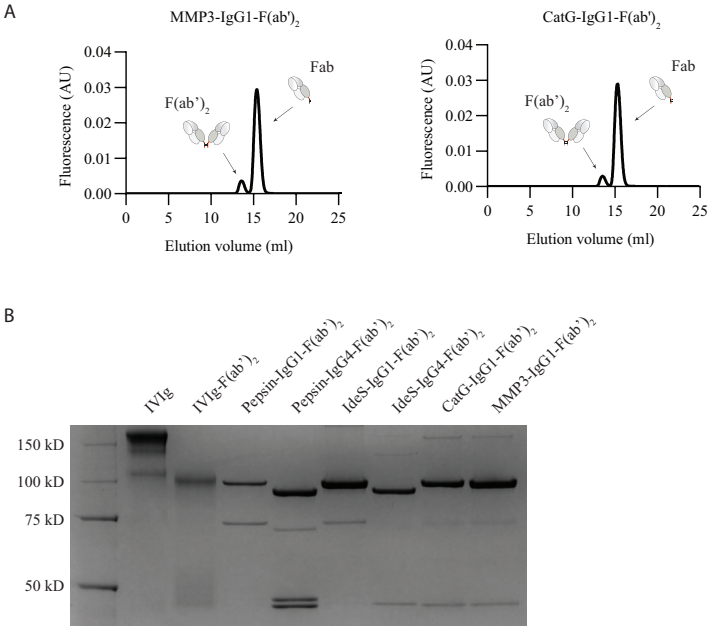

Figure S1. Evaluation of recombinantly produced F(ab')$_2$ targets. *(**A**) The large fraction of Fab byproducts in the purified anti-κ light chain product were extracted from the F(ab')$_2$ fragments using size-exclusion chromatography. (**B**) SDS-PAGE of all F(ab')$_2$ targets, IgG F(ab')$_2$ ~100 kD, full-length IgG ~150 kD, IgG Fab ~50 kD.*

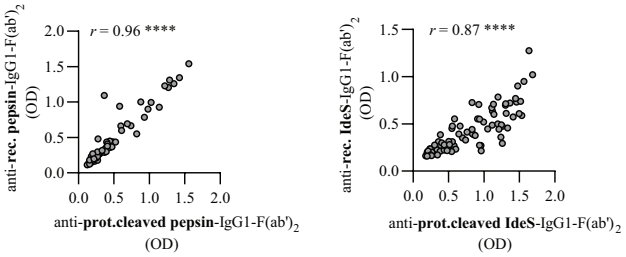

Figure S2. Comparison of AHA reactivity for proteolytically cleaved IgG1-F(ab')$_2$s versus recombinantly expressed IgG1-F(ab')$_2$s of the same protease. *We found that the reactivity was highly similar (HCs, n = 86; pepsin r = 0.96; IdeS r = 0.87, Figure S2). For both reactivities the Spearman rank correlation coefficient (r) was determined; **** p < 0.0001.*

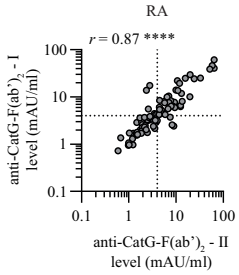

Figure S3. AHA ELISA reproducibility. *Reproducibility was evaluated for anti-CatG-IgG1-F(ab')$_2$ reactivity in RA patients (n=69; r =0.87****).*

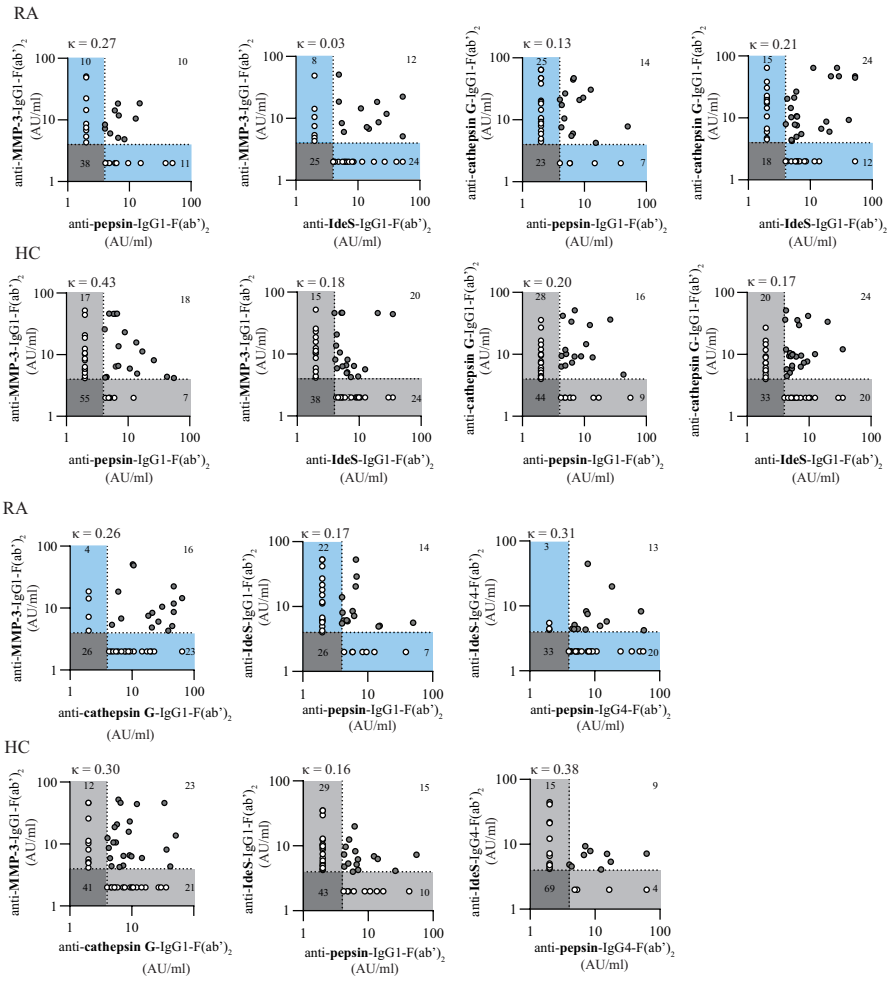

Figure S4. Pairwise comparisons of AHA reactivities. *Pairwise comparisons show levels of AHA reactivity for all evaluated AHA responses in RA patients (blue) and HCs (light grey). Dashed lines represent cut-off level for positivity at 4 AU/ml. For each plot the number of single-positive (white dots), double-positive (grey dots), and double-negative (dark grey square) subjects are depicted. Cohen's Kappa coefficients (κ) are presented at the top of each graph.*

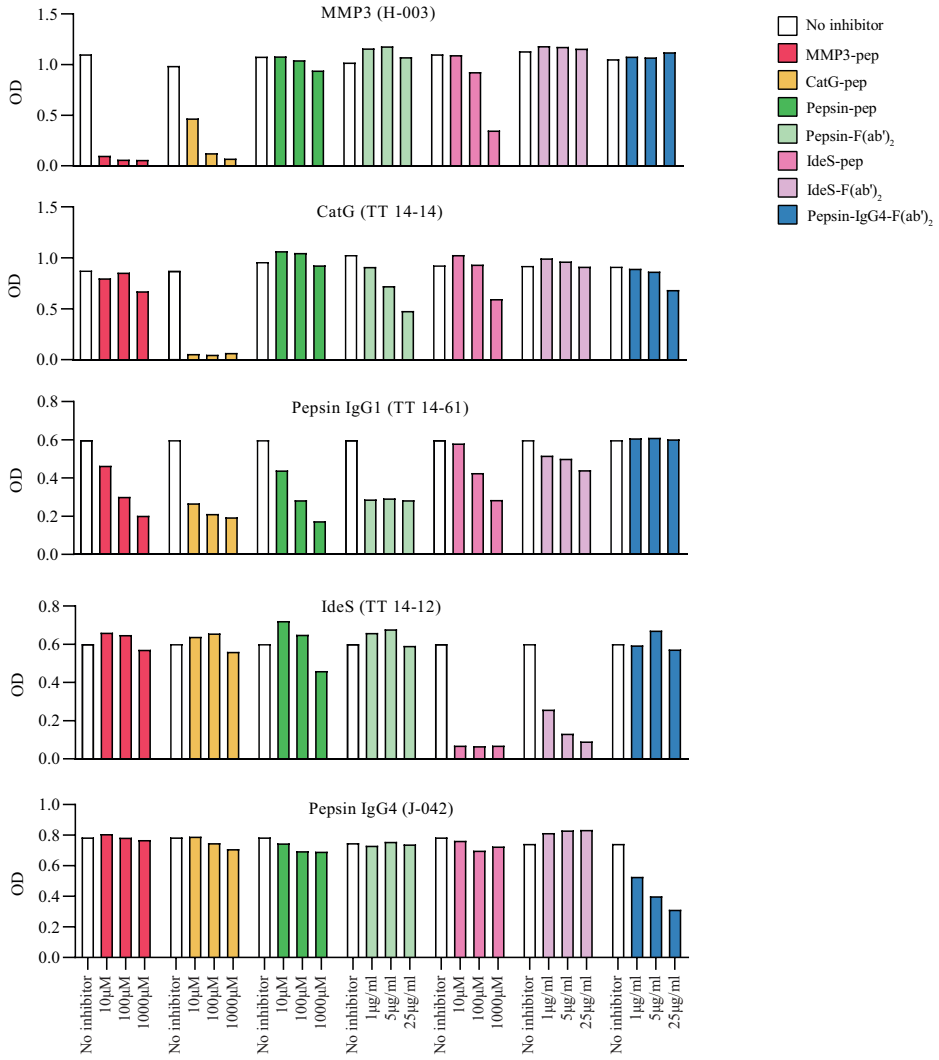

Figure S5. Inhibition assay of AHA reactivity. *Inhibition of AHA reactivity using increasing concentrations of peptides (10, 100, or 1000µM) or F(ab')$_2$s (1, 5, or 25µg/ml). Sera from representative HC or RA patients (indicated by a number above each panel) with an AHA response against the tested F(ab')$_2$ were incubated with the inhibitor before they were tested in the AHA ELISA (n=4).*

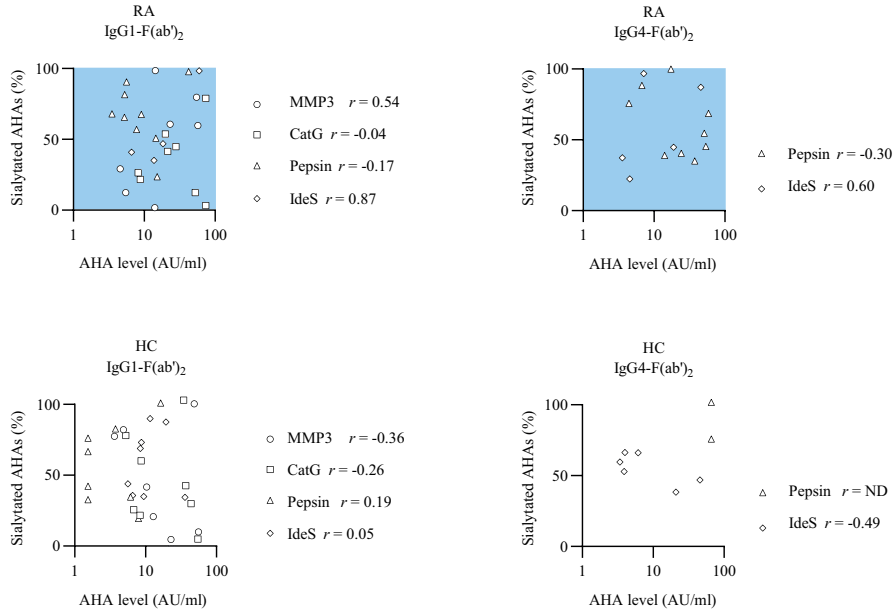

Figure S6. Correlation between the percentage of Fab glycosylated AHAs and AHA levels. *Spearman rank correlation coefficients (r) are presented at the right side of each graph. Due to the limited number of subjects in the analysis significance could not be determined. ND, not determined.*

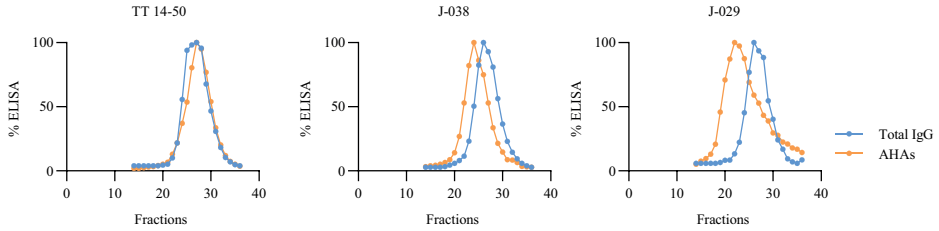

Figure S7. Confirmation of AHA Fab glycosylation using size-exclusion chromatography and ELISA. *Serum from subjects J-038 and J-029, that previously showed moderate and high AHA SNA-binding, fractionated by gel filtration chromatography, followed by ELISA detection, elute earlier than other IgG molecules indicating the presence of Fab glycans on AHAs. Serum TT 14-50, that did not show increased AHA SNA-binding previously, eluted simultaneously with other IgG molecules.*

Table SI. Synthetic peptide analogs of the IgG lower hinge

Name	Amino acid sequence	IgG subclass	Length	First a.a. position**	Final a.a. position	N-terminal tag
MMP3-pep	DKTHTCPPCPAP	IgG1	12	221	232	
Cathepsin G-pep	DKTHTCPPCPAPE	IgG1	13	221	233	
Pepsin-pep	DKTHTCPPCPAPEL	IgG1	14	221	234	
IdeS-pep	CPPCPAPELLG	IgG1	11	226	237	
IdeS biotin-pep	CPPCPAPELLG	IgG1	11	226	237	Biotin
Cathepsin G biotin-pep	DKTHTCPPCPAPE	IgG1	13	221	233	Biotin
Pepsin IgG4 biotin-pep	KYGPPCPSCPAPEF	IgG4	14	221	234	Biotin

*pep = synthetic peptide, a.a. = amino acid
**EU numbering of a.a. positions

CHAPTER 9

Summarizing discussion

Adaptive immune responses have high specificity for pathogens and depend on the activation of B and T cells. These responses provide long-lasting protection with rapid and specific response to re-call infection of the same pathogen, or their variants. A fundamental feature of the adaptive immune system is the ability to distinguish self from non-self. Occasionally, the immune system fails to make this distinction which can lead to self-damaging immune responses and the generation of autoimmune diseases. Upon initiation of the humoral immune responses, initial T cell-dependent B cell activation leads to generation of a germinal center (GC) reaction, which is preceded by a short period of extrafollicular B cell activation in which naive B cells differentiate into plasma blasts (PBs) and early memory B cells (MBCs)[1,2]. During a GC reaction, GC B cells may be positively selected to continue GC-cycling. After initial fate decision, differentiation may proceed and cells exit the GC reaction as plasma cell (PCs), PBs or MBCs[3–5]. Both extrafollicular and GC responses result in the formation of pathogen-specific antibodies of which different isotypes exist. IgG is the most abundant antibody isotype in human peripheral blood followed by IgM, IgA, IgD and IgE.

Glycans can be found attached to proteins and abundantly found on cellular surfaces. Common glycan structures include O- and *N*-linked glycans that are attached to specific amino acid motifs. Glycans are important for proper protein folding, cell-cell interaction, lymphocyte migration, antibody effector functions and may play a role in discrimination between self and non-self structures[6], the latter may be relevant in the pathophysiology of autoimmune diseases[7,8]. Many unanswered questions remain with regards to the role of glycans in immunity.

In this thesis, the contribution of glycans to B cell subset classification during B cell differentiation and antibody repertoire diversification by Fab glycans during health and autoimmune diseases was studied. To this end, we performed comprehensive B cell phenotyping and studied patterns and biases of the acquisition of antibody Fab glycosylation during health and disease, specifically in B cell-mediated autoimmune diseases. Understanding the role of glycans in B cell and antibody biology may provide insights in the phenotypic and functional progression of differentiating B cell subsets. Furthermore, Fab glycans on autoantibodies may contribute to pathogenesis and aid in diagnostics.

Human B cell subset classification

The human B cell population is a heterogenous immune compartment composed of many different B cell subsets, which play distinct roles in protective and pathogenic immune responses. The monitoring of B cell subsets in health and disease may have potential utility as disease biomarkers and therapeutic targets. Technical advances have allowed deep-phenotyping of new and previously identified B cell subsets[9]. Unfortunately, a harmonized

approach for defining different B cell phenotypes and subsets is lacking. Due to the lack of consistent classifications, most studies use imprecisely defined B cell subsets by the use of limited or inconsistent phenotypic markers and lack functional characterization, making comparison of separate studies difficult. Hence, harmonizing B cell classification approaches is of importance. In this thesis, we aimed to improve phenotypic and functional classification of several human B cell subsets. In **Chapter 2,** we evaluated and optimized naive B cell cell-sorting strategies from human peripheral blood to acquire a population of non-mutated, non-expanded and phenotypical non-antigen experienced B cells. CD27 expression is used in general to separate naive from antigen-experienced B cells as its expression correlates with detectible levels of somatic hypermutation in the V region, regardless of cells being Ig isotype switched or not[10,11]. Here, we show that isolation of naive B cells using absence of CD27 expression ($CD27^-$) was insufficient illustrated by a high mean mutation level and low percentage of non-mutated BCRs. This is most likely due to the presence of contaminating $CD27^-$ cells that carry highly mutated BCRs, such as $CD27^-IgG^+/IgA^+$ cells or $CD27^-IgD^-IgM^+$ cells[12,13]. Another commonly used strategy to isolate naive B cells, i.e., $CD27^-IgD^+$, showed low levels of mutated BCRs and a high percentage of non-mutated BCRs. However, it must be noted that there is a large fraction (~30%) of anergic B cells ($CD27^-IgD^+IgM^{low}$ B cells) present when using this isolation strategy[14–16], highlighting the importance to include functional studies for precise classification of B cell subsets. From **Chapter 2** we concluded that current naive B cell isolation strategies using $CD27^-IgD^+$ are adequate, but can be improved considerably by including markers for IgM and CD45RB glycosylation.

Technical advances have allowed deep-phenotyping of B cell subsets. Novel phenotypic characterizations of B cell subsets occasionally omit to include Ig isotype-specific markers. It is, however, of importance to always include Ig isotype markers. For example, in **Chapter 3** we observed that B cell subsets defined by several known and novel phenotypic markers needed further segregation by Ig isotype as their functionality depended on the Ig isotype they expressed.

Glycan remodeling during B cell differentiation

The number of studies investigating changes in glycosylation of surface proteins for B cell subset classification is sparse. A well-known glycan-dependent marker used for GC B cell classification is reactivity for lectin peanut agglutinin (PNA), which binds O-linked glycans containing the asialylated disaccharide Gal-β1,3-GalNAc-Ser/Thr[9,17]. Regulation of glycan remodeling enzymes, including ST3Gal1 and GCNT1, can alter global cellular glycosylation profiles during B cell differentiation. On GC B cells PNA-reactive O-linked glycans were mainly found on BCR co-receptor CD45, which changed compositions during differentiation[18]. In line, a glycan-dependent epitope on CD45RB has recently been identified to mark antigen-experienced B cells, independent of their CD27 expression[19–21].

Hence, identifying different glycan profiles does not only generate insight in phenotypic differences, but may also provide insight into functional differences. In **Chapter 3** we have used a combination of markers including CD45RB glycosylation, CD27 and IgM/IgD isotype expression to segregate human peripheral blood B cell subsets and investigated their IGHV repertoire and *in vitro* functionality. We confirmed that glycosylation of CD45RB is indicative for antigen-primed $CD27^-$ B cells, which are functionally distinct depending on the Ig isotype,. Even though using the glycosylation epitope on CD45RB helps to identify antigen-primed B cells among $CD27^-$ cell, there is, however, a population of $CD27^+$ cells, presumably memory B cells, that do not have this distinct glycosylation of CD45RB, meaning that glycosylation of CD45RB does not mark all antigen primed B cells. Further research should provide insight in the maturation stage and functionality of these $CD27^+$ B cells not expressing CD45RB glycosylation. This work provides novel insights in the phenotypic and functional progression from naive B cells via CD45RB glycosylated $CD27^-$ cells to memory B cells in human peripheral blood and how changing glycan profiles can contribute to B cell subset classification. It is not well understood what the physiological significance of these distinct glycan profiles may be. For one, it may intrinsically tune receptor signaling. For example, in T cells CD45 sialylation and O-glycosylation were found to inhibit CD45-homodimerization resulting in less suppression of T cell receptor signaling[22]. Moreover, depending on the types of glycans present on the B cell surface, interaction in *cis* or *trans* with endogenous lectins such as galectins and SIGLECs may occur[23–25].

Antibody Fab glycosylation

Antibodies are glycoproteins that can contain *N*-linked glycans within their variable (V) regions, so-called Fab glycans, in addition to conserved *N*-linked glycans within the constant domain. Although the role of *N*-linked glycans in the constant domains has been extensively studied, the function of *N*-linked glycans present in antibody V regions is only just being appreciated. Fab glycans are the result of co-translational covalent addition of carbohydrate groups to specific *N*-glycosylation sites, which consist of an asparagine (N), followed by any amino acid but proline, followed by serine (S) or threonine (T) (N-X-S/T; X-P). Because 15% of serum IgG has V regions that carry *N*-linked glycans, and only few germline alleles carry *N*-glycosylation sites, the majority of Fab glycosylation is therefore the result of somatic hypermutation (SHM)[26–28]. *N*-linked glycans found on plasma IgG are predominantly of the complex biantennary type. In comparison with Fc glycans, Fab glycans on IgG contain low percentages of fucose and high percentages of sialic acids (>90%), bisecting GlcNAc and galactoses[29,30], with some differences observed during pregnancy and ageing[31]. Importantly, the presence of a glycosylation site within the antibody V region does not guarantee the presence of a glycan and is highly dependent on the location of the site within the native antibody structure and a proper functioning glycosylation machinery[32,33].

The mechanisms and functions of Fab glycosylation are less well-understood as compared to Fc glycosylation for which the immune-related impact and immune modulatory effects are well defined[34,35]. Furthermore, it is unclear under which circumstances Fab glycans accumulate and what their relevance is in normal physiology as well as in pathologies. Nevertheless, it is highly conceivable that Fab glycosylation can also have an impact on immune function, since they exhibit distinct patterns in pathophysiological conditions.

The function of Fab glycosylated antibodies and B cell receptors

In recent years it has become increasingly clear that Fab glycans play a role in antibody function as well as in immune function. Besides diversification of the antibody repertoire, several functional attributes have been demonstrated to involve Fab glycans.

For several monoclonal antibodies (mAbs) the presence of Fab glycans increases antigen-binding affinity, presumably due to additional hydrophilic interactions between Fab glycans and glycans on antigens[32,36–39]. Differently acquired Fab glycans may enhance antibody selectivity by diminishing off-target binding rather than enhancing on-target binding, which was shown in a model system of anti-idiotype antibodies[40]. Impaired binding to antigen in the presence of Fab glycans has also been described[32,36,40,41]. This was explained by either steric hinderance of the bulky glycan, conformational changes in the absence of the Fab glycan or charge repulsion between the negatively charged terminal sialic acid residues present in most Fab glycans and a negatively charged antigen or antigen-context[28,42,43]. Although several studies show that Fab glycans can influence antigen-binding affinity, in the majority of cases Fab glycans will presumably leave antigen-binding affinity essentially unaffected.

The high frequency of Fab glycans exhibiting terminal sialic acid residues is likely attributed to the fast clearance of glycoproteins with unnatural high-mannose glycans or glycans exhibiting terminal galactose and N-acetylgalactosamine residues[44,45] or by more complete glycan processing due to the high accessibility of Fab glycans to glycan-editing enzymes. Hence, Fab glycan sialylation can enhance the antibody serum half-life, as was shown for Cetuximab and PankoMab[46]. Furthermore, depending on their position, Fab glycans could enhance or decrease antibody half-life *in vivo* and *in vitro*[32,47]. Fab glycans have also been described to affect antibody aggregation propensity[48,49] and modulation of immune complex formation[50]. Since Fab glycans have been implicated to affect antigen binding, it has been postulated that Fab glycans may reduce autoimmunity by masking autoantigen binding sites of autoantibodies[41,51]. Likewise, Fab glycans present on autoreactive B cell receptors (BCRs) have been shown to enhance BCR-signaling and prolong the expression of the BCR on the cell-surface after antigenic triggering[52]. An increasing number of studies hint at involvement of (endogenous or exogenous) lectins that can interact with these glycans, thereby potentially exerting immunomodulatory effects. In certain B cell lymphomas, such

as follicular- or diffuse large B cell lymphoma, the introduction of Fab glycans on the BCR via somatic hypermutation allow interaction with lectins in the germinal center and thereby provide survival signals to sustain tumor growth[53–56]. Furthermore, Fab glycans are also associated with the anti-inflammatory activity of IVIg[57] an intravenous IgG compound that successfully ameliorates symptoms of a number of autoimmune diseases.

Biases in Fab glycan repertoires

The question remains whether Fab glycans and thus introduction of V region *N*-glycosylation sites, is a mere bystander effect of the process of somatic hypermutation or whether Fab glycans accumulate under specific conditions, i.e. in an antigen-dependent manner or during inflammation. Recent studies by us and others observed inherent biases in Fab glycan repertoires which opposes Fab glycans as a bystander effect.

Bulky glycan structures in suboptimal positions may interfere with antibody folding and function. Therefore, one might expect that the introduction of *N*-glycosylation sites is restricted. In **Chapter 6** we observed that *N*-glycosylation sites clustered specifically around the CDRs and DE loop in both light and heavy chain sequences among the different isotypes[28,40,58]. In other words, it appears that the germline repertoire contains a predefined set of locations where *N*-glycosylation sites may be easily introduced upon somatic hypermutation. *N*-glycosylation sites were mostly situated in or near the paratope such that an attached glycan may have the potential to influence the binding properties of the antibody. However, for one region in particular, the CDR3 of the heavy chain, we observed that relatively few sequences acquired N-glycosylation sites, irrespective of the accumulation of mutations[28]. Interestingly, of all CDRs, this CDR3 is most important for antigen recognition[59]. Hence, introduction of a glycan here is likely a highly unfavorable event, which can explain the local negative selection for *N*-glycosylation sites.

The majority of *N*-glycosylation sites within memory rearranged sequences correspond to “progenitor sites”, i.e. a tripeptide in the germline sequence that can become an *N*-glycosylation site with a single nucleotide mutation[28,40]. In **Chapter 6**, we systematically introduced *N*-glycosylation sites at predicted ‘pre-disposed’ locations in a model antibody (adalimumab) and found that over 95% of tested *N*-glycosylation site in the heavy chain and 60% in the light chain become fully occupied[28,40]. Hence, the majority of *N*-glycosylation sites introduced at progenitor sites by somatic hypermutation are in fact glycosylated, which suggests that progenitor sites in general are located at positions that allow facile glycosylation.

Most studies on Fab glycans have focused only on IgG, while the level of Fab glycans on other Ig isotypes was largely unexplored. In **Chapter 6**, we showed that frequencies of variable region *N*-glycosylation sites are Ig isotype- and subclass-dependent, lowest for

naive, followed by IgM memory and κ and λ light chains, and highest for switched memory B cells[28]. Both IgE and IgG4 were shown to contain significantly more variable domain N- glycosylation sites than other isotypes[28,40,60,61], despite the fact that they carried fewer or similar mutation levels as other antibody subclasses. Also for ACPAs, which are highly Fab glycosylated autoantibodies in rheumatoid arthritis, no correlation was observed between the number of mutations and the frequency of *N*-glycosylation sites[62]. These findings suggest that the introduction of *N*-glycosylation sites is not the mere consequence of a high mutation rate. Rather, the mutation rate is likely a consequence of continuous (re-) activation of (autoreactive) B cells, while the Fab glycans provide additional signals that grant a selective advantage to these cells[62,63].

Besides differences in Fab glycosylation levels between different Ig isotypes and subclasses, Fab glycosylation levels can also greatly vary for specific antibody responses (**Chapter 7**). Fab glycosylation levels on anti-RhD, anti-EBV, anti-Spike were significantly lower compared to total IgG. Anti-tetanus and anti-CMV had Fab glycan levels similar to total IgG. Not surprisingly, for IgG4-mediated responses, such as anti-PLA2, anti-ADL and anti-IFX, increased levels of Fab glycosylation were observed compared to total IgG, some even significantly higher than levels of total IgG4[40]. In addition, several autoantibody responses, such as anti-CCP2, anti-MuSK and anti-Dsg3, displayed elevated levels of Fab glycosylation. Interestingly, within the anti-MuSK response, elevated Fab glycosylation was restricted to the IgG4 subclass, in contrast to patients with pemphigus vulgaris that showed elevated levels for both anti-Dsg3 IgG4 and IgG1. Moreover, anti-PR3 IgG1 Fab glycosylation levels, but not IgG3 nor IgG4, were elevated in a fraction of AAV patients. Antibody responses thus widely differ in the level of Fab glycosylation and subclass-specific enrichment of Fab glycans may occur under conditions where Fab glycans are functionally relevant.

Selection and regulation of Fab glycans during B cell responses

Both positive and negative selection for Fab glycans during antigen-specific responses is becoming increasingly evident. Above, we opposed the idea that Fab glycans are a mere side effect of the process of somatic hypermutation, for example by the observation of different levels of Fab glycosylation for different antigen-specific antibody responses. Besides antigen-associated selection, Fab glycosylation is likely subject to additional forms of selection and regulation. However, the question remains how antibodies with or without Fab glycans are selected. This selection likely occurs via several mechanism (**Figure 1**). First, Fab glycans on B cell receptors (BCRs) that result in impaired antigen binding probably get outcompeted by B cells that bind with higher affinity to the antigen (antigen-associated selection). In contrast, if Fab glycans improve antigen binding they may get positively selected. Second, BCRs with Fab glycans may alter their signaling, resulting in an altered threshold for activation (activation-threshold selection). Indeed,

citrullinated-antigen directed B cells demonstrated enhanced BCR-signaling when the BCR had Fab glycans[52]. Alternatively, Fab glycans on BCRs may interact with lectins present in the micro-environment and thereby acquire a survival advantage compared to non-Fab glycosylated BCRs (survival advantage selection), as suggested for B cell lymphomas and primary Sjogren's syndrome[54,64].

For antigen-associated selection of Fab glycans, the charge of the antigen or the context of the antigen seem to be of importance. Structural analysis of patient derived anti-MuSK antibodies revealed that somatic mutations, which led to the introduction of Fab glycans and a large increase in binding affinity, also resulted in an increasingly negatively charged antigen-binding surface. Due to the largely positively charged surface on the MuSK antigen, it is tempting to speculate that the negative charge of sialylated Fab glycans contributed to the increased binding affinity and thereby promoted the selection of these B cell clones[65,66]. In line, anti-RhD antibodies and antibodies against herpes viruses (CMV, EBV, VZV) and SARS-CoV-2 showed decreased levels of Fab glycosylation compared to total IgG. Here, the negatively charged cell membrane or viral envelope may potentially hamper antibody binding due to charge repulsion by antibodies carrying negatively charged sialylated Fab glycans and may result in negative selection for antibodies with Fab glycans.

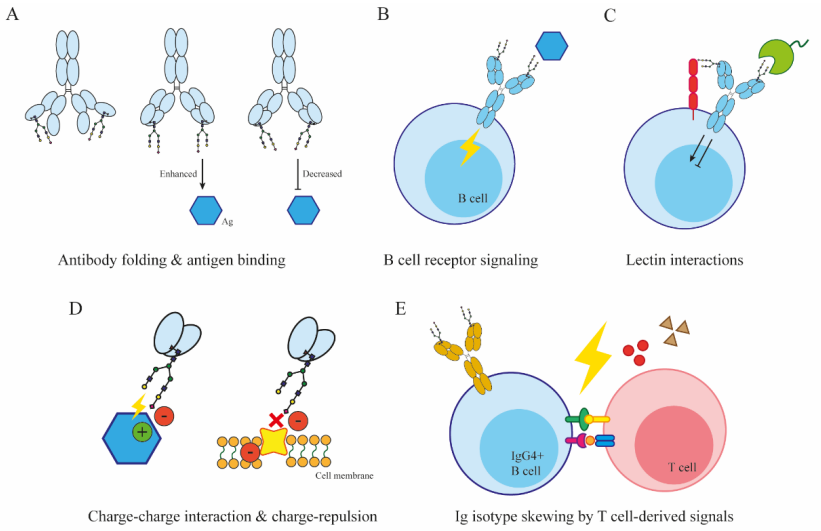

Figure 1. Proposed selection mechanisms for Fab glycosylated BCRs and antibodies. *(**A**) Bulky glycan structures in suboptimal positions may interfere with antibody folding and function. (**B**) BCRs with Fab glycans may alter their signaling, resulting in an altered threshold for activation. (**C**) Fab glycans on BCRs may interact in cis and trans with lectins present in the micro-environment and thereby acquire a survival advantage compared to non-Fab glycosylated BCRs. (**D**) Hydrophobicity and/or charge interactions between Fab glycans and antigens or antigen-context. (**E**) T cell help can skew class switch recombination (CSR) towards Ig isotypes IgG4 and IgE with enriched Fab glycosylation levels.*

Fab glycosylation may in part be regulated by the mode of B cell activation. The introduction of mutations resulting in *N*-glycosylation sites is a determining event for the accumulation of Fab glycans. Since SHM as well as class switch recombination depend on activation-induced deaminase (AID) expression, which is mainly under control of T cell help, it is plausible that different T cell helper profiles may result in different Fab glycosylation levels. For example, IgG4 and IgE antibodies, that are associated with Tfh responses that require in addition to IL-21 expression of IL-4 and/or IL-13, accumulate more Fab glycans than other Ig isotypes and subclasses. That different types of T cell help generate different *N*-glycan profiles has previously been shown for Fc glycans[67]. Whether T cell help can influence the structure of Fab glycans has not been studied so far. Future research should investigate the role of different cytokines in the regulation of Fab glycosylation.

Fab glycans on IgG4 and IgE antibodies

Fundamental differences were observed in the level of Fab glycosylation between isotypes and subclasses in healthy donors (**Chapter 6**). Both IgG4 and IgE antibodies have elevated levels of Fab glycans despite having similar or even fewer variable region mutations as other isotypes, nor did they display a biased V gene usage[28,60,61]. Tfh responses that require in addition to IL-21 expression of IL-4 and/or IL-13 (TF_H2 type response) promote class switching to both IgG4 and IgE[68,69]. The question arises why these responses have elevated Fab glycan levels in general and whether this has functional consequences for IgG4/IgE BCRs and antibodies.

IgG4 antibodies often develop after prolonged antigen exposure and are associated with immune tolerance, as they are poor activators of effector functions because of weak C1q/FcγR binding and their inability to form large immune complexes because of Fab-arm exchange[70–72]. IgE antibodies play a pivotal role in response to allergens[69,73] and are capable of triggering anaphylaxis, one of the most rapid and severe immunological reactions. Although Fab glycans can positively contribute to antigen binding, it is unlikely that antigens provoking a TF_H2 type response would generally be better recognized by antibodies carrying Fab glycans. Alternatively, Fab glycans may be selected to dampen antigen binding contributing to the tolerogenic phenotype of IgG4 antibodies and for IgE antibodies to create a lower-affinity repertoire, which could protect against exacerbated allergic reaction[60]. For both IgG4 and IgE responses, there are indications for impaired germinal center responses[68,74], which tentatively might provide the environment that positively selects for enhanced levels of Fab glycosylation. IgE^+ B cells are rare due to low GC participation, high rates of short-lived antibody secreting cell formation and absence from long-lived compartments[74–79]. The tight regulation of IgE responses, critical for constraining allergic responses, is amongst others, driven by intrinsic signals from the ectopic IgE BCR in activated B cells which drives ASC differentiation in an antigen-independent manner[4,78]. The autonomous signaling observed for IgE^+ B cells might originate

from *in cis* interactions of Fab glycans with surface lectins, i.e. inhibitory co-receptor SIGLEC CD22, which consequently drives the tendency towards apoptosis in IgE^+ B cells, similar to what was observed for IgM BCRs and Galectin-9[75,80–82]. On the other hand, introduction of Fab glycans improves antibody stability, therefore the elevated levels of Fab glycans observed for IgE may function to contribute to stabilization of the highly flexible IgE BCR[83,84].

Fab glycans are thus contributing to antibody diversification and are found with elevated levels on IgG4 antibodies in both infectious and non-infectious settings. In **Chapter 7** we found that IgG4 autoantibodies associated with MuSK myasthenia gravis and pemphigus vulgaris were enriched in Fab glycans and antibodies against therapeutic proteins were previously found to display elevated Fab glycosylation levels[40]. The role for IgG4 antibodies in disease is highly diverse and both pathogenic and protective roles have been described. IgG4 antibodies confer mostly 'blocking' effector functions by not engaging with the complement system or FcγRs. IgG4-mediated pathologies generally involve blocking of protein or receptor functions. The role, if any, of elevated Fab glycans in IgG4-mediated pathology has not been established (**Figure 2**). As previously suggested, Fab glycans may improve the functional monovalency of Fab-arm exchanged IgG4 antibodies by enhancing antigen binding or inversely hamper binding or provide a survival advantage for $IgG4^+$ B cells with Fab glycosylated BCRs via lectin interaction.

B cell-mediated autoimmune diseases

Enrichment of autoantibody Fab glycans has recently been associated as a novel feature of some autoimmune diseases (RA, AAV). **Chapter 7** therefore addresses the important question whether this may be a general characteristic acquired by autoantibodies that develop in the context of autoimmunity. By comparing Fab glycosylation levels on autoantibodies across a broad range of autoimmune diseases we could demonstrate Fab glycosylation indeed is a regular feature in multiple autoimmune diseases, but is restricted to chronic B cell-mediated autoimmune diseases. Importantly, the disease-overarching nature of this study, points towards a common pathophysiological mechanism of immune dysregulation.

Antibodies against latent herpes viruses, vaccine antigen tetanus toxoid and HIV did not show elevated levels of Fab glycans, suggesting that chronic antigen-stimulation as such does not necessarily lead to increased Fab glycosylation levels and may be more specific for chronic inflammation/autoimmune settings. In line, ACPA-IgG exhibits remarkably high levels of Fab glycosylation. Moreover, a rise in ACPA Fab glycosylation levels precedes onset of clinical symptoms, increased ACPA levels and affinity maturation. This implies that affinity maturation does not drive the selection of ACPA-expressing B cells but rather their propensity to introduce V region glycosylation sites that potentially support

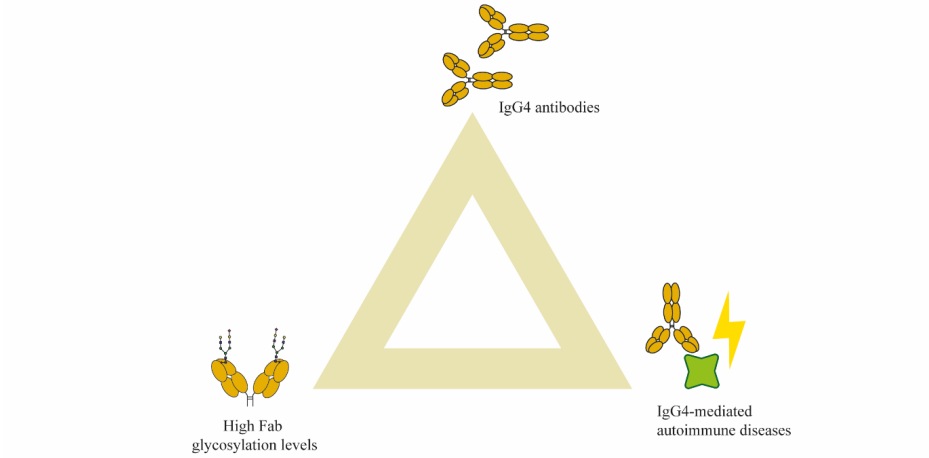

Figure 2. Association between IgG4 antibodies, Fab glycosylation levels and autoimmune diseases.

their expansion and/or survival. Moreover, anti-hinge antibody responses against hinge neoepitopes generated by endogenous (MMPs) but also exogenous proteases (bacterial derived cathepsins) demonstrated elevated levels of Fab glycosylation in RA patients but also in healthy controls (**Chapter 8**), suggesting that extensive Fab glycosylation may also develop in response to an inflammatory proteolytic microenvironment not restricted to autoimmunity.

Autoantibody responses in patients with acute autoimmune diseases, such as GBS, TTP and anti-GBM were characterized by low levels of Fab glycans (**Chapter 7**). The majority of GBS, TTP and anti-GBM glomerulonephritis patients report a viral or bacterial infection before disease onset. The immune system generates antibodies to fight infection, that coincidently trigger autoimmunity in genetically susceptible individuals due to cross-reactivity with self-antigens[85,86]. The low levels of Fab glycans observed on autoantibodies in GBS, TTP and anti-GBM glomerulonephritis might stem from these antibodies originating from cross-reactive anti-microbe immune responses that have evolved in a microbe-specific context in which Fab glycans are not favorable, for example due to charge repulsion as described above.

In addition to Fab glycan levels, glycan composition may also be altered upon chronic inflammation/autoimmune settings, as was previously observed during ageing and pregnancy[31]. Several studies investigated the Fab glycan composition of IgG autoantibodies or BCRs in patients with different autoimmune diseases (RA, AAV and IgG4-RD) and revealed an enrichment of highly sialylated Fab glycans compared to polyclonal serum IgG in healthy controls[26,30,87]. Glycosylation can be influenced by a variety of factors, e.g. type of cell, its activation state and presence of inflammatory mediators such as cytokines

and chemokines. Autoimmune diseases display specific (local) cytokine signatures[88] that are able to modulate expression of glycosidases, sialidases and glycosyltransferases, which impact glycan structure[6] and may explain enrichment of sialylated Fab glycans in several autoimmune diseases. Thereby, Fab glycosylated autoantibodies may locally shape immunological microenvironments at inflamed sites, in line with the observation that synovial fluid-derived ACPA exhibited higher Fab glycan prevalence than ACPA obtained from peripheral blood[26].

The abundant presence of highly sialylated Fab glycans in autoimmune diseases might potentially support their expansion and/or survival or impart an immune-modulatory function[26,89,90] for which mechanisms are not fully understood. This could be cell intrinsic as sialylation can have modest contributions to enhanced antigen-affinity[40,42], but could also rely on the local interaction with sialic acid-binding immunoglobulin-type lectins (SIGLECs). A recent study observed that Fab glycans expressed by autoreactive BCRs result in enhanced BCR-signaling and prolonged expression of the BCR on the cell-surface after antigenic-triggering, which was independent of the SIGLEC CD22[52]. The prolonged surface expression might modulate BCR signaling strength and duration[91] or alternatively, differences in molecular organization of surface BCR clusters with or without Fab glycans alter B cell activation thresholds[52,92]. It cannot be ruled out that interactions with other SIGLECs or (soluble-secreted) lectins may be involved in altered signaling, similar to the role of Galectin-9 described in IgM BCR signaling[82]. In primary Sjogren's syndrome, antigen-independent B cell proliferation within parotoid glands is suggested to arise from interaction of Fab glycans with microenvironmental lectins[64]. Moreover, high sialic acid levels may convey a survival advantage similar to what was observed for $CD4^+$ T helper 2 cells resistant to Galectin-1 mediated apoptosis. $CD4^+$ T helper 2 cells exhibit high α2,6-linked sialic acid surface expression, opposed to activated naive T cells that have significantly lower α2,6-linked sialic acid levels, resulting in galectin-1 mediated apoptosis[6,93]. Whether highly sialylated Fab glycans aid in escape from apoptosis needs to be investigated.

B cell lymphoma

High levels of Fab glycans have not only been observed in autoimmune diseases, but also in certain lymphomas, e.g. Follicular lymphoma (FL) and diffuse large B cell lymphoma (DCBCL). FL BCRs feature a unique enrichment of rare oligomannoses, even though the Fc glycans feature complex-type glycans[94–96]. The high-mannose type glycans are rare in healthy individuals, estimated to represent only 4% of IgG Fab glycans[36]. Moreover, SHM-induced *N*-linked glycosylation sites within FL BCRs were observed on specific hotspots at positions 38 (CDR1), 55 (FR2), 107 (CDR3), and 125 (FR4)[58], suggesting that not only the presence of an *N*-linked glycan but also its exact position seems important to drive lymphomagenesis. Presumably, these high mannose Fab glycans interact with endogenous

lectins, or alternatively with lectins from opportunistic bacteria. This interaction would result in antigen-independent BCR activation via precisely positioned high-mannose Fab glycans and in doing so provide additional growth and survival signals to the lymphoma cell[54–56,97]. Indeed, experimental models confirmed an interaction between lectins, such as DC-SIGN but also lectins on opportunistic bacteria, and FL high-mannose Fab glycans, thereby stimulating the lymphoma B cells[54,97]. As mentioned, in healthy donors high-mannose structures are normally absent on the cell surface, sparking the hypothesis that in FL the Fab glycans do not fully mature inside the Golgi complex due to enzyme inaccessibility[94,95]. For instance, increased serum concentration of IL-6 in patients with non-Hodgkin's lymphoma[98,99], of which 40% represents FL, can enhance the expression of oligosaccharyltransferase, which catalyzes attachment of the *N*-linked glycan precursor to the polypeptide chain in the lumen of the endoplasmic reticulum, resulting in increased IgG Fab glycosylation with a proportional increase in high-mannose structures up to 30%[100–102]. Also the precise positioning of the *N*-glycosylation site can direct glycan composition as introduction of *N*-glycosylation sites in the CDR2 of otherwise identical antibodies resulted in complex-type biantennary glycans at Asp54 and Asp58 but in high-mannose structures at Asp60[33].

Challenges in antibody Fab glycosylation research

Besides IgG, all other immunoglobulin (Ig) isotypes also have V region *N*-glycosylation sites, likely resulting in the presence of Fab glycans. While Fab glycosylation of IgG has been more extensively studied, less is known about the Fab glycosylation patterns of other Igs. This is due -in part- to the fact that the other Ig isotypes are more glycosylated compared to IgG that has only a single conserved *N*-glycosylation site (see **Figure 4**, General introduction), hampering their analysis using well-established methods. For example, IgM which typically exists as a pentamer, has 10 *N*-glycosylation sites on each monomer[103]. We and others use Sambucus nigra agglutinin (SNA) lectin-affinity chromatography to fractionate serum antibodies. For IgG, this technique allows for enrichment of Fab sialylated antibodies, but not for Fc glycans because these are shielded within the 3D-conformation[27,29,104]. Due to a large number of additional sialylated C_H glycans present on other isotypes, the majority of antibodies will end up in the SNA enriched fraction. Several glycans are found in the C_{H1}-domain or hinge-region thus using proteases to generate $F(ab')_2$s prior to fractionation is not a solution. Another limitation of SNA affinity chromatography is that it captures only sialylated glycans. Since a large proportion (>90%) of polyclonal serum IgG contains Fab glycans with at least one terminal sialic acid residue[104] this method provides a good estimation for the level of Fab glycosylation. However, antibodies with non-sialylated Fab glycans end up in the SNA depleted fraction, potentially resulting in a slight underestimation of antibody Fab glycan levels. Thus, using this method the frequency and glycan composition of antibodies with non-sialylated Fab glycans remains unclear. It may be feasible that under certain conditions levels of non-

sialylated Fab glycans increase and that a fraction of Fab glycosylated antibodies is missed that could be functionally relevant, e.g. high-mannose glycans found in B cell malignancies.

Antigen-independent B cell *in vitro* models provide a great opportunity to systematically investigate the relationship between antigen and the introduction of V region *N*-glycosylation sites. The majority of *N*-glycosylation sites are the result of somatic hypermutation. Therefore, the use of naive B cells that carry unmutated Ig genes is beneficial to determine *in vitro* acquired *N*-glycosylation sites. In **Chapter 2** and **3**, we have shown that current isolation strategies for naive B cells ($CD27^-IgD^+$) harbor contamination from mutated non-naive B cells, and use of $CD27^-IgD^+$ is adequate but can be improved by including markers for CD45RB glycosylation and IgM to obtain a population of non-clonally expanded and non-mutated naive B cells.

Somatic hypermutation as well as class switch recombination depend on the activity of AID. In **Chapter 5** and unpublished data, we have observed that *in vitro* AID activity is sufficient for CSR but not for SHM. Studies that are able to induce SHM in primary B cell cultures at physiological relevant rates have not been published. Lack of SHM in cultured primary B cells may stem from several reasons. First, AID expression levels may be limiting, suggesting that relevant signals to induce AID levels necessary for SHM are lacking *in vitro*. Future studies on antibodies produced in B cell in vitro cultures stimulated with T cell dependent and independent cytokines stimulation such as IL-4, IL-13, IL-10, IFN-γ, IL-21, BAFF/APRIL, as well as CD40L should be performed to learn more about the T cell-mediated potential to regulate antibody Fab glycosylation. Second, AID may be able to introduce uracils within the V region, but those are repaired by high-fidelity repair mechanism resulting in an absence of alterations to the DNA. DNA polymerases are important players within DNA repair pathways[105,106]. Physiological relevant oxygen levels influence expression profiles of different repair proteins and DNA polymerases, resulting in higher levels of low-fidelity DNA polymerases, such as POLη, under hypoxia (0.5-1% pO_2)[107,108]. Human B cell *in vitro* studies have so far largely neglected the role of oxygen levels in human B cell studies. Hence, performing *in vitro* experiments at physiological relevant oxygen levels, rather than atmospheric oxygen levels, may be pivotal for the introduction of detectible somatic mutations. For germinal centers, the region within follicles where B cells undergo somatic hypermutation, tissue oxygen levels ranging from normoxic (3-6% pO^2) to hypoxic (0.5-1% pO_2) have been described. In **Chapter 5**, by using optimized *in vitro* cultures mimicking T cell-dependent B cell activation together with in-depth flow cytometric assessment of B cell phenotype, metabolic status and signaling pathways, we show that oxygen is a critical regulator of human naive B cell differentiation and class switch recombination. In addition to local oxygen pressure, other factors such as availability of nutrients, migratory and physical signals such as shear stress are also likely to contribute to B cell fate decision during both extrafollicular and GC B cell responses.

Taken together, we suggest future research that aims to recapitulate the human germinal center response *in vitro* should be performed at physiological relevant oxygen pressures (0.5-6% pO_2).

Fab glycans as an unconventional strategy for antibody diversification: future opportunities, applications and perspectives

The gradual progression of chronic autoimmune diseases often results in serious tissue damage before the disease is diagnosed clinically. Therefore, early diagnosis of autoimmune diseases is desired. Measurement of autoantibodies is a major diagnostic tool in many autoimmune diseases. Besides autoantibody levels and Fc glycosylation, Fab glycosylation might function as another pathogenic determinant in autoimmune diseases. For RA, Fab glycans on autoantibodies are described to predict progression to RA[109]. However, in a large cross-sectional study where Fab glycosylation levels were assessed on pre-symptomatic, early and established RA patients after specific treatment decisions, Fab glycans were less informative after disease onset[110]. The value of Fab glycans as clinical biomarkers may depend on the disease stage, type of treatment and the location of the B cell compartment that produces the autoantibodies. It will be of interest to study the relative abundance of different Ig class and subclasses and integrating this with site-specific *N*-glycosylation profiles in order to generate disease-specific glycan signatures.

The generation of recombinant monoclonal antibodies tremendously revolutionized the landscape of treatment options for different diseases including many cancers, autoimmune, metabolic and infectious diseases. The first monoclonal antibody was approved by the United Stated Food and Drug administration in 1986. Currently 79 therapeutic mAbs have made it onto the market. Since then, antibody engineering has dramatically evolved and mAbs have become a prominent class of new drugs due to their high specificity and limited side-effects.

For therapeutic antibodies glycan modifications are often considered critical quality attributes and can be engineered for therapeutic efficacy and safety improvements. The *N*-linked glycan at position N297 in the Fc of IgG molecules plays an essential role in Fc effector functions including antibody-dependent cellular cytotoxicity (ADCC) and complement-dependent cytotoxicity (CDC) which are among the mechanisms of action of therapeutic antibodies. Hence, engineering Fc glycans on mAbs is a rational strategy to improve safety and adjust efficacy. Nowadays, therapeutic mAbs are generated that are for example non-fucosylated (mogamulizumab, benralizumab, obinutuzumab) or overall non-glycosylated. In addition, introducing Fab glycans onto strategic positions within the variable region of a monoclonal antibody can substantially enhance its activity (ibalizumab)[111].

Above, we described several mechanisms of how Fab glycans can influence antigen binding, including the bulk size of *N*-linked glycans to fill out the space between epitope and paratope, charge–charge interaction and through steric hinderance. A major drawback from mAbs therapy is their immunogenicity. Frequently, individuals that are treated with mAbs develop antibodies against the mAb (anti-drug antibodies) which results in rapid clearance of the drug by which the effectiveness of therapy reduces greatly. In a pilot study, we immunized mice with adalimumab (ADL) wild-type (without Fab glycans) or several ADL variants with Fab glycans. After several weeks and multiple ADL boosters, mice that received ADL with Fab glycans showed significant lower anti-drug antibody levels than mice injected with the non-Fab glycosylated ADL (non-published data). These findings are in line with the beneficial use of the SNA enriched fraction of IVIg (enriched for Fab glycosylated IgG) used to treat patients with autoimmune diseases and B cell malignancies[112,113]. One potential mechanism of action relies on the fact that Fab glycans are very motile and therefore make the epitope, that is often recognized by anti-drug antibodies, more variable and thus less well recognized by anti-drug antibodies. These preliminary results suggest that the addition of Fab glycans may aid to lower immunogenicity of antibodies used for therapeutic purposes. Moreover, introduction of Fab glycans at predisposed locations was able to improve IgG antibody stability[47] and Fab glycans with high sialic acid content could extend antibody half-life[46]. Taken together, Fab glycan engineering serves as a potential new avenue to be explored for new or existing therapeutic antibodies. Of note, the precise positioning of these Fab glycans on locations that do not interfere with antigen binding is important. Furthermore, Fab glycan structures should mimic *in vivo* glycans to avoid immunogenicity against aberrant glycan structures. Current *in vitro* systems have been optimized to generate antibodies with *in vivo*-like Fab glycans[114] (**Figure 3**).

In this thesis, we describe how glycans can contribute to repertoire diversification and classification on both B cell subsets and antibodies. The results presented in this thesis support that glycans can be considered an undistinguishable part of the immunological repertoire through diversity generation and subset classification. We found that glycan profiles can give insight in the phenotypic and functional progression from differentiating B cell subsets and we describe novel patterns and biases of the acquisition of antibody Fab glycosylation during health and disease. The majority of Fab glycans is introduced by somatic hypermutation at predictable locations surrounding the antigen-binding site of antibodies and are introduced to various degrees during antibody responses depending on the antigen, antigen-context as well as Ig isotype/subclass. These findings increase our understanding of the role for Fab glycans in immunity, specifically in the context of B cell-mediated autoimmune diseases. Our findings suggest that future research on mapping cellular and antibody glycan profiles could be very useful, for example to improve B cell subset classification and to determine whether monitoring of Fab glycans can aid in

diagnostics and disease progression and their contribution to pathogenesis. Moreover, the introduction of Fab glycans is a potential new avenue to be explored for improving new or existing therapeutic antibodies.

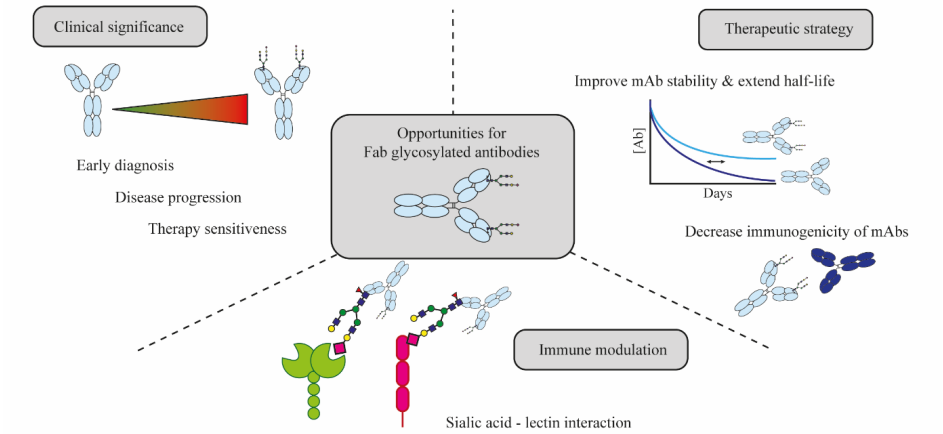

Figure 3. Fab glycans as an unconventional strategy for antibody diversification: future opportunities, applications and perspectives.

REFERENCES

1. Weisel FJ, Zuccarino-Catania G V., Chikina M, Shlomchik MJ. A Temporal Switch in the Germinal Center Determines Differential Output of Memory B and Plasma Cells. *Immunity*. 2016;44(1):116-130. doi:10.1016/j.immuni.2015.12.004
2. Laidlaw BJ, Cyster JG. Transcriptional regulation of memory B cell differentiation. *Nat Rev Immunol*. 2021;21(4):209-220. doi:10.1038/s41577-020-00446-2
3. Laidlaw BJ, Schmidt TH, Green JA, Allen CDC, Okada T, Cyster JG. The Eph-related tyrosine kinase ligand Ephrin-B1 marks germinal center and memory precursor B cells. *J Exp Med*. 2017;214(3):639-649. doi:10.1084/jem.20161461
4. Shinnakasu R, Inoue T, Kometani K, et al. Regulated selection of germinal-center cells into the memory B cell compartment. *Nat Immunol*. 2016;17(7):861-869. doi:10.1038/ni.3460
5. Victora GD, Nussenzweig MC. Germinal centers. *Immunol Rev*. 2022;247(1):5-10. doi:10.1111/j.1600-065X.2012.01125.x
6. Maverakis E, Kim K, Shimoda M, et al. Glycans in the immune system and The Altered Glycan Theory of Autoimmunity: a critical review. *J Autoimmun*. 2015;57:1-13. doi:10.1016/j.jaut.2014.12.002
7. Bermingham ML, Colombo M, McGurnaghan SJ, et al. N-Glycan Profile and Kidney Disease in Type 1 Diabetes. *Diabetes Care*. 2018;41(1):79-87. doi:10.2337/dc17-1042
8. Nakagawa H, Hato M, Takegawa Y, et al. Detection of altered N-glycan profiles in whole serum from rheumatoid arthritis patients. *J Chromatogr B, Anal Technol Biomed life Sci*. 2007;853(1-2):133-137. doi:10.1016/j.jchromb.2007.03.003
9. Sanz I, Wei C, Jenks SA, et al. Challenges and opportunities for consistent classification of human b cell and plasma cell populations. *Front Immunol*. 2019;10(OCT):1-17. doi:10.3389/fimmu.2019.02458
10. Dunn-Walters DK, Isaacson PG, Spencer J. MGZ of Human Spleen Is a Reservoir of Memory. *J Exp Med*. 1995;182(August):559-566.
11. Pascual BV, Liu Y, Magalski A, Bouteiller O De, Banchereau J, Capra JD. Analysis of Somatic mutation in Five B cell Subsets of Human Tonsil. *J Exp Med*. 1994;180.
12. Wei C, Anolik J, Cappione A, et al. A New Population of Cells Lacking Expression of CD27 Represents a Notable Component of the B Cell Memory Compartment in Systemic Lupus Erythematosus. *J Immunol*. 2007;178(10):6624-6633. doi:10.4049/jimmunol.178.10.6624
13. Fecteau JF, Côté G, Néron S. A New Memory CD27 − IgG + B Cell Population in Peripheral Blood Expressing V H Genes with Low Frequency of Somatic Mutation . *J Immunol*. 2006;177(6):3728-3736. doi:10.4049/jimmunol.177.6.3728
14. Merrell KT, Benschop RJ, Gauld SB, et al. Identification of Anergic B Cells within a Wild-Type Repertoire. *Immunity*. 2006;25(6):953-962. doi:10.1016/j.immuni.2006.10.017
15. Duty JA, Szodoray P, Zheng NY, et al. Functional anergy in a subpopulation of naive B cells from healthy humans that express autoreactive immunoglobulin receptors. *J Exp Med*. 2009;206(1):139-151. doi:10.1084/jem.20080611
16. Quách TD, Manjarrez-Orduño N, Adlowitz DG, et al. Anergic responses characterize a large fraction of human autoreactive naive B cells expressing low levels of surface IgM. *J Immunol*. 2011;186(8):4640-4648. doi:10.4049/jimmunol.1001946
17. Rose ML, Malchiodi F. Binding of peanut lectin to thymic cortex and germinal centres of lymphoid tissue. *Immunology*. 1981;42(4):583-591.

18. Giovannone N, Antonopoulos A, Liang J, et al. Human B Cell Differentiation Is Characterized by Progressive Remodeling of O-Linked Glycans. *Front Immunol*. 2018;9:2857. doi:10.3389/fimmu.2018.02857

19. Glass DR, Tsai AG, Oliveria JP, et al. An Integrated Multi-omic Single-Cell Atlas of Human B Cell Identity. *Immunity*. 2020;53(1):217-232.e5. doi:10.1016/j.immuni.2020.06.013

20. Bemark M, Friskopp L, Saghafian-Hedengren S, et al. A glycosylation-dependent CD45RB epitope defines previously unacknowledged CD27-IgMhigh B cell subpopulations enriched in young children and after hematopoietic stem cell transplantation. *Clin Immunol*. 2013;149(3 PB):421-431. doi:10.1016/j.clim.2013.08.011

21. Koethe S, Zander L, Koster S, et al. Pivotal Advance: CD45RB glycosylation is specifically regulated during human peripheral B cell differentiation. *J Leukoc Biol*. 2011;90(1):5-19. doi:10.1189/jlb.0710404

22. Xu Z, Weiss A. Negative regulation of CD45 by differential homodimerization of the alternatively spliced isoforms. *Nat Immunol*. 2002;3(8):764-771. doi:10.1038/ni822

23. Giovannone N, Liang J, Antonopoulos A, et al. Galectin-9 suppresses B cell receptor signaling and is regulated by I-branching of N-glycans. *Nat Commun*. 2018;9(1):3287. doi:10.1038/s41467-018-05770-9

24. Gasparrini F, Feest C, Bruckbauer A, et al. Nanoscale organization and dynamics of the siglec CD22 cooperate with the cytoskeleton in restraining BCR signalling. *EMBO J*. 2016;35(3):258-280. doi:10.15252/embj.201593027

25. Coughlin S, Noviski M, Mueller JL, et al. An extracatalytic function of CD45 in B cells is mediated by CD22. *Proc Natl Acad Sci U S A*. 2015;112(47):E6515-24. doi:10.1073/pnas.1519925112

26. Hafkenscheid L, Bondt A, Scherer HU, et al. Structural analysis of variable domain glycosylation of anti-citrullinated protein antibodies in rheumatoid arthritis reveals the presence of highly sialylated glycans. *Mol Cell Proteomics*. 2017;16(2):278-287. doi:10.1074/mcp.M116.062919

27. van de Bovenkamp FS, Hafkenscheid L, Rispens T, Rombouts Y. The Emerging Importance of IgG Fab Glycosylation in Immunity. *J Immunol*. 2016;196(4):1435-1441. doi:10.4049/jimmunol.1502136

28. Koers J, Derksen NIL, Ooijevaar-de Heer P, et al. Biased N -Glycosylation Site Distribution and Acquisition across the Antibody V Region during B Cell Maturation . *J Immunol*. 2019;202(8):2220-2228. doi:10.4049/jimmunol.1801622

29. Anumula KR. Quantitative glycan profiling of normal human plasma derived immunoglobulin and its fragments Fab and Fc. *J Immunol Methods*. 2012;382(1-2):167-176. doi:10.1016/j.jim.2012.05.022

30. Holland M, Yagi H, Takahashi N, et al. Differential glycosylation of polyclonal IgG, IgG-Fc and IgG-Fab isolated from the sera of patients with ANCA-associated systemic vasculitis. *Biochim Biophys Acta - Gen Subj*. 2006;1760(4):669-677. doi:10.1016/j.bbagen.2005.11.021

31. Bondt A, Wuhrer M, Kuijper TM, Hazes JMW, Dolhain RJEM. Fab glycosylation of immunoglobulin G does not associate with improvement of rheumatoid arthritis during pregnancy. *Arthritis Res Ther*. 2016;18(1):1-6. doi:10.1186/s13075-016-1172-1

32. Coloma MJ, Trinh RK, Martinez AR, Morrison SL. Position Effects of Variable Region Carbohydrate on the Affinity and In Vivo Behavior of an Anti-(1 → 6) Dextran Antibody. Published online 2018.

33. Endo T, Wright A, Morrison SL, Kobata A. Glycosylation of the variable region of immunoglobulin G-site specific maturation of the sugar chains. *Mol Immunol*. 1995;32(13):931-940. doi:10.1016/0161-5890(95)00078-S

34. Dekkers G, Rispens T, Vidarsson G. Novel Concepts of Altered Immunoglobulin G Galactosylation in Autoimmune Diseases. *Front Immunol*. 2018;9:553. doi:10.3389/fimmu.2018.00553

35. Wang TT. IgG Fc Glycosylation in Human Immunity. *Curr Top Microbiol Immunol*. 2019;423:63-75. doi:10.1007/82_2019_152

36. Wright A, Tao M, Kabat EA, Morrison SL. Antibody variable region glycosylation : position effects on antigen binding and carbohydrate structure. *EMBO*. 1991;10(10):2717-2723.

37. Wallick BYSC, Kabat EA, Morrison SL. Glycosylation of a VH residue of a monoclonal antibody against alpha (1----6) dextran increases its affinity for antigen. *JEM*. 1988;168(September):1099-1109.

38. Tachibana H, Kim J, Shirahata S. Building high affinity human antibodies by altering the glycosylation on the light chain variable region in N -acetylglucosamine-supplemented hybridoma cultures. *Cytotechnology*. 1997;23(1-3):151-159.

39. Leibiger H, Wu D, Stigler R, Marx U. Variable domain-linked oligosaccharides of human monoclonal IgG: structure and influence on antigen binding. *Biochem J*. 1999;538:529-538.

40. van de Bovenkamp FS, Derksen NIL, Ooievaar-de Heer P, et al. Adaptive antibody diversification through N -linked glycosylation of the immunoglobulin variable region. *Proc Natl Acad Sci U S A*. 2018;115(8):1901-1906. doi:10.1073/pnas.1711720115

41. Sabouri Z, Schofield P, Horikawa K, et al. Redemption of autoantibodies on anergic B cells by variable-region glycosylation and mutation away from self-reactivity. *Proc Natl Acad Sci*. 2014;111(25):E2567-E2575. doi:10.1073/pnas.1406974111

42. Khurana S, Raghunathan V, Salunke DM. The variable domain glycosylation in a monoclonal antibody specific to GnRH modulates antigen binding. *Biochem Biophys Res Commun*. 1997;234(2):465-469. doi:10.1006/bbrc.1997.5929

43. Jacquemin M. Variable region heavy chain glycosylation determines the anticoagulant activity of a factor VIII antibody. *Haemophilia*. 2010;16(102):16-19. doi:10.1111/j.1365-2516.2010.02233.x

44. ASHWELL G, MORELL AG. THE ROLE OF SURFACE CARBOHYDRATES IN THE HEPATIC RECOGNITION AND TRANSPORT OF CIRCULATING GLYCOPROTEINS. *Adv Enzymol Relat Areas Mol Biol*. 1974;41. doi:10.1002/9780470122860

45. Alessandri L, Ouellette D, Acquah A, et al. Increased serum clearance of oligomannose species present on a human IgG1 molecule. *MAbs*. 2012;4(4):509-520. doi:10.4161/mabs.20450

46. Goletz, SA, Czyk, D, Stoeckl L. Fab-glycosylated antibodies. Patent WO 2012/020065. Published online 2012.

47. van de Bovenkamp F, Derksen N, van Breemen M, et al. Variable Domain N -linked glycans acquired During antigen-specific immune responses can contribute to immunoglobulin g antibody stability. *Front Immunol*. 2018;9(April):1-9. doi:10.3389/fimmu.2018.00740

48. Retamozo S, Brito-Zerón P, Bosch X, Stone JH, Ramos-Casals M. Cryoglobulinemic disease. *Oncology (Williston Park)*. 2013;27(11):1098-1105,1110-1116.

49. Middaugh CR, Litman GW. Atypical glycosylation of an IgG monoclonal cryoimmunoglobulin. *J Biol Chem*. 1987;262(8):3671-3673.

50. Borel IM, Gentile T, Angelucci J, Margni RA, Binaghi RA. Asymmetrically glycosylated IgG isolated from non-immune human sera. *Biochim Biophys Acta*. 1989;990(2):162-164. doi:10.1016/s0304-4165(89)80029-7

51. Canellada A, Gentile T, Dokmetjian J, Margni RA, Margni RA. Occurrence, properties, and function of asymmetric IgG molecules isolated from non-immune sera. *Immunol Invest*. 2002;31(2):107-120. doi:10.1081/IMM-120004802

52. Kissel T, Ge C, Hafkenscheid L, et al. Surface Ig variable domain glycosylation affects autoantigen binding and acts as threshold for human autoreactive B cell activation. 2022;1759(February):1-22.

53. Schneider D, Minden MD Von, Alkhatib A, et al. Lectins from opportunistic bacteria interact with acquired variable-region glycans of surface immunoglobulin in follicular lymphoma. *Blood*. 2015;125(21):3287-3296. doi:10.1182/blood-2014-11-609404

54. Coelho V, Krysov S, Ghaemmaghami AM, et al. Glycosylation of surface Ig creates a functional bridge between human follicular lymphoma and microenvironmental lectins. *Proc Natl Acad Sci U S A*. 2010;107(43):18587-18592. doi:10.1073/pnas.1009388107

55. Amin R, Mourcin F, Uhel F, et al. DC-SIGN-expressing macrophages trigger activation of mannosylated IgM B-cell receptor in follicular lymphoma. *Blood*. 2015;126(16):1911-1920. doi:10.1182/blood-2015-04-640912

56. Linley A, Krysov S, Ponzoni M, Johnson PW, Packham G, Stevenson FK. Lectin binding to surface Ig variable regions provides a universal persistent activating signal for follicular lymphoma cells. doi:10.1182/blood-2015-04-640805

57. Schwab I, Nimmerjahn F. Role of sialylation in the anti-inflammatory activity of intravenous immunoglobulin - F(ab')2 versus Fc sialylation. *Clin Exp Immunol*. 2014;178(S1):97-99. doi:10.1111/cei.12527

58. Koning MT, Quinten E, Zoutman WH, et al. Acquired N-Linked Glycosylation Motifs in B-Cell Receptors of Primary Cutaneous B-Cell Lymphoma and the Normal B-Cell Repertoire. *J Invest Dermatol*. 2019;139(10):2195-2203. doi:10.1016/j.jid.2019.04.005

59. Xu JL, Davis MM. Diversity in the CDR3 Region of V H Is Sufficient for Most Antibody Specificities. *Immunity*. 2000;13(1):37-45.

60. Koning MT, Trollmann IJM, Van Bergen CAM, et al. Peripheral IgE repertoires of healthy donors carry moderate mutation loads and do not overlap with other isotypes. *Front Immunol*. 2019;10(JULY):1-8. doi:10.3389/fimmu.2019.01543

61. Levin M, Levander F, Palmason R, Greiff L, Ohlin M. Antibody-encoding repertoires of bone marrow and peripheral blood—a focus on IgE. *J Allergy Clin Immunol*. 2017;139(3):1026-1030. doi:10.1016/j.jaci.2016.06.040

62. Vergroesen RD, Slot LM, van Schaik BDC, et al. N-Glycosylation Site Analysis of Citrullinated Antigen-Specific B-Cell Receptors Indicates Alternative Selection Pathways During Autoreactive B-Cell Development. *Front Immunol*. 2019;10(September). doi:10.3389/fimmu.2019.02092

63. Vergoessen R, Slot L, Hafkenscheid L, et al. B-cell receptor sequencing of anti-citrullinated protein antibody (ACPA) IgG-expressing B cells indicates a selective advantage for the introduction of N-glycosylation sites during somatic hypermutation. *Ann Rheum Dis*. 2018;77(6):955-958.

64. Hamza N, Hershberg U, Kallenberg CGM, et al. Ig Gene Analysis Reveals Altered Selective Pressures on Ig-Producing Cells in Parotid Glands of Primary Sjögren's Syndrome Patients. *J Immunol*. 2015;194(2):514-521. doi:10.4049/jimmunol.1302644

65. Fichtner ML, Jiang R, Winton VJ, et al. Elevated N-glycosylation of immunoglobulin G variable regions in myasthenia gravis highlights a commonality across autoantibody- associated diseases. Published online 2021:1-40.

66. Fichtner ML, Vieni C, Redler RL, et al. Affinity maturation is required for pathogenic monovalent IgG4 autoantibody development in myasthenia gravis. *J Exp Med*. 2020;217(12). doi:10.1084/JEM.20200513

67. Oefner CM, Winkler A, Hess C, et al. Tolerance induction with T cell-dependent protein antigens induces regulatory sialylated IgGs. *J Allergy Clin Immunol*. 2012;129(6):1647-55.e13. doi:10.1016/j.jaci.2012.02.037

68. Unger PPA, Lighaam LC, Vermeulen E, et al. Divergent chemokine receptor expression and the consequence for human IgG4 B cell responses. *Eur J Immunol*. 2020;50(8):1113-1125. doi:10.1002/eji.201948454

69. Wade-Vallance AK, Allen CDC. Intrinsic and extrinsic regulation of IgE B cell responses. *Curr Opin Immunol*. 2021;72:221-229. doi:10.1016/j.coi.2021.06.005

70. Aalberse ROBC, Schuurman J. 2002_Immunology_IgG4 breaking the rules.pdf. Published online 2002.

71. Schuurman J, Van Ree R, Perdok GJ, Van Doorn HR, Tan KY, Aalberse RC. Normal human immunoglobulin G4 is bispecific: It has two different antigen-combining sites. *Immunology*. 1999;97(4):693-698. doi:10.1046/j.1365-2567.1999.00845.x

72. Davies AM, Sutton BJ. Human IgG4: A structural perspective. *Immunol Rev*. 2015;268(1):139-159. doi:10.1111/imr.12349

73. Allen CDC. Features of B Cell Responses Relevant to Allergic Disease. *J Immunol*. 2022;208(2):257-266. doi:10.4049/jimmunol.2100988

74. He JS, Meyer-Hermann M, Xiangying D, et al. The distinctive germinal center phase of IgE+ B lymphocytes limits their contribution to the classical memory response. *J Exp Med*. 2013;210(12):2755-2771. doi:10.1084/jem.20131539

75. Haniuda K, Fukao S, Kodama T, Hasegawa H, Kitamura D. Autonomous membrane IgE signaling prevents IgE-memory formation. *Nat Immunol*. 2016;17(9):1109-1117. doi:10.1038/ni.3508

76. Talay O, Yan D, Brightbill HD, et al. IgE + memory B cells and plasma cells generated through a germinal-center pathway. *Nat Immunol*. 2012;13(4):396-404. doi:10.1038/ni.2256

77. Talay O, Yan D, Brightbill HD, et al. Erratum: IgE+ memory B cells and plasma cells generated through a germinal-center pathway (Nature Immunology (2012) 13 (396-404)). *Nat Immunol*. 2013;14(12):1302-1304. doi:10.1038/ni.2770

78. Ramadani F, Bowen H, Upton N, et al. Ontogeny of human IgE-expressing B cells and plasma cells. *Allergy Eur J Allergy Clin Immunol*. 2017;72(1):66-76. doi:10.1111/all.12911

79. Erazo A, Kutchukhidze N, Leung M, et al. Unique Maturation Program of the IgE Response In Vivo. *Immunity*. 2007;26(2):191-203. doi:10.1016/j.immuni.2006.12.006

80. Laffleur B, Duchez S, Tarte K, et al. Self-Restrained B Cells Arise following Membrane IgE Expression. *Cell Rep*. 2015;10(6):900-909. doi:10.1016/j.celrep.2015.01.023

81. Davis AC, Shulman MJ. IgM - molecular requirements for its assembly and function. *Immunol Today*. 1989;10(4):118-128. doi:10.1016/0167-5699(89)90244-2

82. Cao A, Alluqmani N, Buhari FHM, et al. Galectin-9 binds IgM-BCR to regulate B cell signaling. *Nat Commun*. 2018;9(1). doi:10.1038/s41467-018-05771-8

83. Drinkwater N, Cossins BP, Keeble AH, et al. Human immunoglobulin E flexes between acutely bent and extended conformations. *Nat Struct Mol Biol*. 2014;21(4):397-404. doi:10.1038/nsmb.2795

84. Wurzburg BA, Jardetzky TS. Conformational Flexibility in Immunoglobulin E-Fc3-4 Revealed in Multiple Crystal Forms. *J Mol Biol*. 2009;393(1):176-190. doi:10.1016/j.jmb.2009.08.012

85. Aminov R. Editorial : Microbial and Environmental Factors in autoimmune and inflammatory diseases. 2017;8(March):6-8. doi:10.3389/fimmu.2017.00243

86. Smatti MK, Cyprian FS, Gheyath KN, Almishal RO, Yassine HM. Viruses and Autoimmunity: A Review on the Potential Interaction and Molecular Mechanisms Maria. 2019;(Figure 1):1-18.

87. Culver EL, van de Bovenkamp FS, Derksen NIL, et al. Unique patterns of glycosylation in immunoglobulin subclass G4-related disease and primary sclerosing cholangitis. *J Gastroenterol Hepatol*. 2019;34(10). doi:10.1111/jgh.14512

88. Raphael I, Nalawade S, Eagar TN, Forsthuber TG. T cell subsets and their signature cytokines in autoimmune and inflammatory diseases. *Cytokine*. 2015;74(1):5-17. doi:10.1016/j.cyto.2014.09.011.T

89. Kempers AC, Hafkenscheid L, Dorjée AL, et al. The extensive glycosylation of the ACPA variable domain observed for ACPA-IgG is absent from ACPA-IgM. *Ann Rheum Dis*. 2018;77(7):1087-1088. doi:10.1136/annrheumdis-2017-211533

90. Suwannalai P, Britsemmer K, Knevel R, et al. Low-avidity anticitrullinated protein antibodies (ACPA) are associated with a higher rate of joint destruction in rheumatoid arthritis. *Ann Rheum Dis*. 2014;73(1):270-276. doi:10.1136/annrheumdis-2012-202615

91. Stoddart A, Jackson AP, Brodsky FM. Plasticity of B cell receptor internalization upon conditional depletion of clathrin. *Mol Biol Cell*. 2005;16(5):2339-2348. doi:10.1091/mbc.e05-01-0025

92. Hou P, Araujo E, Zhao T, et al. B cell antigen receptor signaling and internalization are mutually exclusive events. *PLoS Biol*. 2006;4(7):e200. doi:10.1371/journal.pbio.0040200

93. Toscano MA, Bianco GA, Ilarregui JM, et al. Differential glycosylation of TH1, TH2 and TH-17 effector cells selectively regulates susceptibility to cell death. *Nat Immunol*. 2007;8(8):825-834. doi:10.1038/ni1482

94. Radcliffe CM, Arnold JN, Suter DM, et al. Human follicular lymphoma cells contain oligomannose glycans in the antigen-binding site of the B-cell receptor. *J Biol Chem*. 2007;282(10):7405-7415. doi:10.1074/jbc.M602690200

95. McCann KJ, Ottensmeier CH, Callard A, et al. Remarkable selective glycosylation of the immunoglobulin variable region in follicular lymphoma. *Mol Immunol*. 2008;45(6):1567-1572. doi:10.1016/j.molimm.2007.10.009

96. Chiodin G, Allen JD, Bryant DJ, et al. Insertion of atypical glycans into the tumor antigen-binding site identifies DLBCLs with distinct origin and behavior. *Blood*. 2021;138(17):1570-1582. doi:10.1182/blood.2021012052

97. Schneider D, Dühren-von Minden M, Alkhatib A, et al. Lectins from opportunistic bacteria interact with acquired variable-region glycans of surface immunoglobulin in follicular lymphoma. *Blood*. 2015;125(21):3287-3296. doi:10.1182/blood-2014-11-609404

98. Kato H, Kinoshita T, Suzuki S, et al. Production and effects of interleukin-6 and other cytokines in patients with non-Hodgkin's lymphoma. *Leuk Lymphoma*. 1998;29(1-2):71-79. doi:10.3109/10428199809058383

99. Guo Y, Xu F, Lu T, Duan Z, Zhang Z. Interleukin-6 signaling pathway in targeted therapy for cancer. *Cancer Treat Rev*. 2012;38(7):904-910. doi:10.1016/j.ctrv.2012.04.007

100. Canellada A, Blois S, Gentile T, Margni Idehu RA. In vitro modulation of protective antibody responses by estrogen, progesterone and interleukin-6. *Am J Reprod Immunol*. 2002;48(5):334-343. doi:10.1034/j.1600-0897.2002.01141.x

101. Miranda S, Canellada A, Gentile T, Margni R. Interleukin-6 and dexamethasone modulate in vitro asymmetric antibody synthesis and UDP-Glc glycoprotein glycosyltransferase activity. *J Reprod Immunol*. 2005;66(2):141-150. doi:10.1016/j.jri.2005.04.001

102. Gutiérrez G, Malan Borel I, Margni RA. The placental regulatory factor involved in the asymmetric IgG antibody synthesis responds to IL-6 features. *J Reprod Immunol*. 2001;49(1):21-32. doi:10.1016/s0165-0378(00)00074-7

103. Maverakis E, Kim K, Shimoda M, et al. Glycans In The Immune system and The Altered Glycan Theory of Autoimmunity: A Critical Review. *J Autoimmun*. 2015;(0):1-13. doi:10.1007/978-3-642-16712-6_100386

104. Bondt A, Rombouts Y, Selman MHJ, et al. Immunoglobulin G (IgG) Fab Glycosylation Analysis Using a New Mass Spectrometric High-throughput Profiling Method Reveals Pregnancy-associated Changes. *Mol Cell Proteomics*. 2014;13(11):3029-3039. doi:10.1074/mcp.M114.039537

105. Seki M, Gearhart PJ, Wood RD. DNA polymerases and somatic hypermutation of immunoglobulin genes. *EMBO Rep*. 2005;6(12):1143-1148. doi:10.1038/sj.embor.7400582

106. Masuda K, Ouchida R, Hikida M, et al. DNA polymerases eta and theta function in the same genetic pathway to generate mutations at A/T during somatic hypermutation of Ig genes. *J Biol Chem*. 2007;282(24):17387-17394. doi:10.1074/jbc.M611849200

107. Chan N, Ali M, McCallum GP, et al. Hypoxia provokes base excision repair changes and a repair-deficient, mutator phenotype in colorectal cancer cells. *Mol Cancer Res*. 2014;12(10):1407-1415. doi:10.1158/1541-7786.MCR-14-0246

108. Bahjat M, Stratigopoulou M, Pilzecker B, et al. DNA polymerase β prevents AID-instigated mutagenic non-canonical mismatch DNA repair. *bioRxiv*. Published online 2020. doi:10.1101/2020.01.30.926964

109. Hafkenscheid L, de Moel E, Smolik I, et al. N-Linked Glycans in the Variable Domain of IgG Anti–Citrullinated Protein Antibodies Predict the Development of Rheumatoid Arthritis. *Arthritis Rheumatol*. 2019;71(10):1626-1633. doi:10.1002/art.40920

110. Kissel T, Hafkenscheid L, Wesemael TJ, et al. ACPA-IgG variable domain glycosylation increases before the onset of rheumatoid arthritis and stabilizes thereafter; a cross-sectional study encompassing over 1500 samples. Published online 2021.

111. Song R, Oren DA, Franco D, Seaman MS, Ho DD. Strategic addition of an N-linked glycan to a monoclonal antibody improves its HIV-1-neutralizing activity. *Nat Biotechnol*. 2013;31(11):1047-1052. doi:10.1038/nbt.2677

112. Käsermann F, Boerema DJ, Rüegsegger M, et al. Analysis and functional consequences of increased Fab-sialylation of intravenous immunoglobulin (IVIG) after lectin fractionation. *PLoS One*. 2012;7(6):e37243. doi:10.1371/journal.pone.0037243

113. Guhr T, Bloem J, Derksen NIL, et al. Enrichment of sialylated IgG by lectin fractionation does not enhance the efficacy of immunoglobulin G in a murine model of immune thrombocytopenia. *PLoS One*. 2011;6(6):1-8. doi:10.1371/journal.pone.0021246

114. Dekkers G, Plomp R, Koeleman CAM, et al. Multi-level glyco-engineering techniques to generate IgG with defined Fc-glycans. *Sci Rep*. Published online 2016. doi:10.1038/srep36964

APPENDIX

ENGLISH SUMMARY

B cell and antibody differentiation
the contribution of glycans to repertoire diversification and classification

Our immune system has two lines of defense, innate and adaptive immunity, that work together to enable rapid and specific elimination of pathogens. Adaptive immunity depends on the activation of B and T cells for specific and long-lasting protection. The response of B cells to infection or immunization can be broadly divided into T cell-dependent B cell responses that feature a germinal center and T cell-independent B cell responses that lack GCs and feature B cell proliferation and differentiation at extrafollicular sites. B cells that receive help from T cells can differentiate into memory B cells, plasmablasts or plasma cells, of which the latter two produce antibodies.

An antibody, also called immunoglobulin, consists of two domains; a constant domain and a variable domain. The constant domain determines the (sub)class of the antibody; the possibilities are IgD, IgM, IgG1-4, IgA1-2 or IgE. The different classes exert different effector functions such as Fc-receptor binding and complement activation. The variable domain is important for the recognition and opsonization of pathogens. Each B cell has a unique specificity. In order to protect our body against a plethora of potential pathogens, the same number of antibody specificities must therefore be generated at minimum. Two processes underlying the broad diversity of the antibody repertoire are V(D)J recombination and somatic hypermutation.

During somatic hypermutation, mutations are introduced in the variable domain which can result in increased affinity of the antibody for the pathogen. In addition, it may also lead to the formation of a glycosylation site consisting of the amino acid sequence Asn -X -Ser/Thr (where X is any amino acid except proline), which may result in the generation of Fab-glycosylated antibodies. The obtained Fab glycosylation is an additional extension of the antibody repertoire diversity. The absence or presence of specific glycans may also contribute to the classification and diversification of the B cell repertoire. Different stages of B cell development and differentiation are characterized by the presence of specific glycans on proteins on the B cell surface, such as PNA-reactive O-glycans found on B cells within germinal centers. The contribution of glycans to both B cell and antibody repertoire diversification and classification is the subject of this thesis.

Antibody Fab glycosylation in itself and the location of glycosylation sites in the variable domain may be controlled by antigen-specific properties. B cell culture systems are well suited to systematically investigate the relationship between antigen and the introduction of glycosylation sites in the variable domain. To this end, it is essential that studies are

performed using true naive B cells with still unmutated antibody (Ig) genes to identify the culture-induced somatic hypermutation and potentially acquired glycosylation sites. Common strategies for the isolation of naive B cells utilize CD27 surface expression to differentiate antigen-experienced from inexperienced B cells, as CD27 expression correlates with having mutated Ig genes. However, a significant proportion of class-switched and non-class-switched B cells that do not express CD27 still carry mutated BCRs. In **Chapter 2**, we improved current isolation strategies for naive B cells ($CD27^{-}IgD^{+}$) by using markers for specific glycosylation on CD45RB and IgM. Using this optimized strategy, we obtained a population of virtually non-clonally expanded and non-mutated naive B cells.

As mentioned before, surface expression of CD27 is often used as a marker for antigen-experienced B cells, but also a fraction of $CD27^{-}$ B cells show mutated and class-switched Ig genes, characteristic of antigen-priming. In **Chapter 2**, we observed that specific O-glycosylation on CD45RB marks antigen-experienced B cells, independent of their CD27 expression. In **Chapter 3,** we therefore investigated human peripheral blood B cell subsets separated by CD45RB glycosylation, CD27 and IgM/IgD isotype expression and studied their Ig repertoire and *in vitro* functionality. We observed distinct maturation stages for $CD27^{-}$ B cells with glycosylated CD45RB, defined by differential expression of IgM and IgD. From this we concluded that glycosylation of CD45RB is indicative for antigen-primed B cells, which are, depending on the Ig isotype, functionally distinct. These findings provide new insights into the phenotypic and functional progression of naive B cells into memory B cells.

Since most glycosylation sites are the result of somatic hypermutation, it is essential to be able to induce this process during culture experiments. To date, studies able to induce somatic hypermutation in primary human B cell cultures at physiological relevant rates have not been published. Thus, optimization of B cell culture systems is needed. In **Chapter 4** we have compared and improved previously published human naive B cell cultures in order to gain more insight into the role of different T cell-dependent (TD) and -independent (TI) stimulations on B cell differentiation, antibody production and somatic hypermutation. We used optimized TD and TI stimulation protocols for in-depth analysis of B cell differentiation and antibody production in primary B cell and PBMC cultures. We found that the level of CD40L co-stimulation, cytokines IL-21 and IL-4 and the initial starting number of B cells had the greatest effects on B cell differentiation, class switch and antibody production. These insights resulted in the development of efficient B cell differentiation culture protocols that use small amounts of B cells, making these assays ideally suited for future clinical research studies with valuable patient material.

An important factor that is often overlooked during B cell culture experiments is the possible effects of oxygen pressure on B cell differentiation. In **Chapter 5** we therefore

investigated how partial oxygen pressure (pO_2) found in human lymphoid tissues (pO_2 ~1-3%) regulates naive B cell differentiation and class switching and how this compares to atmospheric oxygen pressure (pO_2 21%) generally used in culture experiments. Culturing naive B cells at 3% pO_2 promoted differentiation into antibody-secreting cells while culturing at 1% pO_2 generated a unique $CD27^{++}$ B cell population. During germinal center reactions, B cells cycle between regions with different oxygen pressures. Therefore, we also investigated the effect of time-dependent switching of cultures between 1% and 3% pO_2. We found that time-dependent pO_2 switching during culture have major effects on the ability of naive B cells to differentiate and can promote class switching and secretion of IgG antibodies. Together, we have shown that oxygen plays a crucial role during B cell differentiation and class switch to IgG and the relevance of applying physiological oxygen pressure in future research.

Diversification of the antibody repertoire may occur through the emergence of glycosylation sites in the variable domain that result in the generation of Fab-glycosylated antibodies. Insights into antibody Fab glycosylation patterns during different stages of B cell development are scarce and most studies have focused only on IgG, while the level of Fab glycans on other antibody isotypes and subclasses remains largely unknown. In **Chapter 6,** we established patterns of glycosylation sites in variable domains of naive and memory B cell repertoires. We found that for all isotypes the glycosylation sites clustered specifically around antigen binding regions (CDR1-3, DE loop). We found no evidence of site-specific selection against acquisition of a glycosylation site, except for antigen-binding region CDR3. In addition, we found increased frequencies of glycosylation sites for IgE and IgG4 antibodies compared to IgG1-3 or IgA. Together, these results point toward a differential selection pressure of glycosylation site acquisition during affinity maturation of B cells, which depends on the location within the variable domain and is isotype/subclass dependent.

Several autoantibody responses have been characterized with increased Fab glycosylation levels. However, it is unknown whether this is a common feature for antibodies that develop in the context of autoimmunity. In **Chapter 7** have we performed a disease-overarching study and determined the Fab glycosylation levels for ten different autoantibodies associated with B cell-mediated autoimmune diseases. We found that Fab glycosylation is a common feature of autoantibodies, but restricted to chronic autoimmune diseases. The importance of this finding resides, among other things, in the disease-overarching nature of this study, which points to a possible common pathophysiological mechanism of immune dysregulation in chronic autoimmune diseases.

Elevated levels of Fab glycans are thus regularly observed on antibodies that develop in the context of autoimmunity. It is unclear whether elevated Fab glycosylation levels also

occur on antibodies generated during alternative inflammatory states. Anti-hinge antibodies recognize neo-epitopes within the hinge of IgG. These neo-epitopes become exposed after proteolytic cleavage of the IgG molecule by inflammation or infection-associated endogenous or exogenous proteases. In **Chapter 8**, the levels of Fab glycosylation on anti-hinge antibodies are compared between rheumatoid arthritis (RA) patients and healthy individuals. Anti-hinge antibodies specific for neo-epitopes generated by both endogenous and exogenous proteases showed increased levels of Fab glycans in both RA patients and healthy individuals. These results suggest that elevated Fab glycosylation levels may also develop in response to an inflammatory proteolytic microenvironment, not restricted to autoimmunity.

Finally, the results presented in this thesis are summarized and put in perspective in **Chapter 9**. In this thesis we describe how glycans can contribute to repertoire diversification and classification for both B cells and antibodies. We found that glycan profiles provide insight into phenotypic and functional progression of differentiating B cell subpopulations. Moreover, we found novel patterns and biases of the acquisition of antibody Fab glycosylation during health and disease and increased our understanding of the role for Fab glycans in immunity. Our findings suggest that in-depth mapping of glycan profiles for antibodies and B cells during differentiation may be very useful, for example to improve the classification of B cell subpopulations or to monitor Fab glycans for diagnostic purposes.

NEDERLANDSE SAMENVATTING

B cel en antistof differentiatie
de bijdrage van glycanen aan repertoire diversificatie en classificatie

Ons immuunsysteem heeft twee verdedigingslinies, de aangeboren en verworven immuniteit, die samenwerken om een snelle en specifieke eliminatie van ziekteverwekkers mogelijk te maken. Verworven immuniteit is afhankelijk van de activering van B en T cellen voor specifieke en langdurige bescherming. De response van B cellen op infectie of immunisatie kan grofweg worden onderverdeeld in T cel afhankelijke B cel reacties waarbij kiemcentra worden gevormd en T cel onafhankelijke B cel reacties zonder kiemcentra waarbij B cel proliferatie en differentiatie in extrafolliculaire regio's plaatsvindt. B cellen die hulp krijgen van T cellen kunnen differentiëren tot geheugen B cellen, plasmablasten of plasmacellen waarvan de laatste twee antistoffen produceren.

Een antistof, ook wel immuunglobuline genoemd, bestaat uit twee verschillende domeinen; een constant domein en een variabel domein. Het constante domein bepaald de (sub) klassen van de antistof; de mogelijkheden zijn IgD, IgM, IgG1-4, IgA1-2 of IgE. De verschillende klassen voeren verschillende effectorfuncties uit zoals Fc-receptorbinding en complementactivering. Het variabele domein is van belang voor de herkenning en opsonisatie van ziekteverwekkers. Elke B cel heeft een unieke specificiteit. Om ons lichaam tegen grote hoeveelheden potentiële ziekteverwekkers te beschermen moeten er dus minstens evenveel antistofspecifiteiten worden gegenereerd. Twee processen die ten grondslag liggen aan de grote diversiteit van het antistof repertoire zijn V(D)J recombinatie en somatische hypermutatie.

Tijdens somatische hypermutatie worden er mutaties geïntroduceerd in het variabele domein wat kan resulteren in verhoogde affiniteit van de antistof voor de ziekteverwekker. Daarnaast kan het ook leiden tot het ontstaan van een glycosyleringsplaats wat kan resulteren in de productie van Fab-geglycosyleerde antistoffen. De verkregen Fab glycosylatie is een additionele uitbereiding van de diversiteit van het antistofrepertoire. De af- of aanwezigheid van specifieke glycanen kan tevens bijdragen aan de classificatie en diversificatie van het B cel repertoire. Verschillende stadia van B cel ontwikkeling en differentiatie worden gekenmerkt door de aanwezigheid van specifieke glycanen op eiwitten op het membraan van de B cel. Een voorbeeld hiervan zijn PNA-reactieve O-glycanen die op B cellen in de kiemcentra worden aangetroffen. De bijdrage van glycanen aan zowel B cel als antistof repertoire diversificatie en classificatie is het onderwerp van dit proefschrift.

Antistof Fab glycosylering an sich en de locatie van glycosyleringplaatsen in het variabele domein worden mogelijk gestuurd door antigeenspecifieke eigenschappen. B

cel kweeksystemen zijn zeer geschikt om systematisch de relatie tussen antigeen en de introductie van glycosyleringsplaatsen in het variabele domein te onderzoeken. Hiervoor is het essentieel dat studies worden uitgevoerd met behulp van echte naïeve B cellen met nog ongemuteerde antistof (Ig)-genen om de in kweek geïnduceerde somatische hypermutatie en mogelijk verworven glycosylatieplaatsen te identificeren. Veel gebruikte strategieën voor de isolatie van naïeve B cellen maken gebruik van CD27 membraanexpressie om antigeen-ervaren en onervaren B cellen te onderscheiden, aangezien CD27-expressie correleert met het hebben van gemuteerde Ig-genen. Echter, een aanzienlijk deel van de klasse geswitchte en niet-klasse geswitchte B cellen die geen CD27 tot expressie brengen, dragen toch gemuteerde BCR's. In **Hoofdstuk 2** hebben we de huidige isolatiestrategieën voor naïeve B cellen ($CD27^-IgD^+$) verbeterd door gebruik te maken van markers voor een specifieke glycosylering op CD45RB en IgM. Gebruikmakende van deze geoptimaliseerde strategie hebben we een populatie van vrijwel niet-klonaal geëxpandeerde en niet-gemuteerde naïeve B cellen verkregen.

Membraanexpressie van CD27 wordt zoals eerder genoemd vaak gebruikt als een marker voor antigeen-ervaren B cellen, maar ook een fractie van $CD27^-$ B cellen vertoont gemuteerde en klasse geswitchte Ig-genen, kenmerkend voor antigeen-ervaring. In **Hoofdstuk 2** hebben we waargenomen dat specifieke O-glycosylering op CD45RB antigeen-ervaren B cellen markeert, onafhankelijk van hun CD27 expressie. In **Hoofdstuk 3** bestudeerde we daarom humane B cel subsets uit perifeer bloed gescheiden door CD45RB-glycosylatie, CD27 en IgM/IgD expressie en bestudeerden we hun Ig-repertoire en *in vitro* functionaliteit. We hebben verschillende ontwikkelingsstadia waargenomen voor CD27- B cellen met geglycosyleerd CD45RB, gedefinieerd door differentiële expressie van IgM en IgD. Hieruit concludeerden we dat glycosylering van CD45RB indicatief is voor antigeen-ervaren B cellen die afhankelijk van hun klassen functioneel verschillend zijn. Deze bevindingen bieden nieuwe inzichten in de fenotypische en functionele progressie van naïeve B cellen naar geheugen B cellen.

Aangezien de meeste glycosyleringsplaatsen het resultaat zijn van somatische hypermutatie, is het essentieel om dit proces te kunnen induceren tijdens kweekproeven. Tot op heden zijn er geen studies gepubliceerd waarin somatische hypermutatie met fysiologisch relevante mutatielevels werd geïnduceerd in primaire humane B cellen. Dus optimalisatie van B cel kweeksystemen is nodig. In **Hoofdstuk 4** hebben we eerder gepubliceerde humane naïeve B celkweken vergeleken en verbeterd met als doel om meer inzicht te krijgen in de rol van de verschillende T cel afhankelijke (TA) en onafhankelijke (TO) stimulaties op B cel differentiatie, antistof productie en somatische hypermutatie. We hebben geoptimaliseerde TA- en TO-stimulatieprotocollen gebruikt voor een diepgaande analyse van B cel differentiatie en antistof productie in primaire B cel en PBMC kweken. We ondervonden dat de mate van CD40L co-stimulatie, cytokines IL-21 en IL-4 en het initiële

beginaantal B cellen de grootste effecten hadden op B cel differentiatie, klasse switch en antistof productie. De verkregen inzichten resulteerde in de ontwikkeling van efficiënte B cel differentiatie kweekprotocollen die gebruik maken van kleine hoeveelheden B cellen wat deze tests bij uitstek geschikt maakt voor toekomstige klinische onderzoekstudies met kostbaar patiëntmateriaal.

Een belangrijke factor die vaak over het hoofd wordt gezien tijdens B cel kweekproeven zijn de mogelijke effecten van zuurstofdruk op B cel differentiatie. In **Hoofdstuk 5** hebben we daarom onderzocht hoe partiële zuurstofdruk (pO_2) gevonden in humaan lymfoïde weefsel (pO_2 ~1-3%) naïeve B cel differentiatie en klasse switch reguleert en hoe dit zich verhoud tot atmosferische zuurstofdruk (pO_2 21%) die over het algemeen wordt toegepast bij kweekproeven. Het kweken van naieve B cellen bij 3% pO_2 bevorderde differentiatie tot antistof-secreterende cellen terwijl bij 1% een unieke $CD27^{++}$ B cel populatie werd gegenereerd. Tijdens kiemcentra reacties migreren B cellen tussen regio's met verschillende pO_2. Daarom onderzochten we ook het effect van tijdsafhankelijke wisselingen tussen 1% en 3 % pO_2. Hier ondervonden we dat pO_2 wisselingen grote effecten hebben op de mogelijkheid van naïeve B cellen om te differentiëren en de klasse switch en de secretie van IgG antistoffen kan bevorderen. Hiermee hebben we laten zien dat zuurstof een cruciale rol speelt tijdens B cel differentiatie en klasse switch naar IgG en de relevantie van het toepassen van fysiologische zuurstofdruk in toekomstig onderzoek.

Diversificatie van het antistof repertoire kan plaatsvinden door het ontstaan van glycosyleringsplaatsen in het variabele domein die kunnen resulteren in de generatie van Fab-geglycosyleerde antistoffen. Inzicht in antistof Fab glycosylerings patronen tijdens verschillende stadia van B cel ontwikkeling zijn schaars en de meeste onderzoeken hebben zich alleen gericht op IgG, terwijl het niveau van Fab glycanen op andere antistof (sub)klassen nog grotendeels onbekend is. Daarom hebben we in **Hoofdstuk 6** patronen van glycosyleringsplaatsen in kaart gebracht van de variabele domeinen van antistoffen behorende bij naïeve en geheugen B cellen. Hierbij vonden we dat voor alle klassen de glycosyleringsplaatsen zich specifiek clusterden rondom antigeenbindingregio's (CDR1-3, DE lus). We vonden geen bewijs dat er locatie-specifieke selectie plaats vond tegen het verkrijgen van een glycosyleringsplaats, behalve voor de antigeenbindingsregio CDR3. Daarnaast vonden we voor IgE en IgG4 antistoffen verhoogde frequenties van glycosyleringsplaatsen ten opzichte van IgG1-3 of IgA. Samen wijzen deze resultaten op een differentiële selectiedruk voor het verkrijgen van glycosyleringsplaatsen tijdens affiniteitsrijping van B cellen, die afhangt van de locatie binnen het variabele domein en van de (sub)klassen van de antistof.

Meerdere auto-antistof responsen zijn gekarakteriseerd met verhoogde Fab glycosylerings niveaus. Het is echter niet bekend of dit een algemeen kenmerk is voor antistoffen die zich

ontwikkelen in de context van auto-immuniteit. In **Hoofdstuk 7** hebben we een ziekte-overstijgend onderzoek uitgevoerd en de Fab glycosylerings niveaus bepaald voor tien verschillende auto-antistoffen geassocieerd met B cel gemedieerde auto-immuunziekten. We ontdekten dat Fab glycosylatie een veelvoorkomend kenmerk is van auto-antistoffen geassocieerd met auto-immuunziekten, maar zich beperkte tot chronische auto-immuunziekten. Het belang van deze bevinding ligt onder andere in de ziekte-overstijgende aard van deze studie, die wijst op een mogelijk gemeenschappelijk pathofysiologisch mechanisme van immuun ontregeling bij chronische auto-immuunziekten.

Verhoogde niveaus van Fab glycanen worden dus regelmatig geobserveerd op antistoffen die zich ontwikkelen in de context van auto-immuniteit. Het is onduidelijk of verhoogde Fab glycosylerings niveaus ook voorkomen op antistoffen die ontstaan tijdens andere inflammatoire toestanden. Anti-hinge antistoffen herkennen neo-epitopen in de hinge van IgG. Deze neo-epitopen zijn blootgesteld nadat het IgG molecuul door midden is geknipt door ontsteking of infectie-geassocieerde endogene of exogene proteasen. In **Hoofdstuk 8** worden de niveaus van Fab glycanen op anti-hinge antistoffen vergeleken tussen patiënten met reuma en gezonde individuen. Anti-hinge antistoffen die binden aan neo-epitopen gegenereerd door zowel endogene als exogene proteasen vertoonden verhoogde niveaus van Fab glycanen bij zowel reuma patiënten als gezonde individuen. Deze resultaten suggereren dat verhoogde Fab glycosylering niveaus zich ook kunnen ontwikkelen in een inflammatoir proteolytisch micro-milieu, en dus niet beperkt is tot auto-immuniteit.

Ten slotte worden de in dit proefschrift gepresenteerde resultaten samengevat en in perspectief geplaatst in **Hoofdstuk 9**. In dit proefschrift beschrijven we hoe glycanen kunnen bijdragen aan repertoirediversificatie en classificatie voor zowel B cellen als voor antistoffen. Zo ontdekten we dat glycaanprofielen inzicht geven in fenotypische en functionele progressie van differentiërende B cel subpopulaties. Bovendien vonden we nieuwe en afwijkende Fab glycosylerings patronen op antistofresponsen tijdens gezondheid en ziekte en vergrootten we ons begrip van de rol van Fab glycanen in immuniteit. Onze bevindingen suggereren dat toekomstig onderzoek om glycaanprofielen op antistoffen en op B cellen tijdens differentiatie in kaart te brengen zeer nuttig kan zijn, bijvoorbeeld om de classificatie van B cel subpopulaties te verbeteren of om Fab glycanen te monitoren voor diagnostische doeleinden.

LIST OF PUBLICATIONS

1. **Koers J**, Sciarrillo R, Derksen NIL, Vletter EM, Fillié-Grijpma YE, Raveling-Eelsing E, et al., Differences in IgG autoantibody Fab glycosylation across autoimmune diseases. *Journal of Allergy and Clinical Immunology (2023).*
2. **Koers J**, Marsman C, Steuten J, Tol S, Derksen NIL, ten Brinke A, van Ham SM, Rispens T. Oxygen level is a critical regulator of human B cell differentiation and IgG class switch recombination. *Frontiers in Immunology (2022).*
3. **Koers J**, Pollastro S, Tol S, Niewold ITG, van Schouwenburg PA, de Vries N, Rispens T. Improving naive B cell isolation by absence of CD45RB glycosylation and CD27 expression in combination with BCR isotype. *European Journal of Immunology (2022).*
4. Marsman C, Verhoeven D, **Koers J**, T2B consortium, Rispens T, ten Brinke A, van Ham SM, Kuijpers TW. Optimized protocols for in vitro T cell-dependent and T cell-independent activation for B cell differentiation studies using limited cells. *Frontiers in Immunology (2022).*
5. **Koers J**, Pollastro S, Tol S, Pico-Knijnenburg I, Derksen NIL, van Schouwenburg PA, van der Burg M, van Ham SM, Rispens T. CD45RB glycosylation and BCR isotype define maturation of functionally distinct B cell subsets in human peripheral blood. *Frontiers in Immunology (2022).*
6. **Koers J**, Derksen NIL, Falkenburg WJJ, Ooijevaar-de Heer P, Nurmohamed MT, Wolbink GJ, Rispens T. Elevated Fab glycosylation of anti-hinge antibodies. *Scandinavian Journal of Rheumatology* (2021).
7. Falkenburg WJJ, Oskam N, **Koers J**, van Boheemen L, Ooijevaar-de Heer P, Verstappen GM, Bootsma H, Kroese FGM, van Schaardenburg D, Wolbink G, Rispens T. Identification of Clinically and Pathophysiologically Relevant Rheumatoid Factor Epitopes by Engineered IgG Targets. *Arthritis Rheumatology* (2020).
8. Temming AR, de Taeye SW, de Graaf EL, de Neef LA, Dekkers G, Bruggeman CW, **Koers J**, Ligthart P, Nagelkerke SQ, Zimring JC, Kuijpers TW, Wuhrer M, Rispens T, Vidarsson G. Functional Attributes of Antibodies, Effector Cells, and Target Cells Affecting NK Cell–Mediated Antibody-Dependent Cellular Cytotoxicity. *Journal of Immunol*ogy (2019).
9. **Koers J**, Derksen NIL, Ooijevaar-de Heer P, Nota B, van de Bovenkamp FS, Vidarsson G, Rispens T. Biased *N*-glycosylation site distribution and acquisition across the antibody V region during B cell maturation. *Journal of Immunol*ogy (2019).
10. Culver EL, van de Bovenkamp FS, Derksen NIL, **Koers J**, Cargill T, Barnes E, de Neef LA, Koeleman CAM, Aalberse RC, Wuhrer M, Rispens T. Unique patterns of glycosylation in immunoglobulin subclass G4-related disease and primary sclerosing cholangitis. *Journal of Gastroenterology and Hepatol*ogy (2018).
11. Falkenburg WJ, von Richthofen HJ, **Koers J**, Weykamp C, Schreurs MWJ, Bakker-Jonges LE, Haagen I, Lems WF, Hamann D, Schaardenburg D, Rispens T. Clinically relevant discrepancies between different rheumatoid factor assays. *Clinical Chemistry and Laboratory Medicine* (2018).
12. Falkenburg WJ, Schaardenburg D, **Koers J**, Ooijevaar-de Heer P, Wolbink G, Bentlage AEH, Vidarsson G, Rispens T. Rheumatoid factors may potentiate immune complex formation of anti-citrullinated protein antibodies. *Arthritis Rheumatology* (2016).

CONTRIBUTING AUTHORS

CHAPTER 2

Koers J[1], Pollastro S[1], Tol S[2], Niewold ITG[3], de Vries N[3], Rispens T[1]

Improving naive B cell isolation by absence of CD45RB glycosylation and CD27 expression in combination with BCR isotype

1 Sanquin Research, Department of Immunopathology, and Landsteiner Laboratory, Amsterdam University medical centers, University of Amsterdam, Amsterdam, The Netherlands.
2 Sanquin Research, Department of Research facilities, and Landsteiner Laboratory, Amsterdam University medical centers, University of Amsterdam, Amsterdam, The Netherlands.
3 Amsterdam Rheumatology and Immunology Center, Amsterdam University medical centers, University of Amsterdam, Amsterdam, The Netherlands.

JK, SP and TR designed research. JK, ST, and IN performed research. SP and JK analyzed data. JK, SP, NV and TR wrote the paper. All authors critically reviewed the manuscript, gave final approval of the version to be published, and agreed to be accountable for all aspects of the work ensuring that questions related to the accuracy or integrity of any part of the work are appropriately investigated and resolved.

CHAPTER 3

Koers J[1], Pollastro S[1], Tol S[2], Derksen NIL[1], Pico I[3], Schouwenburg P[4], van der Burg M[4], van Ham SM[1,4], Rispens T[1]

CD45RB glycosylation and Ig isotype define maturation of functionally distinct B cell subsets in human peripheral blood

1 Sanquin Research, Department of Immunopathology, and Landsteiner Laboratory, Amsterdam UMC, University of Amsterdam, Amsterdam, The Netherlands.
2 Sanquin Research, Department of Research Facilities, and Landsteiner Laboratory, Amsterdam UMC, University of Amsterdam, Amsterdam, The Netherlands.
3 Department of Pediatrics, Laboratory for Pediatric Immunology, Leiden University Medical Center, Leiden, Netherlands.
4 Swammerdam Institute for Life Sciences, University of Amsterdam, Amsterdam, the Netherlands.

JK, SP, ST, PS, MB and TR designed research. JK, ST, IP and ND performed research. JK, SP and ND analyzed data. JK, SH and TR wrote the paper. All authors critically reviewed the manuscript, gave final approval of the version to be published, and agreed to be accountable for all aspects of the work ensuring that questions related to the accuracy or integrity of any part of the work are appropriately investigated and resolved.

CHAPTER 4

Marsman C[1], Verhoeven D[2,3], Koers J[1], T2B consortium, Rispens T[1], ten Brinke A[1], van Ham SM[1,4], Kuijpers TW[2]

Optimized protocols for *in vitro* T cell-dependent and T cell-independent activation for B cell differentiation studies using limited cells

1 Sanquin Research, Department of Immunopathology, and Landsteiner Laboratory, Amsterdam UMC, University of Amsterdam, Amsterdam, The Netherlands.
2 Amsterdam UMC, University of Amsterdam, Department of Pediatric Immunology, Rheumatology and Infectious Diseases, Emma Children's Hospital, Amsterdam, the Netherlands.
3 Amsterdam UMC, University of Amsterdam, Department of Experimental Immunology, Amsterdam Institute for Infection & Immunity, Amsterdam, the Netherlands.
4 Swammerdam Institute for Life Sciences, University of Amsterdam, Amsterdam, the Netherlands.

JK, CM, JS, AB, SH and TR designed research. JK, CM, JS, ST and ND performed research. JK, CM and JS analyzed data. JK, CM, JS, AB, SH and TR wrote the paper. All authors critically reviewed the manuscript, gave final approval of the version to be published, and agreed to be accountable for all aspects of the work ensuring that questions related to the accuracy or integrity of any part of the work are appropriately investigated and resolved.

CHAPTER 5

Koers J[1], Marsman C[1], Steuten J[1], Tol S[2], Derksen NIL[1], ten Brinke A[1], van Ham SM[1,3], Rispens T[1]

Oxygen level is a critical regulator of human B cell differentiation and IgG class switch recombination

1 Sanquin Research, Department of Immunopathology, and Landsteiner Laboratory, Amsterdam UMC, University of Amsterdam, Amsterdam, The Netherlands.

[2] Sanquin Research, Department of Research Facilities, and Landsteiner Laboratory, Amsterdam UMC, University of Amsterdam, Amsterdam, The Netherlands.
[3] Swammerdam Institute for Life Sciences, University of Amsterdam, Amsterdam, the Netherlands.

JK, CM, JS, AB, SH and TR designed research. JK, CM, JS, ST and ND performed research. JK, CM and JS analyzed data. JK, CM, JS, AB, SH and TR wrote the paper. All authors critically reviewed the manuscript, gave final approval of the version to be published, and agreed to be accountable for all aspects of the work ensuring that questions related to the accuracy or integrity of any part of the work are appropriately investigated and resolved.

CHAPTER 6

Koers J[1], Derksen NIL[1], Ooijevaar-de Heer P[1], Nota B[2], van de Bovenkamp FS[1,3], Vidarsson G[4], Rispens T[1]

Biased *N*-glycosylation site distribution and acquisition across the antibody V region during B cell maturation

[1] Department of Immunopathology, Sanquin Research and Landsteiner Laboratory, Amsterdam University Medical Center, University of Amsterdam, Amsterdam, the Netherlands.
[2] Department of Research Facilities, Sanquin Research and Landsteiner Laboratory, Amsterdam University Medical Center, University of Amsterdam, Amsterdam, the Netherlands.
[3] Department of Immunohematology and Blood Transfusion, Leiden University Medical Center, Leiden, the Netherlands.
[4] Department of Experimental Immunohematology, Sanquin Research and Landsteiner Laboratory, Amsterdam University Medical Center, University of Amsterdam, Amsterdam, the Netherlands

JK and TR designed research. JK and TR collected data used in this study. JK, ND, PO performed research. JK, BN and TR analyzed data. JK, FB, GV and TR wrote the paper. All authors critically reviewed the manuscript, gave final approval of the version to be published, and agreed to be accountable for all aspects of the work ensuring that questions related to the accuracy or integrity of any part of the work are appropriately investigated and resolved.

CHAPTER 7

Koers J[1], Sciarrillo R[1], Derksen NIL[1], Vletter EM[2], Fillié-Grijpma YE[3], Raveling-Eelsing E[4], Graça NAG[5], Leijser T[1], Pas HH[6], van Nijen-Vos LL[6], Braham MVJ[7], Buisman A[7], de Jong J[8], Schriek AI[13], Tio-Gillen AP[9,10], Teng YKO[11], Steenhuis M[1], Swaneveld FH[12], de Taeye SW[13], van Gils MJ[13], Verschuuren JJGM[14], Rutgers B[4], Heeringa P[15], Horváth B[6], Jacobs BC[9,10], de Leeuw K[4], Franssen CFM[16], Veyradier A[17,18], Coppo P[18,19], Gelderman KA[8], van Ham SM[1,20], van Els CACM[7], van der Woude D[2], Huizinga R[9], Huijbers MG[3,14], Kuijpers TW[21,22], Toes REM[2], Bos NA[4], Rispens T[1], on behalf of the T2B consortium

Differences in IgG autoantibody Fab glycosylation across autoimmune diseases

1 Sanquin Research, Department of Immunopathology, and Landsteiner Laboratory, Amsterdam University Medical Center, University of Amsterdam, Amsterdam, The Netherlands
2 Department of Rheumatology, Leiden University Medical Center, Leiden, The Netherlands
3 Department of Human Genetics, Leiden University Medical Center, Leiden, The Netherlands
4 Department of Rheumatology and Clinical Immunology, University Medical Center Groningen and University of Groningen, Groningen, The Netherlands
5 Department of Molecular Hematology, and Landsteiner Laboratory, Amsterdam University Medical Center, University of Amsterdam, Amsterdam, The Netherlands
6 Centre for Blistering Diseases, Department of Dermatology, University Medical Center Groningen, University of Groningen, Groningen, The Netherlands
7 Centre for Infectious Disease Control, National Institute for Public Health and the Environment, Bilthoven, The Netherlands
8 Sanquin Diagnostic Services, Amsterdam, The Netherlands
9 Department of Immunology, Erasmus MC, University Medical Center Rotterdam, Rotterdam, The Netherlands
10 Department of Neurology, Erasmus MC, University Medical Center Rotterdam, Rotterdam, The Netherlands
11 Department of Nephrology, Leiden University Medical Center, Leiden, The Netherlands
12 Department of Transfusion Medicine Sanquin Blood Bank Amsterdam The Netherlands
13 Department of Medical Microbiology and Infection Prevention, Amsterdam University Medical Center, University of Amsterdam, Amsterdam Infection and Immunity Institute, Amsterdam, The Netherlands
14 Department of Neurology, Leiden University Medical Center, Leiden, The Netherlands
15 Deptarment of Pathology and Medical Biology, University Medical Center Groningen and University of Groningen, Groningen, The Netherlands

[16] Department of Internal Medicine, University Medical Center Groningen and University of Groningen, Groningen, The Netherlands
[17] Service d'Hématologie biologique, Hôpital Lariboisière and EA-3518 Institut de Recherche Saint Louis, Assistance Publique-Hôpitaux de Paris, Université de Paris, France
[18] Centre de Référence des Microangiopathies Thrombotiques, Hôpital Saint-Antoine, AP-HP, Paris, France
[19] Service d'Hématologie, Hôpital Saint-Antoine, AP-HP, Paris, France Sorbonne Université, UPMC Univ Paris, Paris, France
[20] Swammerdam Institute for Life Sciences, University of Amsterdam, Amsterdam, The Netherlands
[21] Department of Pediatric Hematology, Immunology and Infectious Diseases, Emma Children's Hospital, Amsterdam University Medical Centre, Amsterdam, The Netherlands
[22] Department of Blood Cell Research, Sanquin Research and Landsteiner Laboratory, Amsterdam University Medical Centre, University of Amsterdam, Amsterdam, The Netherlands

JK, RS, NB, TK, and TR designed research. JK, RS, ND, TL, YF, ER, EV, HP, MB, LN, JJ and NG performed research. JK, RS, ND, YF, ER, EV, HP, NG and TR analyzed data. JK, NB, TK, DW, RT, RH, CE, MH, and TR wrote the paper. All authors critically reviewed the manuscript, gave final approval of the version to be published, and agreed to be accountable for all aspects of the work ensuring that questions related to the accuracy or integrity of any part of the work are appropriately investigated and resolved.

CHAPTER 8

Koers J[1], Derksen NIL[1], Falkenburg WJJ[2], Ooijenvaar-de Heer P[1], Nurmohamed MT[3,4], Wolbink GJ[4], and Rispens T[1]

Elevated Fab glycosylation on anti-hinge antibodies

[1] Sanquin Research, Department of Immunopathology, and Landsteiner Laboratory, Amsterdam University Medical Center, University of Amsterdam, Amsterdam, The Netherlands.
[2] Department of Medical Microbiology, Amsterdam University Medical Centers, University of Amsterdam, Amsterdam, The Netherlands.
[3] Reade, Department of Rheumatology, Amsterdam Rheumatology and Immunology center, Amsterdam, The Netherlands.
[4] Amsterdam Rheumatology and Immunology center, Amsterdam University Medical Center, VU University Medical Center, Amsterdam, The Netherlands

JK, WF, GW and TR designed research. JK, ND, PO and WF performed research. JK, ND, WF and TR analyzed data. JK, TR, GW and MN wrote the paper. All authors critically reviewed the manuscript, gave final approval of the version to be published, and agreed to be accountable for all aspects of the work ensuring that questions related to the accuracy or integrity of any part of the work are appropriately investigated and resolved.

PHD PORTFOLIO

Name PhD student: Jana Koers
PhD period: May 1st 2017 – July 31st 2022
Promotor: Prof. dr. S.M. van Ham
Co-promotor: dr. T. Rispens

PHD TRAINING

	Year	ECTS
General courses		
Advanced Immunology	2018	2.5
Sanquin science course (*oral*)	2017	0.5
ENII - Advanced Immunology Summer School (*poster*)	2018	2.0
Scientific Integrity	2018	0.2
Personal development program (module 2 - 4)	2018 – 2021	1.5
Specific courses		
Project Management	2018	1.5
R course	2018	1.5
Advanced Flow Cytometry	2018	1.5
Personal Leadership	2021	0.5
Seminars and workshops		
Weekly IP Department meetings	2017 – 2022	5.0
Biweekly Journal Club	2017 – 2022	2.5
Monthly IP seminar	2017 – 2020	2.5
Weekly Sanquin Research Staff Meeting	2017 – 2022	5.0
Landsteiner Lectures and guest speaker seminars	2017 – 2022	2.5
Sanquin Science Day (*posters 4x*)	2017/8/9/21	3.0
Masterclasses		
Master class Brian Sutton	2017	0.2
Master class Andre Veillette	2017	0.2
Master class Meinrad Busslinger	2017	0.2
Master class Muzlifa Hanifa	2018	0.2

	Year	ECTS
National and international conferences		
Keystone symposia B cell - T cell interactions (*poster 2x*)	2019, 2022	5.0
NVVI Winter School (*posters 2x*)	2017-2022	3.0
AI&II (*poster, orals 2x*)	2017-2019	3.0
European Congress of Immunology (*posters 2x*)	2018, 2021	2.0
European B cell network	2021	0.5
T2B symposia (*orals 2x*)	2021, 2022	1.0
Teaching and Supervision		
Practical course assistant – "Immunology: research and clinic"	2017-2021	4.0
MSc student Ikram Sarti (internship, 8 months)	2019	3.0
MSc student Thiemo Leijer (internship, 5 months)	2020	2.0

CURRICULUM VITAE

Jana Koers is geboren op 23 december 1993 te Nijmegen. In 2011 behaalde ze haar VWO diploma aan de Stedelijke Scholen Gemeenschap Nijmegen (SSGN) met het dubbelprofiel natuur & gezondheid en natuur & techniek. In 2011 verhuisde ze naar Amsterdam en begon ze aan haar studie Biomedische Wetenschappen aan de Universiteit van Amsterdam (UvA). Tijdens haar bachelor liep ze stage bij AMOLF academische instituut voor fundamentele natuurkunde in Amsterdam onder leiding van Prof. dr. Tom Shimizu, waar ze onderzoek deed naar genen betrokken bij veroudering in modelorganisme C. elegans. Gedurende haar bachelor was ze vicevoorzitter van de opleidingscommissie, waar ze meedacht over het optimaliseren van het bachelor curriculum biomedische Wetenschappen.

In 2014 ronde ze haar bachelor af, en vervolgde haar opleiding aan de Vrije Universiteit van Amsterdam met de master Biomolecular Sciences en specialiseerde zich in Biological Chemistry en Molecular Cell Biology. Gedurende haar master werkte ze als practicum assistent voor bachelor studenten Biomedische Wetenschappen van de UvA zowel als van de VU. Haar eerste masterstage deed ze bij het Charité academisch ziekenhuis van Berlijn, Duitsland, waar ze onder leiding van Prof. dr. Michael Schupp retinol metabolisme in vetcellen onderzocht. Haar afstudeerstage vond plaats op de afdeling Immunopathologie van Sanquin, waar ze onder leiding van dr. Theo Rispens onderzoek deed naar autoantistoffen in reumatoïde artritis. De resultaten van deze stage hebben bijgedragen aan meerdere publicaties. Ze ronde haar master af begin 2017 met een onderzoeksvoorstel wederom onder leiding van dr. Theo Rispens. Hierin formuleerde ze onderzoeksstrategieën voor het karakteriseren en onderscheiden van humane IgM pentameren en hexameren, waarvan de inhoud heeft bijgedragen aan huidig promotieonderzoek.

In mei 2017 begon haar promotieonderzoek op de afdeling Immunopathologie van Sanquin Research onder de begeleiding van dr. Theo Rispens. Tijdens haar promotietraject werkte ze aan antistof Fab glycosylering in gezondheid en ziekte. De resultaten van dit onderzoek hebben bijgedragen aan het tot stand komen van dit proefschrift.

DANKWOORD

Dit proefschrift is het resultaat van vijf jaar onderzoek. Ik wil graag iedereen bedanken die heeft bijgedragen aan het tot stand komen van dit proefschrift, waarbij een aantal van jullie in het bijzonder.

Theo, mijn co-promotor en wetenschappelijke allesweter. Al tijdens mijn stage op Sanquin kwam ik er achter dat ik wilde gaan promoveren maar op één voorwaarde dat dat onder jouw begeleiding zou gaan gebeuren. En zo geschiedde het. Natuurlijk wil ik je bedanken voor je input, kritische blik en wetenschappelijke discussies, maar bovenal wil ik je bedanken voor de autonomie die je me hebt gegeven de afgelopen vijf jaar. Het vertrouwen dat je me gaf dat ik mijn eigen projecten kon en mocht runnen heeft mijn persoonlijke groei een enorme boost gegeven. Theo bedankt, wat waren we een super team!

Marieke, mijn promoter en de 'mammie' van deze geweldige afdeling. De coronapandemie was een uitdaging van de bovenste plank met name om de afdeling bij elkaar te houden en verbinding te blijven zoeken ondanks fysieke afwezigheid. Ik bewonder hoe je dat hebt getackeld met bijvoorbeeld jouw persoonlijke mailtjes om ons op te vrolijken en ons te overtuigen de moed erin te houden. Bedankt voor af en toe dat duwtje in de rug en een goed gesprek. De B cel werkbesprekingen waren mijn absolute favoriet, fijn dat ik hier welkom was.

Naast mijn promotor en co-promotor wil ik natuurlijk ook de andere leden van mijn OIO-begeleidingscommissie bedanken. **Gestur** en **Martijn** bedankt voor de nuttige en leuke discussies en het waarborgen van mijn PhD planning.

Mijn paranimfen: **Ninotska** en **Simon**, wat een eer dat jullie mijn paranimfen willen zijn en wat hebben jullie dit verdiend! Ik kan me geen betere voorstelling maken dan dat ik jullie aan mijn zij heb tijdens de verdediging van mijn proefschrift. **Ninotska**, mijn steun en toeverlaat. Proeven doen met jou was altijd gezellig. Team Ninja, Kip en eekhoorn of toch jut en jul. Ik kan genieten van je neurotische trekjes op het lab en ik ben dankbaar voor je altijd betrouwbare proeven. Naast dat je onmisbaar bent geweest op het gebied van wetenschappelijke input kon ik ook altijd bij je terecht voor een goed gesprek, advies een lach en een traan, dankjewel dat je er altijd voor me was. Hopelijk blijven we onze traditie van theekransjes met taart voortzetten. **Simon**, mijn held! Wat heb jij een onmisbare input gegeven aan de cellulaire projecten in dit proefschrift. Bedankt voor al je geduld en uitleg over het FACSen en sorten van mijn B celletjes. Ik heb goede herinneringen aan onze memorabele sort-sessies tot diep in de nacht met Netflix, een vette hap van McDonalds en tussen de samples door een tukje op de groene bankjes. Bedankt dat je altijd weer in

was voor een nieuwe proef die nog gekker, nog langer, nog meer gates of nog meer platen nodig had.

Graag wil ik ook de andere PI's van de afdeling bedanken. **Anja**, bedankt voor je kritische en pragmatische aanpak die vaker dan eens mijn projecten een goede impuls vooruit hebben gegeven. **Ilse**, ontzettend bedankt voor je ondersteuning om een baan te veroveren bij Genmab. Wat gezellig dat we nu weer collega's zijn. Ook **Robbert**, **Diana**, **Gert-jan**, en **Sascha** erg bedankt voor jullie nuttige feedback en input de afgelopen jaren.

Lieve oud AIOs, ik ben bevoorrecht dat ik samen met jullie heb mogen promoveren. Bedankt voor jullie warme welkom en fijn dat ik altijd met mijn vragen bij jullie terecht kon, en nog steeds kan. Maar bovenal wil ik jullie bedanken voor alle gekkigheid en gezelligheid die we samen hebben meegemaakt op borrels, feestjes, kerstdiners, OIO+ diners en weekendjes weg.

Willem, mijn avontuur op Sanquin begon onder jouw vleugel, een fijne plek. Jij hebt mij het vertrouwen gegeven dat ik 'slim' genoeg zou zijn om een PhD te gaan doen en daar ben ik je heel dankbaar voor. Ook bedankt voor al je goede adviezen en gezelligheid door de jaren heen. B cell boys **Casper**, **Niels** en **Peter-Paul** bedankt dat jullie mij alles leerden over B cellen. Ik koester nog goede herinneringen aan onze kweeklabsessies waar we pipetteerden en twerkten onder het genot van de SlamFM mix marathon. De B cell Keystone symposia in Keystone en Hannover met **Casper**, **Niels**, **Erik**, **Nieke** en **Dorit** waren een absoluut hoogtepunt tijdens mijn PhD. **Sanne**, **Anna van Beek**, **Anna Kroeze** en **Marlieke** bedankt voor alle gezellige weekendjes weg, high-tea en shop sessies. Hopelijk volgen er nog veel meer. **Laura** (culo, Guapi, dushi) mijn fantastische danspartner en tequila zusje. Ik heb genoten van onze avonturen! **Lea,** bedankt dat je zo'n gezellige buurvrouw was. **Juulke**, bedankt voor je aanstekelijke lach en gezelligheid. Ik heb goede herinneringen aan onze hypoxia thuiswerk sessies vergezeld door Betty en Worias. Ook bedankt aan **Inge**, **Karin**, **Richard**, **Anouk**, **Twan**, **Astrid**, **Anno**, **Saskia, Jorn** en **Judith**.

Aan alle huidige PhDs: **Nieke**, **Esther**, **Tamara**, **Yasmin**, **Nienke**, **Myrddin**, **Christine**, **Milou**, **Lisan, Bert** en **Laura Kummer**, bedankt voor de gezelligheid.

Bella **Sabrina**, het was leuk om met jou samen te werken. Bedankt voor je onmisbare bijdrage aan dit proefschrift en je vrolijke en doortastende spirit.

Jolanda en **Irma**, wat heb ik genoten van het les geven op het Science park zowel tijdens mijn master als later tijdens mijn PhD. **Jolanda**, zonder jou was dit avontuur nooit begonnen jij bent de drijfveer geweest van mijn carrière op Sanquin. Uit de grond van mijn hart wil

ik je bedanken voor je vertrouwen en geloof in mijn kunnen, iets wat jij al veel eerder zag dan ik zelf.

Ook bedankt aan alle andere IP-ers die bijdragen of hebben bijgedragen aan deze fantastische afdeling: **Pleuni**, **Gerard**, **Angela**, **Dorina**, **Dorien**, **Mieke**, **Ingrid**, **Ellen**, **Lisanne**, **Simone**, **Annelies**, **Kim**, **Iris**, **Gijs**, **Tineke**, **Miranda**, **Jorn**, **Floris**, **Christina**, **Sophie**, **Henk**, **John**, **Rocco**, **Daniela**, **George**, **Ina**, **Jerry**, **Brenda**, **Bruno**, **Virginia**, **Amelie**, **Mariel**, **Suzanne**, **Marij**, **Rob**, **Jolinde**, **Olvie**, **Sofie**, **Jim**, **Arend**, **Maurice**, **Julian**, **Sinead**, **Veronique**, **Domenique** en **Nadine**.

Fatima, als er toch iemand de koningin van het regelen is ben jij het! Ontzettend bedankt voor al je hulp en steun in het bijzonder tijdens de laatste fase van mijn promotieonderzoek. Jij bent, samen met **Kaoutar**, onmisbaar voor deze afdeling!

Tijdens mijn promotie heb ik met veel plezier studenten mogen begeleiden en ook hen wil ik graag bedanken. **Ikram**, jij was de eerste student die ik mocht begeleiden. Ik vond het leuk te zien hoe enthousiast en doortastend je was ondanks het lastig project. **Thiemo**, I have admired your motivation and perseverance even though you had to switch supervisors and was held back due to restrictions of the pandemic.

De Sardinië 2018 crew: **Casper**, **Laura**, **Loreto**, **Judith**, **Ammarina**, **Max** en **Twan**. Het was een legendarische week van tequila party's, volvreten, wijn drinken, Doerak spelen en af en toe ook een beetje science. Bedankt dat jullie deze trip zo memorabel hebben gemaakt en is zonder twijfel een van de hoogtepunten van mijn PhD.

De leukste en baddest boys in town: de leden van G-unit **Arthur, Steven**, **Max**, **Zoltan**, **Robin**, **Erik**, **Mads**, **Thijs** en **Timon. Arthur**, het is altijd gezellig met jou door dik en dun. Je kww filosofie gaf regelmatig een relativerend steuntje in de rug. Ik heb genoten van onze gymsessies, cheat days en borrels. **Steven**, HOEEE bedankt voor alle gezelligheid maar ook voor je bijdrage aan dit proefschrift met AHA en PLWH. **Max**, heerlijk hoe jij science kan bedrijven…mic drop. **Timon**, I loved dancing with you on the floor.

Alex, thank you for all the fun, delicious food and helping me design my thesis.

Bedankt ook aan alle andere party people die de vele borrels fantastisch hebben gemaakt: **Rivelino** (wanneer gaan we weer Pisang drinken?), **Mark**, **Carlijn**, **Felix**, **Anna Oja**, **Florencia**, **Roos**, **Milena**, **Franscesca**, **Bram**, **Bogac** en **Natasja**.

Graag wil ik ook de mensen van **Cryobiologie** bedanken. Fijn dat jullie altijd zo goed voor mijn ingevroren B celletjes hebben gezorgd en alle keren dat ik vergeten was cellen

aan te vragen en jullie zo vriendelijk waren deze last-minute nog voor mij uit de kou te trekken. **Susan Cavay** bedankt voor het opspeuren van bloeddonoren. En **Erik**, **Simon**, **Mark**, **Floris** en **Tom** bedankt voor de ongelofelijke gesmeerde Faciliteit die jullie runnen op Sanquin. Daar mogen jullie trots op zijn!

Graag wil ik ook **alle leden van het Target-2-B consortium** bedanken en in het bijzonder alle leden van work package 3/6: **Nico**, **Rene**, **Diane**, **Taco**, **Esther** en **Theo**. Ik heb genoten van onze gezellige en nuttige werkbesprekingen en ons gezamenlijk enthousiasme over Fab glycanen.

Ik wil ook graag een aantal co-auteurs bedanken voor hun inzet en enthousiasme. In Leiden, **Mirjam**, **Pauline** en **Ingrid** bedankt voor jullie expertise en input rondom de BCR sequencing projecten. Van Sanquin, **Maartje**, **Arjan** en F**loris**, bedankt voor de prettige samenwerking rondom de B cel subset MS metingen en analyses.

Graag wil ik ook hen bedanken die zich hebben ingezet voor mijn mentale gezondheid. Coaches **Louise Mennen** en **Caroline Rebach** bedankt voor alle onvergetelijke inzichten die jullie me hebben geven tijdens de personal development en project management cursussen.

Mijn lieve vriendinnetjes uit Nimma: **Milou**, **Marieke**, **Lotte** en **Nikki** bedankt voor alle gezelligheid naast werk met Harry Potter marathons, vierdaagse feesten en weekendjes weg. **Mike**, **Sven** en **Rosan** fijn om met jullie te sparren over de wetenschap en om het promoveren wat te relativeren terwijl we ons misselijke aten bij Sumo of hard gingen op Metaxa.

Lieve schoonfamilie, **Wilma**, **Leo**, **Willem**, **Winnie**, **Manu** en **Kian**. Bedankt voor jullie interesse, steun, afleiding en toepasselijke sinterklaas surprises. **Cees**, je was een fantastische vader en een fantastisch mens.

Ook wil ik graag mijn super science grootvader en naamgenoot **Jan. A. van den Heuvel** bedanken. Zijn thuis-laboratorium in Vlijmen is met zekerheid de aanwakkering van mijn interesse in chemie en biologie geweest. Samen met de precisie die ik van **Oma** leerde hebben jullie mij de grondbeginsels voor een wetenschappelijke carrière bijgebracht.

Wat fijn om zulke geweldige ouders te mogen hebben. **Pap** en **Mam**, jullie leerden mij dat met hard werken, een goed plan en passie alles mogelijk is. Bedankt voor jullie oneindige steun en praktische adviezen. Mam, ook bedankt voor de mooie illustratie op de cover. Mijn grote zus en broer, **Lena** en **Tale**, fijn om twee van zulke kanjers als voorbeeld te mogen hebben.

Lieve **Janne**. We did it! Tegelijkertijd promoveren wat een avontuur en het is ons gelukt. Bedankt voor je altijd kritische blik, leuke soms verhitte inhoudelijke discussies en het benaderen van mijn projecten vanuit een andere hoek. Bedankt ook voor je onvoorwaardelijke liefde en steun. Ik ben benieuwd wat de toekomst gaat brengen. Met jou aan mijn zij wordt het hoe dan ook fantastisch. Ik hou van je!

Lieve kleine **Betty**, bedankt dat je altijd mijn schoot lekker warm kwam houden tijdens het vele thuiswerken en met aandacht heb geluisterd als ik een presentatie voor je oefende.

Einde.